A MULTI-PROXY PALAEOENVIRONMENTAL RECONSTRUCTION OF THE HOMA PENINSULA, WESTERN KENYA

THOMAS HENRY VINCENT

A thesis submitted in partial fulfilment of the requirements of Liverpool John Moores University for the degree of Doctor of Philosophy

August 2020

<u>ABSTRACT</u>

The Plio-Pleistocene of East Africa marks a crucial yet poorly understood period for hominin evolution. To better understand hominin activities from this time, the environmental substrate on which they resided must first be understood, as changes in the environment most likely influenced hominin evolutionary developments. Detailed palaeoenvironmental reconstructions throughout East Africa have been implemented using multi-proxy approaches to address this. Such records thus far are spatially and temporally limited. This thesis aims to rectify this by producing a multi-proxy palaeoenvironmental reconstruction of two sites on the Homa Peninsula, western Kenya – a novel palaeoenvironmental setting which hosts Plio-Pleistocene sedimentary sequences containing traces of hominin activity. These sites include Nyayanga (~ 2.6 Ma) and Sare River (~ 1.77 Ma).

The multi-proxy approach implemented in this research encompasses analyses of stratigraphy, particle size and phytoliths to reconstruct site sedimentary dynamics, depositional environment and palaeovegetation. End-member mixing analysis is additionally utilised to 'unmix' multimodal particle size distributions and provide more detailed information on sedimentary dynamics.

Nyayanga is interpreted as an alluvial plain environment upon which deposition occurred via episodic hyperconcentrated flows and intermittent unconfined fluvial flows. During flow hiatuses, secondary processes including fluvial runoff and aeolian deposition occurred, as well as stable land surface development. Higher energy hyperconcentrated flows became absent from the record throughout time, whilst unconfined fluvial activity became more infrequent. This was likely caused by a migration of the active sector of the alluvial plain. Bushy grasslands and grassy bushlands with infrequent sedges and woodland characterised the landscape during this time.

An alluvial plain is also identified as the depositional environment for sediments at Sare River. Intermittent unconfined fluvial activity deposited sediments on gentle slopes. This activity became more infrequent throughout time and flow hiatuses, characterised by the occurrence of secondary processes and stable land surface development, became more frequent. This could be attributed to a migration of the

active sector of the alluvial plain, or to aridification at the site. Bushy grasslands with infrequent woodland characterised the landscape here. Cosmogenic nuclide dating suggests sediments here could be younger than previously thought.

An interplay of both regional and local tectonics as well as climate drove palaeoenvironmental change at both sites. The development of the East African Rift System created extensive space for the accumulation of sediment, whilst also altering base-level through the formation and destruction of palaeolakes. A variable climate regime influenced variations in deposition at Nyayanga. Both sites experienced an overall trend towards greater aridity throughout deposition. Changes in palaeoclimate at Nyayanga are attributed to the intensification of the Northern Hemisphere Glaciation, whilst the development of an intensified Walker Circulation is identified as the cause of aridification at Sare River.

Environmental preferences of *Paranthropus* at Nyayanga ~ 2.6 Ma are similar to those presented at other East African sites. This suggests these hominins inhabited or frequented similar depositional settings in open landscapes characterised by bushy grasslands with infrequent wooded vegetation. Evidence from Nyayanga provides support for the pulsed-climate hypothesis linking environmental change to hominin evolution, which suggests that the long term drying trend observed in East Africa was punctuated by periods of extreme climate variability in which large lakes appeared and disappeared. During these periods evolutionary changes in hominins are suggested to have occurred.

Sediments from Sare River provide support that hominin activity ~ 1.5 Ma thrived in open environments characterised by alluvial/fluvial deposition much like other East African sites. A trend towards greater aridity and an increase in hominin activity throughout the sediments at this site is interpreted. This suggests that hominin activity here might provide support for the aridity hypothesis linking palaeoenvironmental change to hominin evolution, which suggests progressive aridity across Africa initiated grassland expansion and the novel adaptations associated with these environments.

<u>CONTENTS</u>

LIST OF TABLES

LIST OF FIGURES

DECLARATION OF COPYRIGHT

I confirm that no part of the material presented in this thesis has previously been submitted by me or any other person for a degree in this or any other university. In all cases, where it is relevant, material from the work of others has been acknowledged.

The copyright of this thesis rests with the author. No quotation from it should be published without prior written consent and information derived from it should be acknowledged.

<u>ACKNOWLEDGEMENTS</u>

This thesis would have not been successful without the constant support, guidance, encouragement and patience of a number of people whom I would like to thank here.

Firstly, thank you to my supervisory team that have advised and guided me throughout my time at Liverpool. My director of studies, Dr. Elizabeth Whitfield, gave me the opportunity to investigate such a fascinating topic, and I am grateful for her support and guidance throughout my PhD. I am also thankful for her aid during fieldwork on the Homa Peninsula, where it would not have been possible to collect the sufficient samples and information needed for this research alone. Dr. Jason Kirby, whom not only aided my supervision throughout this PhD, but also throughout my undergraduate degree. I am extremely grateful to him for allowing me the chance to study geography at Liverpool John Moores University, from which this research developed, as well as for his advice and feedback. Prof. Laura Bishop also aided this thesis with her inputs from a geoarchaeological and faunal perspective.

My extreme gratitude is owed to Prof. Tom Plummer from the Central University of New York, whom allowed me to participate in the novel research he is conducting as part of the Homa Peninsula Project. In addition to this, I would like to thank him for his constant interest in my work and the discussions he initiated whilst on fieldwork. May his humbleness, kindness and support also be noted.

I also owe Dr. Rahab Kinyanjui special thanks. Rahab hosted me at the National Museum of Kenya and aided in the development of my work with phytoliths. This element of the thesis would not have been possible without here guidance, support and wisdom.

I would also like to thank several other academic and laboratory staff at Liverpool John Moores University, whom although weren't part of my supervisory team, helped guide this thesis to completion. Prof. Chris Hunt provided lengthy discussions on multiple elements of my PhD. I am very thankful for his wisdom and approachability. I would also like to thank Dr. Tim Lane for his support and guidance on cosmogenic nuclide dating, as well his aid during fieldwork on the Homa

CHAPTER 1.   INTRODUCTION

1.1. Rationale

By 2.6 Ma the first widespread hominin use of stone tools, otherwise termed Oldowan technology, marked an important evolutionary milestone. With this came large mammal butchery, dietary changes and lithic raw material transportation (Plummer et al., 1999; 2009a; 2009b; Bishop et al., 2006; Braun et al., 2008; 2009a; 2009b; Ditchfield et al., 2018; Plumer and Bishop, 2016; Plummer and Finestone, 2018; Finestone, 2019). Despite this, our understanding of hominin activities and behaviour at this time is lacking, due to the existence of only a handful of archaeological sites containing both plentiful artefacts and well-preserved fauna (Ditchfield et al., 2018). In order to better understand hominin activities and behaviour, the environmental substrate on which they resided must first be understood, as changes in the environment most likely influenced hominin evolutionary developments (Potts, 1994; Plummer et al., 1999; Albert et al., 2015). To achieve this, multi-proxy approaches are often employed to form a more robust and accurate reconstruction of the palaeoenvironment by utilising an array of palaeoenvironmental proxies in conjunction (Ashley & Driese, 2000; Hay & Kyser, 2001; Albert et al., 2006; 2015; Bamford et al., 2006; Ashley et al., 2009; Deocampo et al., 2009).

Well known sites such as Olduvai Gorge in Tanzania and the Turkana Basin in Kenya and Ethiopia, currently act as the main sources of palaeoanthropological data from the late Pliocene of East Africa. This has been highlighted as one of the most important time periods for evolutionary developments of Hominids (Leakey, 1971; Bonnefille, 1984; Fernandez-Jalvo et al., 1998; Ditchfield et al., 1999; Plummer et al., 1999; 2009b; Blumenschine et al., 2003; Hernández Fernández & Vrba, 2006; Bamford et al., 2006; 2008; Ashley et al., 2010a; Albert et al., 2015). During this period, hominins adapted to a shift from C_3 (wooded) habitats to larger amounts of C_4 (grasses) vegetation, most likely caused by global cooling and tectonic uplift (Plummer et al., 1999). This information is based on the use of multi-proxy approaches at the previously mentioned sites (Kibunjia et al., 1992; Rogers et al., 1994; Plummer & Bishop, 1994; Behrensmeyer, 1997; Fernandez-Jalvo et al., 1998; Andrews & Humphrey, 1999; Potts et al., 1999; Hay & Kyser, 2001; Blumenschine

et al., 2003; Hover & Ashley, 2003; Schoeninger et al., 2003; Wynn, 2004; Hernández Fernández & Vrba, 2006; Bamford et al., 2006; 2008; Sikes & Ashley, 2007; Harris et al., 2008; Deocampo et al., 2009; Magill et al., 2013a; 2013b; 2016; Albert et al., 2015; Uno et al., 2016b; 2016a). Other localities in East Africa outside of Olduvai Gorge and the Turkana Basin have by comparison received considerably less attention from palaeoanthropologists. In terms of understanding the behaviour of Oldowan tool using hominins, their activities need to be investigated in different environmental settings (Potts, 1994; Plummer et al., 1999).

To learn more about Oldowan hominin activities in a new geographic setting, research on the Homa Peninsula, western Kenya was initiated as part of an interdisciplinary palaeoanthropological project — the Homa Peninsula Paleoanthropological Project (HPPP) (Plummer et al., 1999). By comparing hominid activities at different spatial locations, behavioural variability in hominins can be assessed (Plummer et al., 1999). As part of the HPPP, significant archaeological traces of our hominin ancestors have been uncovered within sedimentary contexts coupled with well-preserved fauna. These date back to at least ~ 2.6 Ma BP and record novel behaviours in an open environment, rather than in the more wooded Oldowan sites (Plummer et al., 1999; Bishop et al., 2006; Plummer & Bishop, 2016; Ditchfield et al., 2018). Included within these are traces of *Paranthropus sp.* and abundant lithics spanning the range of the Oldowan Industrial Complex (Finestone, 2019).

However, the palaeoenvironment in this region is not well understood, owing to the focus on mainly one archaeological site, Kanjera South, where palaeoenvironmental interpretations are limited to field-based sedimentary investigations, isotopic analysis of pedogenic carbonates, and more recently, particle size analysis (Behrensmeyer et al., 1995; Plummer et al., 2009a; Plummer & Bishop, 2016; Ditchfield et al., 2018;). Thus there is a clear need to further develop and refine palaeoenvironmental reconstructions in this geographical area.

1.2. Research aims and objectives

The Homa Peninsula contains significant Oldowan archaeology in a novel palaeoenvironmental setting, which is positioned within a poorly understood temporal period in East Africa. For this reason, it is essential that hominin activities

and their associations with the environment here are better understood. To achieve this, the palaeoenvironment must first be reconstructed.

As part of the HPPP, the role this thesis is to improve the understanding of the palaeoenvironment in which archaeological occurrences are found across the Homa Peninsula. The research here specifically aims to build a palaeoenvironmental reconstructions of two new sites, Nyayanga and Sare River, through the utilisation of a multi-proxy approach. This encompasses analyses of stratigraphy, particle size and phytolith assemblages. By refining the resolution of reconstructions here, our understanding of hominin behaviours and activities in different environmental settings will be enhanced, and the palaeoenvironment of the Homa Peninsula will be comparable with better known East African sites (Ditchfield et al., 1999; Plummer et al., 1999; 2009a; Blumenschine et al., 2003; Ashley et al., 2010a). This will be achieved through completion of the following objectives:

1. Reconstructing the sedimentary dynamics and depositional environment at both sites

2. Reconstructing the palaeovegetation at both sites

3. Identifying the driving mechanisms of palaeoenvironmental change on the Homa Peninsula by analysing changes in (1) and (2)

4. Resolving the environmental factors driving palaeoenvironmental evolution and determining the relationship between hominin activity and palaeoenvironmental change.

1.3. Thesis structure

In **Chapter 2**, the geographical location of the study sites is introduced and their climatic, environmental and geological settings are described. Research findings from previous work on the Homa Peninsula are synthesized.

Chapter 3 reviews literature surrounding East African palaeoenvironmental records from the Miocene to the Pleistocene and its relationship with hominin activity. Reconstructive techniques are identified and evaluated. Driving mechanisms of

palaeoenvironmental change are also outlined and evaluated, as well as major climate transitions.

Chapter 4 outlines the methods/proxies that are used to reconstruct the palaeoenvironment of the study sites. Each method is reviewed in terms of its usefulness to palaeoenvironmental reconstructions and specifically to this study. Methodological approaches are detailed for each technique, as well as the laboratory technique and data analysis.

In **Chapter 5**, the results for each method applied in this research are presented and described. Based on these results, sediments are divided into different units based on their lithofacies. Some of these units are further divided into subunits. Subsequently, a table of lithology is presented summarising the characteristics of each sedimentary unit based on the results. Results are first presented for the Nyayanga study site and subsequently for the Sare River site.

Chapter 6 makes interpretations based on the results presented in the previous chapter, beginning with the Nyayanga study site and followed by the Sare River site. It begins by attributing end-members to transport/depositional mechanisms and sediment sources, based on the end-member characteristics and evidence from the other methods applied at each site. Following this, the palaeoenvironment is interpreted for each sedimentary unit identified at the two sites. Palaeoenvironmental evolution at each site is then discussed subsequently to this, based on the changes observed through each of the sedimentary units. Driving mechanisms for palaeoenvironmental change at each site are then discussed. To conclude, the relationship between hominin activity and the palaeoenvironmental substrate at both sites on the Homa Peninsula is discussed, as well as the impact that changes in palaeoenvironmental settings may have had on such activity.

The overall findings of this thesis are presented in **Chapter 7.**

CHAPTER 2.   STUDY SITES

2.1. Introduction

Within this chapter, the geographical location of the study sites will be introduced, including their climatic, environmental and geological settings. Research findings thus far on the Homa Peninsula will also be synthesized herein.

2.2. Location, Geology and Geoarchaeology

2.2.1. The Homa Peninsula

The Homa Peninsula is located in western Kenya on the southern shores of the Winam Gulf of Lake Victoria (Figure 2.1) in the Nyanza Province of the East African Rift Valley (EARV), an elongate EW to NE – SW fault bounded rift-system which emanates from the Kenya dome (Pickford, 1982; Behrensmeyer et al., 1995; Ditchfield et al., 1999; Plummer et al., 1999; Bishop et al., 2006). The rift stretches 133 km long east of Lake Victoria, with a width of approximately 25 – 50 km (Behrensmeyer et al., 1995). Located on this peninsula are the two study sites that form the basis for this research: Nyayanga (0º 23' 55.597" S, 34º 27' 5.767" E) and Sare River (0º 24' 33.239" S, 34º 37' 4.580" E), as well as the previously studied site of Kanjera South (Figure 2.1).

The geologic context of the Homa Peninsula is described extensively by various authors (Pickford, 1984; Plummer & Potts, 1989; Behrensmeyer et al., 1995; Plummer et al., 1999; Ditchfield et al., 1999). The peninsula is dominated by the Homa Mountain carbonatite complex (Figure 2.1), formed of intrusive volcanic masses on a foundation of shattered and fenitized Nyanzian rocks (Behrensmeyer et al., 1995). Doming of Homa Mountain began between 10 – 11 Ma and continued until ~ 5 Ma, with the latest dated episode being at 1.3 ± 0.1 Ma (Le Bas, 1977; Pickford, 1984; Behrensmeyer et al., 1995) . Contemporary thermal activity is limited to hot springs at various sites on the peninsula (Behrensmeyer et al., 1995).

The geology in the immediate vicinity of Homa Mountain includes Homa carbonatite, Homa phonolite, Homa ignimbrite, Homa limestone, and fenitized Nyanzian (Braun et al., 2008; Finestone, 2019). Homa Mountain acts as a radial drainage system for the peninsula, and from 6 Ma throughout the Pleistocene, fluvial-lacustrine sediments were deposited on its flanks (Behrensmeyer et al., 1995; Ditchfield et al.,
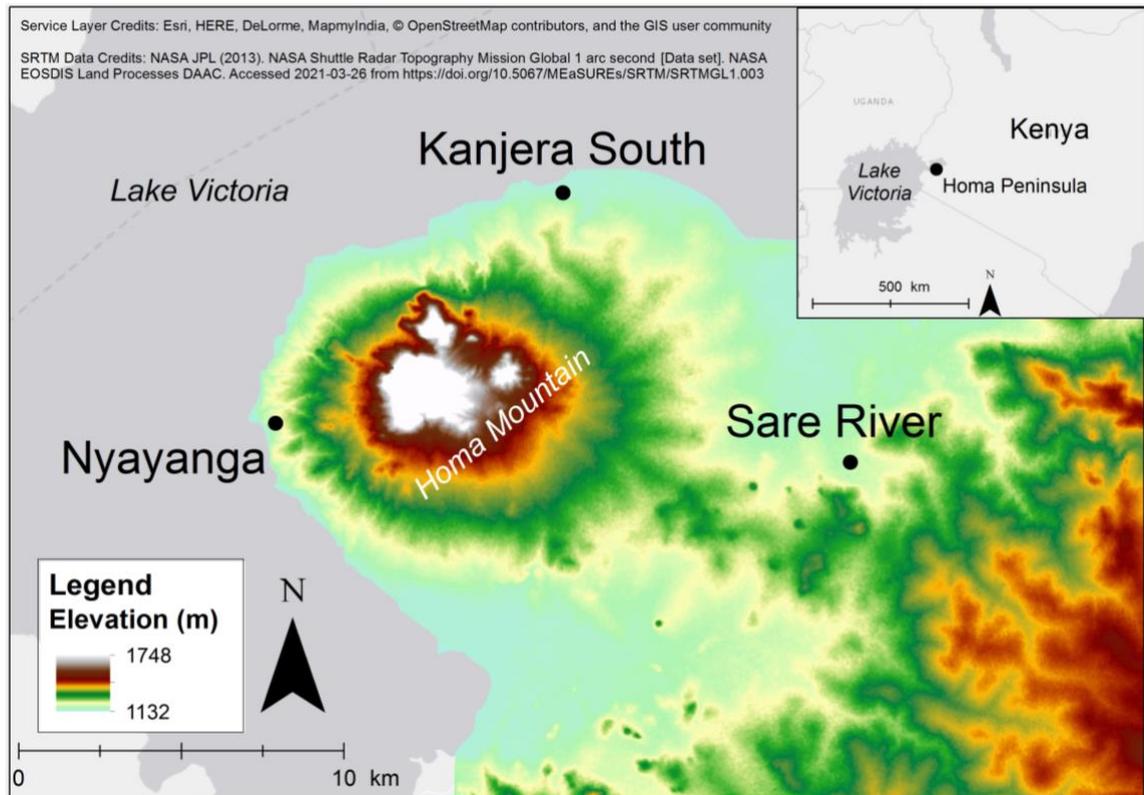
Figure 2.1:The Homa Peninsula, located in western Kenya on the southern shores of the Winam Gulf of Lake Victoria.
The position of the two study localities (Nyayanga and Sare River) and Kanjera South (focus of previous work) are
highlighted, as well as Homa Mountain. A 30 m digital elevation model (DEM) is overlaid to illustrate topographic
variations across the peninsula (DEM data source credited in figure)

1999; Plummer et al., 1999; Braun et al., 2008). Extensive geological mapping, geochemical analyses (Energy Dispersive X-ray Fluorescence [ED XRF]) and conglomeratic surveys revealed that the drainage system across the peninsula is predominantly comprised of material from the carbonatite complex, indicating this is the primary sediment source (Braun et al., 2008; Finestone, 2019).

The geology associated with the carbonatite complex on the peninsula as well as its drainage system is divided from the surrounding geological provinces by the Samanga fault (Figure 2.2), which has existed since the Pliocene (Le Bas, 1977; Braun et al., 2008; Finestone, 2019). These provinces include Nyanzian rhyolites, Oyugis granite, Nyanzian chert, Bukoban quartzite, Bukoban felsite, and Bukoban basalt (Braun et al., 2008; Finestone, 2019). Material from these sources are found in the Awach drainage system which flows towards the peninsula from the east before being diverted either side of the peninsula due to faulting and uplift associated with the doming of Homa Mountain (Braun et al., 2008; Finestone, 2018).
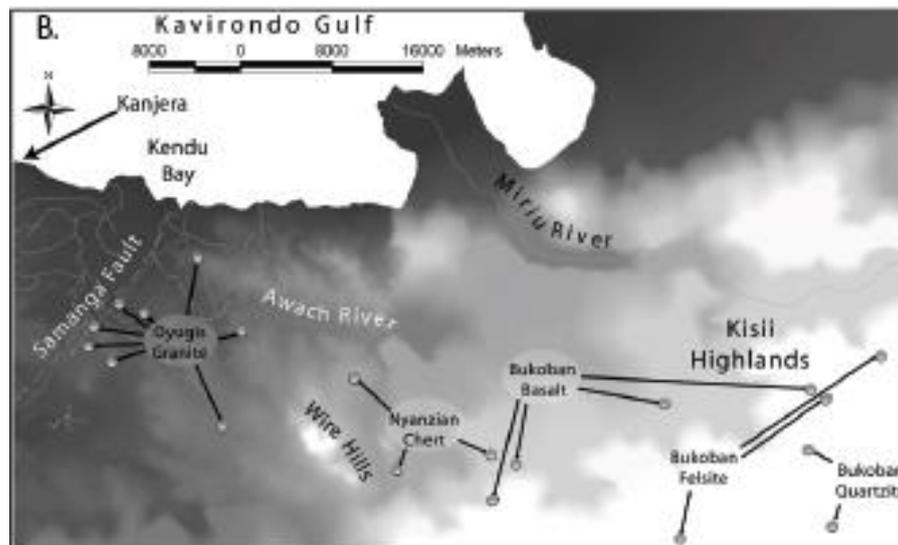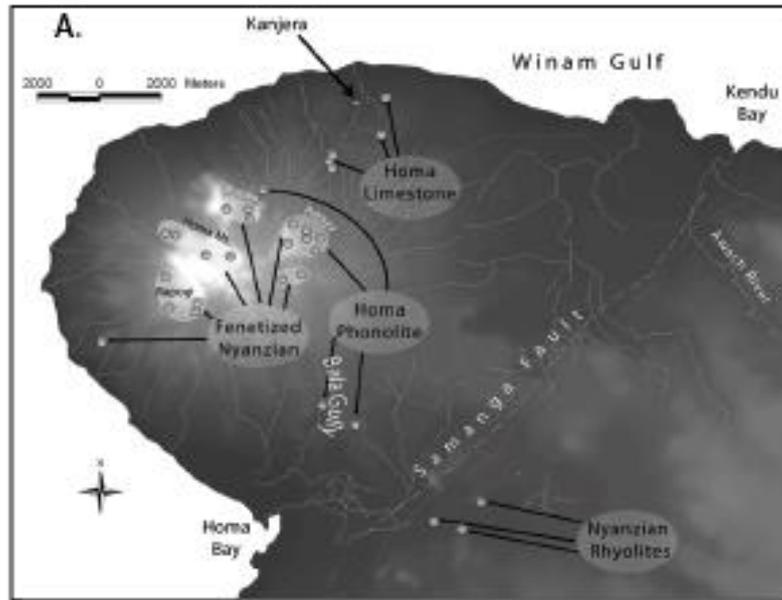
Figure 2.2:The geological provinces surrounding the Homa Peninsula. Figures from Braun et al. (2008). Figure A shows the provinces surrounding Homa Mountain. Figure B shows the provinces to the east of the Samanga fault, which is also displayed on both images

2.2.2. Nyayanga

The Nyayanga study site is located west of Homa Mountain (Figure 2.1), characterised by faulting and fluvial incision into clays, silts and sands which has shaped a 40,000 m² westward facing amphitheatre, where well-stratified beds can be observed in a ~ 16 m thick sequence. Elevation can be seen to steeply decrease from east to west here (Figure 2.3), with Homa Mountain acting as the only sediment source for the site. Vegetation here can be described as an open wooded grassland. Shrubs and grasses are most common, although wooded vegetation is present. Much of the surrounding vegetation is now farmland.
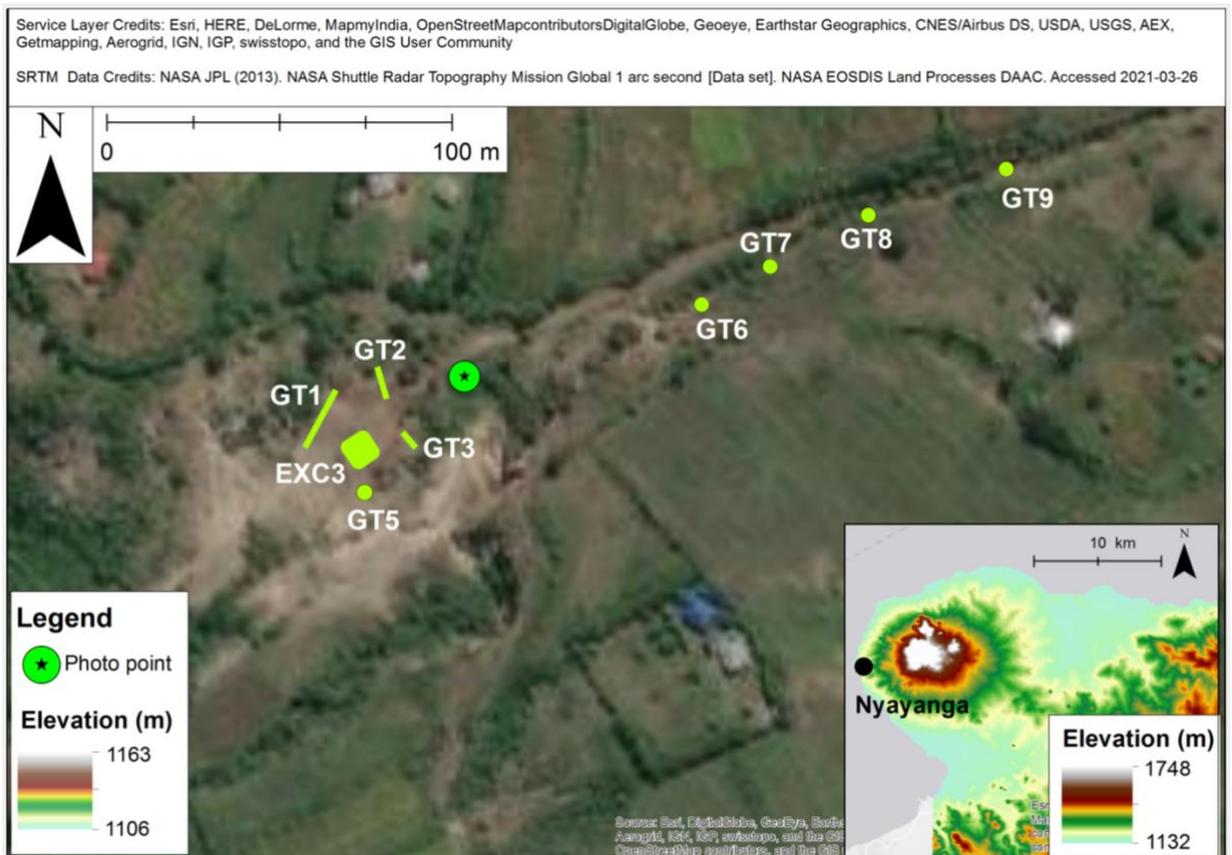
Figure 2.3: Geological trenches (GT) and excavations (EXC) at Nyayanga (satellite imagery credited in figure). The position from which the site photograph displayed in Figure 2.4 is also highlighted.. A difference in elevation of ~ 600 m can be observed between Homa Mountain and Nyayanga

Current chronology at the site is based upon biostratigraphy and magnetostratigraphy, placing the deposits at 3.05 – 2.595 Ma in age (Finestone, 2019). Resultantly, evidence of hominin activity here is of great significance (Plummer, *pers. comms.).* From 2015 to 2017 six excavations and nine geological trenches were laid out at Nyayanga (Figure 2.3 & Figure 2.4). 402 artifacts were discovered across the site as well as fossil taxa with cut marks and percussion damage. Of these, 227 artifacts were found on the surface, whilst 175 were found *in* situ in excavations. Two hominin teeth were also uncovered at the site, determined to be *Paranthropus sp.* molars based on size and overall morphology by Professor Shara Bailey. Identification to species level was unavailable based on the isolated teeth alone.

Excavation 3 (25 m^2) (Figure 2.5) yielded the largest abundance of artifacts and fauna, including 116 artifacts spatially associated with fossil taxa. Notably, a *Paranthropus sp.* molar (Figure 2.6) and a fossil Hippopotamidae were part of the assemblage and were found in close proximity to stone tools. These included flakes,

Figure 2.4: A ~ 150 m panoramic site photograph taken by the author in 2016 from the point displayed in Figure 2.3 facing southwest (0° 23' 54.384'' S, 34° 27' 8.273'' E). Geological trenches and excavations placed in the main amphitheatre of the Nyayanga locality are highlighted. Geological trenches placed further up the canyon cannot be seen in this picture. Vegetation here can be described as an open wooded grassland

cores, a hammerstone and several manuports (Figure 2.7). Excavation 1 (9 m^2) and Excavation 2 (10 m^2) revealed no artifacts, whilst Excavation 4 (4 m^2), 5 (10 m^2) and 6 (3 m^2) uncovered further artifacts in association with fauna.

Artifacts from Nyayanga include both fresh and weathered specimens, and are composed of Bukoban quartzite (27.4%), vein quartz (23.6%), fenitized rhyolite (22.9%) and Nyanzian rhyolite (17.7%) (Finestone, 2019). Durable lithologies were selected for flake production here, some of which were not locally available, suggesting that hominins travelled a distance of at least 2 – 4 km to access the lithologies to the southeast unrelated to the Homa Mountain carbonatite complex

Figure 2.5:Photograph of Excavation 3 (0° 23' 54.384'' S, 34° 27' 8.2728'' E) at Nyayanga taken by the author facing east. A fossil Hippopotamidae can be seen the bottom left of the image

Figure 2.6:Photograph of a Paranthropus sp. *molar retrieved from Excavation 3 at Nyayanga taken by Prof. Tom Plummer in 2016*

(Finestone, 2019). This might be explained by the comparably soft/flawed lithologies available in local conglomerates, which is why hominins travelled further to procure higher quality materials (Finestone, 2019). However, this record indicates greater selectivity and transport than existing knowledge from other early Oldowan occurrences (Finestone, 2019).

Figure 2.7:Photograph of the examples of in situ artifacts surrounding a fossil hippopotimidae in Excavation 3 at Nyayanga taken by Prof. Tom Plummer in 2016

2.2.3. Sare River

The Sare River study site (Figure 2.1 & Figure 2.8) is located ~ 55 km east of Homa Mountain and most likely dates to the Early Stone Age of East Africa based upon the fossil assemblage. The sedimentary sequence here reaches up to 7 m in thickness and is exposed for over 2 km with no evidence of disturbance. The highlands to the southeast at Nyamira act as the primary sediment source for Sare River.

Highly weathered granite bedrock makes up the base of this sequence, which is overlain by a ~ 1 – 2 m thick palaeosol, a ~ 1 – 2 m volcanic tuff, and capped by a further palaeosol (Figure 2.9). Magnetostratigraphy has indicated a normal to reversed polarity in the lower unit, with reversed polarity persisting through the upper units (Finestone, 2019). The overlying tuff, termed the 'Orio tuff', has been suggested to coincide with the late Pliocene/early Pleistocene depositional events that occurred in the vicinity of Homa Mountain (Le Bas, 1977). This places the upper palaeosol just above the Olduvai subchron, indicating they are just younger than ~
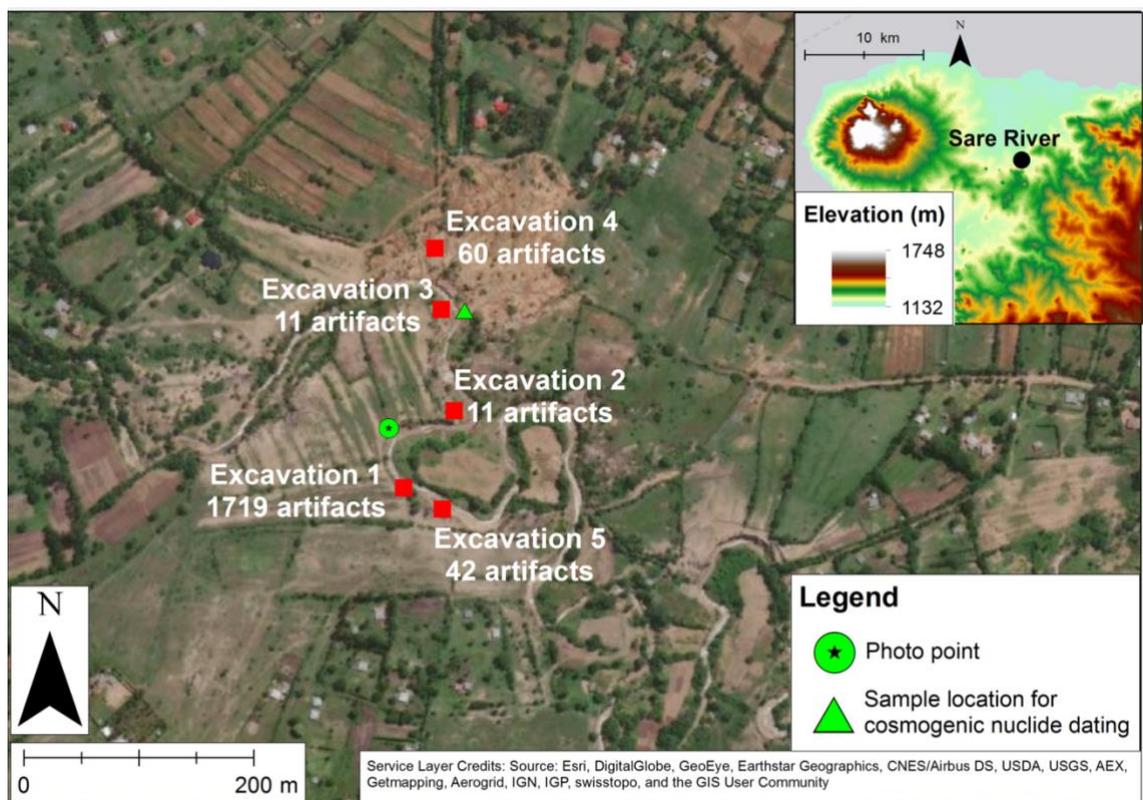
Figure 2.8: The Sare River study site (satellite imagery credited in source). Excavation locations and the number of artifacts uncovered in each are highlighted. The location of sampling for cosmogenic nuclide dating is also displayed. The position from which the site photograph shown in Figure 2.9 is also shown. Elevation surrounding Sare River can be seen to steeply decrease from southeast to northwest in the DEM (data source credited in figure)

1.77 Ma (Sier et al., 2017; Finestone, 2019). Analysis of stable isotopes of pedogenic carbonates is ongoing here, and has suggested that the palaeoenvironment may have been that of a heterogeneous landscape consisting of dense woodlands and wooded grasses (Plummer*, pers. comms.*).

Between 2015 and 2017, five excavations were laid out at Sare River across a 250 m transect primarily targeting the upper palaeosol (Figure 2.9), although the lower palaeosol also contains a conglomerate in which artefacts and quartzite cobbles can be found in a sandy matrix. Excavations 2 – 5 were 2 m^2 in size, whilst excavation 1 was 12 m^2 in size. Together these excavations yielded nearly 2000 *in situ* artifacts (Figure 2.10) which were all fresh, whilst no faunal remains were uncovered (Finestone, 2019). Artifact density was variable between excavations, with excavation 1 preserving a considerably denser accumulation of artifacts (143.3/m^2) than excavations 2 (5.5/m^2), 3 (5.5/m^2), 4 (30/m^2) and 5 (21/m^2). This suggests that this location was a hotspot for hominin activity and that they favoured specific locations for activities utilising stone tools (Finestone, 2019). Stone tools at Sare River were primarily composed of quartz (84%), which was readily available from local conglomerates (Finestone, 2019). The differences between transport difference of raw materials at Nyayanga and Sare River likely relates to the quality and availability of high quality raw materials, which were more abundant at Sare River (Finestone, 2019).

Figure 2.9:Site photograph displaying the upper palaeosol at Sare River taken by the author in 2017 from the position shown in Figure 2.8 facing south (0° 24' 33.2388'' S, 34° 37' 4.5804'' E). The contemporary vegetation here is notably denser, with trees being much more frequent than Nyayanga.

Figure 2.10: Photograph taken by Prof. Tom Plummer in 2017 displaying an example of artifact scatter in Excavation 1 at Sare River

2.2.4. Previous work: Kanjera South

Kanjera South (Figure 2.1) hosts the only other record of Oldowan archaeology on the Homa Peninsula aside from Nyayanga and Sare River (Oswald, 1914; Leakey, 1935; Boswell, 1935; Plummer & Potts, 1989; Behrensmeyer et al., 1995; Plummer et al., 1999; 2009a; Bishop et al., 2006; Plummer & Bishop, 2016;). It is home to the recovery of the first monkey fossils found in East Africa (Oswald, 1914), as well as the recovery of modern hominin fossils (Leakey, 1935; Behrensmeyer et al., 1995; Ditchfield et al., 1999). Based on the artefactual and faunal assemblage in the sequence, the hominin fossils were suggested to be of a middle Pleistocene age (Leakey, 1935; Behrensmeyer et al., 1995). However, this age was contested by claims that sediment slumping had caused bones and artefacts of different ages to become mixed (Boswell, 1935; Kent, 1942), thus adding controversy to the provenance of the hominin finds (Behrensmeyer et al., 1995).

The sediments at Kanjera South were first described as a tripartite series of beds, with a greenish tuff with ash at the base, overlain by a middle group of clays with limestone and an upper bed of clay, believed to be middle Pleistocene in age (Kent, 1942). Following this, a number of studies refined the geology and palaeontology of the locale and sampling for magnetostratigraphy was initiated (Saggerson, 1952;

Pilbeam & Gould, 1974; Le Bas, 1977). Five units were outlined and were suggested to be early/middle Pleistocene in age (Pickford, 1984; 1987).

Later work defined six units (Table 2.1) within the sequence at Kanjera South (KS1 – 6) (Behrensmeyer et al., 1995). Sampling for magnetostratigraphy and biostratigraphy identified that deposition of sediments occurred ~ 2.3 Ma in the late Pliocene (Plummer & Potts, 1989; Ditchfield et al., 1999; Plummer et al., 1999). Moreover, evidence of sediment slumping previously identified (Boswell, 1935) was not observed; sediments were shown to be preserved in good stratigraphic context (Behrensmeyer et al., 1995; Ditchfield et al., 1999). Subsequently, taphonomically controlled excavations have taken place here as part of the HPPP (Bishop et al., 2006), with a number of excavations and geological trenches being placed, on which an interdisciplinary team of archaeologists, palaeontologists and geologists have since worked (Behrensmeyer et al., 1995; Ditchfield et al., 1999; Plummer et al., 1999; 2009a; Bishop et al., 2006; Braun et al., 2008; 2009b; 2009a; Ferraro et al., 2013; Lemorini et al., 2014; Plummer & Bishop, 2016).

Over 4400 artifacts as well as thousands of faunal remains have been uncovered at the site across three excavations: Excavation 1 (169 m^2), Excavation 2 (15 m^2), and Excavation 5 (4 m^2) (Plummer et al., 2009a; 2009b; Finestone, 2019). Artifacts are composed of durable materials including quartz, quartzite, basalt, felsite, chert and granite and reflect hominin preference for hard and easily-flaked materials (Braun et al., 2008; 2009a; 2009b; Finestone, 2019). Although much of the assemblage is composed of locally sourced materials (70%), exotic artifacts also make up a noteworthy proportion (30%). This again points to hominins selecting for high-quality durable materials and travelling greater distances to acquire them (Braun et al., 2008; 2009a; 2009b; Finestone 2019).

Reconstructions of the palaeoenvironment at Kanjera South have been based on field investigations and isotopic data from pedogenic carbonates, palaeosol carbonates and tooth enamel (Behrensmeyer et al., 1995; Ditchfield et al., 1999; 2018; Plummer et al., 2009a; Plummer & Bishop, 2016). Deposition generally took place in alluvial and lake marginal environments on a grassy plain, between wooded slopes and a permanent water body (Behrensmeyer et al., 1995; Ditchfield et al., 1999; 2018; Plummer et al., 2009a; Plummer & Bishop, 2016). More detailed

descriptions of the palaeoenvironment for each bed at Kanjera South have been made (Behrensmeyer et al., 1995; Ditchfield et al., 1999; Plummer et al., 2009a; Plummer & Bishop, 2016); this information is summarised in Table 2.1.

Bed	Description	Palaeoenvironmental interpretation
KS1	Grey-brown silty, gravelly sand and sandy silt, with layers of hard $CaCO_3$ nodules. These preserve fine horizontal lamination and indicate post-depositional calcification. Clasts including granite, grey and red chert, some volcanic material and large biotites present in gravel associated with coarser sand. Some thin clayey silt beds in upper 1 m. Bimodal grain size distribution of medium-grained sand and fine silt-clay.	Deposition initially began as a flow of pyroclastic material from the Homa Mountain complex towards depocentre Nyanza Rift graben in the north. These deposits were reworked by ephemeral streams running across the fan of the original pyroclastic flows. Possibly a nearshore lacustrine or wet floodplain environment.
KS2	c. 1.3 m of orange and yellow-grey gravelly sand, with a thin patchy conglomerate. Contains fresh biotites and angular and rounded volcanic and basement clasts. Cross-stratification orientated 150–155° (SE). Variable cementation, locally very mottled with irregular limonitic staining.	Fluvial channel fill, with deposition by anastomosing channels flowing with intermittent, diffuse, generally low-energy flow regimes.
KS3	c. 60 cm of homogeneous and massive light-orange to yellow-grey sandy silt with some tuffaceous silt. Some horizontal orange mottling. Includes partial *Hippopotamus* skeleton. Ostracods and fish scales also present.	Continuation of KS2, with a transition to a wetter depositional environment. Small channel present with more stable land surfaces.
KS4	c. 3.2 m thick grey-green and brown clay, with some silty clay and occasional sandy clay in lower bed. Clays generally dense, homogeneous, calcareous and mottled, with occasional slickensides and soft patches of $CaCO_3$. Sandy clay channel features 1.5 m above the base, with root traces and reworked clay clasts. Irregular bedding contacts within the clays suggest pedobioturbation. Increased $CaCO_3$ in upper half of unit; this occurs as vertical patches and small nodules. Pedogenesis evidenced by vertical cracking, decreased homogeneity of clay and abundant nodules. Ostracods and fish debris in lower parts of bed.	Very-low energy lacustrine or swamp deposition. Periodic sub-aerial exposure with some sub-aqueous deposition. Clays deposited either during the transgression of a lake or during the formation of a wetland system
KS5	~2–2.5 m of brown clayey sandy gravel, with matrix-supported grains and pebbles. Some resistant $CaCO_3$ layers interbedded; abundant volcanic gravel and cobbles present in some of these. One limestone bed has plant stem and root moulds, whereas others are massive and caliche-like. Clayey sand and gravel beds generally massive and bimodal, with some grain-supported gravel lenses and abundant small $CaCO_3$ nodules throughout.	Fluvial deposition with a variable energy regime combined with pedogenesis and stable land surface development.
KS6	2 m of brown clay, grading upwards to light-grey mottled gravelly clay and capped by an irregular, massive $CaCO_3$ bed up to 40 cm in thickness. Lower part has fewer $CaCO_3$ nodules than KS5. Upper part of bed has patches of gravelly and sandy clay, which are dark grey and have yellow streaks and mottling. Relatively pure clay with no coarser clast components.	Continuation of KS5. Wet conditions, possibly near a spring or other source of calcium-saturated water.

Table 2.1: Bed descriptions and palaeoenvironmental interpretations published previously for Kanjera South, including Behrensmeyer et al. (1995), Ditchfield et al. (1999; 2018), and Plummer et al. (2009)

2.3. Contemporary climate and vegetation
2.3.1. Climate

East African climate is complex and influenced by a variety of factors; Kinyanjui (2012) gives a detailed overview of these. The main influences on East African climate appear to be: the movement of the Inter-Tropical Convergence Zone (ICTZ); the El Niño-Southern Oscillation (ENSO); disturbances in monsoon trade winds;

changes in Sea Surface Temperature (SST); and large scale atmospheric weather patterns (Kinyanjui, 2012).

The ITCZ (a low-pressure belt) migrates from south to north and vice versa, forming sub-tropical high pressure cells. Consequently, high rainfall belts are created corresponding to the area of maximum insolation and spanning the distance of the tropics, causing significant climate variation within this area, due to latitude, distance from the coast, and topography (Mutai & Ward, 2000; Marchant et al., 2007; Kinyanjui, 2012). The migration of the ITCZ is most likely also the cause for the two rainy seasons that characterise the eastern Rift Valley, occurring from March to June and from October to December. The intervening climate is arid/dry. Periods of maximum rainfall follow the latitudinal position of the ITCZ with a lag of ~ 4 weeks, although maximum surface temperatures appear to follow periods of maximum solar radiation (Kinyanjui, 2012; Nicholson, 2018).

Additionally, disturbances in the monsoon and trade winds, changes in the sea surface temperature (SST) and large scale atmospheric weather patterns all cause variability in inter-annual rainfall variability (Mutai & Ward, 2000; Kinyanjui, 2012; Nicholson, 2018). Moist westerly winds originating from the South Atlantic through the Congo basin during the austral winter also influence rainfall variability in the western part of East Africa, as well as the rainy seasons (Bergner et al., 2003).

The El Niño-Southern Oscillation (ENSO) also influences climate, particularly in the eastern rift valley. Periods of high rainfall are most likely associated with warm ENSO events, and vice versa (Mutai & Ward, 2000; Kinyanjui, 2012). The complex topography of this region also results in a highly diverse set of mean rainfall totals, with highlands receiving ~ 1000 – 1500 mm of mean annual rainfall, and lowlands receiving only ~ 250 – 500 mm. The mountain ranges surrounding the central rift valley also act as an orographic barrier producing a rain shadow effect that results in irregular rainfall throughout the long rainy season between March and May (Mutai & Ward, 2000; Kinyanjui, 2012).

The Homa Peninsula receives an average of ~ 11,400 mm of precipitation annually, and has a temperature of 24ºC (Le Bas, 1977; Behrensmeyer et al., 1995). Although classified as a tropical climate, rainfall in the region is erratic and prolonged droughts

are a common feature of the climate, which can result in widespread fires (Edwards, 1940).

2.3.2. Vegetation

Edwards (1940) provides an overview of the vegetation throughout Kenya. Edwards characterises the area surrounding Nyayanga as an 'Acacia-tall grass savannah and open grassland'. However, Nyayanga has been subject to agricultural practice, and so the vegetation in the immediate vicinity of this locality differs slightly from the wider description. Despite this, the vegetation here and in the surrounding area is described as having an even cover of grass approximately 120 cm in height, with trees widely spaced apart (~ 15 m) and varying in height (~ 3 – 15 m), or even non-existent. The most frequently occurring trees are species of *Acacia*, but *Euphorbia* and other succulents are also present of which are seen frequently. The most characteristic species include: *A. stenocarpa, A. abyssinica, A. hebecladoides, A. drepanolobium, A. lahai, A. pennata, A. seyal* and *A. xanthophloea.*

At higher altitudes, *Acacia* become less important to the vegetative composition, and their place is most commonly taken by sclerophyllous bush. The grass component of the vegetation is made up of tall grass that appears to have almost complete cover, but is relatively open at its base. Grasses are comprised mainly of *Themeda trianda, Pennisetum masaicum, Eragrostis* spp.*, Hyparrhenia* spp., *Andropogon* spp., *Setaria* spp., *Panicum* spp., and more commonly in drier areas, *Pennisetum stramineum* and *Digitaria* sp. aff. D. *nodosa.* In localised areas such as near streams and on ancient lake beds, species of *Cynodon* also occur. Legumes are particularly infrequent, occurring mainly as *Indigofera* and *Crotalaria*. Burning has also significantly altered the vegetation throughout the region; burning is performed by pastoral tribes, degrading large portions of evergreen thicket and allowing species of *Acacia* to invade. On the upper slopes of the Homa Mountain however, evergreen woodland and bushes are largely undisturbed by human activity.

The vegetation at Sare River differs to that of the vegetation found near Nyayanga (Figure 2.9). Edwards (1940) characterises this area as a high moisture savannah, forming under higher rainfall amounts. Thickly scattered trees ~ 3 – 5 m in height along with tall grasses ~ 1.5 – 2.5 m high. Similar to the previous vegetation type

described, *Acacia* are a frequently important feature of the vegetation, although broad-leafed trees appear more often. Of these, frequently appearing types include *Combretum*, *Terminalia*, *Ficus*, and *Faurea*. The herbage is made up primarily of *Themeda triandra*, *Hyperrhenia* spp., and *Cymbopogon* spp.. Some of the most common grasses in this vegetation type are *Chloris gayana*, *Setaria trinervia*, *Trichopteryx kagerensis*, Digitaria diagonalis*, Beckeropsis uniseta*, *Paspalum scrobiculatum,* and *Cynodon* spp..

2.4. Summary

This chapter has presented an overview of the study sites, including their geographical, geological and archaeological characteristics. Additionally, the contemporary climate and vegetation has also been overviewed. Previous research in the study region has also been summarised here.

CHAPTER 3.   LITERATURE REVIEW

3.1. Introduction

To fully understand the complex nature of hominid activities and behaviour, it is essential that the environmental substrate and general character of the landscape they occupied is fully understood (Plummer et al., 1999; Albert et al., 2015). Such an understanding is paramount when determining how changes in the environment shaped human evolution and the emergence of key hominin traits, if at all (Reed, 1997; Potts, 1998; 2013). For this reason, hominid activities in varied geographic settings have been, and remain under investigation by palaeoanthropologists (Potts, 1998; 2013; Plummer et al., 1999). The East African Rift System (EARS) has been the focus of such investigations, owing to its extensive stratigraphic sequences that preserve records of human evolution, as well as a suite of palaeoenvironmental indicators (Potts, 2013) spanning from the late Miocene to the early Pleistocene.

This chapter reviews literature surrounding East African palaeoenvironmental records from the Miocene to the Pleistocene and its relationship with hominin activity. The effect of palaeoenvironmental change on hominin evolution in East Africa is first reviewed. Reconstructive techniques are then identified and evaluated. Driving mechanisms of palaeoenvironmental change are also outlined and evaluated, as well as other major climate transitions.

3.2. The effect of palaeoenvironmental change on Hominin evolution in East Africa

At present, it is widely accepted that all the main stages in human evolution occurred primarily in East Africa, despite the existence of the World Heritage Site in South Africa, the Cradle of Humankind (Dirks and Berger, 2013) and the appearance of the genera *Sahelanthropus* (Brunet et al., 2002). The earliest specimens for each of the main genera were found in the EARS. Four stages of human evolution are apparent in the fossil record. These include: 1) the appearance of the first proto hominins around 7 – 4 Ma, attributed to the genera *Sahelanthropus*, *Orrorin* and *Ardipithecus*, 2) the appearance of the *Australopithecus* genus at ~ 4 Ma and of the robust *Paranthropus* genus ~ 2.7 Ma, 3) the appearance of the genus *Homo*

between 2.5 and 1.8 Ma and 4) the appearance of anatomically modern humans around 300 ka (Stern & Susman, 1983; Hopf et al., 1993; Leakey et al., 1995; Senut et al., 2001; Antón, 2003; Bramble & Lieberman, 2004; Haile-Selassie et al., 2004; White et al., 2009; Cerling et al., 2010; 2013; Roach et al., 2013; Maslin et al., 2014; Gibbons, 2017). These are summarised in Figure 3.1.

The notion that human evolutionary changes have been caused by extrinsic forces, which in this case are changes in their surrounding environment, is one that has received much attention (Vrba, 1985; deMenocal, 1995; Potts, 1996; 1998; 2013; Trauth et al., 2005; 2010; Maslin et al., 2014). A number of hypotheses have been proposed to explain this relationship; the most prominent of these include: 1) the turnover-pulse hypothesis (Vrba, 1985), 2) the aridity hypothesis (deMenocal, 1995), 3) the deep-lakes hypothesis (Trauth et al., 2005; 2010), 4) the variability selection hypothesis (Potts, 1996; 1998; 2013), and 5) the pulsed variability hypothesis (Maslin et al., 2014). These are summarised in Table 3.1: The differing hypotheses linking hominin evolution to palaeoenvironmental change in East Africa. An explanation for each theory is given as well as the authors that have proposed them; a more detailed review of each of the hypotheses is provided by Maslin et al. (2014).

An environmental theory of hominin evolution not discussed above is that of the savannah hypothesis (Lewin and Foley, 2004; Maslin et al., 2014). This suggests that with the reduction in tree cover and the emergence of savannahs, hominins were forced to descend from the trees of their preferential wooded habitats and adapt to life on the savannah (Lewin and Foley, 2004; Bender et al., 2012; Maslin et al., 2014). The primary adaptation associated with this is the emergence of bipedalism (Lewin and Foley, 2004). This theory later developed into the aridity hypothesis (discussed above), in which the long-term trend towards aridity and the expansion of the savannah associated with this was the major driver hominin evolution (deMenocal, 1995; 2004; Reed, 1997; Maslin et al., 2014). Moreover, the savannah hypothesis has been challenged since the discovery of *Orrorin*, which displays features suggesting that it was a part time tree-dweller, but was also bipedal when on the ground prior to the expansion of open savannah environments (Senut et al., 2018).
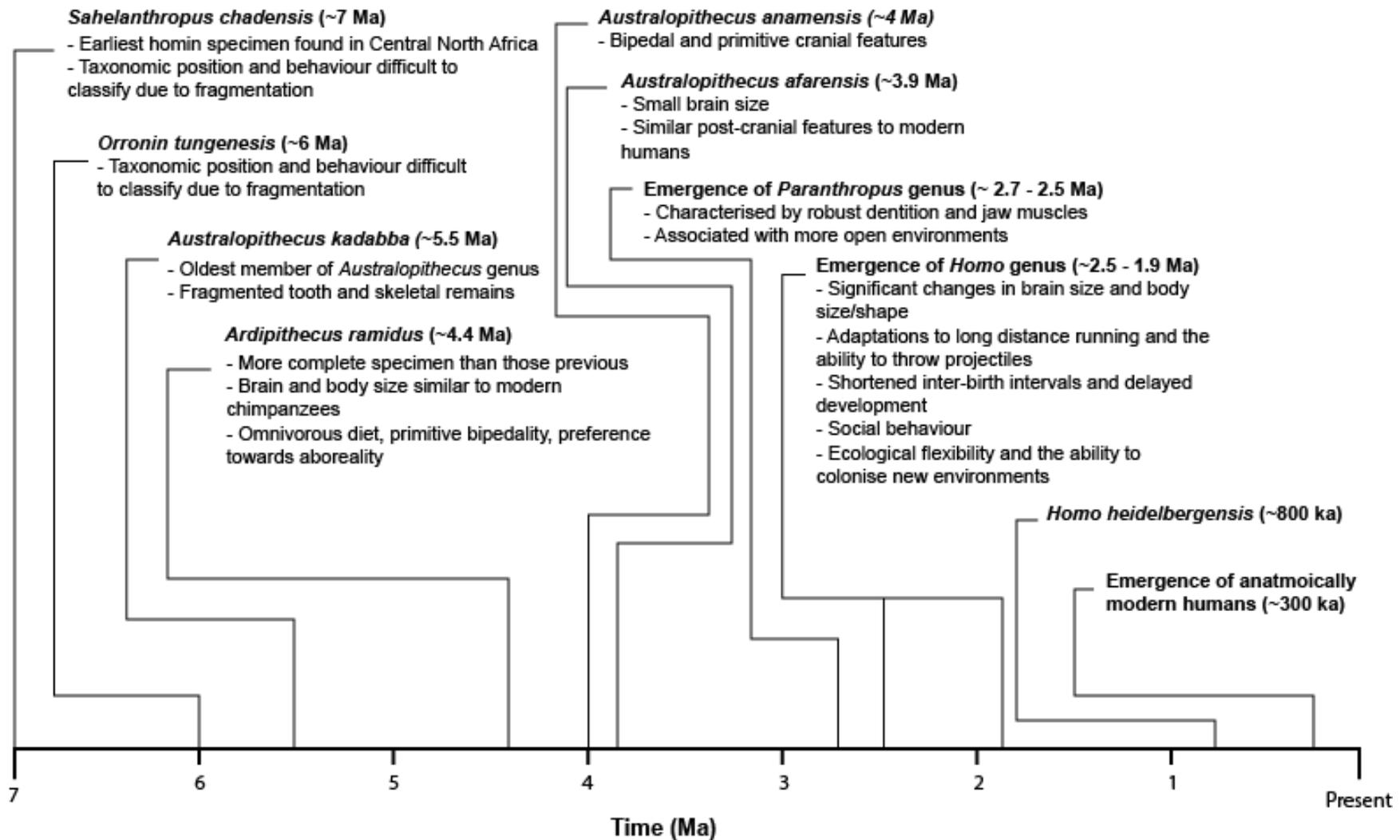
Figure 3.1:Timeline of significant developments in human evolution throughout East Africa (Stern & Susman, 1983; Hopf et al., 1993; Leakey et al., 1995; Senut et al., 2001; Antón, 2003; Bramble & Lieberman, 2004; Haile-Selassie et al., 2004; White et al., 2009; Cerling et al., 2010; 2013; Roach et al., 2013; Maslin et al., 2014)

Table 3.1: The differing hypotheses linking hominin evolution to palaeoenvironmental change in East Africa. An explanation for each theory is given as well as the authors that have proposed them

Hypothesis	Theory	Sources
Turnover-Pulse	The idea that global cooling between 2.8 – 2.4 Ma had a significant influence on habitat change across Africa. This coincides with the emergence of *Homo*, *Paranthropus*, stone toolmaking, and other African mammalian evolutionary changes (eg. speciation pulse in bovids). The hypothesis refers to a concentration of speciation and extinction events within a narrow temporal window, forced primarily by changes in the environment.	Vrba, 1985
Aridity	Progressive aridity across Africa initiated grassland expansion and the novel adaptations associated with these environments. Fragmentation of pre-existing habitats also promoted directional selection and population vicariance, which in turn resulted in speciation.	deMenocal, 1995; 2004
Deep-Lakes	Occurrence of deep expansive lakes during major humid periods, more specifically at 2.7 – 2.5 Ma, 1.9 – 1.7 Ma and 1.1 – 0.9 Ma, within which key events in hominin evolution took place. The periodic formation of these lakes is thought to have been precessionally-driven, causing the dispersal of hominins, which resulted in speciation and adaptive changes, as well as an increase in cranial capacity.	Trauth et al., 2007; 2010
Variability	Environment instability resulted in its temporal and spatial variability, consequently shaping the adaptations observed in hominins and other biota. This is because adaptable behavioural and morphological mechanisms may have been selected for during periods of extreme environmental variability, explaining how organisms developed the capacity to adjust to novel habitats that were introduced as a result of environmental variability or population dispersal.	Potts, 1996; 1998; 2013
Pulsed Climate	Hypothesis that the long term drying trend observed in East Africa was punctuated by periods of extreme climate variability, much like a combination of the variability selection hypothesis and the aridity hypothesis. During these periods, large deep lakes appeared and disappeared, with their fluctuations controlled by precessional forcing. It is during these periods that evolutionary change is suggested to occur, including speciation and dispersal events.	Maslin & Trauth, 2009

It has also been hypothesised that active tectonics have been a key driving factor in hominin evolution (King and Bailey, 2004). With the EARS being one of the largest and most consistently active tectonic structures in the world, as well as being the home to some of the most extensive fossiliferous and archaeological material associated with hominin evolution, a relationship between the two has been subject to closer investigation (King and Bailey, 2004). It is suggested that active tectonics created topographically complex landscapes which allowed hominins to seek refuge or gain tactical advantages against predators or prey in largely open environments, where they would otherwise be considered as relatively defenceless species (King and Bailey, 2004). Moreover, active tectonics shaped widely variable landscapes, and so it is proposed that these differing environments encouraged the development of adaptational behaviors and potentially speciation (King and Bailey, 2004). Tectonic activity is widely considered to be one of the primary drivers of environmental change throughout East Africa and is discussed later in section 3.4.1..

3.3. Palaeoenvironmental records throughout East Africa (Miocene – Pleistocene)

Extensive research has been carried out to provide detailed palaeoenvironmental evidence from hominin occupation areas (Table 3.2). Although lacking in spatial extent, the number of such palaeoenvironmental records is increasing (Maslin et al., 2014). Some of the most detailed palaeoenvironmental records are from Omo-Turkana, Olduvai Gorge, Laetoli, Hadar, Olorgesaillie and the Homa Peninsula (Table 3.2 and references therein). East African palaeoenvironment change from the Miocene to Pleistocene is extremely complex, undergoing changes in characteristic environments, vegetation structure and climate (Table 3.2). This will be discussed in this section, as well as the methods of palaeoenvironmental reconstruction utilised at different geological formations.

3.3.1. Palaeoenvironmental interpretations

Table 3.2 shows that the most common environment of deposition amongst sites is generally represented by alternating phases of both lacustrine and fluvial deposition in floodplain and marginal lacustrine environments. Alluvial deposition is also apparent in some formations (Mursi fm., Nachukui fm., Kanjera South fm.), although

this is less frequent than other modes of deposition. Variations in these environments are most likely owed to the extreme climate variability experienced in East Africa throughout the Plio-Pleistocene, which is observed in isotopic and lipid biomarker records (Cerling & Hay, 1986; Cerling et al., 1988; Wynn, 2004; Levin et al., 2004; 2011; Sikes & Ashley, 2007; Cerling et al., 2011a; Magill et al., 2013a; 2013b), pollen records (Bonnefille, 1976; 1984; 2010; Bonnefille & Dechamps, 1983; Bonnefille & Riollet, 1987) and other sources (Bamford, 2005; 2011b; 2011a; 2012; Owen et al., 2008; 2009; Andrews & Bamford, 2008; Deocampo et al., 2009; Deocampo & Tactikos, 2010; Rossouw & Scott, 2011; Albert et al., 2015;).

Lake level fluctuations are also apparent in many formations, indicating frequent transgressions and regressions, further highlighting the variability in wet/dry phases experienced throughout the Plio-Pleistocene (Brown & Feibel, 1991; Hay & Kyser, 2001; Ashley, 2007; Lepre et al., 2007; Campisano & Feibel, 2008; Deocampo et al., 2009; Magill et al., 2013b; Ashley et al., 2014a). Some of the most noticeable lake level fluctuations are recorded between 1.9 and 1.7 Ma at Koobi Fora (Brown & Feibel, 1991; Lepre et al., 2007) and Olduvai Gorge, with those at Olduvai being attributed to precessional forcing (Hay & Kyser, 2001; Ashley, 2007; Deocampo et al., 2009; Magill et al., 2013b; Ashley et al., 2014a). However, tectonics also possess the ability to impact lake conditions through the alteration of wider catchment and drainage networks, as well as lake morphology (Bergner et al., 2009; Trauth et al., 2010; Olaka et al., 2010; Feibel, 2011; Maslin et al., 2014).

Vegetation structure among the formations appears to generally follow a mosaic type environment dominated by wooded grasslands or grassy woodlands, before having an overall increase in the abundance of grasslands as time goes on, particularly C_4 grasslands (Table 3.2). This most likely relates to the progressive aridification experienced throughout the Plio-Pleistocene of East Africa (deMenocal, 1995; 2004). This aridification could be linked to the expansion of C_4 grasslands, leading environments to become gradually more open over time, as shown in these palaeoenvironmental records (Tipple & Pagani, 2007; Ségalen et al., 2007; Edwards et al., 2010).

Table 3.2: Significant locations containing geological formations (fm) that preserve hominin bearing sediments dating from the Miocene to the Pleistocene in East Africa. An overview of the palaeoenvironment interpreted at each formation is given, as well the methods used for palaeoenvironmental reconstruction

Location and associated fossils		Associated time period and palaeoenvironmental description	Methods	References
Omo-Turkana, Kenya/Ethiopia (*Australopithecus anemensis, Australopithecus afarensis, Paranthropus Boisei, Paranthropus aethiopicus, Homo habilis, Homo rudolfensis, Homo erectus, Kenyanthropus platyops*)	Nawata fm.	**Miocene:** Heterogeneous environments, including forest, woodland and grassland in proximity to a broad river, with conditions becoming more open about 6.5 Ma. No evidence of significant lake formation, only small shallow floodplain ponds.	Sedimentology; Fauna; Stable isotopes; Plant wax biomarkers; Plant Macrofossils; Pollen	Bonnefille, 1976; Brown et al., 1978; Bonnefille & Dechamps, 1983; Brown & Feibel, 1986; Howell et al., 1987; Cerling et al., 1988; 2003; 2011a; 2015; Feibel et al., 1989; Leakey et al., 1995; 1996; Wynn, 2000; 2004; Bobe & Eck, 2001; Bobe et al., 2002; 2007; Alemseged, 2003; Harris & Leakey, 2003; Feibel, 2003; Macho et al., 2003; Schoeninger et al., 2003; Bobe & Behrensmeyer, 2004; Gathogo & Brown, 2006; Hernández Fernández & Vrba, 2006; Manthi, 2006; Bobe, 2006; 2011; Lepre et al., 2007; Quinn et al., 2007; 2013; Gathogo et al., 2008; Harris et al., 2008; Bobe & Leakey, 2009; Levin et al., 2011;
	Kanapoi fm.	**Pliocene:** Mixture of woodlands and grasslands, but with a predominance of woodland (fauna). Complex mosaic of palaeoenvironments, but relatively dry and open (isotopes).		
	Mursi fm.	**Pliocene:** Prevalent closed woodlands and forests, although some indication of open dry grasslands. Potentially ecotonal environments at the edges of woodlands and grasslands. Deposition in deltaic and alluvial settings.		
	Usno fm.	**Pliocene:** Woodlands/ecotonal environments at the edges of woodlands and grasslands. Close to water.		
	Shungura fm.	**Pliocene:** Alternating lacustrine and fluvial depositional environments. Mosaic of forest, woodland and grassland in varying proportions. Closed wet system. **Pleistocene:** Fluvial deposition with the exception of a large lake phase at ~ 2.1 Ma. Mosaic of forest, woodland and grassland in varying proportions. An increase in grassland presence, although not significantly until after 2 Ma. Still more wooded than other areas of the Turkana basin.		
	Koobi Fora fm.	**Pliocene:** Alternating lacustrine and fluvial phases. Mosaic woodlands along large river, with open savanna at the basin margins and uplands. Gallery forest, floodplain grasslands and dry marginal bushland. Evidence for seasonal fluctuations in moisture.		

		Pleistocene: Closed lacustrine system with deep lake which shifts to a large, open meandering river system with streams and ponds. Expansion of large subaerial floodplain landscapes suitable for grassland expansion. Grassland expansion between 2 and 1.75 Ma, coincident with shift to fluvial system.		Drapeau et al., 2014; Barr, 2015; Plummer et al., 2015; Uno et al., 2016b; Bamford, 2017; Manthi et al., 2017; Plummer & Finestone, 2017; Field, 2020
	Nachukui fm.	**Pliocene:** Woodlands with patches of grassland. Dry conditions. Primarily mixed C3/C4 ecosystems, with an increase in grasses towards the end of the Pliocene. **Pleistocene:** Slight decrease in the proportion of woodland to open grassland, with C4 vegetation now dominating the ecosystem. Riparian woodland present. Deposition under fluvial and alluvial conditions, with some periods of lacustrine deposition.		
Olduvai Gorge, Tanzania (*Paranthropus boisei, Homo habilis, Homo rudolfensis, Homo erectus*)		**Pleistocene:** Fluvio-lacustrine deposition, contemporaneous volcanism and faulting. Generally a tropical semi-arid setting, mainly centred around a palaeolake. Several climate fluctuations between wet and cooler conditions and arid and hot conditions, generally trending towards aridity. Mosaic microenvironments and palaeoecology. Freshwater availability through springs and wetland systems fed by groundwater. Fluctuations between abundant grasslands with shrubs and fruit baring trees to dense forests.	Geochemistry; Stable isotopes; Phytoliths; Pollen; Fauna; Sedimentology; Plant wax biomarkers; Total organic carbon; Plant macrofossils	Cerling & Hay, 1986; Fernandez-Jalvo et al., 1998; Ashley & Driese, 2000; Hay & Kyser, 2001; Liutkus & Ashley, 2003; Liutkus et al., 2005; Bamford, 2005; Albert et al., 2006; 2015; Bamford et al., 2008; Deocampo et al., 2009; Ashley et al., 2009; 2010a; 2010b; 2014a; 2014b; Barboni et al., 2010; Bennett et al., 2012; Magill et al., 2013a; 2013b

Site	Environment	Proxies	References
Laetoli, Ethiopia (*Australopithecus afarensis, Paranthropus aethiopicus, Homo sapiens*)	**Pliocene:** Wood dominated vegetation, shifting to mosaic wooded habitats with C3 grasses, gradually trending to more bushland, before shifting to wooded grasslands with C4 grasses. Mainly riparian/gallery woodland with grassland. Gradual trend towards a more arid and open environment. Fluvial environment with some lacustrine deposition.	Phytoliths; Fauna; Stable isotopes; Plant macrofossils; Pollen; Sedimentology/Geology	Bonnefille & Riollet, 1987; Cerling, 1992; Foster et al., 1997; Barboni & Bremond, 2009; Bishop et al., 2011; Kingston, 2011; Kovarovic & Andrews, 2011; Reed & Denys, 2011; Rossouw & Scott, 2011; Su & Harrison, 2015; Su, 2011; Bamford, 2011a; 2011b; Barboni, 2014; Harrison, 2017
Hadar (*Australopithecus afarensis*)	**Pliocene:** Dry gallery woodland close to a stream with mosaic savanna vegetation – grassy woodland. Deposition across an extensive floodplain near to an ancestral river and palaeo-lake, but also periods of fluvial and lacustrine deposition. Predominantly C3 plants (mainly trees) with some C4 grasses.	Pollen; Sedimentology; Fauna; Geochemistry; Stable isotopes	Taieb et al., 1972; Bonnefille et al., 1987; 2004; Radosevich et al., 1992; Hailemichael, 2001; Hailemichael et al., 2002; Levin et al., 2004; Quade et al., 2004; Wynn et al., 2008; Campisano & Feibel, 2008; Reed, 2008; Aronson et al., 2008; Bedaso, 2011; Reed & Geraads, 2012; Johanson, 2017
Olorgesaillie, Kenya (*Homo erectus*)	**Pleistocene:** Predominantly C4 grassland with some wooded grassland. Close proximity to a shallow freshwater lake with some phases of fluvial deposition. Cooler and moister than semi-arid climate today.	Stable isotopes; Phytoliths; Diatoms; Sedimentology; Fungal spores; Geochemistry; Plant wax biomarkers; Charcoal; Fauna	Potts, 1998; 2016; Sikes et al., 1997; 1999; Potts et al., 1999; Owen et al., 2009; 2011; 2014; Kinyanjui, 2012; Lee et al., 2013

Homa Peninsula, Kenya

(*Homo*) | Kanam fm. | **Miocene:** Diverse spatially mosaic environment, fluctuating between closed and open environments. Sediments most likely deposited in a lacustrine/marginal lacustrine environment. | Fauna; Stable isotopes; Sedimentology; Geochemistry | Boswell, 1935; Kent, 1942; Plummer & Potts, 1989; Behrensmeyer et al., 1995; Potts et al., 1997; Potts, 1998; Ditchfield et al., 1999; Plummer et al., 1999; 2009b; 2009a; Bishop et al., 2006; Plummer & Bishop, 2016 |
| | Kanjera South fm. | **Pleistocene:** Deposition on an alluvial plain at the margin of a lake basin. Rapid deposition occurring in the form of hyperconcentrated flows. Lightly wooded to open grassland habitat. | | |
| | Kanjera North fm. | **Pleistocene:** Deposition included transitions between fluvial, lacustrine and mudflat environments. | | |

3.3.2. Reconstructive techniques

Multi-proxy approaches appear to be essential to palaeoenvironmental reconstructions (Table 3.2). Sedimentological/geological analyses, isotopic analyses and analyses of faunal remains appear to be among the most frequently used palaeoenvironmental indicators. The use of a suite of palaeoenvironmental indicators improves the accuracy and clarity of palaeoenvironmental reconstructions, in addition to their robustness (Cerling et al., 2010; White et al., 2010; Kinyanjui, 2012; Turner et al., 2014).

Geological formations are first analysed in terms of their sedimentology/geology to develop a facies model, which divides sediments into different lithofacies based on their primary depositional attributes, including bedding, grain size, texture and sedimentary structures (e.g. Hay, 1976; Harris et al., 1988; Behrensmeyer et al., 1995; Ditchfield et al., 1999; Liutkus & Ashley, 2003). Broadly defined lithofacies are utilised to trace stratigraphic units across a site and constrain sampling for more detailed analyses; interpretations are also made on the depositional environment of sediments based on the characteristics of each lithofacies (Hay, 1976; Brown & Feibel, 1986; 1991; Potts, 1989; Behrensmeyer et al., 1995; Campisano & Feibel, 2008; Wynn et al., 2008; Ditchfield & Harrison, 2011; Campisano, 2012). More detailed facies models at the centimetre scale have also been constructed to correlate sediment dynamics to climatic fluctuations and lake transgressions and regressions; this is often performed on continuous sedimentary records, such as the cores taken at Olduvai Gorge (Ashley, 2007; Blumenschine et al., 2012; Stanistreet, 2012).

Palaeovegetation structure in the studied formations are most frequently interpreted using $\delta^{13}C$ isotopes of pedogenic carbonates/palaeosols and fossil tooth enamel, fossil fauna, and pollen (Table 3.2). This provides independent records of the vegetation structure, allowing for more robust and detailed interpretations to be made (Cerling et al., 2010; White et al., 2010; Kinyanjui, 2012; Turner et al., 2014). Stable carbon isotopes provide information on the distribution of C_3 (common in cooler, wetter climates) to C_4 (common in hotter, dryer climates) vegetation (e.g. Levin et al., 2004; Wynn, 2004; Quinn et al., 2007; Sikes & Ashley, 2007; Cerling et al., 2011c). However, caution should be taken in the interpretation of $\delta^{13}C$ records,

as $_\delta$¹³C values may increase as palaeosols mature (Bennett et al., 2012). Fossil fauna can be linked to vegetation based on their dietary preferences and habitats (e.g. Fernandez-Jalvo et al., 1998; Bobe, 2011; Bishop et al., 2011; Drapeau et al., 2014; Plummer et al., 2015). Pollen provides more detailed information on the palaeovegetation structure than both isotopic and faunal analyses, revealing information on plant type/species and spatial distribution; pollen is not always preserved in sediments however (Bonnefille, 1976; 1984; Bonnefille & Dechamps, 1983).

Plant wax biomarker analysis is utilised at both Olduvai Gorge and at the Nachukui formation in the Omo-Turkana basin to provide more detailed insights into palaeovegetation structure. At Olduvai Gorge, it enabled the identification of significant ecosystem variability, with fluctuations in vegetation structure coinciding with precession length cycles (Magill et al., 2013a). Similarly, at the Nachukui formation its use highlighted that C₄ vegetation was present in a higher abundance throughout the Pleistocene than indicated by isotopic analysis (Uno et al., 2016b). Notably, analyses of plant wax biomarkers and total organic carbon allowed the identification of significant ecosystem variability at Olduvai Gorge during the Pleistocene, with fluctuations in vegetation structure coinciding with precession length cycles (Magill et al., 2013a); temporal variations in precipitation were also identified (Magill et al., 2013b).

Phytoliths allow more detailed interpretations to be made on the palaeovegetation in terms of plant type/species and spatial distribution, similar to pollen (Bamford et al., 2006; Kinyanjui, 2012; Barboni, 2014; Albert et al., 2015). Their use at Olorgesaillie (Kinyanjui, 2012), Olduvai Gorge (Bamford et al., 2006; 2008; Albert et al., 2006; 2015; Barboni et al., 2010), and Laetoli (Rossouw & Scott, 2011) highlight this, where they support interpretations made from isotopes and fauna, whilst also revealing additional detail on palaeoclimatic dynamics and palaeovegetation structure. Phytoliths are also well preserved in oxidised environments, and so are often present in dry environments where pollen may be absent (Piperno, 2006; Kinyanjui, 2012). Information can also be provided beyond family level on grasses, which is more accurate than that of grass pollen (Twiss et al., 1969; Mulholland & Rapp, 1992; Piperno & Pearsall, 1998; Mercader et al., 2010; Kinyanjui, 2012).

However, their analysis suffers from issues in multiplicity (a given taxon produces multiple phytoliths) and redundancy (a given phytolith may be produced by many taxa), which can produce a biased record of the palaeovegetation (Barboni & Bremond, 2009; Mercader et al., 2009; Albert et al., 2015).

Plant macrofossils are also utilised to reconstruct palaeovegetation in several of the geological formations (Albert et al., 2006; 2015; Bamford et al., 2006; Andrews & Bamford, 2008; Bamford, 2012; 2017). They provide robust independent records of palaeovegetation on a local scale; this is particularly advantageous, as pollen and phytolith provide more regional records (Bamford, 2012).

$\delta^{18}O$ isotopes are utilised in many of the formations and provide a record of palaeoclimate dynamics (Cerling & Hay, 1986; Sikes et al., 1999; Cerling et al., 2003; 2011a; Wynn, 2004; Quinn et al., 2007; Sikes & Ashley, 2007; Levin et al., 2011; Bennett et al., 2012). In the Hadar formation, $\delta^{18}O$ analysis revealed that the palaeoenvironment underwent gradual aridification throughout the Pliocene, yet still experienced high climate variability within this time (Levin et al., 2004; Quade et al., 2004; Aronson et al., 2008; Bedaso, 2011). This is further highlighted by palynological evidence here, which depicts high climate variability and an array of habitats (Bonnefille et al., 1987; 2004). A similar trend can also be observed from $\delta^{18}O$ analysis of sediments from Olduvai Gorge, where the palaeoclimate gradually became more arid throughout the Pleistocene (Cerling & Hay, 1986; Cerling et al., 1988; Sikes & Ashley, 2007). To contrast this, $\delta^{18}O$ values from Olorgesaillie demonstrate that environment was moister than the modern landscape, indicating that it had the capability to support more C_3 vegetation than today (Sikes et al., 1999). Caution has however been drawn to the interpretation of $\delta^{18}O$ records; the mixture of meteoric waters with lacustrine saline brines can skew $\delta^{18}O$ values, potentially giving a false representation of palaeoclimate dynamics (Bennett et al., 2012).

Other methods less frequently used for palaeoenvironmental reconstructions include geochemical analysis of clays, which enables the identification of freshwater in palaeoenvironments (Deocampo et al., 2009; Deocampo & Tactikos, 2010; Deocampo et al., 2010; Owen et al., 2011; Lee et al., 2013). Analyses of diatomaceous sediments have also aided the identification of wetland systems, as

well as both saline and freshwater lakes (Liutkus & Ashley, 2003; Owen et al., 2008; 2009; 2011; 2014; Lee et al., 2013; Albert et al., 2015).

It should be highlighted that although the use of multi-proxy approaches often increases the robustness of palaeoenvironmental reconstructions, interpretations between different proxy records should be taken with caution. Proxy records from different sources may produce contradictory results due to issues such as preservation, response time and sensitivity (Moore et al., 1991; Barboni & Bremond, 2009; Mercader et al., 2009; Mather et al., 2011; Albert et al., 2015; Vrydaghs et al., 2016). For example, pollen has been shown to have high taxonomic value in palaeoenvironmental reconstructions, but can suffer from issues such as preservation, causing some species to become under-represented in the palaeoenvironmental record (Moore et al., 1991; Dunseth et al., 2019). When comparing this to phytolith proxy data, although a lower taxonomic resolution is obtained, phytoliths are more resilient to post-depositional processes (Albert et al., 2015). To add to this, both of these proxy sources have issues with multiplicity and redundancy, as some plants produce more/less pollen/phytoliths than other, causing them to become over/under-represented in the palaeoenvironmental record (Moore et al., 1991; Barboni & Bremond, 2009; Mercader et al., 2009; Albert et al., 2015; Vrydaghs et al., 2016). Factors such as these must be taken into account when interpreting proxy data from multiple sources.

3.3.3. Chronological control

Chronological control has received much attention at each of the sites (Deino & Potts, 1992; Ditchfield et al., 1999; Campisano, 2007; Deino, 2011; 2012; Brown & McDougall, 2011). A well-constrained and robust chronology is essential in palaeoenvironmental reconstructions to determine the timing of changes that may influence evolutionary events, but also for the cross-comparison of palaeoenvironmental records (Barham et al., 2011; Gibbon et al., 2014; Granger et al., 2015). High-resolution chronologies are also desirable to prevent temporal averaging of palaeoenvironmental change (Hopley & Maslin, 2010; Maslin et al., 2014). Sampling resolution is also responsible for this, but samples taken from long sedimentary sequences with little chronological control can result in fluctuations in the environment being overlooked, resultantly displaying an 'average' environment

for that time, rather than the true environment (Hopley & Maslin, 2010; Maslin et al., 2014).

Multiple dating methods are often used to establish a more reliable chronology (Barham et al., 2011; Gibbon et al., 2014; Turner et al., 2014; Granger et al., 2015). From the sites analysed here, the most frequently used techniques include radiometric dating of volcanic tuffs (Brown & McDougall, 2011; Deino, 2011; 2012), biostratigraphy (Ditchfield et al., 1999; Bishop et al., 2006), magnetostratigraphy (Ditchfield et al., 1999; Brown & McDougall, 2011; Deino, 2012) and tephrostratigraphy (Campisano, 2007; Brown & McDougall, 2011; Deino, 2012).

Radiometric dates (primarily $^{40}Ar/^{39}Ar$ dates) of tuffs and their correlations with other tuffs through tephrostratigraphy has been essential in developing robust timelines at the majority of the hominin baring regions, most notably the Omo-Turkana basin (Cerling et al., 1979; Brown & McDougall, 2011; Feibel, 2011). This has facilitated an accurate chronology to be established across spatially varying geological formations, providing a lengthy record of palaeoenvironmental change (Brown & McDougall, 2011).

Magnetostratigraphy is often used in conjunction with these techniques and provides an independent age control on the correlation of sequences; however, it cannot provide an absolute date like that of radiometric dating techniques (Ditchfield et al., 1999; Brown & McDougall, 2011; Deino, 2012). Biostratigraphy is used in a similar way, yet it can provide some idea on the age of sediments without the use of other dating techniques (Ditchfield et al., 1999; Bishop et al., 2006).

3.4. Drivers of palaeoenvironmental change and their impact on palaeoclimate

From the information discussed thus far, is evident that East African palaeoenvironments were extremely variable. Numerous authors have highlighted that environmental and climatic changes are the result of both major tectonic activity and orbital forcing.

3.4.1. Tectonic activity

Palaeoenvironmental change throughout East Africa was largely driven by the complex formation and development of the East African Rift System (EARS), which

involved substantial faulting and volcanism over an extended period (Crossley & Knight, 1981; Baker et al., 1988; Blisniuk & Strecker, 1990; Strecker et al., 1990; Foster et al., 1997; Ebinger et al., 2000; Trauth et al., 2007; Maslin & Christensen, 2007; Maslin et al., 2014; WoldeGabriel et al., 2016). Significant changes in vegetation structure, climate and topography were triggered by this (Baker et al., 1988; Strecker et al., 1990; Sepulchre et al., 2006; Maslin & Christensen, 2007; Trauth et al., 2007; 2010; Bergner et al., 2009; Olaka et al., 2010; Borchardt & Trauth, 2012; Prömmel et al., 2013; Maslin et al., 2014).

Uplift during the Plio-Pleistocene transformed relatively flat topography throughout the EARS into mountainous terrain, creating an orographic barrier that resulted in reduced moisture availability and aridification in East Africa (deMenocal, 2004; Sepulchre et al., 2006; Maslin & Christensen, 2007; Prömmel et al., 2013; Maslin et al., 2014). A progressive shift from C_3 to C_4 vegetation occurred in response to this which had significant impacts on biota throughout the Plio-Pleistocene (Wynn, 2004; Levin et al., 2004; Feakins et al., 2005; Quinn et al., 2007; Sikes & Ashley, 2007; Harris et al., 2008; Plummer et al., 2009b; Brachert et al., 2010; Cerling et al., 2011a; Maslin et al., 2014; Uno et al., 2016b); these changes can be observed in the environmental records previously discussed (Table 3.2).

Drainage throughout the EARS was also significantly influenced by tectonic activity. Basins suitable for lake formation were created throughout the EARS through the development of graben morphologies, although faulting also destroyed basins over long periods (~ 100 kyrs) of time (Baker et al., 1988; Strecker et al., 1990; Trauth et al., 2010). Faulting also caused the alteration of catchments and drainage networks, as well as the morphology of lake basins through downwarping, drainage reversal and ponding (Baker et al., 1988; Strecker et al., 1990; Rach, 1992; Trauth et al., 2010; Maslin et al., 2014). This may have affected lake conditions over shorter periods of time, as well as their sensitivity to precipitation and evaporation (Bergner et al., 2009; Trauth et al., 2010; Olaka et al., 2010; Feibel, 2011; Maslin et al., 2014).

Although it is clear that tectonic activity had a significant impact on East African palaeoenvironment, ambiguity still surrounds the full extent of this (Maslin et al., 2014). A limited understanding of the timing, altitude and rate of uplift throughout the EARS is partially responsible for this, as these factors control local precipitation

and are consequently essential to climate evolution (Spiegel et al., 2007; Pik et al., 2008; Wichura et al., 2010; Maslin et al., 2014). Additionally, records of palaeovegetation primarily come from hominin sites that are spatially limited in terms of the wider environment, and may also be subject to time-averaging over long sequences (Hopley & Maslin, 2010). This makes it difficult to fully understand the spatial and temporal impact tectonics had on palaeovegetation (Maslin et al., 2014).

3.4.2. Orbital forcing

Orbital forcing is largely responsible for the occurrence of glacial and interglacial periods throughout the Quaternary, either directly or indirectly, through eccentricity, obliquity and precession cycles (Maslin & Christensen, 2007; Maslin et al., 2014). In East Africa, precession cycles largely influenced moisture availability and seasonality prior to and throughout the Miocene to the Pleistocene (deMenocal, 1995; Teaford & Ungar, 2000; Bobe & Eck, 2001; Trauth et al., 2003; Clement et al., 2004; Reed & Fish, 2005; Denison et al., 2005; Deino et al., 2006; Hopley et al., 2007; Kingston, 2007; Lepre et al., 2007; Wilson, 2011; Joordens et al., 2011; Magill et al., 2013b; Ashley et al., 2014a; Maslin et al., 2014).

Supporting evidence for the impact of precession forcing on East African climate and moisture availability is increasing. Fluviolacustrine sediments and diatomites at the Baringo-Bogoria basin (central Kenya rift valley) record the occurrence of wet/dry periods at precession intervals (23 Kyrs) between 2.7 – 2.55 Ma (Deino et al., 2006; Kingston, 2007; Wilson, 2011; Kinyanjui, 2012; Wilson et al., 2014). Similarly, lithological investigations show that lake-level change consistent with timescales of precession or obliquity in the Turkana basin at Koobi Fora occurred between 1.9 – 1.6 Ma (Lepre et al., 2007). Evidence from lithological investigations and analysis of strontium isotope ratios of lacustrine fish fossils at Karari Ridge, Turkana basin, demonstrated that wet/dry periods and monsoon intensity were also influenced by precession between 2 – 1.85 Ma (Joordens et al., 2011). At Olduvai Gorge, episodes of lake expansion and contraction were also recorded within the lithostratigraphy, coinciding with precession intervals between 1.84 – 1.74 Ma (Ashley & Driese, 2000; Ashley, 2007;). Rainfall was shown to increase by a third between the dry and wet portion of each precession cycle (Ashley, 2007). Stable carbon isotopic signatures of lipid biomarkers from ancient plants here also

correlated strongly with precession cycles (Magill et al., 2013a). Similar cycles were recorded more recently (1.1 and 0.9 Ma) in the diatomaceous lacustrine sediment at the Olorgesailie basin (Trauth et al., 2007; Owen et al., 2008; Potts, 2013).

Orbital forcing also has an indirect influence on East African climate. High-latitude orbital forcing impacts glacial-interglacial cycles, which consequently effects East African climate due to changes in: Pole-Equator temperature gradients; sea surface temperatures; wind strength and direction; atmospheric carbon dioxide, methane and water vapour content (Maslin et al., 2014). The effects of these cycles are reflected by the sensitivity of African palaeovegetation throughout the Quaternary, in which changes in atmospheric CO_2 and regional temperatures resulted in rapid shifts in pollen assemblage indices (Lezine, 1991; Bonnefille & Mohammed, 1994; Elenga et al., 1994), charcoal fluxes (Verardo & Ruddiman, 1996), and the ratio of C_3 to C_4 biomarkers (Huang et al., 1999; Ficken et al., 2002; Schefuß et al., 2005). The interaction of glacial-interglacial cycles with high and low latitude orbital forcing, as well as the insolation maxima and minima make this increasingly complex; resultantly, tropical African climate could respond to orbital forcing at both 11.5 kyrs and 5 kyrs intervals, not just at 23 kyrs precession intervals (Trauth et al., 2003; Berger et al., 2006; Verschuren et al., 2009; Maslin et al., 2014).

3.4.3. Other global climate transitions

Aside from tectonic activity and orbital forcing, several significant climatic events occurred through the Miocene to Pleistocene which influenced the palaeoenvironment of East Africa in a number of ways (Table 3.3); these are briefly discussed here.

C_4 grasslands have had a significant impact on vegetation structure globally (Tipple & Pagani, 2007; Ségalen et al., 2007; Brown et al., 2011). In East Africa, forests reduced in size and more open landscapes became increasingly common, evidenced in a wide range of proxies (Sikes et al., 1999; Potts et al., 1999; Bobe et al., 2002; 2007; Cerling et al., 2003; 2011a; 2015; Bobe & Leakey, 2009; Bobe, 2011; Rossouw & Scott, 2011; Kinyanjui, 2012). The faunal community responded to this with large-scale evolutionary changes. Included within this are anatomical and behavioural changes in hominins, whom adapted to more arid and open

environments facilitated by C$_4$ grasslands throughout the Plio-Pleistocene (Plummer et al., 2009a; 2009b).

Aside from weak precipitation changes in East Africa evidenced by climate modelling studies, little is known about the effects of the tectonic closure of the Strait of Gibraltar across East Africa (Murphy et al., 2009; Schneck et al., 2010).

The intensification of the northern hemisphere glaciation (iNHG) may be responsible for changes in African climate from 2.7 Ma onwards. Regional aridity is one postulated response, evidenced by a large increase in the amount of dust leaving the Sahara and Arabia (deMenocal, 1995; 2004); however, this has been debated, as oxygen isotope values show significant transitions at the same time as the iNHG, rather than following it (Trauth et al., 2009). In addition to this, large lakes in the Baringo-Bogoria Basin (Deino et al., 2006; Kingston, 2007), and on the eastern shoulder of the Ethiopian Rift and in the Afar Basin (Williams et al., 1979; Bonnefille, 1983), are thought to have gone through cycles of growth and decline between 2.7 and 2.5 Ma; this is indicative of a highly variable climate regime (Maslin et al., 2014).

Numerous changes in the tropics coincide with a potential change in the Walker circulation at around 1.9 Ma. Despite there being a gradual tend towards more open environments after 3 Ma, it was following 2 Ma that the open, grassy landscapes started to occur in higher abundance, evidenced by δ^{13}C/^{12}C ratios from fossil mammals (Lee-Thorp et al., 2007). Terrestrial dust records from the Arabian Sea (deMenocal, 1995; 2004), the eastern Mediterranean Sea (Larrasoaña et al., 2003), and off subtropical West Africa (Tiedemann et al., 1994) also indicate increased aridity and variability subsequent to 1.9 – 1.5 Ma (Trauth et al., 2009). During this time, evidence for the presence of large, deep and fluctuating lakes also exists in East Africa (Trauth et al., 2005; 2007). In addition to this, the DWC has been suggested to alter the properties of the El Niño-South Oscillation, consequently impacting the Indian Ocean Dipole — the primary cause of modern day interannual variability in precipitation in Africa (Saji et al., 1999); this may have influenced East Africa in a similar way throughout the Plio-Pleistocene (Maslin et al., 2014).

Table 3.3: Significant climatic events occurring through the Miocene to Pleistocene that may have impact East African palaeoenvironment. Each event is explained briefly, as well as the effect each of them may have on East African climate

Event	Explanation	Effect on East African climate	Sources
C₄ Grassland emergence and expansion	Carbon dioxide threshold breached ~ 30 Ma; C$_4$ photosynthetic pathway in plants developed as a response, including C$_4$ grasses	C$_4$ grass dominated biomes had major impact on continental biota. In Africa, forests reduced in size and expansive grasslands became more common	Tipple & Pagani, 2007; Ségalen et al., 2007; Plummer et al., 2009a; Edwards et al., 2010; Brown et al., 2011; Cerling et al., 2013; Maslin et al., 2014
Tectonic closure of the Strait of Gibraltar	Mediterranean Sea isolated from Atlantic Ocean ay ~ 5.59 Ma, resulting in its desiccation and the removal of ~ 6% of dissolved salts, significantly altering the alkalinity. Normal conditions re-established at ~ 5.33 Ma	Weak precipitation changes, little known about any further effects	Hsü et al., 1973; Krijgsman et al., 1999; Bickert et al., 2004; Roveri et al., 2008; Murphy et al., 2009; Schneck et al., 2010; Maslin et al., 2014
Intensification of the Northern Hemisphere Glaciation (iNHG)	Glaciation in Northern Hemisphere intensified dramatically between 2.75 Ma and 2.54 Ma, characterised by repeated advances and retreats of ice sheets (glacial-interglacial cycles)	Variable climate regime and an increase in regional aridity from ~ 2.7 Ma	Keigwin, 1978; 1982; Keller et al., 1989; Ruddiman et al., 1988; Mann & Corrigan, 1990; Raymo, 1991; 1994; Wright & Miller, 1996; Li et al., 1998; Haug & Tiedemann, 1998; Maslin et al., 1998; 2014; Crowley & Hyde, 2008; DeConto et al., 2008; Fedorov et al., 2013; Abe-Ouchi et al., 2013
Development of an intensified Walker Circulation (DWC)	Intensified Walker Circulation (east − west temperature gradient across tropical Pacific Ocean) developed in response to global cooling	Variable climate regime and increased aridity from ~ 2 Ma	deMenocal, 1995; 2004; Saji et al., 1999; Ravelo et al., 2004; McClymont & Rosell-Melé, 2005; Liu et al., 2008; Brierley et al., 2009; Trauth et al., 2009; Fedorov et al., 2013; Larrasoaña et al., 2013; Maslin et al., 2014
Early to Middle Pleistocene Transition (EMPT)	Transition in periodicity of glacial-interglacial cycles from 41 kyrs to a quasiperiodicity of ~ 100 kyrs. Increase in amplitude of global ice volume variations	Variable climate regime and increased aridity from ~ 1 Ma	Prell, 1984; Shackleton et al., 1988; Imbrie et al., 1992; Tiedemann et al., 1994; Berger & Jansen, 1994; Mudelsee & Stattegger, 1997; Maslin & Ridgwell, 2005; Trauth et al., 2005; 2007; Abe-Ouchi et al., 2013; Maslin et al., 2014

African climate had a significant response to the early – middle Pleistocene transition (EMPT). Although C_4 grasses were present throughout Africa, they remained a relatively minor component of the environment until the late Pliocene and early Pleistocene (Ségalen et al., 2007). Open ecosystems dominated by C_4 grass components emerged during the EMPT throughout East Africa, evidenced by pedogenic carbonate $\delta^{13}C$ data (Sikes et al., 1997; Cerling et al., 2011c; Levin et al., 2011). Additionally, large ephemeral lakes throughout East Africa may also have formed as result of the EMPT between 1.1 and 0.9 Ma, such as the Olorgesailie Formation, the Naivasha and Elemnteita-Nakuru basins, and the Afar Basin (Trauth et al., 2005; 2007).

3.5. Summary

Literature suggests that five primary hypotheses linking palaeoenvironmental change to hominin evolution exist. These include the: turnover-pulse, aridity, deep-lakes variability, and pulsed climate hypotheses. Other linkages have also been made between hominin evolution and the emergence and expansion of savannahs, as well as with tectonic activity and the variable environments that it created. After evaluating literature surrounding East African Palaeoenvironmental records from the Miocene to the Pleistocene, research most commonly reports the environment of deposition amongst sites as alternating phases of both lacustrine and fluvial deposition in floodplain and marginal lacustrine environments. Alluvial deposition is also apparent in some formations. Amongst these records, the most frequently used reconstructive techniques in include analyses of stratigraphy, $\delta^{13}C$ isotopes, plant wax biomarkers, phytoliths, plant macrofossils and $\delta^{18}O$ isotopes. Tectonic activity and orbital forcing have been identified as the primary driving mechanisms of palaeoenvironmental change, although global climate transitions including the expansion of C_4 grasslands, the tectonic closure of the Straight of Gibraltar, the EMPT, the iNHG and the EMPT have all had significant impacts on palaeoenvironmental change.

CHAPTER 4.   METHODS

4.1. Introduction

This chapter details the methods/proxies that will be used to reconstruct the palaeoenvironment of the Nyayanga and Sare River sites on the Homa Peninsula. Each method is reviewed in terms of its usefulness to palaeoenvironmental reconstructions and to this study. The methodological approach, including the laboratory technique and data analysis, is also detailed.

4.2. Geology/sedimentology

Investigations into the geology and sedimentology of palaeoenvironments are crucial to develop a framework for further analysis of sediments and often guide/constrain laboratory techniques (Hay, 1976; Hassan, 1979; Boggs, 1995; Vandenberghe, 2013; Miall, 2013; Paterson & Heslop, 2015b). As the environment plays a major role in the formation of sediments, sediments can act as a significant indicator of palaeoenvironmental conditions. Observations are made on colour, composition, sedimentary structures, size class, particle shape, roundness, grain orientation etc. (Hay, 1976; Hassan, 1978; Behrensmeyer et al., 1995; Ditchfield et al., 1999). This information is invaluable and is frequently used to develop and refine a facies model, which divides a sequence into different lithofacies.

Lithofacies are lithologically different yet deposited in environments that are closely related (Hay, 1976). Classification of lithofacies is based on their primary depositional attributes, which can include bedding, grain size, texture, and sedimentary structures (Miall, 2013). The scale of a lithofacies is dependent on the level of detail that its classification incorporates; broadly defined lithofacies are more suitable for tracing stratigraphic units across a site, whilst high levels of detail at the centimetre scale are more applicable to logging a sediment core (Miall, 2013). Lithofacies are then subject to further analysis in order to develop an interpretation of the geological history and environmental evolution; this can subsequently be mapped on a basin scale (Hay, 1976; Hassan, 1978; Liutkus & Ashley, 2003; Miall, 2013; Albert et al., 2015).

Prior to the lithofacies classification system introduced by Miall (1977), sediments were assigned to lithofacies based on a researchers own local classification system.

Resultantly, the identification of common depositional themes between sites were overlooked, as the lack of a standardised classification system between deposits obscured any similarities (Miall, 2013).

Miall's updated classification system (Table 4.1) has since become a standard field methodology when investigating fluvial deposits (e.g. Lepre, 2009; Maurin et al., 2017; Mtelela et al., 2017; Bordy et al., 2019; Saylor et al., 2019; Scardia et al., 2019). Despite this, critics suggest that important detail may be overlooked by assigning sediments to a predetermined lithofacies (Bridge, 1993). Additionally, assigning sediments to predetermined lithofacies can lead to the incorrect assumption that each facies has a unique interpretation (Bridge, 1993). However, Miall acknowledges that there may be differences to the 'standard' lithologies and highlights that the classification system should be used as a basis for field research, whilst researchers should be aware that refinements are always possible (Miall, 2013).

Figure 4.1: Photograph taken by Prof. Tom Plummer of the author collecting a sediment spot sample from Excavation 3 at Nyayanga using a stainless steel trowel

During field investigations on the Homa Peninsula, sediment spot samples were taken from geological trenches and excavations that were dug throughout each of the sites (Figure 4.1). When taking samples, the weathering profile was first removed from the face of the sequence, with the sample then being taken with a stainless-steel trowel. The classification system proposed by Miall (Table 4.1) was used to provide a basis for identifying lithofacies site wide and adhere to a standardised classification system (Miall, 2013). Observations were made on colour, composition, sedimentary structures and size class. A hand lens was also utilised to inspect carbonate nodules after their removal with a stainless steel trowel, whilst the presence of coalescing carbonates and carbonate horizons were also noted. Samples were taken from each of the lithofacies identified, as well as at laterally varying locations. Assessments of both the palaeo- and modern geomorphological profile of each of the sites were also made. Further architectural analysis was not completed due to lack of sediment exposure, as exposures were limited to geological trenches and excavations (Miall, 2013). Moreover, wider conglomeratic surveys identifying geological provenances surrounding the sites have previously been completed (Braun et al., 2008; Finestone, 2019) and were not carried out here.

Facies code	Facies	Sedimentary Structures	Interpretation
Gmm	Matrix-supported, massive gravel	Weak grading	Plastic debris flow (high strength, viscous)
Gmg	Matrix-supported gravel	Inverse to normal grading	Pseudoplastic debris flow (low strength, viscous)
Gci	Clast-supported gravel	Inverse grading	Clast-rich debris flow (high strength), or pseudoplastic debris flow (low strength)
Gcm	Clast-supported massive gravel	-	Pseduoplastic debris flow (inertial bedload, turbulent flow)
Gh	Clast-supported, crudely bedded gravel	Horizontal bedding, imbrication	Longitudinal bedforms, lag deposits, sieve deposits
Gt	Gravel, stratified	Trough cross-beds	Minor channel fills
Gp	Gravel, stratified	Planar cross-beds	Transverse bedforms, deltaic growths from older bar remnants
St	Sand, fine to very coarse, may be pebbly	Solitary or grouped trough cross-beds	Sinuous-crested and linguoid (3-D) dunes
Sp	Sand, fine to very coarse, may be pebbly	Solitary or grouped trough cross-beds	Transverse and linguoid bedforms (2-D dunes)
Sr	Sand, very fine to coarse	Ripple cross-lamination	Ripples (lower flow regime)
Sh	Sand, very fine to coarse, may be pebbly	Horizontal lamination parting or streaming lineation	Plane-bed flow (critical flow)
Sl	Sand, very fine to coarse, may be pebbly	Low-angle (<15°) cross-beds	Scour fills, humpback or washed-out dunes, antidunes
Ss	Sand, fine to coarse, may be pebbly	Broad, shallow scours	Scour fill
Sm	Sand, fine to coarse	Massive, or faint lamination	Sediment-gravity flow deposits
Fl	Sand, silt, mud	Fine lamination, very small ripples	Overbank, abandoned channel, or washed-out dunes, antidunes
Fsm	Silt, mud	Massive	Backswamp or abandoned channel, or waning flood deposits
Fm	Mud, silt	Massive, desiccation cracks	Overbank, abandoned channel, or drape deposits
Fr	Mud, silt	Massive, roots, bioturbation	Root bed, incipient soil
C	Coal, carbonaceous mud	Plant, mud films	Vegetated swamp deposits
P	Paleosol carbonate (calcite, siderite)	Pedogenic features: nodules, filaments	Soil with chemical precipitation

Table 4.1: Facies classification model from Miall (2013)

4.3. Particle size analysis and EMMA
4.3.1. Particle size analysis

Whilst geological provenances and sediment sources surrounding Nyayanga and Sare River have been identified in previous studies utilising ED-XRF and conglomeratic surveys (Braun et al., 2008; Finestone, 2019), little is known about the transport behaviour and depositional mechanisms occurring at these sites. Due to the lack of exposure of sediments and much of the material belonging to the fine fraction (<2 mm), field analysis of sediments can only provide a limited amount of this information. Resultantly, particle size analysis (PSA) was chosen to learn more about the sedimentary processes occurring at Nyayanga and Sare River through the analysis of the fine fraction.

PSA has long been an established technique in reconstructing the environment, transport behaviour and depositional mechanisms of sediments, as particle size trends appear to be the result of sedimentary processes (Hassan, 1978; Friedman, 1979; Le Roux & Rojas, 2007; Liu et al., 2014; Clarke et al., 2014; Amireh, 2015), and due to the ubiquitous nature of sediments, its application spans an array of environmental settings (Bement et al., 2007; Amit et al., 2007; Dill & Ludwig, 2008; Dinakaran & Krishnayya, 2011; de Haas et al., 2014; Guan et al., 2016) and time periods (Gillies et al., 1996; Lekach et al., 1998; Amit et al., 2007; Houben, 2007; Yin et al., 2011; Wang et al., 2015; Schillereff et al., 2015). Traditionally, particle size was measured using the sieve-pipette method (SPM). This consists of sieving the size fraction >63 µm and using the settling method, which relies on Stokes' law, for the fraction <63 µm. This assumes that particles share the same density as quartz, and are rigid, smooth spheres with a known settling velocity, with a mass percentage being given for each defined class (Beuselinck et al., 1998).

More recent advances in particle size analysis using different methods have resulted in a decline in the use of SPM, due to several drawbacks. These include: size variations within defined size-classes, as some particles are platy in shape rather than spherical (Beuselinck et al., 1998; Wang et al., 2013); the requirement of large amounts of sample (Wang et al., 2013); its labour intensive/time consuming nature (Di Stefano et al., 2010; Wang et al., 2013); and its vulnerability to operator error (Beuselinck et al., 1998; Wang et al., 2013).

Laser diffraction poses an attractive alternative, due to its rapid time of analysis, higher resolution and small sample requirement (Konert & Vandenberghe, 1997; Beuselinck et al., 1998; Eshel et al., 2004; Di Stefano et al., 2010; Wang et al., 2013). The technique is based on the light diffraction theory that particles of given sizes diffract light at certain angles whilst pumped through a sample cell in suspension. The diffracted light intensity is then acknowledged by detectors (which measure volume percentage) and processed through one of two diffraction theories (Mie theory or the Fraunhofer theory) (Beuselinck et al., 1998). It should be highlighted that the two techniques may obtain different results, as SPM is a gravimetric technique, whereas laser diffraction is volumetric (Beuselinck et al., 1998).

Despite its advantages, attention should also be drawn to the limitations of laser diffraction. The clay fraction is frequently underestimated by this technique when particles clay particles are platy, as the optical diameter measured is much larger than the spherical dimeter of the particle (Konert & Vandenberghe, 1997; Beuselinck et al., 1998; Eshel et al., 2004; Wang et al., 2013). A standardised diffraction theory used to interpret the data obtained within laser diffraction is also lacking. Two theories exist; the Fraunhofer theory and the Mie theory. The main difference is that the Fraunhofer models assume that only diffraction occurs and no refraction, which is not always the case. Therefore, the Mie theory attempts to rectify this through the use of a refractive index, yet this can also be difficult to choose, due to the multi-sized and poly-mineralic nature of sediments (Beuselinck et al., 1998; Eshel et al., 2004; Di Stefano et al., 2010; Wang et al., 2013). It is suggested that the Fraunhofer theory be applied to instances where particles are >50µm in diameter, and the Mie theory to particles <50µm in diameter; however, this cannot always be satisfied, due to the heterogeneous nature of sediments and must be taken into consideration during the comparison of studies (Di Stefano et al., 2010; Wang et al., 2013).

Textural parameters/descriptive statistics (eg. mean, mode, sorting, skewness, kurtosis etc.) are frequently employed in environmental reconstruction (Folk & Ward, 1957; Friedman, 1979; Clarke et al., 2014; Amireh, 2015), especially with the emergence of larger particle size datasets obtained through more rapid methods of PSA (IJmker et al., 2012). Computer programmes, for example GRADISTAT (Blott

& Pye, 2001), have been developed to rapidly calculate textural parameters from particle size datasets; this has made the task of analysing particle size results in this manner trivial and far less laborious (Hartmann, 2007).

However, it is widely acknowledged that textural parameters, more often than not, are not truly representative of sedimentary processes where polymodal or highly skewed particle size distributions (PSD) are concerned (Weltje & Prins, 2003; Holz et al., 2004; 2007; Dietze et al., 2012; Clarke et al., 2014; Schillereff et al., 2014; Amireh, 2015). Such distributions are often the result of the physical mixing of sediment populations from different transport mechanisms, and/or from various sources (Prins, 1999; Holz et al., 2007; IJmker et al., 2012; Ma et al., 2015). This has long been realised (Curray, 1960; Visher, 1969; Middleton, 1976; Ashley, 1978; Sheridan et al., 1987), and consequently much work has focused on 'unmixing' these subpopulations through an array of statistical and graphical methods (Weltje, 1997; Prins, 1999; Weltje & Prins, 2003; 2007; Dietze et al., 2012; Clarke et al., 2014; Paterson & Heslop, 2015b).

4.3.2. End-member mixing analysis
4.3.2.1. End-member mixing analysis and its use in this research
End-member mixing analysis (EMMA) is the process of decomposing or 'unmixing' PSDs into constituent components, or end-members (EMs), in order to gain more detailed information on the sedimentary processes that occurred within a palaeoenvironment. EMs derive more meaningful interpretations of sediment dynamics from PSDs and often represent the sediment pool, pathway or mixing dynamics of the environment (Weltje, 1997; Weltje & Prins, 2003; 2007; Meyer et al., 2013; Clarke et al., 2014; Paterson & Heslop, 2015b).

EMMA has been utilised in a variety of different sedimentary archives to identify sediment sources and/or transport mechanisms, which Dietze and Dietze (2019) highlight include marine, lacustrine, aeolian, fluvial, alluvial and periglacial environments, across multiple spatial and temporal scales (Prins et al., 2002; Stuut et al., 2002; Weltje and Prins, 2003; Holz et al., 2004; Vriend and Prins, 2005; Garzanti et al., 2007; Hamann et al., 2008; Strauss et al., 2012; Ijmker et al., 2012; Dietze et al., 2012; 2013; Clarke et al., 2014; Borchers et al., 2015; Ma et al., 2015; Toonen et al., 2015; Schillereff et al., 2015; Wündsch et al., 2016; Collins et al.,

2017; Varga et al., 2019). However, it has been highlighted that the physical plausibility, geomorphological, and geological information when performing analyses must always be taken into account, as well as during the interpretation of EMs (Paterson & Heslop, 2015b). Without this information, one cannot be confident whether the EM represents the available sediment source or the mixing dynamics of the environment (Ijmker et al., 2012; Clarke et al., 2014).

Recently EMMA has proven effective in identifying major depositional processes involved in site formation in archaeological contexts, providing a greater understanding of human/environmental interactions (Collins et al., 2017). Such information would prove invaluable to the research at hand. Resultantly, EMs will be used in conjunction with geological and geomorphological information acquired through field analyses of sediments and from previous work (Braun et al., 2008; Finestone, 2019) to identify transport mechanisms/depositional processes at Nyayanga and Sare River.

4.3.2.2. A brief overview of end-member mixing analysis

Multiple methods of EMMA exist and have been discussed comprehensively by various authors (Weltje, 1997; Prins, 1999; Weltje & Prins, 2007; Prins et al., 2007; Dietze et al., 2012; Paterson & Heslop, 2015b; Van Hateren et al., 2018) and will not be covered in detail here. Essentially, these techniques assume that datasets are formed from a fixed number of EMs, which are non-negative and sum to 1/100% (Prins, 1999; Paterson & Heslop, 2015b). The simplest possible explanation of particle size variation within a dataset is sought after, and so the minimum number of EMs to provide an adequate approximation of the data is identified through goodness-of-fit statistics, namely the coefficient of determination (r^2) (Prins et al., 2007). The aim is to achieve a high coefficient of determination whilst maintaining a low linear correlation between EMs (Paterson & Heslop, 2015b). By doing this, overfitting of the EMs to the dataset is prevented, thus meaning that EMs are linearly independent (Paterson & Heslop, 2015b). Two main approaches are taken to unmixing particle size distributions; these can be divided into non-parametric approaches and parametric approaches.

Parametric approaches assume that observed particle size distributions are composed of numerous continuous unimodal EMs that may be described by

analytical functions (eg. normal, lognormal or Weibull distributions) and a small set of descriptive parameters (Prins et al., 2007; Paterson & Heslop, 2015b). They require prior independent genetic knowledge of EM particle size distributions and cannot simultaneously decompose multiple particle size distributions (Prins, 1999; Prins et al., 2007; Vandenberghe, 2013). For these reasons, they will not be discussed further here.

Non-parametric approaches obtain EMs from the dataset itself by using the covariance between samples as a geological context (Weltje & Prins, 2007; Prins et al., 2007; Paterson & Heslop, 2015b). For this reason, no prior independent genetic knowledge of subpopulations is required (Weltje & Prins, 2007; Vandenberghe, 2013; Flood et al., 2015; Paterson & Heslop, 2015b; Liu et al., 2016). Three main methods of non-parametric End Member Mixing Analysis (EMMA) are used; simplex expansion (Weltje, 1997; Prins et al., 2000; Moreno et al., 2002; Stuut et al., 2002; Frenz et al., 2003; Holz et al., 2004; 2007; Wan et al., 2007; Hamann et al., 2008; Meyer et al., 2013), eigenvector rotation (Dietze et al., 2012; 2014; IJmker et al., 2012; Clarke et al., 2014; Ma et al., 2015; Schillereff et al., 2015; Langford et al., 2016; Wang et al., 2016) and nonnegative matrix factorisation (NMF)(Paterson & Heslop, 2015b).

NMF boasts the most easily navigated user interface (AnalySize — based in MatLab), the best EM fits and the highest capability of identifying the true EMs, whilst also having a rapid computing time (Paterson & Heslop, 2015b; Van Hateren et al., 2018). For these reasons, NMF presents the most beneficial non-parametric approach to EM mixing analysis and will be utilised in the research.

4.3.3. Laboratory preparation and data analysis

For this research, samples were first subject to chemical pre-treatment similar to that outlined by Konert & Vandenberghe (1997) in order to isolate the discrete particles and provide evenly dispersed suspension (Liu et al., 2014). 10 ml of 30% H_2O_2 was added to oxidise samples and remove unwanted organic material that may otherwise reduce repeatability of results or skew particle size distributions (Blott et al., 2004; Gray et al., 2010). Subsequently, samples were heated for further oxidation until all reaction ceased. Carbonates were not removed by the use of hydrochloric acid, as these were suspected to make up a large proportion of the

samples and be part of the original deposition. Deionised water was added to neutralise samples. These were then placed in a 40°C oven until almost all the water had evaporated. Calgon was then added to ensure the even dispersal of particles. A Beckman Coulter LS11320 laser granulometer was used measure particle size using the Fraunhofer model, as samples contained coarser material >63µm, nor could a refractive index be obtained. Analyses of samples were repeated 5 times to ensure reproducibility. GRADISTAT was used to calculate textural parameters and size classes in the phi unit using the Folk and Ward method (Folk & Ward, 1957).

AnalySize, the EMMA interface developed within MATLAB, was used to calculate non-parametric EMs through NMF for the datasets (Paterson & Heslop, 2015b). Sedimentary processes associated with each EM were then identified with aid from field sediment logs and previous work (Braun et al., 2008; Finestone, 2019). The percentage of each EM in sediment samples and their distribution spatially and temporally was determined in order to derive the major sedimentary processes involved in site formation (Figure 4.2).
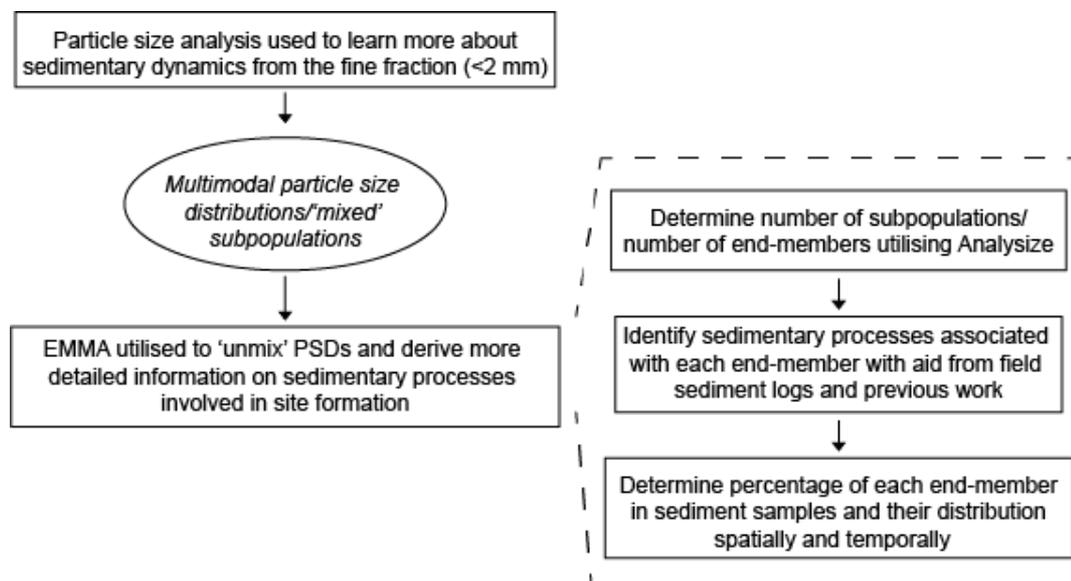
Figure 4.2:The process followed in this study to learn more about sedimentary dynamics at Nyayanga and Sare River through the analysis of the fine fractuon of sediment. PSA is first used. With the acquisition of multimodal PSDs, EMMA is used to 'unmix' PSDs to learn more about the various sedimentary processes involved in site formation. The process of utilising EMMA entails determining the minimum number of EMs that best represent the data from both Nyayanga and Sare River. Sedimentary processes are then attributed to these EMs with the aid of field sediment logs and previous work. The percentage of each EM in sediment samples and their distribution spatially and temporally is then determined to decipher the major sedimentary processes invovled in site formation.

4.4. Phytolith analysis
4.4.1. Phytoliths and palaeoenvironments

Methods such as pollen analysis, lipid biomarker analysis and isotope analysis are most common in reconstructing Plio-Pleistocene palaeovegetation/palaeoclimate in east Africa (section 3.3.2. and references therein). Samples from both Nyayanga and Sare River were examined for pollen, however this was either absent or sparse most likely due to lack preservation (Bamford et al., 2006; Uno et al., 2016a). Lipid biomarker analysis was also attempted with samples, but due to equipment malfunctions and time constraints this was not completed, but may bare potential for future research. Moreover, isotopic analyses are being undertaken by colleagues working on the HPPP, and so were not completed in this research. Despite this, upon laboratory inspection it was found that samples from both sites contained an abundance of phytoliths, and so their analysis was decided to be the best method available for the reconstruction of palaeovegetation in this research.

Phytoliths are morphologically distinct bodies of silica produced within and between plant cells, as a result of the deposition of dissolved silica from evapotranspiration (Piperno, 1997; 2006). Phytolith production within plants is controlled by climatic conditions, soil chemistry and water, plant developmental stage and the taxonomic affinity of the plant (Piperno, 2006; Kinyanjui, 2012). Phytoliths are mainly produced in grasses, but also in some other plants. They are morphologically distinct, meaning that when analysed they can provide partial information on plant taxa and thus on the palaeoecology of a site (Bamford et al., 2006; Lu et al., 2007; Katz et al., 2010; Albert et al., 2015). Phytoliths are produced in all plants, but monocotyledons, specifically grasses, accumulate silica more effectively, and thus produce more phytoliths than dicotyledons (Piperno, 1988; Piperno & Pearsall, 1998; Albert et al., 1999; Barboni et al., 1999; Strömberg, 2004; Piperno, 2006; Mercader et al., 2009; Kinyanjui, 2012).

The use of phytoliths in palaeoenvironmental reconstructions has increased over the previous 30 years (Albert et al., 1999; 2000; 2006; 2009; Mercader et al., 2000; 2009; 2010; Thorn, 2004; Bremond et al., 2005b; 2005a; Bamford et al., 2006; 2008; Barboni et al., 2010; Rossouw & Scott, 2011; Kinyanjui, 2012; Novello et al., 2015). The ratio of C3 to C4 grasses is often calculated through the use of grass phytolith

indices; this provides information on the palaeoclimate and palaeovegetation of a region (Bamford et al., 2006; Barboni & Bremond, 2009; Kinyanjui, 2012; Albert et al., 2015). The ratio of closed to open habitat is also calculated through estimates of grass/tree and shrub composition (Bremond et al., 2005a; Kinyanjui, 2012). Due to their robust chemical composition, phytoliths are also incredibly durable and resistant to post-depositional processes (Bamford et al., 2006). For this reason, they have seen extensive use at Miocene to Pleistocene archaeological and palaeoanthropological sites, where in some cases, pollen is not preserved (Bamford et al., 2006; Uno et al., 2016a). Their use in reconstructing African palaeovegetation is not novel, and hominin sites throughout East Africa have been subject to phytolith analysis with success (Bamford et al., 2006; 2008; Albert et al., 2009; 2015; Mercader et al., 2009; 2010; Rossouw & Scott, 2011; Kinyanjui, 2012). This makes phytoliths an ideal tool for the reconstruction of palaeovegetation on the Homa Peninsula.

However, one must take into account the taxonomic resolution of phytoliths. The issue of differential production, which causes multiplicity and redundancy, can produce a biased record of the palaeovegetation (Barboni & Bremond, 2009; Mercader et al., 2009; Albert et al., 2015). Moreover, different methods of transport can lead to the differential sorting of phytoliths in an environment, dependant on their size, weight and shape; consequently, this may affect interpretations of the palaeovegetation (Lu et al., 2007). These issues must be carefully considered when making interpretations from phytolith assemblages. Often, a reference collection of the modern vegetation of a region and its phytolith production is studied in order to deduce which plants/plant parts produce certain phytoliths, as well as how many phytoliths are produced by each plant/plant part (Albert et al., 1999; 2015; Bamford et al., 2006; Lu et al., 2007). Moreover, the geomorphology of the sample site is frequently taken into account to determine the depositional processes and environment under which phytolith might have been deposited; this is often deduced through the use of a facies model (e.g. Bamford et al., 2006; Bement et al., 2007; Neumann et al., 2009; Albert et al., 2015).

4.4.2. Laboratory technique and data analysis
4.4.2.1.Preparation of ancient sediment for phytolith analysis

Ancient sediment was prepared for phytolith analysis through a method similar to that described by Bamford et al., (2006) and Albert et al., (1999); by following this method, consistency is maintained with other colleagues working on phytoliths on the Homa Peninsula, as well as with studies at better known archaeological sites. The method ensures the recovery of the lightest phytoliths and concentrates phytoliths for further analysis (Bamford et al., 2006). 1g of sediment was first air-dried in a 40^oC oven before being treated with an equivolume solution of 3 N HCL and 3 N HNO_3 for 30 minutes and subsequently being centrifuged at 3000rpm for 2 minutes. This eliminates carbonates and phosphates from the samples. The supernatant was then removed and the pellet was washed with deionised water three times, by centrifuging for 2 mins at 3000rpm and removing supernatant. Following this, 10 ml of 30% H_2O_2 was added to the samples to oxidise organic matter. This was heated to 70^oC and more H_2O_2 was added until the reaction had ceased. The sample were then placed in a 40^oC oven and air-dried before being reweighed. The resultant sample is then termed the acid insoluble fraction (AIF) (Albert et al., 1999; Bamford et al., 2006).

The AIF were then subject to density separation to partition the mineral components by adding 5 ml of sodium polytungstate solution ($Na_6(H_2W_{12}O_{40})H_2O$) of 2.4g/ml density. This density is commonly used, due to the density of phytoliths ranging from 1.5 – 2.3 mg/l (Albert et al., 1999; 2000; 2006; 2015) This was then centrifuged at 3000rpm for 5 minutes. The supernatant was subsequently transferred to another centrifuge tube and 1 ml of deionised water was added. This was vortexed and centrifuged again at 3000rpm for 5 minutes. This process was repeated until no visible mineral particles remained in the supernatant, indicating that all minerals had been retrieved.

4.4.2.2.Preparation of modern plants for phytolith analysis

A modern reference collection situated at the National Museums of Kenya prepared by Rahab Kinyanjui was used to compare phytoliths from ancient sediment with. This was prepared using the methodology outlined by Kinyanjui (2012).

4.4.2.3.Preparation of microscope slides for phytolith description

Slides were prepared following the methods outlined by Bamford et al., (2006) and Albert et al., (1999). 1 mg of sample, accurate to 0.1 mg, was added to a microscope slide. Three to four drops of Entellan were added to the slide and mixed with the sample before adding a cover slide. By counting the total number of fields containing sediment grains, an aerial coverage of sediment on the slide can be estimated. A minimum count of 200 phytoliths with recognisable morphologies were counted to ensure on a 24% error margin in the interpretation of results; by counting only 50 phytoliths, this margin increases to 40% (Bamford et al., 2006).

4.4.2.4.Description and identification of phytoliths

The classification used to describe phytoliths in this study is presented in Table 4.2; pictures of the various morphologies described are presented in Figure 4.3. It is based on an array of literature (Twiss et al., 1969; Brown, 1984; Piperno, 1988; 2006; Albert et al., 1999; 2000; Albert, 1999; Albert et al., 2006; 2015; Bamford et al., 2006; 2008), the PHYTCORE online database (phytcore.org) and morphological classifications described by Kinyanjui (2012). Phytoliths are divided into categories based on the vegetation type they are diagnostic of (grasses, herbaceous, sedges and wood). Where phytoliths are produced most abundantly by a particular vegetation group, but are also produced in other plants, they are categorised as 'nondiagnostic'. Terms used to describe phytolith morphologies relate to the anatomical terminology of the cell in which they developed (Albert et al., 2000). If this was not possible, terms relating to the geometrical characteristics of the phytolith were used, as outlined in the International Code for Phytolith Nomenclature (ICPN) (Madella et al., 2005; Bamford et al., 2006; Albert et al., 2015). Previous quantitative studies were used to inform interpretations on the abundance of phytoliths from different plants/plant parts (Albert et al., 2000; Albert & Weiner, 2001; Albert, 2003; Bamford et al., 2006; Albert et al., 2015).

Table 4.2: Classification system used to describe phytoliths in this study. Phytolith morphologies are presented based on the vegetation group they relate to, and classed as nondiagnostic if they are also produced in other plants. A description for each morphotype is given, as well as sources that describe/identify such morphotypes. Pictures of the majority of morphotypes are presented in Figure 4.3; these are distinguished in the 'Figure no.' column.

Vegetation type	Subgroup	Name	Fig. no. (Figure 4.3)	Morphotype description	References
Grasses	Grass Silica Short Cell	Rondel/ Trapeziform	b.i – b.v/ c.i – c.ii	Varying shapes including conical, keeled and pyramidal. Sometimes described as trapeziforms	Fredlund & Tieszen, 1994; Albert et al., 1999; Strömberg, 2004; Madella et al., 2005; Piperno, 2006; Bremond et al., 2008; Rossouw, 2009; Mercader et al., 2010
		Saddle	d.	Two convex edges opposite each other, with two straight or concave edges	Twiss et al., 1969; Fredlund & Tieszen, 1994; Piperno & Pearsall, 1998; Thorn, 2004; Strömberg, 2004; Madella et al., 2005; Piperno, 2006; Bremond et al., 2008; Mercader et al., 2010
		Bilobate	e.i – e.iii	Two distinct lobes connected by a shank/shaft	Twiss et al., 1969; Brown, 1984; Fredlund & Tieszen, 1994; Piperno & Pearsall, 1998; Albert et al., 1999; Thorn, 2004; Strömberg, 2004; Madella et al., 2005; Piperno, 2006; Bremond et al., 2008; Rossouw, 2009; Barboni & Bremond, 2009; Mercader et al., 2010
		Cross	i.	Four lobes arranged in a cross shape. Both symmetrical and asymmetrical	Twiss et al., 1969; Mulholland & Rapp, 1992; Fredlund & Tieszen, 1994; Alexandre et al., 1997; Strömberg, 2004; Madella et al., 2005; Barboni & Bremond, 2009; Rossouw, 2009
	Non-diagnostic	Scutiform	f.i – f.ii	Short cells with swollen bases and a conical point. Occasionally referred to as 'shield-shaped' or 'lanceolate'	Mulholland & Rapp, 1992; Thorn, 2004; Madella et al., 2005; Kinyanjui, 2012
		Bulliform	g.i – g.iv	Fan-shaped cells	Mulholland & Rapp, 1992; Piperno & Pearsall, 1998; Albert et al., 1999; Strömberg, 2004; Madella et al., 2005; Piperno, 2006; Kinyanjui, 2012

		Acicular	h.	Needle-shaped cells	Twiss et al., 1969; Madella et al., 2005; Bremond et al., 2005b; 2008
Sedges	-	Achene	o.i – o.iv	Thin plates with cone shapes. Rounded cones	Piperno, 1988; 2006; Ollendorf, 1992; Strömberg, 2004; Madella et al., 2005; Kinyanjui, 2012
		Papillae	p.i – p.iii	Thin plates with cone shapes. Hat-shaped	Piperno, 1988; 2006; Ollendorf, 1992; Strömberg, 2004; Madella et al., 2005; Kinyanjui, 2012
Herbaceous	-	Elongate	a.i – a.vi	Plates with a length greater than their width	Twiss et al., 1969; Piperno, 1988; 2006; Strömberg, 2004; Madella et al., 2005; Novello et al., 2015
Woody	Diagnostic	Sclereid	j.i – j.iii	Elongate/irregular in shape with tapered ends. Can be branched or facetted with knobs on surface	Albert et al., 1999; Strömberg, 2004; Madella et al., 2005; Piperno, 2006; Kinyanjui, 2012
		Tracheid	k.i – k.v	Elongate in shape with ornamentation in an annular, reticulate or helical fashion	Albert et al., 1999; Strömberg, 2004; Madella et al., 2005; Piperno, 2006; Kinyanjui, 2012
		Spheroid	l.i – l.iv	Spherical in shape	Piperno, 1988; 2006; Albert et al., 1999; 2000; 2006; Strömberg, 2004; Madella et al., 2005; Barboni et al., 2007; Mercader et al., 2009; Albert et al., 2009; Kinyanjui, 2012
	Non-diagnostic	Irregular	m.i – m.ii	Undefined in shape	Albert et al., 1999; 2006; 2015; Bamford et al., 2006; Kinyanjui, 2012
		Blocky polyhedron	-	Plate-like cells with a polyhedral outline. Often faceted and either compact or elongated	Albert et al., 1999; Strömberg, 2004; Madella et al., 2005; 2006; 2015; Barboni et al., 2010; Kinyanjui, 2012
Unknown	-	Tabular	n.i – n.ii	Table shaped with opposite sides parallel to each other	Madella et al., 2005
		Unidentified	-	Morphotypes that have not been assigned	-
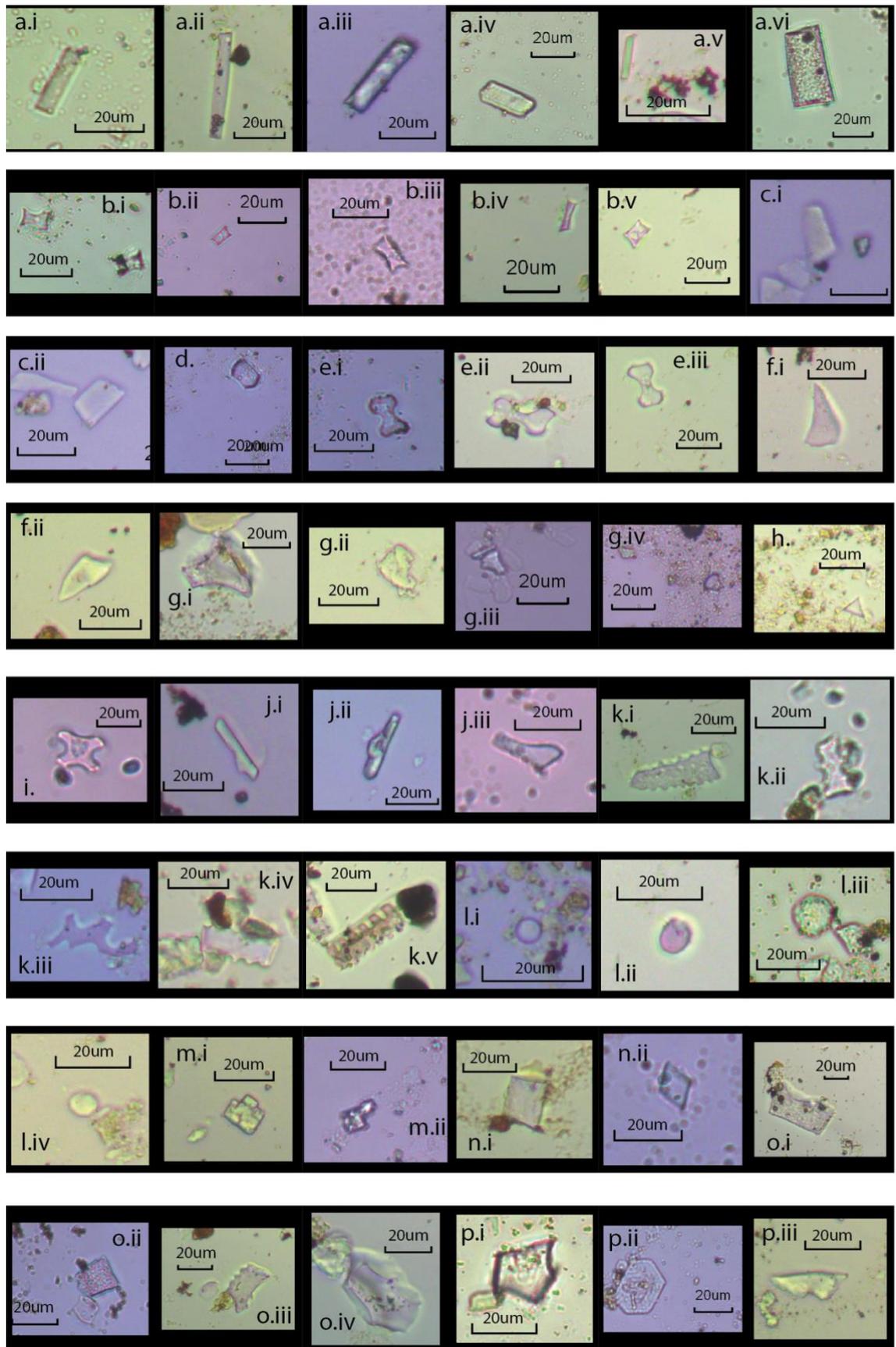
Figure 4.3: Phytolith morphologies identified in this study. a.i – vi) Elongate, b.i – v) Rondel, c.i – ii) Trapeziform rondel, d.) Saddle, e.i – iii) Bilobate, f.i – ii) Scutiform, g.i – iv) Bulliform, h.) Acicular, i.) Cross. j.i – iii) Sclereid, k.i – v) Tracheid, l.i – iv) Spheroid, m.i – ii) Irregular, n.i – ii) Tabular, o.i – iv) Achene, p.i – iii) Pappilae

56

4.4.2.5.Data analyses

Morphotypes identified in the phytolith assemblage were counted and presented as TILIA diagrams for each geological trench. Counts for each morphotype were displayed as a percentage of the total count; this was plotted against depth of the geological trench. Morphotypes were grouped based on the type of vegetation they relate to. Groups included: herbaceous, grass, nondiagnostic grass, wood, nondiagnostic wood, and unknown. The percentages of diagnostic groups are presented on the right of the diagram. Changes in the percentages of these groups is assumed to relate to changes in the structure of the palaeovegetation (Kinyanjui, 2012). Diagrams were delineated into zones where the vegetation structure was suspected to undergo shifts. Although the interpretation of vegetation structure utilising phytoliths may be subject to biases surrounding differential production, transport and preservation, the information provided by phytoliths is invaluable where methods such as analyses of pollen, lipid biomarkers and carbon isotopes are unavailable (Lu et al., 2007).

Morphotypes and groups differ slightly between Sare River and Nyayanga. Counts for Sare River were completed prior to the awareness of several morphotypes including achene, papillae and sclereid type phytoliths. Due to time constraints, it was not possible to complete the counts for Sare River again. For this reason, the sedge and wood components of the vegetation structure at Sare River may be under-represented.

4.5. Cosmogenic nuclide dating
4.5.1. Cosmogenic nuclides and the importance of dating

The establishment of a robust regional geochronology on the Homa Peninsula is essential in determining the age of the sites here in order to place them in a comparable timeframe to other east African palaeoanthropological sites (Barham et al., 2011; Gibbon et al., 2014; Granger et al., 2015). Whilst Kanjera South has been subject to dating in previous studies using biostratigraphy and magnetostratigraphy (Ditchfield et al., 1999; 2019; Bishop et al., 2006; Plummer et al., 2009b), Nyayanga and Sare River have not. Magnetostratigraphy, geochemical tuff sourcing, single crystal laser fusion $^{40}Ar/^{39}Ar$ dating and biostratigraphy are all work in progress at these sites by other colleagues working on the HPPP. It is essential that sediments

are dated with multiple techniques, as all dating methods face various limitations and can potentially provide contrasting ages for the same sediment, highlighting the need for verification between independent dating techniques (Barber et al., 2000; Smith, 2001; Marshall et al., 2007).

With sediments suspected to be Plio-Pleistocene in age and much of the more common methods of dating (section 3.3.3.) already work in progress on the Homa Peninsula, few methods of dating are available for utility here. The use of cosmogenic nuclide dating however has become more common in archaeological contexts, providing accurate, precise and independent dates up to c. 5 Ma (Granger & Muzikar, 2001; Granger, 2014; Gibbon et al., 2014; Granger et al., 2015; Çiner et al., 2015; Liu et al., 2015). Resultantly, this technique was utilised herein to constrain the age of archaeological occurrences and act as an independent chronological control (Barham et al., 2011) for other dating methods utilised on the Homa Peninsula. An application to the Natural Environment Research Council (NERC) for samples taken from both Nyayanga and Sare River was submitted for cosmogenic nuclide dating, although only the samples from Sare River were accepted.

Of the different methods of cosmogenic dating (Dunai, 2010), the isochron burial method was used (Balco & Rovey, 2008). Burial dating uses the differential decay rates of cosmogenic nuclides where samples have become shielded (burial) from cosmic rays (high energy charged particles that penetrate the earth's atmosphere and collide with the surface from outer space) (Dunai, 2010). Commonly, and in this study, the ratio of the different half-lives of cosmogenic radionuclides ^{26}Al and ^{10}Be are utilised, due to their simultaneous occurrence in quartz, as well as the accurate knowledge of their decay constants and half-lives (Dunai, 2010). By using the differential decay rates of the cosmogenic nuclides, a ratio is obtained which is used to acquire a single age for the point at which the samples was taken from, assuming that the sample was *in situ* (Balco & Rovey, 2008; Dunai, 2010). This aids in constraining magnetostratigraphy data to the sedimentary sequence at Sare River, dramatically improving the chronological framework here.

4.5.2. Field and Laboratory technique

Nine samples were collected from conglomerate deposits using a stainless steel trowel at Sare river thought to be rapidly buried. Samples included one sample of

c.60 quartzite pebbles, two samples of sand, and six individual clasts. These were acquired from a 3 – 4 m facies of fluvial sands and gravels at the base of a 5.1 m section, above a highly weathered granite bedrock and below a clear 30 – 50 cm tuff layer (location in Figure 2.8). All samples were buried at a depth greater than 3 m, as suggested by Granger (2014), and comprised mainly of Quartz (Figure 4.4).

After being awarded the NERC funding to complete cosmogenic nuclide dating on samples taken from Sare River, samples were taken to the Scottish Universities Environmental Research Centre's (SUERC) cosmogenic isotope analysis laboratory in East Kilbride in November 2016. The laboratory procedure followed here is similar to that outlined by Balco & Rovey (2008). Much of this procedure was carried out by the authour under the guidance and supervision of staff at SUERC, whilst the remainder of the laboratory procedure and age calculations were completed by Dr. Ángel Rodés.

Samples were crushed and sieved to the size fraction 250 – 500 um. These were then franzed, which separates magnetically charged particles from non-magnetic particles in order to isolate the non-magnetic quartz grains. Isolated quartz grains were then placed in a solution of HNO_3 and HCl and heated on a hot plate overnight. Following this, samples were subject to froth flotation to remove feldspars, before being repeatedly etched in dilute HF. Al and Be were extracted from quartz separates using standard methods of HF dissolution and column chromatography (Stone, 2004). ICP optical emission spectrophotometry is to be used to calculate Al concentrations on aliquots of the dissolved sample. Al and Be isotope ratios were then calculated through accelerator mass spectrometry.
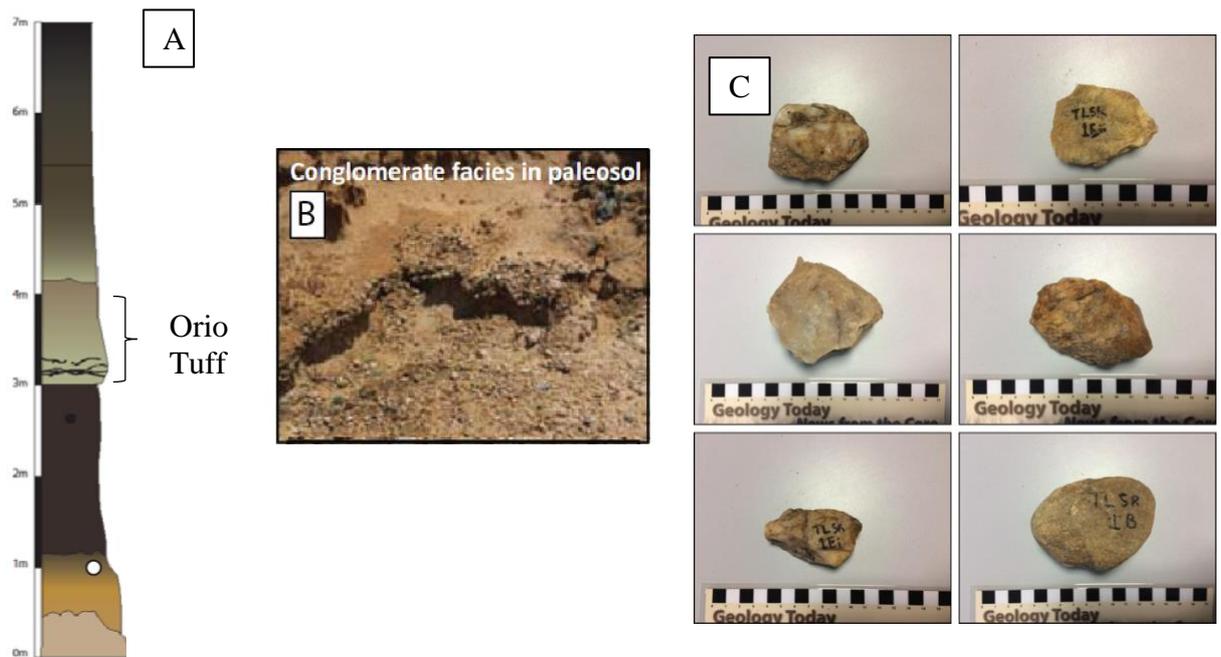
Figure 4.4: A) Composite sedimentological log of the visible exposures at Sare River. White circle at c. 1 m shows the location from which samples were taken. The Orio tuff suggested to be ~ 1.77 Ma in age is also highlighted B) The conglomerate facies at the base of the palaeosol from which samples were taken C) Several of the samples acquired for cosmogenic dating; all are quartz or quartzite in lithology and were sampled from the same stratigraphic unit

4.6. Summary

This chapter has reviewed each method in terms of its usefulness to palaeoenvironmental reconstructions and to this study. Each method has been evaluated in terms of its advantages, whilst the weaknesses of each method have also been acknowledged. Information has also been detailed on the field and laboratory based technique of each method, as well as the data analysis involved..

Geological/sedimentological investigations provide invaluable information on the sedimentary dynamics of a palaeoenvironment, whilst also establishing a framework for more detailed analysis of sediments using a facies model that can be traced site-wide. The use of PSA provides information on the sedimentary dynamics involved in site formation through analysis of the fine fraction. This is limited due to the mixing of different sedimentary processes creating multimodal PSDs. EMMA provides a way to 'unmix' the PSDs into EMs which can be attributed to sediment sources or processes with aid of field sediment logs. By analysing the spatial and temporal distribution of these EMs in samples at both sites, detailed information on the major sedimentary processes involved in site formation can be learned. Palaeovegetation structure and palaeoclimate can be interpreted using phytolith analysis. Detailed information can be gathered on the proportion of various vegetation types,

particularly grasses, but the wood component may be poorly represented. Cosmogenic nuclide dating of quartzite pebbles, sand and clasts acquired from fluvial sands and gravels below the tuff layer at Sare River will also provide an absolute date here through the use of the isochron burial method. This will aid chronological control at this site. Together, these methods will provide a detailed multi-proxy palaeoenvironmental reconstruction of the Homa Peninsula that will form the basis for further analysis. This information is summarised in the workflow diagram shown in Figure 4.5
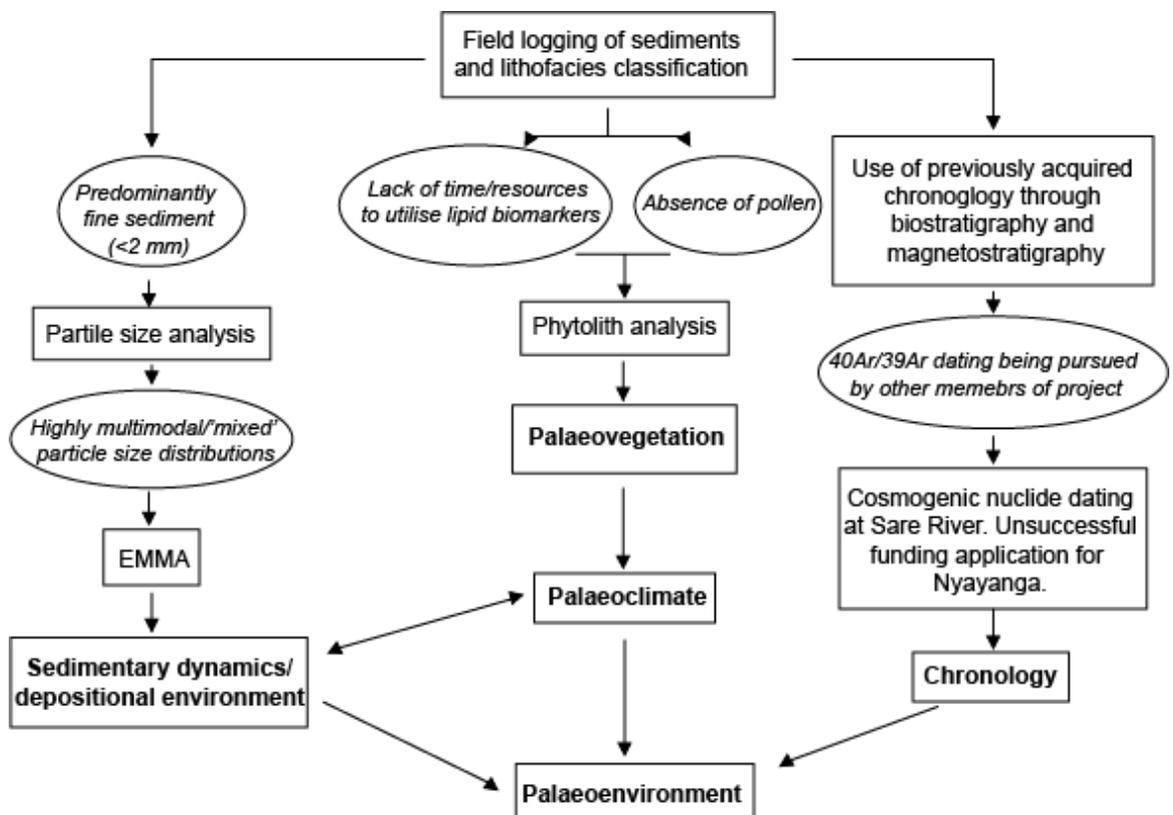
Figure 4.5: A summary workflow diagram overviewing the methods utilised in this study and their role in developing palaeoenvironmental reconstructions of the study sites. Square boxes with standard text indicate actions taken/methods used in this study. Italic text in circular boxes indicate rationale for each action/method, or the results of methods. Bold text in square boxes indicate the aspects of the palaeoenvironment reconstructions that methods contribute towards.

CHAPTER 5.   RESULTS

5.1. Introduction

In this chapter, the results of field investigations, particle size analysis, EMMA and phytolith analysis will be presented for both Nyayanga and Sare River. A workflow diagram which overviews the order in which results are described is shown in Figure 5.1. Results are first presented for Nyayanga, and subsequently for Sare River. For both sites, results of EMMA are presented first, as well a description of each EM in terms of the sedimentary characteristics they represent. Sediment sections for each geotrench/excavation are then presented, displaying sediment logs acquired in the field, PSA results, EM distribution and vegetation type distribution. For each section, sediments and their variation up-sequence are first described based on results from field analyses and PSA. PSA results are presented as size class divisions, as the majority of sediments are polymodal in nature. The distribution of EMs throughout samples is subsequently described. Following this, phytolith distributions throughout the sequences are described, with the distribution of vegetation types plotted for each sample. TILIA diagrams are used to display more detailed information on the phytolith distributions throughout sequences. Finally, the results of cosmogenic nuclide dating of samples taken from Sare River will also be presented.
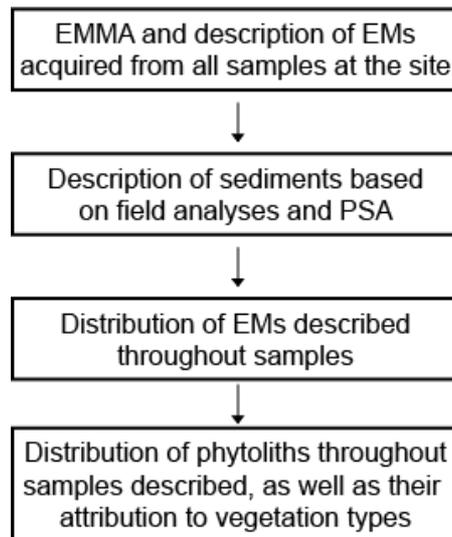
Figure 5.1: Workflow diagram overviewing the order in which results are presented for both sites

5.2. Nyayanga
5.2.1. EMMA

At Nyayanga, a three EM model was chosen to best represent the dataset without overfitting (Figure 5.2), as explained in section 4.3.2. Both a high coefficient of determination ($r^2=0.952$) and 95th percentile were obtained with this model, whilst also maintaining a low linear correlation between the EMs ($r^2=0.138$). A low angular deviation was also obtained ($\theta=9.759$), which displays the angular difference in degrees between the reconstructed and observed data. If a sample has a low r^2 and/or a high angular deviation, it indicates that the sample has not been well represented by the EM model. Such samples are shown as outliers, represented by the red crosses in Figure 5.2. These outliers remain present in all the simulated EM models (Figure 5.2), so it was decided not to increase the number of EMs further. Instead, significant outliers will be highlighted and described in terms of their individual textural parameters in addition to how they are represented by the EM model.

EM densities were exported from AnalySize and imported to GRADISTAT to compute descriptive statistics and size classes in order to maintain consistency with the original particle size distributions.

5.2.1.1. EM1

EM1 is a symmetrical poorly sorted silty clay (Figure 5.2). Despite this, it has a mean grain size of 8.8Φ, resembling a very fine silt. Since it is multimodal, the mean becomes a less reliable descriptor for the average grain size; in cases of multimodality the median is often more reliable. Here, the median is very similar to the mean and still classes the average grain size as a very fine silt. Although identified as being a symmetrical distribution, EM1 can be seen to have a slight coarse tail which incorporates a very small amount of fine sand. With a kurtosis value of 1.06, EM1 is classed as mesokurtic, suggesting that the sorting of the distribution remains relatively consistent between the tails and the central portion of the distribution.

5.2.1.2. EM2

EM2 is similar to, yet slightly coarser than EM1 and can be identified as a symmetrical poorly sorted silt (Figure 5.2). Almost the entire distribution is made of

silts, with a small amount of clay also being present. It is a unimodal distribution with a mean of 7.34 Φ, classing it as a fine silt. The kurtosis is 0.99 classing it as mesokurtic, like that of EM1.

5.2.1.3. EM3

EM3 differs to the previous two EMs. It can be classed as a very fine skewed poorly sorted sandy silt (Figure 5.2). Although classed as a unimodal distribution in GRADISTAT, it can be seen to have a small fine peak that incorporates a small amount of clays in addition to its coarser primary peak. For this reason, the median may be more appropriate to classify the average grain size; this can be identified as a very coarse silt. The kurtosis of EM3 is higher than that of previous EM's; it can be classed as very leptokurtic. This suggests that its central peak of coarse silts is better sorted than that of the tails of the distribution.
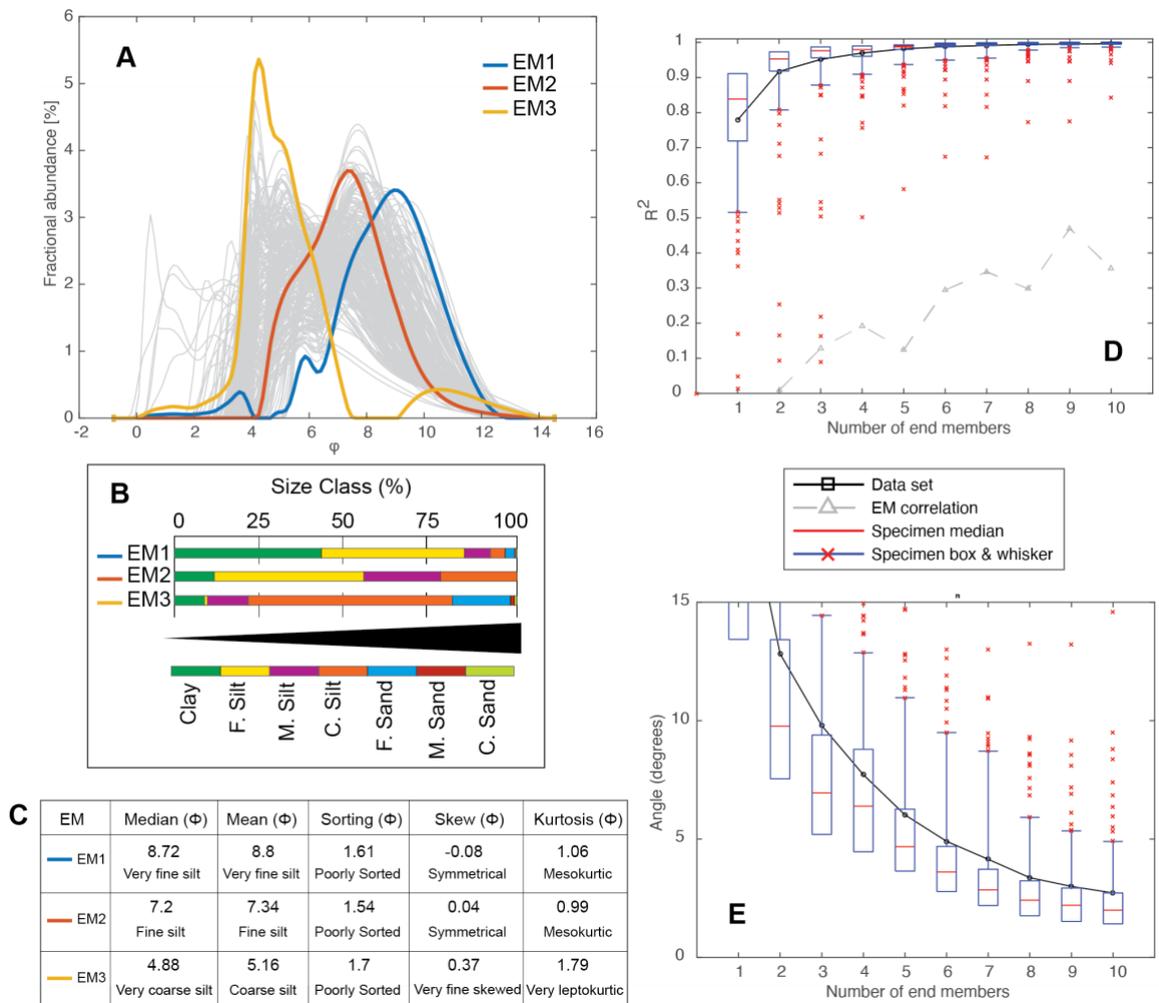
Figure 5.2: EM plots for particle size distributions at Nyayanga. (A) The three EM model overlaid on particle size distributions from Nyayanga, (B) Size fractions of each EM, (C) Textural parameters of each EM, (D) Linear correlations for each EM scenario (E) Angular deviations for each EM scenario

5.2.2. Geotrench 1
5.2.2.1.Sedimentology
Geotrench 1 (Figure 5.3 & Figure 5.4) is ~ 5.4 m in depth. At its base, it is comprised of matrix-supported angular clasts in a clayey silt conglomerate with occasional cobbles, before gradationally transitioning to a grey brown clayey silt with some sandy lenses, occasional granules and carbonate nodules at ~ 4.8 m. Overlying this is a grey brown clayey silt with sandy orange lenses, which are overlain by a grey green silt with occasional pebbles. The unit subsequently fines to a grey brown clayey silt. At ~ 3.9 m, an erosive contact exists with the overlying light orange grey massive silty sands. Over a metre of massive grey brown clayey silts with carbonate nodules are then observed from ~ 3.7 m, before sharply transitioning to light orange clayey silts with some gravel, as well as coalescing carbonate nodules up to pebbles in size at ~ 2.4 m. Finally, a sharp transition at ~ 0.8 m to a massive red brown clayey silt with pedogenic carbonate nodules characterises the top of this trench.

5.2.2.2.EMMA
At the base of Geotrench 1, EM's 1 and 2 explain the majority of particle size distributions (Figure 5.3), with a smaller percentage of EM3. From ~ 4.4 m to ~ 4.2 m, EM3 increases in percentage whilst EM1 decreases, following which EM1 significantly increases again and explains over 50% of particle size distributions. This trend is interrupted at ~ 3.9 m, where EM3 increases to over 50%, whilst EM2 decreases further to ~ 10%. However, at this depth the particle size distribution is very poorly explained by the EM model (R^2=0.16), as an outlier is present (OL2). The sample at this depth incorporates higher percentages of sands, with over 50% of the sample ranging in sizes from fine to coarse sand. Sand is not present in large amounts in any of the EMs, especially in sizes greater than fine sand; this most likely explains why this sample is poorly explained by the EM model.

At ~ 3.8 m in depth EM1 accounts for over 50% of the distributions up to ~ 2.3 m in depth. The percentage of EM2 reduces from ~ 2 5% to 0 during this period, whilst EM3 increases from ~ 15% to ~ 30%. An outlier is present (OL1) at ~ 2.4 m. Similar to the previous outlier, the particle size distribution of this sample incorporates higher percentages of fine sand, which is most likely why it is poorly represented by the EM model.

Figure 5.3: Sediment log of Geotrench 1(Figure 2.3) at Nyayanga. Sediment log depth is presented in metres. Facies codes outlined by Miall (2013) are included on sediment logs. Particle size distributions, EM abundances and vegetation types are also included at corresponding sample depths. Two outliers are present (OL1 and OL2). These samples incorporate higher percentages of sand. Letters a – f. relate to sediment pictures displayed in Figure 5.4

From ~ 2.1 m in depth to ~ 0.8 m, EM2 best explains the majority PSD's with percentages over 75% in all but one sample, of which is dominated by EM1. Aside from this sample, EM1 is present percentages <25%, decreasing upwards. EM3 shows the opposite trend and increases from absence to ~ 20%.
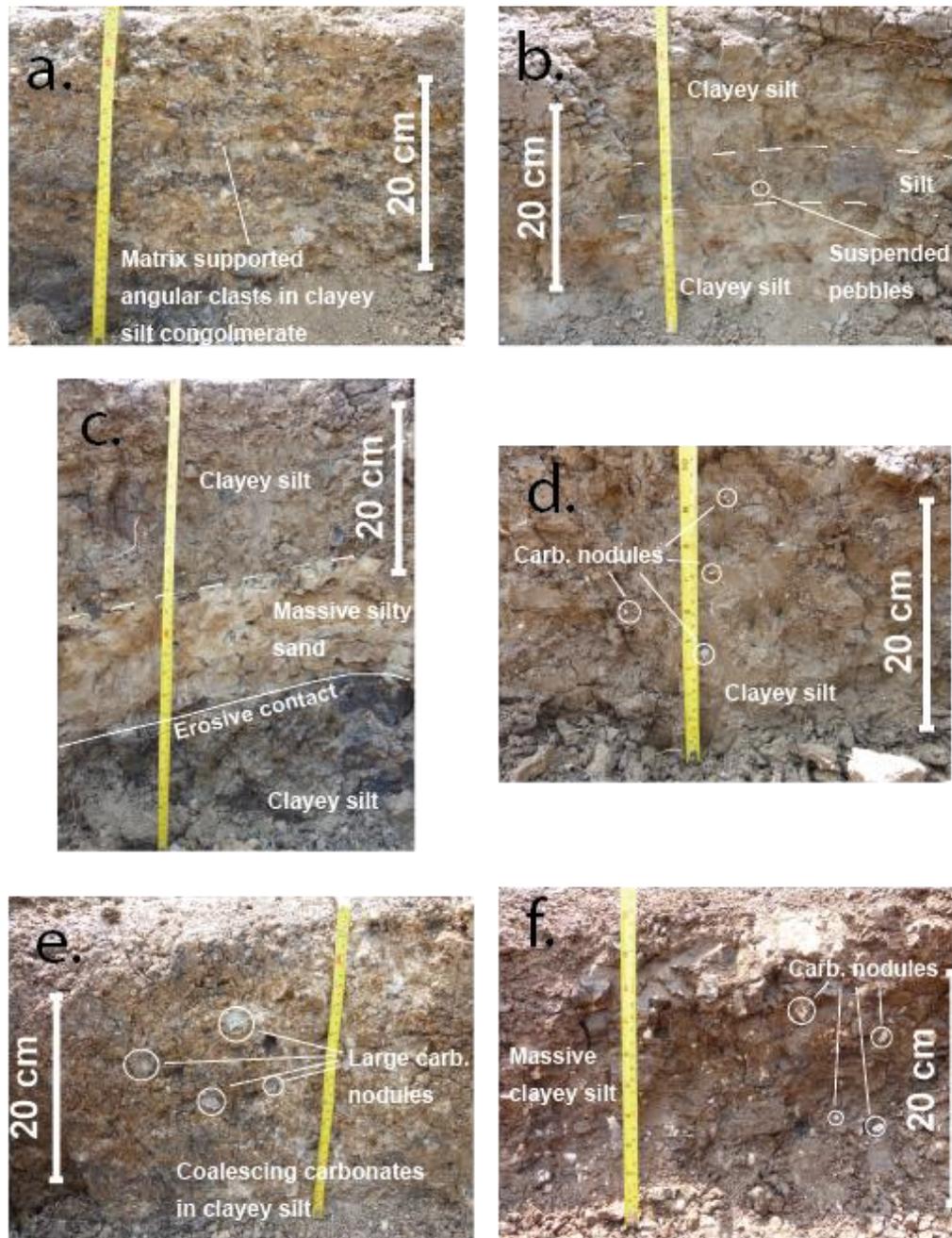
Figure 5.4: Photos of sediments in GT1 at Nyayanga. Letters a – f correspond to the depths sections highlighted in Figure 5.3. Sediment features are highlighted in the images

At ~ 0.8 m in depth, the best explanation of PSD's alternates between EM's 1 and 2; whilst EM1 is present in percentages >50%, EM2 is present is in percentages <25%, and vice versa. EM3 is consistently present in percentages <25%.

5.2.2.3. Phytoliths

Throughout the trench, grass and herbaceous phytoliths dominate the assemblage (Figure 5.5). Sedge and wood phytoliths remain present in abundances of ~ 10%. However, to better describe the dynamics of the phytolith distribution throughout the trench, four zones were identified.

Zone 1 characterises the base of the trench between 5.4 m and 4.5 m. Grass phytoliths increase from ~ 30% to ~ 50%, whilst wood and herbaceous phytoliths both reduce in percentage. An increase in rondels characterises the increase in grass phytoliths, whilst a reduction in spheroids are responsible for the reduction of wood phytoliths. Irregular phytoliths however are seen to increase, most likely relating to wooded vegetation, although they are nondiagnostic of this.

At 4.5 m to 2.9 m, zone 2 is delineated. This zone has the most consistent trend in vegetation types indicated by phytoliths. Wood phytoliths remain ~ 10%, whilst sedge phytoliths are slightly fewer ~ 5%. Grass and herbaceous phytoliths generally remain ~ 40% in abundance, with some variations. Rondel phytoliths show the most variation in this zone, showing repeated increases and decreases of at least 15%. Saddles gradually decrease in this zone, as do bilobates and sclereids. Tracheids characterise much of the wood phytoliths.

Zone 3 lies at 2.9 m to 1.6 m. Sedge phytoliths increase to ~ 10% in this zone, characterised primarily by achene phytoliths. Grass phytoliths also increase in percentage and dominate this zone, composed mainly of rondel and saddle
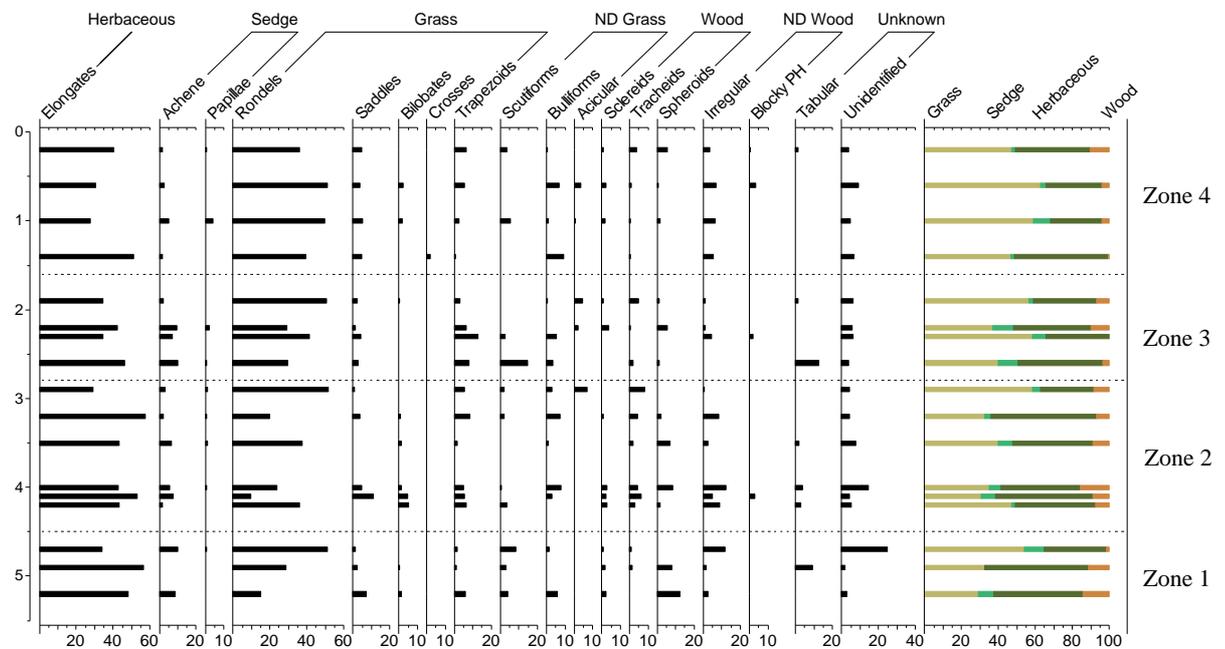
Figure 5.5: Phytolith morphotypes counted at GT1 and their respective percentages. Morphotypes are categorised into vegetation types (Herbaceous, Sedges, Grasses, nondiagnostic (ND) Grasses, Wood, ND Wood and Unknown). The percentages of these vegetation types are presented on the right of the diagram (ND morphotypes are not included here). The diagram is delineated into four zones representing shifts in the vegetation structure

phytoliths. Herbaceous phytoliths show a small decrease in percentage from zone 2.

From 1.6 m to the top of the trench is zone 4. Grass phytoliths dominate this zone, more so than zone 3. These are primarily composed of rondels, although saddles are present throughout. Herbaceous phytoliths reduce in percentage, as do sedge phytoliths. Wood phytoliths show a reduction in percentage from zone 3 at the base of zone, but steadily increase to ~ 10%.

5.2.3. Geotrench 2
5.2.3.1.Sedimentology

~ 4.2 m in depth, Geotrench 2 (Figure 5.6 & Figure 5.7) consists of relatively different sediments than that of Geotrench 1. At its base, it is comprised of massive grey silts with carbonate nodules and occasional granules. Overlying this at ~ 3.5 m in depth are massive red brown clayey silts with carbonate nodules, like that of those towards at the top of Geotrench 1; evidence for faulting here may also exist. A sharp change to massive light orange clayey silts occurs at ~ 2.3 m in depth, with occasional carbonate nodules and manganese staining also present. This is overlain by a massive grey orange granular clayey silt at ~ 1.7 m, where carbonate nodules are still present. Massive light orange grey granular clayey silts overlie these sediments at ~ 1.2 m, with a thin band of carbonate nodules running through the centre of this layer at ~ 1.1 m. A metre of brown silts with carbonate nodules throughout make up the top of Geotrench 2, with carbonate nodules being particularly more concentrated at ~ 0.8 m in depth.

5.2.3.2.EMMA

From the base to ~ 3.8 m in depth, EM2 best explains PSD's, with EM1 present in percentages <10% at the very base and then absent, whilst EM3 is absent at the base and then present in percentages ~ 25% (Figure 5.6).

EM2 best explains the PSD's between ~ 3.8 m and ~ 1.7 m in depth. At this depth and below, EM3 is present in percentages <10% or absent. EM1 infrequently better explains PSD's than EM2, and is generally present in percentages <30%.

From 1.7 m to 1 m in depth, EM2 best represents PSD's, but EM1 still represents ~ 25% of each PSD. EM3 increases in percentages at ~ 1.7 m and above, and at

times better represents PSD's than EM2, before becoming less present (<25%) at ~ 1.3 m.

From 1 m to the top of the trench EM3 best represents PSD's , present at percentages >50% in both samples, whilst EM2 is present in slightly higher percentages than EM1.

Figure 5.6: Sediment log of Geotrench 2 (Figure 2.3) at Nyayanga. Sediment log depth is presented in metres. Facies codes outlined by Miall (2013) are included on sediment logs Particle size distributions, EM abundances and vegetation types are also included at corresponding sample depths. Letters a – g. relate to sediment pictures displayed in Figure 5.7

Figure 5.7: Photos of sediments in GT2 at Nyayanga. Letters a – g correspond to the depths sections highlighted in Figure 5.6. Sediment features are highlighted in the images

5.2.3.3. Phytoliths

The distribution of phytoliths in Geotrench 2 appears more consistent than that of Geotrench 1 (Figure 5.8). Herbaceous phytoliths dominate the majority of this geotrench, although grass phytoliths are present in abundance. Two zones are identified here.

Zone 1 spans from 4 m to 2 m in depth. It is dominated by herbaceous vegetation in abundances of over 50%. Grass phytoliths generally comprise ~ 35% of the phytolith known distribution; this is made up primarily of rondel phytoliths, although

Figure 5.8: Phytolith morphotypes counted at GT2 and their respective percentages. Morphotypes are categorised into vegetation types (Herbaceous, Sedges, Grasses, nondiagnostic (ND) Grasses, Wood, ND Wood and Unknown). The percentages of these vegetation types are presented on the right of the diagram (ND morphotypes are not included here). The diagram is delineated into two zones representing shifts in the vegetation structure

saddle phytoliths are present throughout. Wood phytoliths are almost entirely absent from this zone. Sedge phytoliths are present in abundances <10%.

From 2 m in depth to the top of the trench is zone 2. Grass phytoliths, composed mainly of rondel phytoliths, dominate this zone between 2 m and 1.3 m in depth with abundances of ~ 50%,before reducing to ~ 40% for the remainder of the zone. Saddles steadily decrease throughout zone 2, whilst bilobates increase. Herbaceous phytoliths are present in abundances of ~ 40% between 2 m and 1.3 m, before becoming dominant from 1.3 m to the top of the trench, with abundances of ~ 50%. Wood phytoliths can be seen to steadily increase in percentage throughout this zone, from <5% at the base, to ~ 10% at the top of the trench. Sedge phytoliths are present in abundances of ~ 5% throughout the zone.

5.2.4. Geotrench 3
5.2.4.1.Sedimentology

Geotrench 3 (Figure 5.9 & Figure 5.10), ~ 3.1 m in depth, is comprised of a massive dark grey brown clayey silt with isolated carbonate nodules at its base. Overlying this at ~ 2.9 m is a massive grey buff coloured silt with carbonate nodules coalescing, which gradationally develops more light orange silts at ~ 2.5 m. Subsequently, a massive dark grey brown clayey silt with carbonate nodules overlies these sediments at ~ 1.9 m. At ~ 1.5 m, grey brown clayey silts with some

granules and increased carbonate content appear, with carbonate content hardening into rock-like clasts. Following this, between ~ 1.2 m and ~ 0.6 m, alternating laminations of light grey yellow and orange brown grey sandy silts exist, with carbonate nodules dispersed throughout, as well as lenses of orange sands and silts. Orange brown sandy silts with carbonate nodules cap this trench.

5.2.4.2. EMMA

Throughout Geotrench 3, EM's 1 and 3 follow a consistent pattern (Figure 5.9). At the base of the trench, EM1 is seen to increase in percentage until ~ 2.9 m in depth.
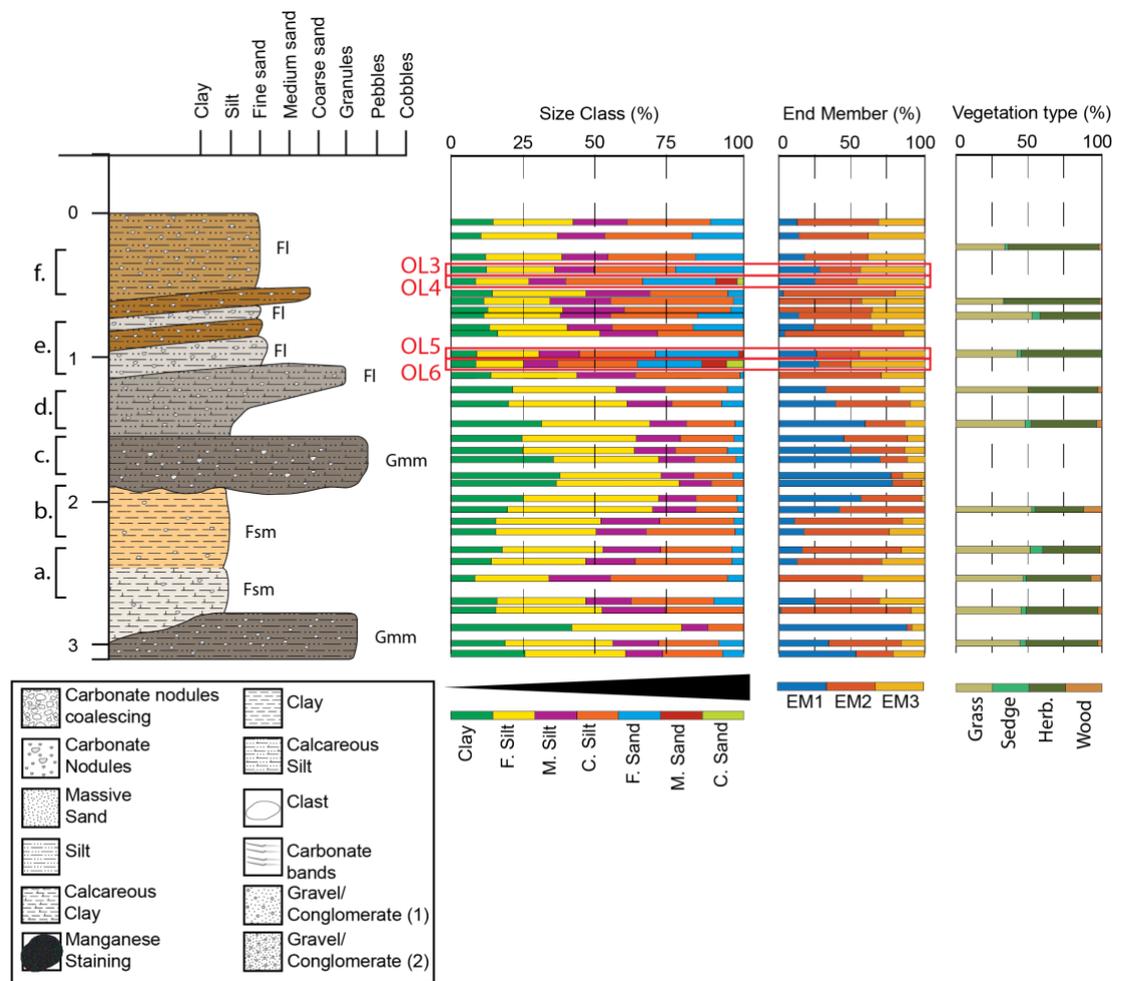
Figure 5.9: Sediment log of Geotrench 3 (Figure 2.3) at Nyayanga. Sediment log depth is presented in metres. Facies codes outlined by Miall (2013) are included on sediment logs. Particle size distributions, EM abundances and vegetation types are also included at corresponding sample depths. Four outliers are present in the trench (OL3 – 6), two at ~ 1.1 m in depth, and two at ~ 0.6 m in depth. these samples incorporate higher percentages of sand in their distribution. Letters a – f. relate to sediment pictures displayed in Figure 5.10
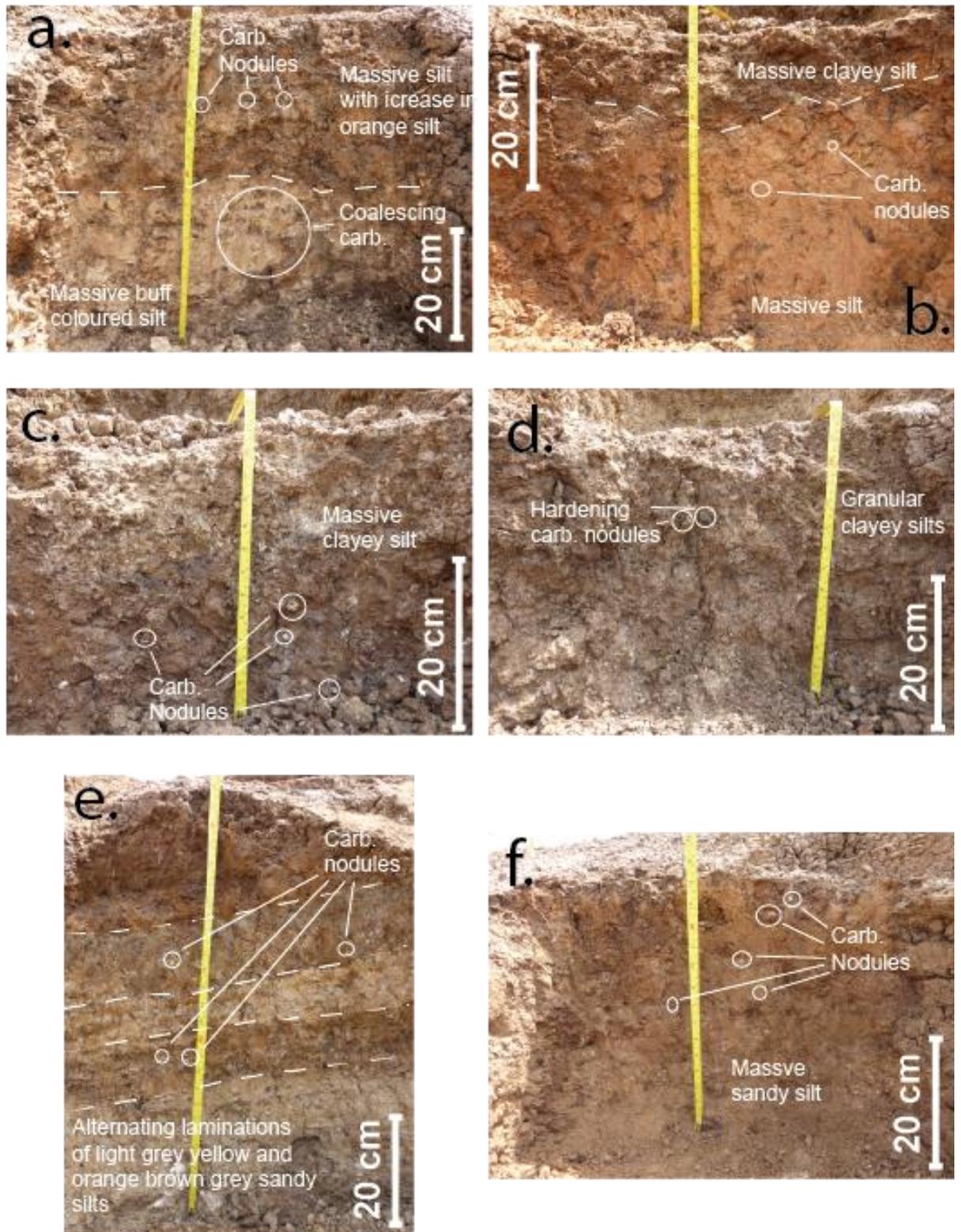
Figure 5.10: Photos of sediments in GT3 at Nyayanga. Letters a – f correspond to the depths sections highlighted in Figure 5.9. Sediment features are highlighted in the images

Following this, it decreases to ~ 20%, before increasing in percentage again between ~ 2.8 m and ~ 2 m, from which point it generally decreases in abundance towards to the top of the trench. EM3 shows the opposite trend throughout the

trench. EM2 is consistently present throughout the trench in percentages between ~ 25% and 50%, with the occasional exceptions. It is at its lowest percentages in the middle of the trench ~ 1.9 m in depth, either side of which it increases in percentage.

Four outliers are present in the trench (OL3 – 6), two at ~ 1.1 m in depth, and two at ~ 0.6 m in depth. Like the outliers identified in Geotrench 1, these samples incorporate higher percentages of sand in their distribution, up to coarse sand in size, and so will be poorly presented by the EM model. These samples do not fit the EM model well, even by increasing the number of EMs, most likely due to the infrequency of coarser PSD's.

5.2.4.3.Phytoliths

Like previous trenches, grass and herbaceous phytoliths dominate the assemblage throughout Geotrench 3 (Figure 5.11). Wood and sedge phytoliths are present throughout the trench, although in low percentages. Three zones can be identified in this trench.

Zone 1 spans from 3.1 m to 1.8 m. Grass phytoliths dominate this zone, comprising at least 45% of the known phytolith distribution and gradually increasing throughout the zone. Herbaceous phytoliths are present in similar abundances of 45% at the base of the zone, but gradually decrease to abundance of ~ 30% towards the top of the zone. Wood phytoliths display an over

increase in percentage from <5% at the base of the zone to ~ 20% at the top; these are composed primarily of tracheid phytoliths. Sedge phytoliths are present throughout in abundances of 5 – 10%.

 Zone 2, which spans from 1.8 m to 0.8 m in depth, is dominated by grass and herbaceous phytoliths, which have relatively even abundances of ~ 45%. A reduction in wood phytoliths can be observed throughout the zone; percentages drop to <5%. Abundances of sedge phytoliths remain consistent with zone 1.

From 0.8 m to the top of the trench is zone 3. This is dominated by herbaceous phytoliths, which increase in percentage from ~ 45% in zone 2 to ~ 70% in zone 3.

Grass phytoliths reduce in abundance to ~ 30%. Wood and sedge phytoliths are present in low abundances of <5%.

Figure 5.11: Phytolith morphotypes counted at GT3 and their respective percentages. Morphotypes are categorised into vegetation types (Herbaceous, Sedges, Grasses, nondiagnostic (ND) Grasses, Wood, ND Wood and Unknown). The percentages of these vegetation types are presented on the right of the diagram (ND morphotypes are not included here). The diagram is delineated into three zones representing shifts in the vegetation structure

5.2.5. Geotrench 5
5.2.5.1.Sedimentology

Only ~ 2 m in depth, Geotrench 5 (Figure 5.12) is the smallest of the Nyayanga trenches. At its base, it is comprised of a massive buff coloured laminated clayey silt. Overlying this are poorly sorted gravels and occasional cobbles supported by a grey brown clayey silt matrix. At ~ 1 m, a massive well sorted grey brown clayey silt with some manganese characterises the rest of these sediments. The two uppermost sediment units are consistent with lower parts of Geotrench 1 and 2.

5.2.5.2.EMMA

From the base to ~ 0.5 m in depth, Geotrench 5 is largely dominated (~ 50%) by EM2 (Figure 5.12). EM3 is present in percentages <20%. EM1 is generally more present with percentages ~ 30%, although it falls to ~ 10% at 1.7 m and has a peak of ~ 65% at 0.9 m. At the top of the trench, EM3 is largely present in PSD's, with over 50% presence in two of three samples. EM2 decreases in presence to ~ 25% for these two samples but remains at ~ 50% for the third. EM1 is present in percentages <15%.
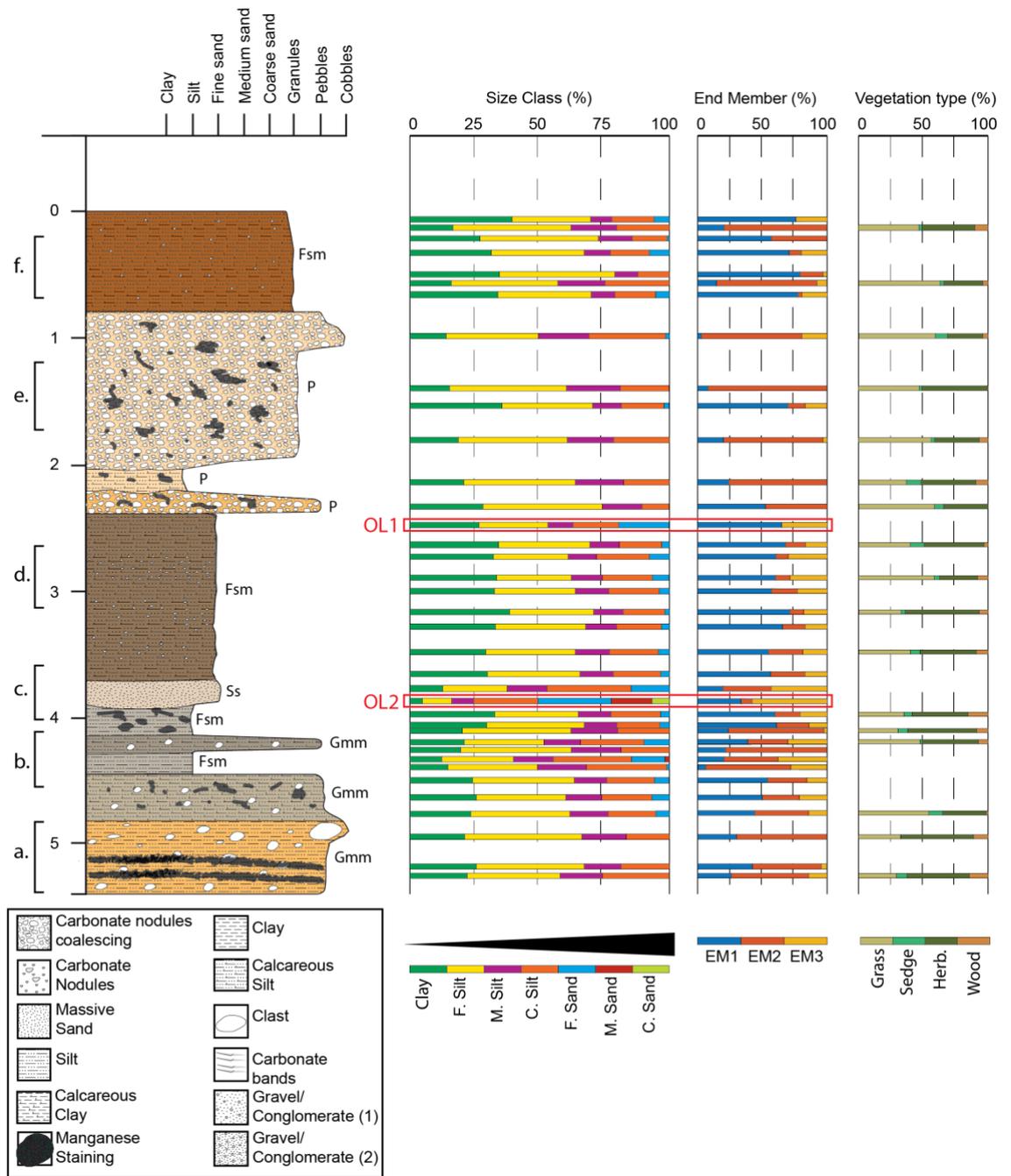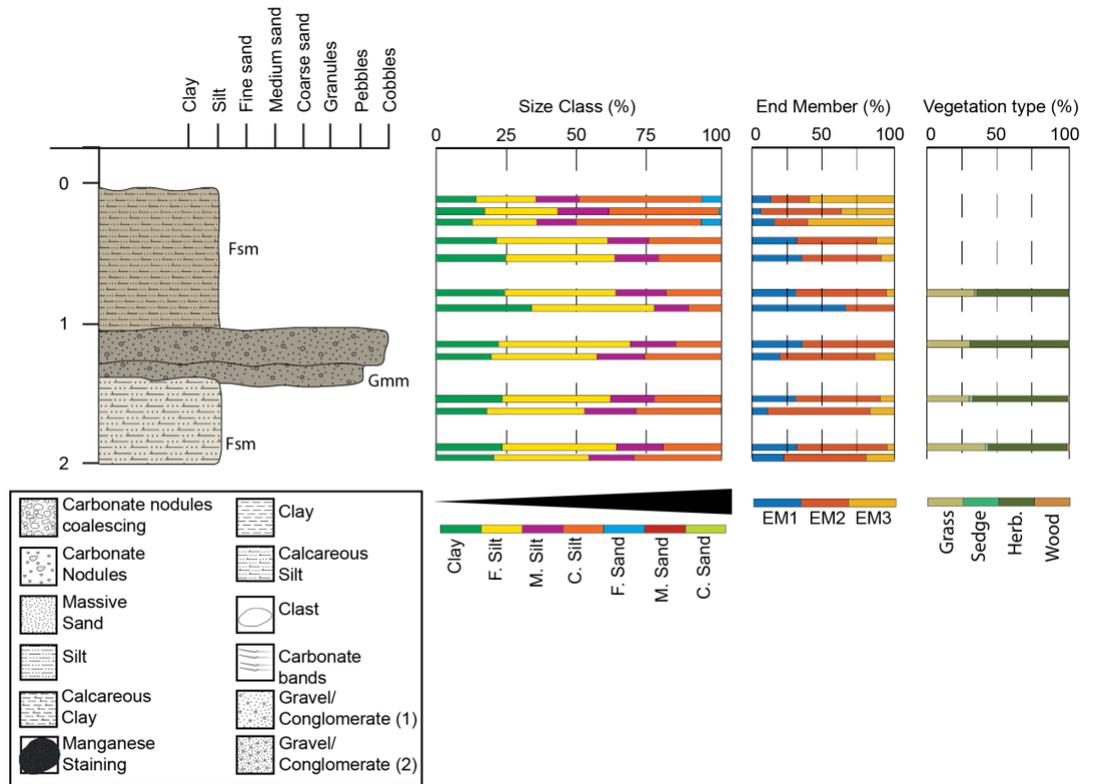
Figure 5.12: Sediment log of Geotrench 5 (Figure 2.3) at Nyayanga. Sediment log depth is presented in metres. Facies codes outlined by Miall (2013) are included on sediment logs. Particle size distributions, EM abundances and vegetation types are also included at corresponding sample depths

5.2.5.3.Phytoliths

Throughout Geotrench 5, herbaceous phytoliths are dominant in abundances of >50% (Figure 5.13). Grass phytoliths are present throughout in abundances of 30% to 45%. Sedge and wood phytoliths are almost completely absent from this trench, with abundances <5%.
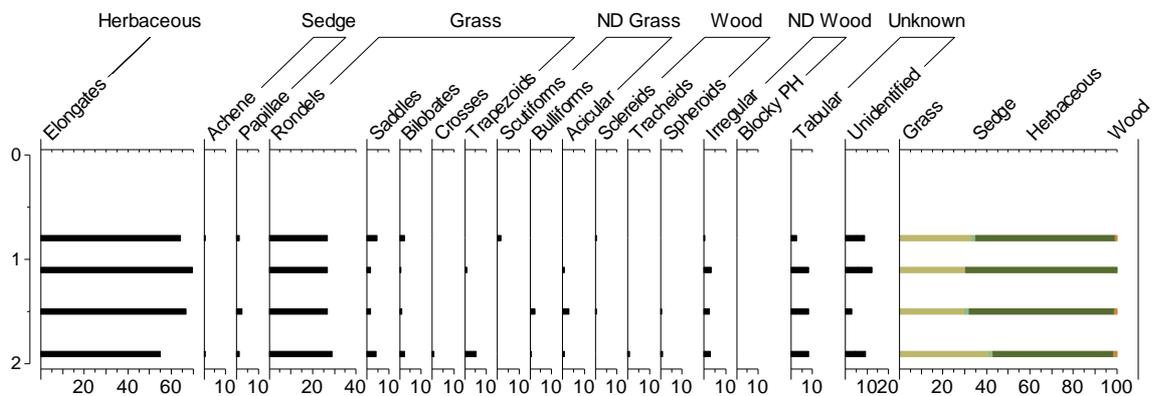
Figure 5.13: Phytolith morphotypes counted at GT5 and their respective percentages. Morphotypes are categorised into vegetation types (Herbaceous, Sedges, Grasses, nondiagnostic (ND) Grasses, Wood, ND Wood and Unknown). The percentages of these vegetation types are presented on the right of the diagram (ND morphotypes are not included here)

5.2.6. Geotrench 6
5.2.6.1.Sedimentology

Geotrench 6 (Figure 5.14 & Figure 5.15) is ~ 3.2 m in depth, with sediments here apparently coarser overall than other previous units. At the base of the trench, an outcrop of a fairly massive cobble conglomerate exists, which is not depicted in the log. Overlying this is a ~ 35cm massive granular grey brown clayey silts with diffuse carbonate nodules. This has a gradational contact with the overlying massive grey orange brown clayey silts at ~ 2.8 m, where diffuse carbonate nodules also exist. Up sequence a gradational shift towards alternating faintly laminated clayey silts and sandy silts with fine gravel at ~ 2.3 m, with a lower concentration of carbonate nodules is identified. Overlying these sediments at ~ 1.3 m is a massive clayey silt with large amount of carbonate nodules, up to pebbles in size, as well as clasts up
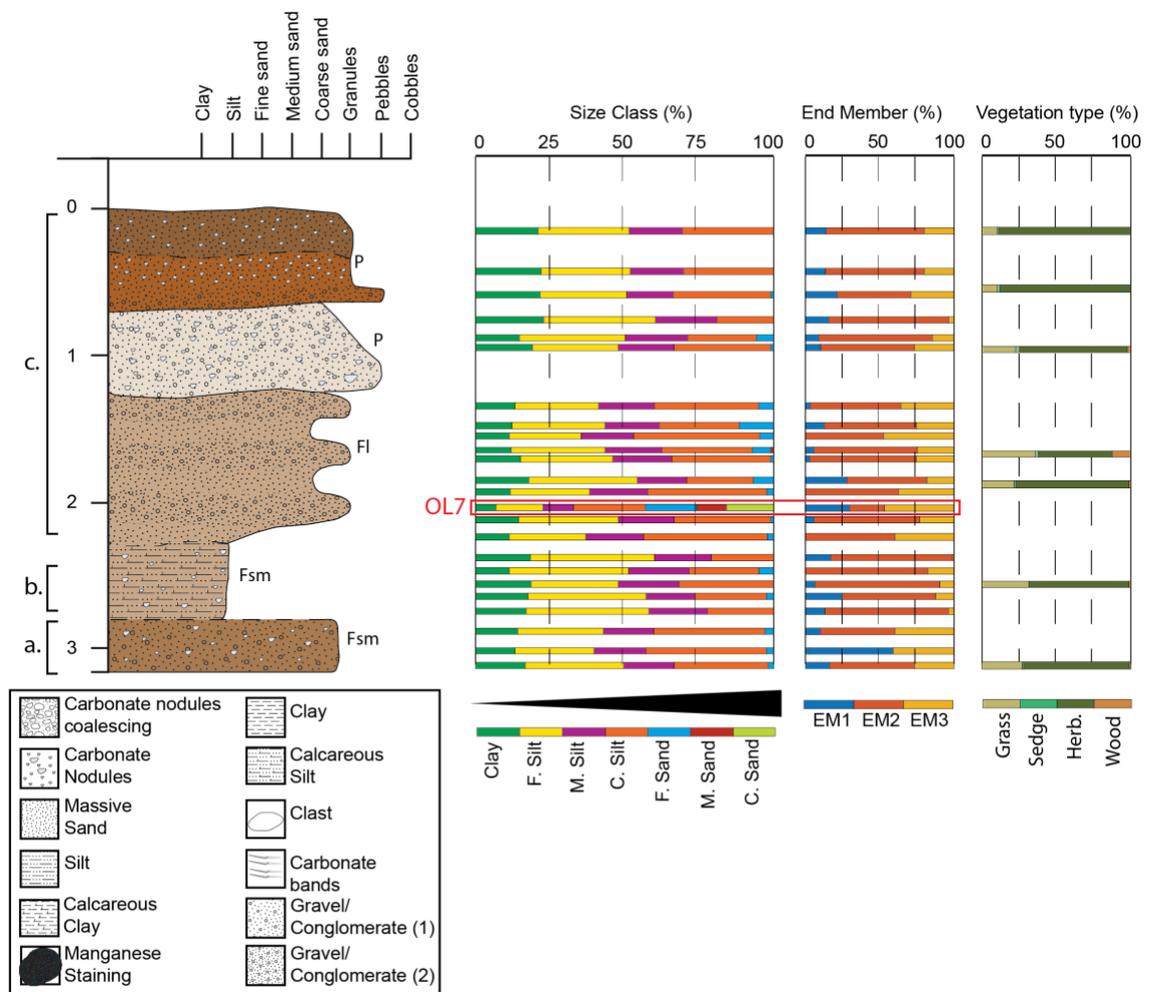
Figure 5.14: Sediment log of Geotrench 6 (Figure 2.3) at Nyayanga. Sediment log depth is presented in metres. Facies codes outlined by Miall (2013) are included on sediment logs. Particle size distributions, EM abundances and vegetation types are also included at corresponding sample depths. One outlier is present at ~ 2 m (OL7). This sample incorporates a large percentage of sand. Letters a – c. relate to sediment pictures displayed in Figure 5.15

to pebbles in size. These sediments have a sharp contact with the overlying massive dark brown orange granular clayey silt at ~ 0.7 m, which contains carbonate nodules and occasional granules; these sediments are similar to the red brown orange sediments seen in previous trenches.

5.2.6.2. EMMA

There is little change in EM compositions in Geotrench 6 (Figure 5.14). EM2 dominates much of the sequence and accounts for over 50% of the EM composition for most samples. EM3 fluctuates between 15% and 40% throughout the trench, showing a peak from the base to ~ 2.8 m in depth, a trough to ~ 2 m in depth, followed by a peak to ~ 1.4 m in depth, tailed by a steady general decrease to the top of the trench. EM1 is present in low percentages (<20%) for much of the trench, with exceptions at ~ 3 m and ~ 2 m, where it's percentages rises. One outlier is present at ~ 2 m (OL7). This sample incorporates a large percentage of sand, like previous outliers.
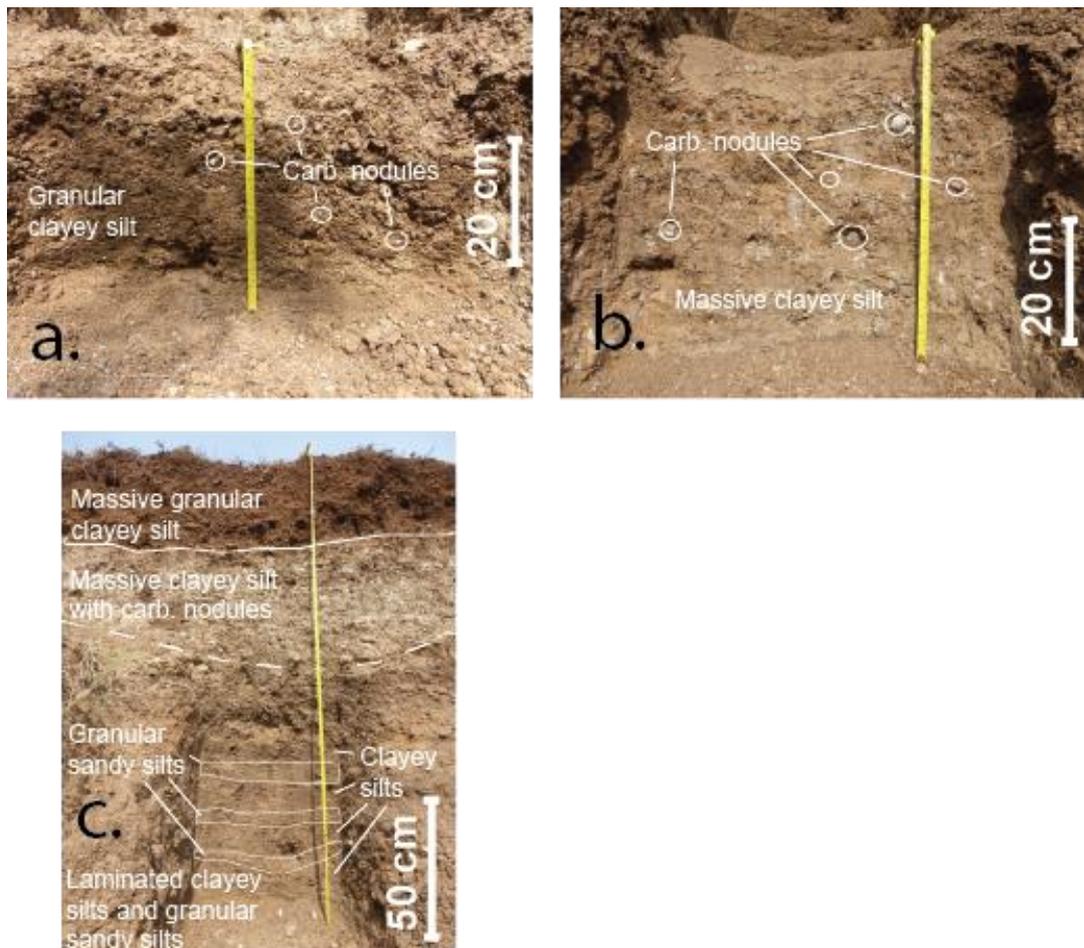
Figure 5.15: Photos of sediments in GT6 at Nyayanga. Letters a – c correspond to the depths sections highlighted in Figure 5.14. Sediment features are highlighted in the images

5.2.6.3. Phytoliths

The phytolith assemblage at Geotrench 6 is dominated by herbaceous phytoliths (Figure 5.16). These are present in very high abundances of 70% to 90%. Grass phytoliths are present in abundances of 10% to 35%; the heist instance is located at 1.6 m in depth. Sedge phytoliths are almost absent, with abundances <5%. Wood phytoliths show a similar trend, although have a single instance where abundances are >10% at 1.6 m; this is the same location grass phytoliths also reach their highest abundance.
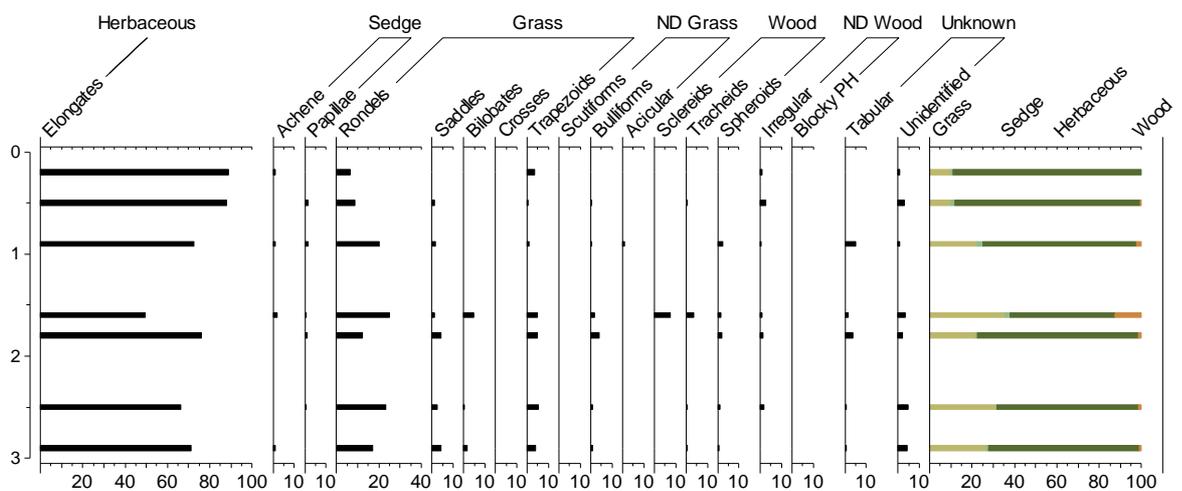
Figure 5.16: Phytolith morphotypes counted at GT6 and their respective percentages. Morphotypes are categorised into vegetation types (Herbaceous, Sedges, Grasses, nondiagnostic (ND) Grasses, Wood, ND Wood and Unknown). The percentages of these vegetation types are presented on the right of the diagram (ND morphotypes are not included here)

5.2.7. Geotrench 7
5.2.7.1. Sedimentology

At the base of Geotrench 7 (Figure 5.17 & Figure 5.18), a massive light grey buff clayey silt exists between ~ 3.3 m and ~ 2.7 m in depth, with cobbles and pebbles in its lowermost parts. This is overlain by a massive orange grey clayey silt with carbonate nodules diffusely dispersed throughout. At ~ 1.8 m the sediments coarsen to more sandy silts with faint horizontal laminations. At ~ 1.6 m, orange sandy silts supporting pebbles and carbonate nodules appear; these sediments have a diffuse contact with overlying massive brown silts at ~ 0.5 m, which contain a clear pedogenic carbonate horizon at ~ 0.25 m.

5.2.7.2.EMMA

Geotrench 7 displays some of the most consistent PSD's up sequence throughout the site, and this is reflected in the EMs (Figure 5.17). EM2 accounts for over 75% of the EM compositions at the base of the trench, and steadily decreases in percentage from the base to the top. EM3 shows the opposite trend and rises from ~ 10% at the base, to ~ 70% at the top of the trench. EM1 is absent for much of the trench, but is infrequently present in percentages <10%.
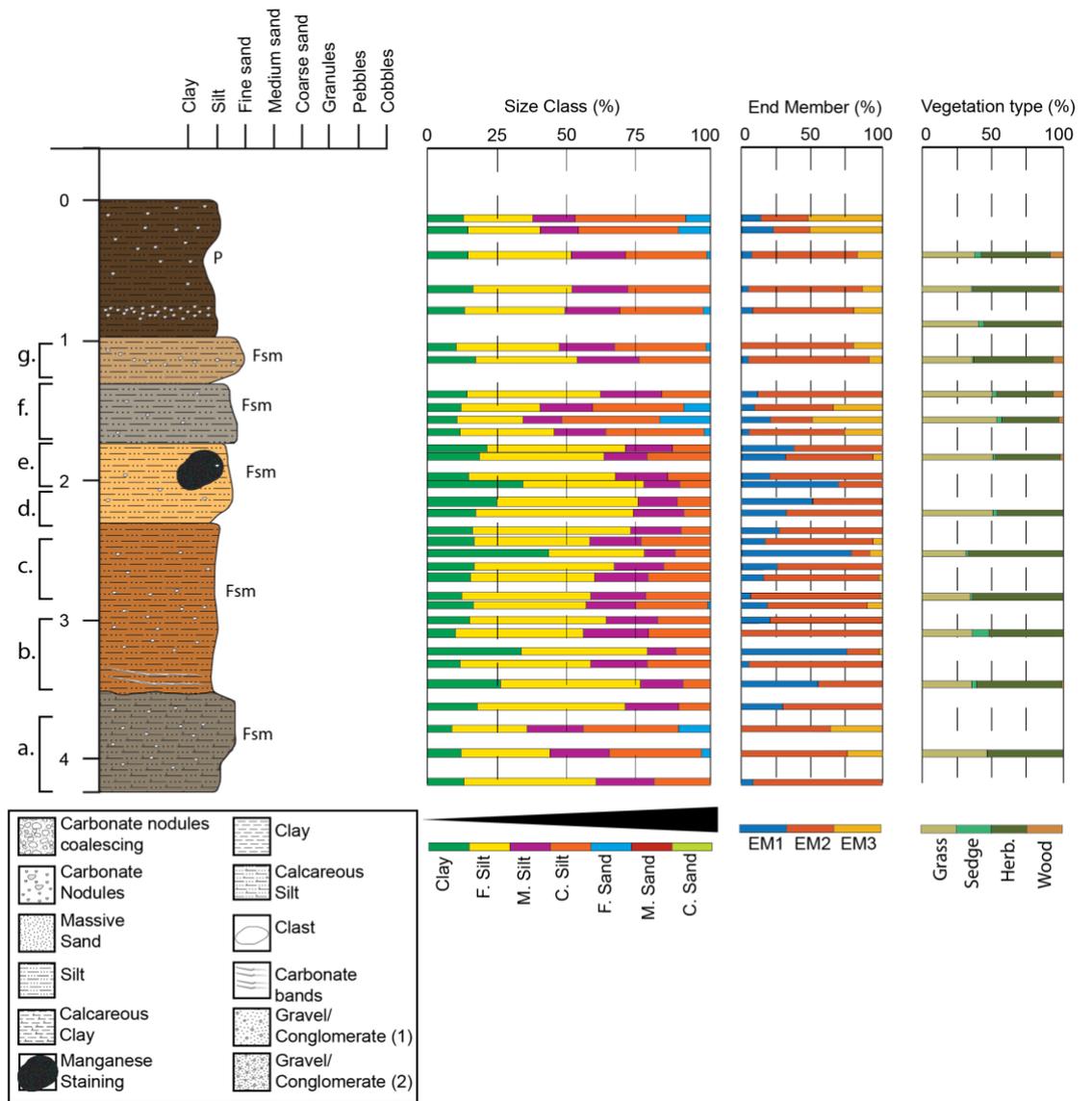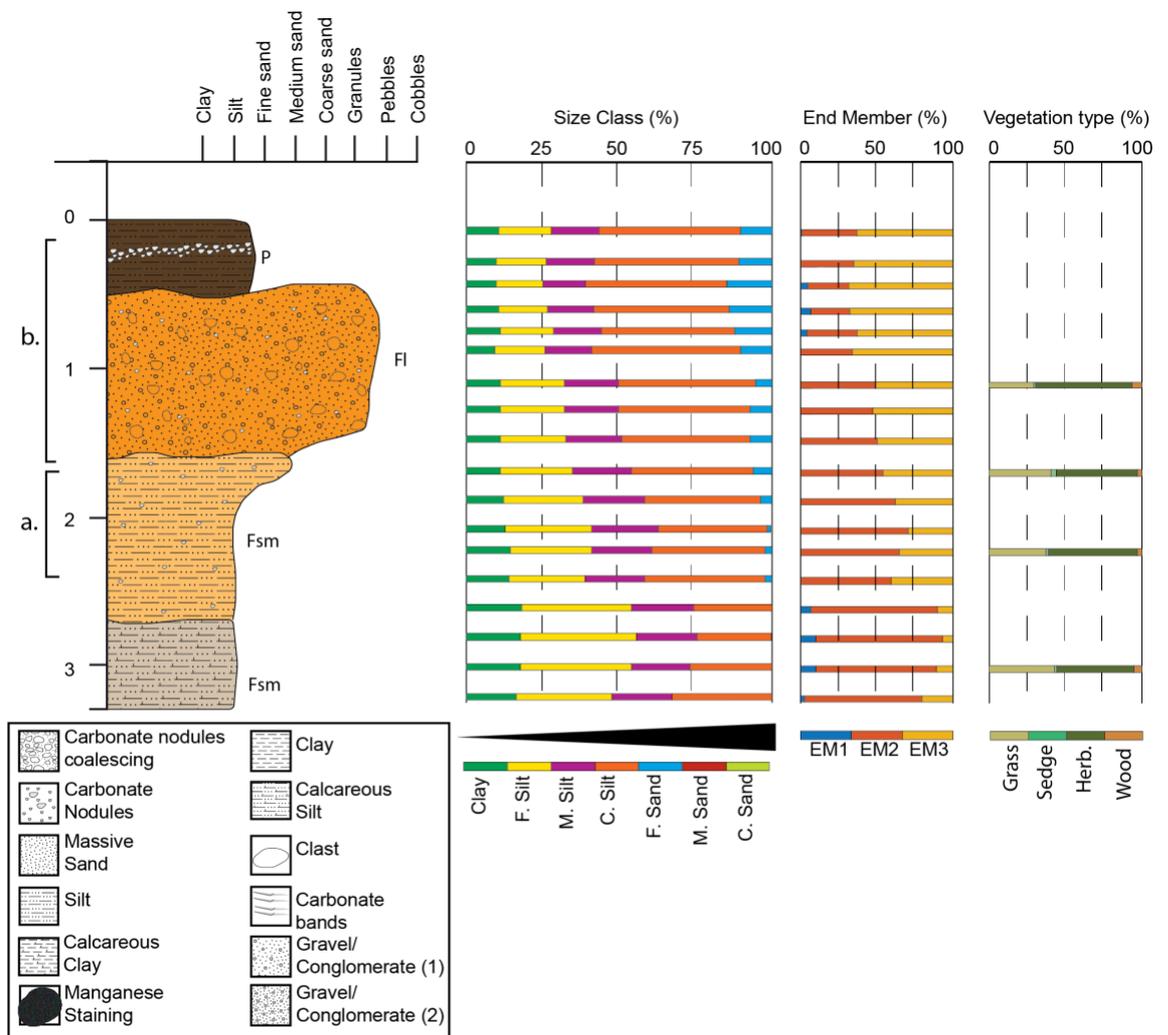

Figure 5.17: Sediment log of Geotrench 7 (Figure 2.3) at Nyayanga. Sediment log depth is presented in metres. Facies codes outlined by Miall (2013) are included on sediment logs. Particle size distributions, EM abundances and vegetation types are also included at corresponding sample depths. Letters a – b. relate to sediment pictures displayed in Figure 5.18
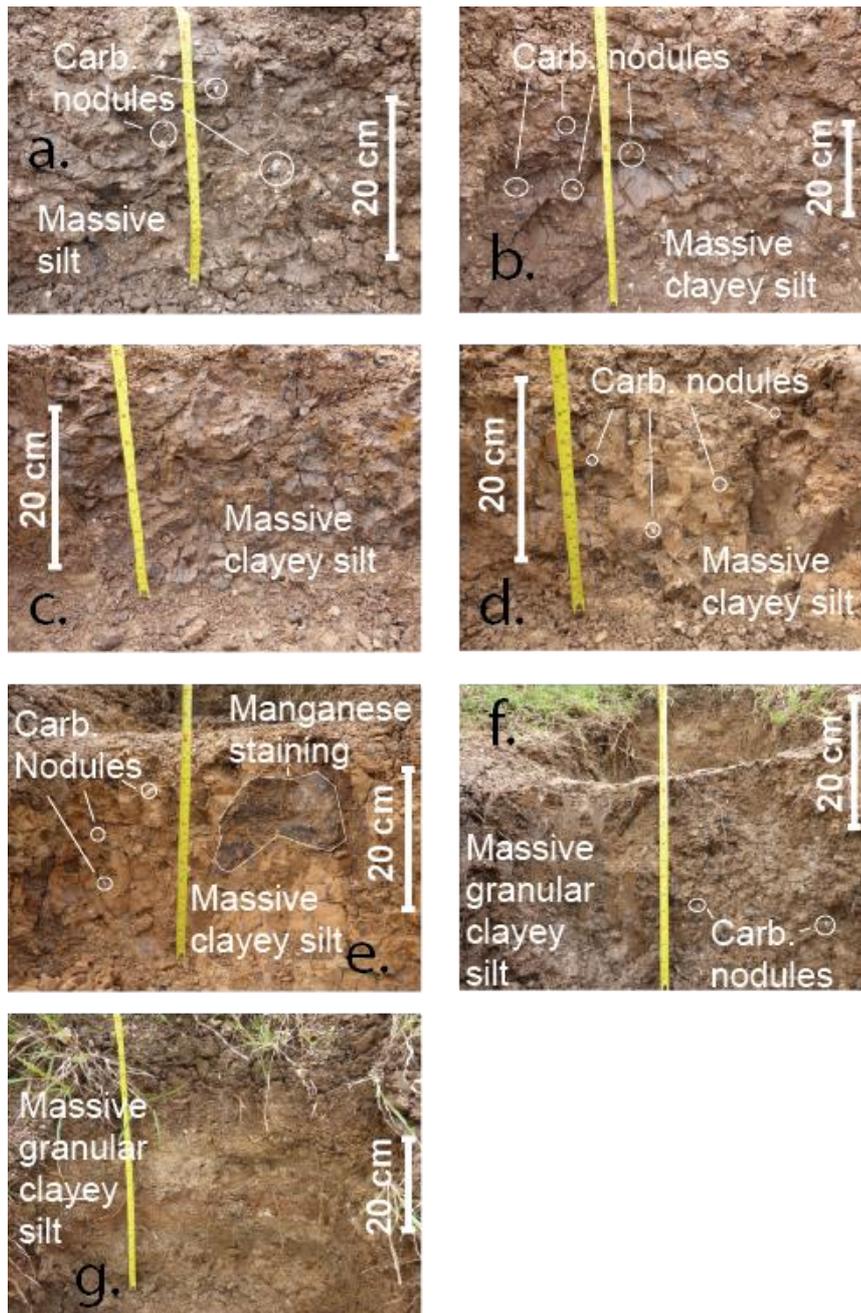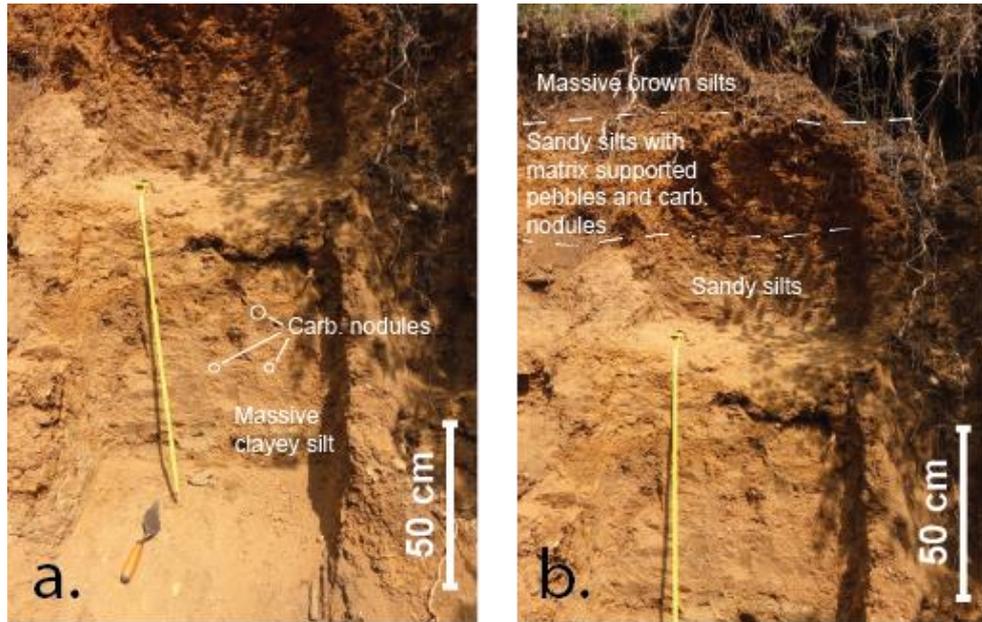
Figure 5.18: Photos of sediments in GT7 at Nyayanga. Letters a – b correspond to the depths sections highlighted in Figure 5.17. Sediment features are highlighted in the images

5.2.7.3.Phytoliths

Geotrench 7 displays a consistent phytolith distribution throughout (Figure 5.19). It is dominated by herbaceous phytoliths, which have an abundance of ~ 50%. Grass phytoliths have

an average abundance of ~ 40% throughout the trench. Wood phytoliths are present in low abundances of ~ 5% throughout, whilst sedge phytoliths are present in even lower abundances.
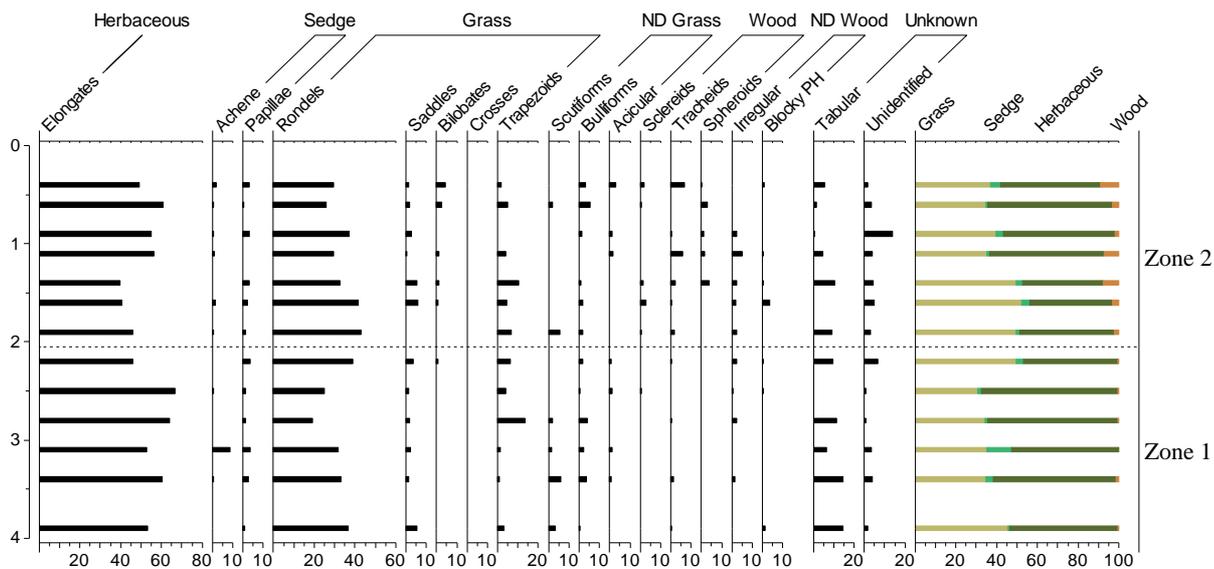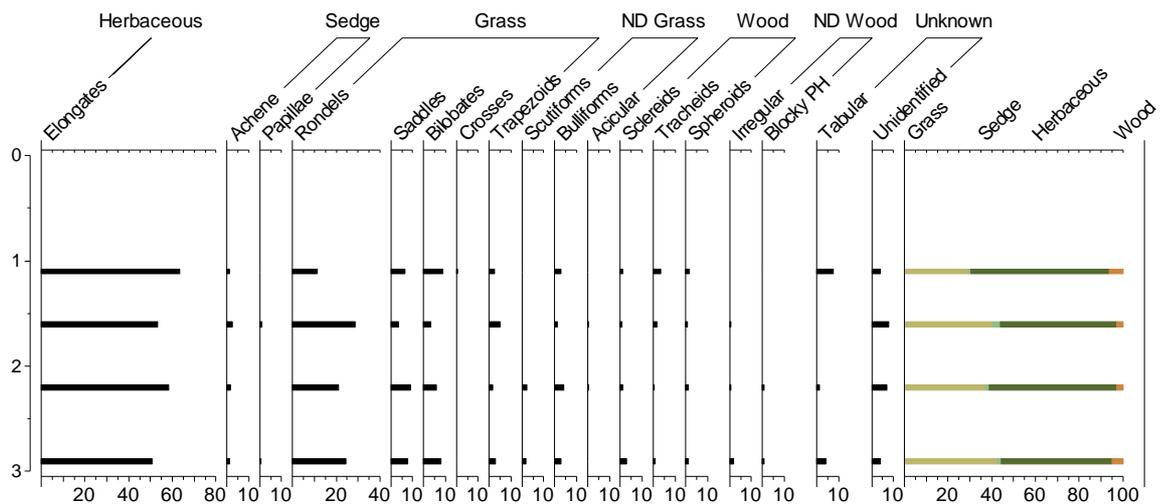

Figure 5.19: Phytolith morphotypes counted at GT7 and their respective percentages. Morphotypes are categorised into vegetation types (Herbaceous, Sedges, Grasses, nondiagnostic (ND) Grasses, Wood, ND Wood and Unknown). The percentages of these vegetation types are presented on the right of the diagram (ND morphotypes are not included here)

5.2.8. Geotrench 8
5.2.8.1.Sedimentology

Geotrench 8 (Figure 5.20 & Figure 5.21) is ~ 3.1 m in depth. At its base, a ~ 60cm massive red brown silt with carbonate nodules exists, overlain by a thin grey clayey silt with diffuse carbonate nodules throughout at ~ 2.5 m. A massive grey silt with reworked carbonate nodules and cementing overlies this at ~ 2.4 m. A diffuse contact exists between these sediments and the overlying massive orange silts at ~ 2.1 m, which are characterised by carbonate nodules and light cementing. At ~ 1.6 m, these sediments have a gradational contact with brown silts, where there is also manganese alteration. A sharp, undulating contact with the overlying light brown silts exists at ~ 1.5 m. These sediments incorporate some larger carbonate nodules towards 1 m.
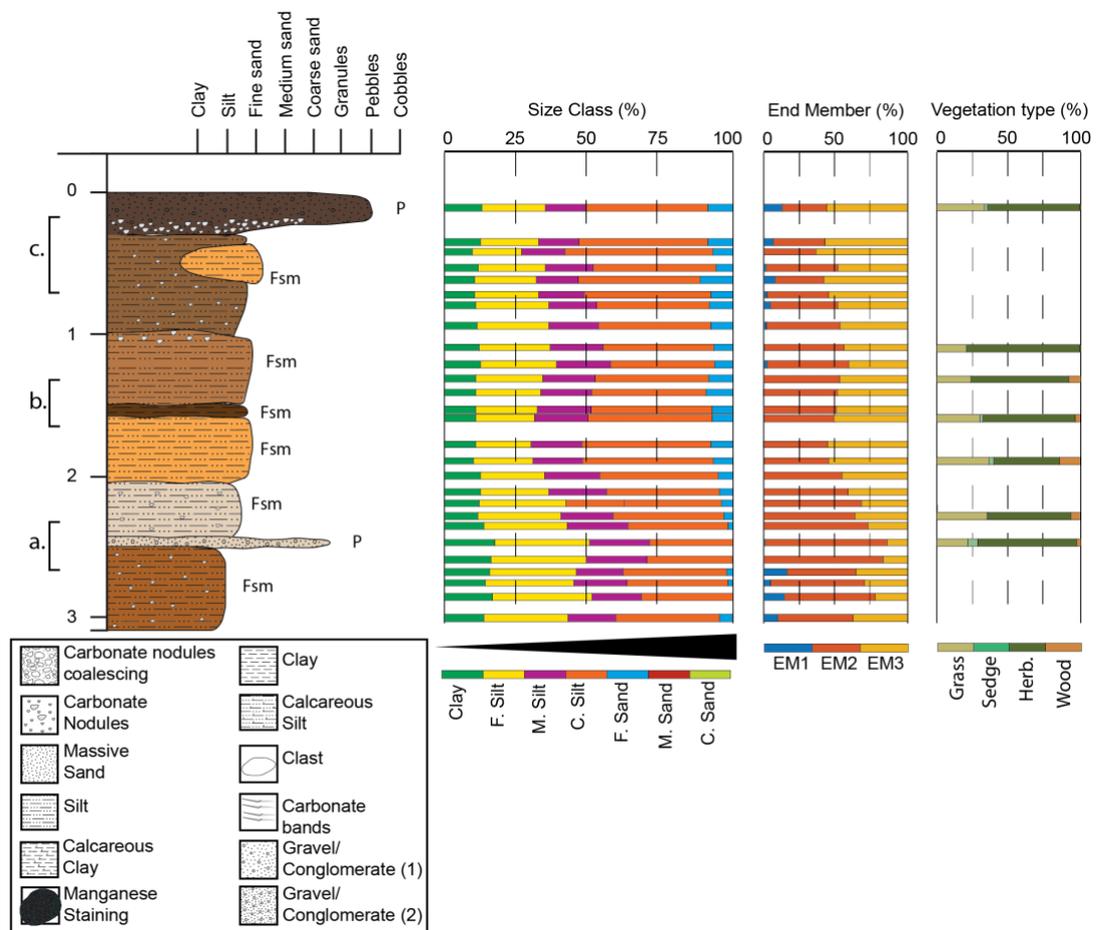
Figure 5.20: Sediment log of Geotrench 8 (Figure 2.3) at Nyayanga. Sediment log depth is presented in metres. Facies codes outlined by Miall (2013) are included on sediment logs. Particle size distributions, EM abundances and vegetation types are also included at corresponding sample depths. Letters a – c. relate to sediment pictures displayed in Figure 5.21

Overlying this at ~ 1 m, a brown clayey silt with diffuse carbonate nodules exists. Within these sediments an isolated light orange silt exists at ~ 0.5 m, which could potentially be a small channel structure. At the top of the trench at ~ 0.3 m there is a massive brown silt with a clear carbonate horizon. This unit is similar to the sediments preserved in the uppermost unit of Geotrench 7.

5.2.8.2. EMMA

Like Geotrench 7, Geotrench 8 has extremely consistent PSD's up sequence throughout all of the units present (Figure 5.20). From the base to ~ 0.9 m, EM2 accounts for most of the EM compositions, but decreases from ~ 75% to ~ 50%. Above this depth, it decreases further to ~ 30% at the top of the trench. EM3 displays the opposite trend and displays a general increase from the base of the trench, where its percentage is ~ 25/35%, to the top of the trench, where it accounts for over
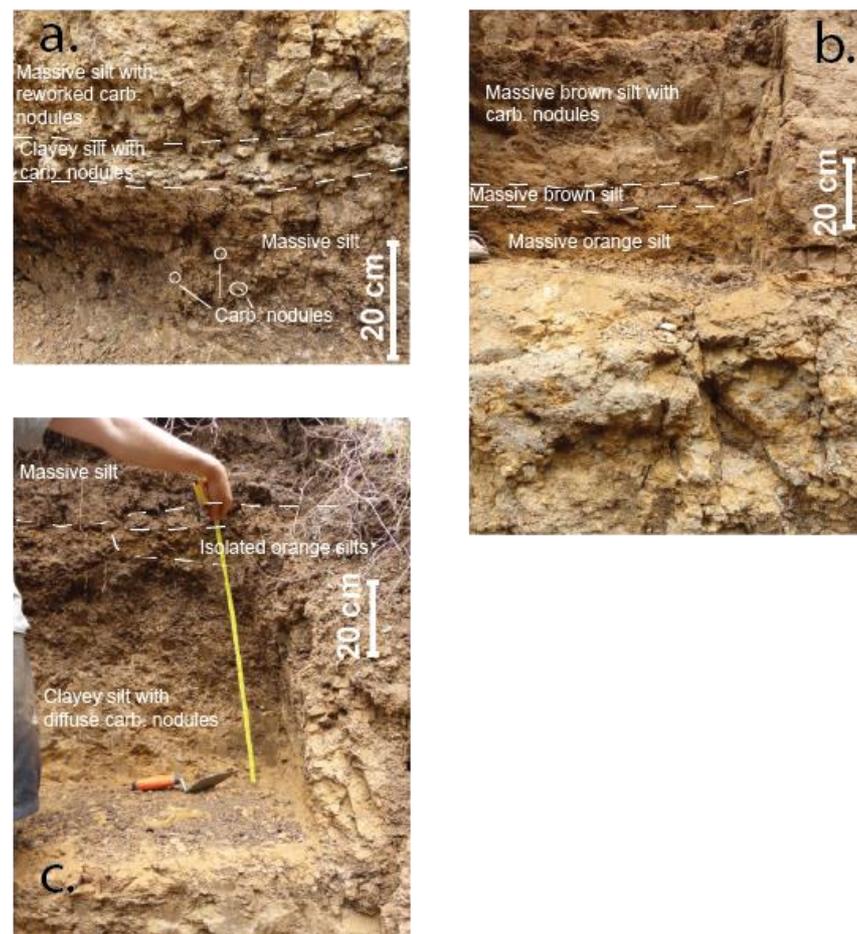
Figure 5.21: Photos of sediments in GT8 at Nyayanga. Letters a – c correspond to the depths sections highlighted in Figure 5.20. Sediment features are highlighted in the images

50% of the EM composition. Like the previous trench EM1 is infrequently present in percentages <20%, but shows a gradual increase from ~ 1.5 to the top of the trench.

5.2.8.3. Phytoliths

Geotrench 8 is dominated by herbaceous phytoliths throughout (Figure 5.22). Grass phytoliths are consistently present in abundances of over 20%. Wood phytoliths show a reduction in percentage throughout the trench, whilst sedge phytoliths are almost absent. Two zones are identified.

Zone 1, which spans from 2.4 m to 1.2 m is dominated by herbaceous phytoliths. Between 2.4 and 1.9 m, grass and wood phytoliths both see an increase in percentage, before decreasing between 1.9 m and 1.2 m. Sedge phytoliths are present in abundances of ~ 5%.

Zone 2 spans from 1.2 m to the top of the trench. It is characterised by an almost complete absence of wood and sedge phytoliths. Herbaceous phytoliths see a reduction in percentage from ~ 75% to ~ 60% throughout this zone, but are still dominant. Grass phytoliths increase from~ 25% to ~ 40% in this zone.
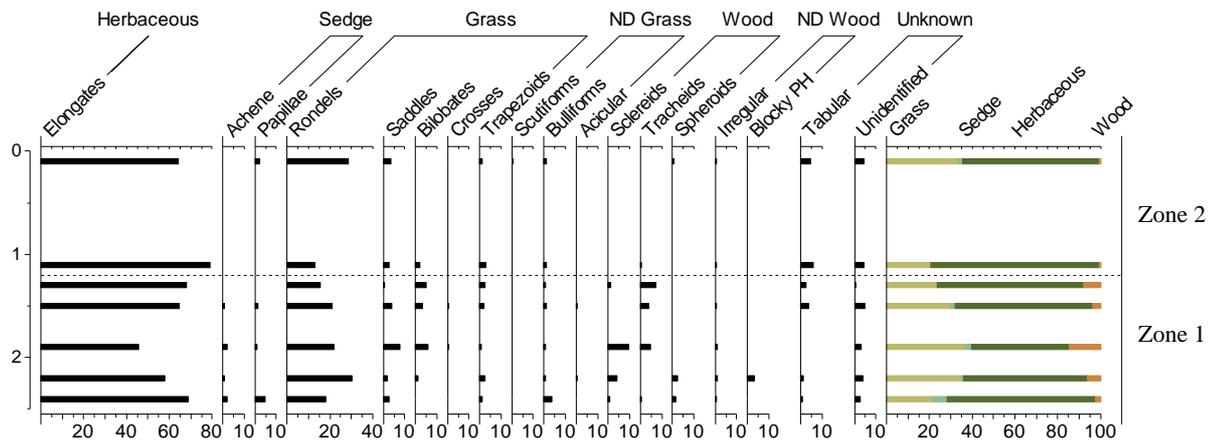
Figure 5.22: Phytolith morphotypes counted at GT8 and their respective percentages. Morphotypes are categorised into vegetation types (Herbaceous, Sedges, Grasses, nondiagnostic (ND) Grasses, Wood, ND Wood and Unknown). The percentages of these vegetation types are presented on the right of the diagram (ND morphotypes are not included here). The diagram is delineated into two zones representing shifts in the vegetation structure

5.2.9. Geotrench 9
5.2.9.1.Sedimentology

Geotrench 9 (Figure 5.23 & Figure 5.24), also ~ 3.1 m in depth, contains massive grey green silts at its base, with occasional carbonate nodules. Overlying this at ~ 2.1 m are massive well sorted brown clayey silts, with no obvious carbonate nodules. At ~ 1.9 there is an orange massive silt with carbonate nodules within. This gradationally changes to a brown clayey silt at ~ 1.7 m which gradually coarsens upwards, but remains predominantly a silt. At ~ 1.3 m, this gradationally shifts towards a massive orange clayey silt with carbonate nodules. A gradational contact with these sediments is also present at ~ 0.9 m, where the sediments become a massive red brown clayey silt with occasional carbonate nodules. This is overlain
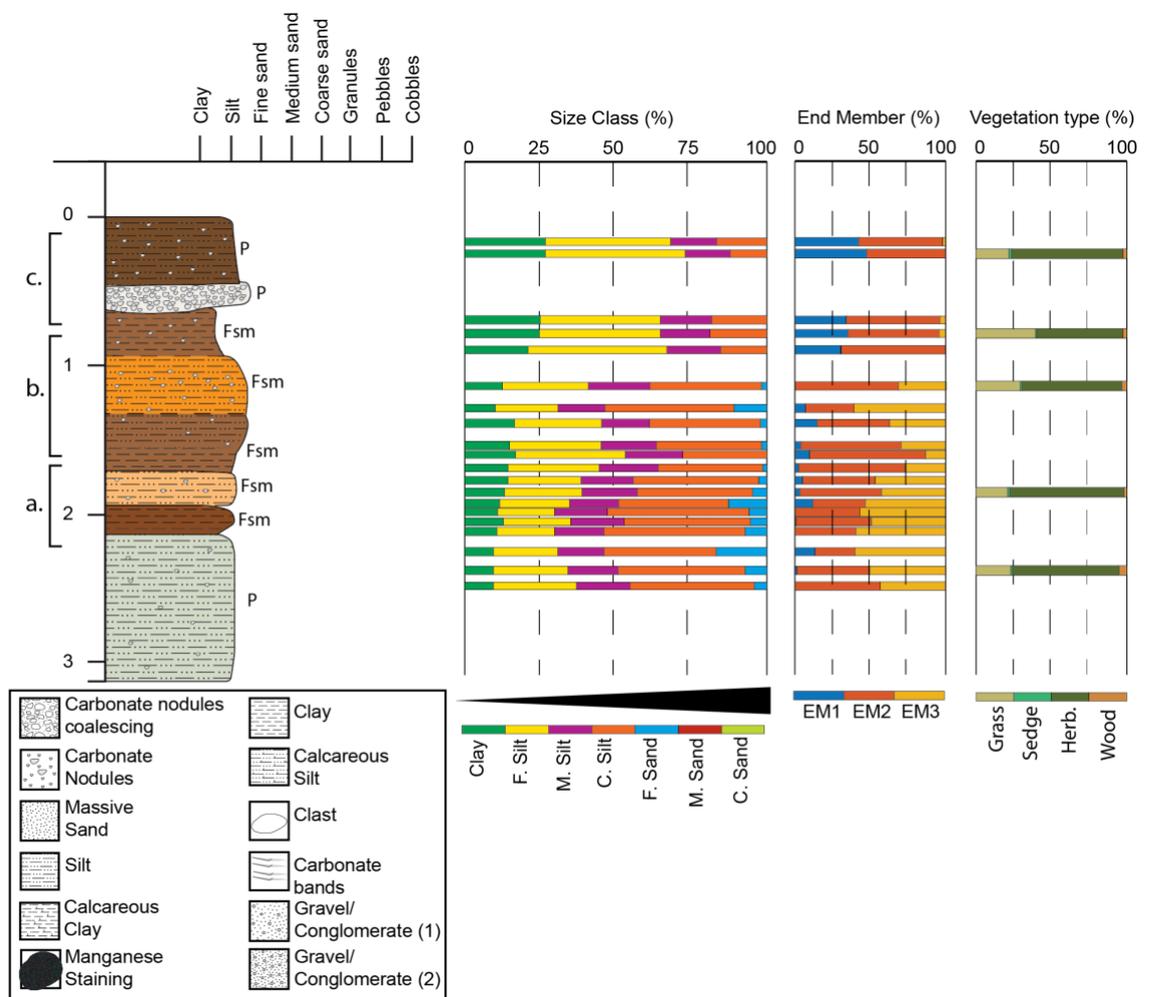
Figure 5.23: Sediment log of Geotrench 9 (Figure 2.3) at Nyayanga. Sediment log depth is presented in metres. Facies codes outlined by Miall (2013) are included on sediment logs. Particle size distributions, EM abundances and vegetation types are also included at corresponding sample depths. Letters a – c. relate to sediment pictures displayed in Figure 5.24

Figure 5.24: Photos of sediments in GT9 at Nyayanga. Letters a – c correspond to the depths sections highlighted in Figure 5.23. Sediment features are highlighted in the images

by a ~ 10cm band of white micrite and carbonate nodules at ~ 0.6 m, which is overlain by a massive brown clayey silt with carbonate nodules.

5.2.9.2.EMMA

In Geotrench 9, EM1 generally displays a gradual increase from its base to the top of trench, from which it goes from being absent in the EM composition to accounting for ~ 50% of it by ~ 0.5 m in depth (Figure 5.23). EM3 shows the opposite trend; at the base of

the trench it is accountable for ~ 50% of the EM composition, but is absent by the top of the trench. EM2 is present throughout the entire trench, generally in abundances of at least 50%, but in places, such as ~ 1 m, reaching almost 75%.

5.2.9.3.Phytoliths

Herbaceous phytoliths dominate Geotrench 9 throughout, with abundances of over 50% (Figure 5.25). Grass phytoliths can be seen to increase in percentage from 25% to 40% between the base of the trench to 1.8 m, before decreasing to 25% at
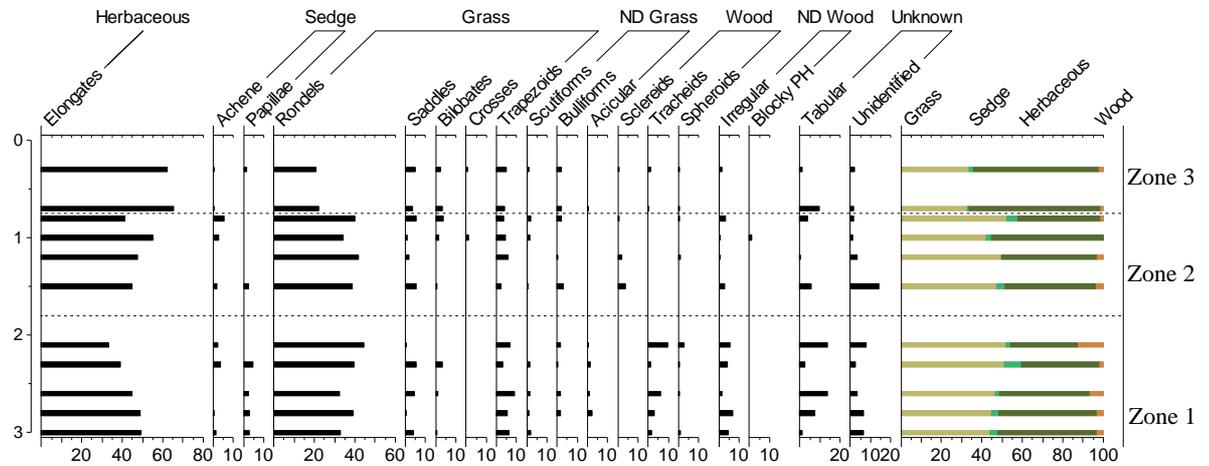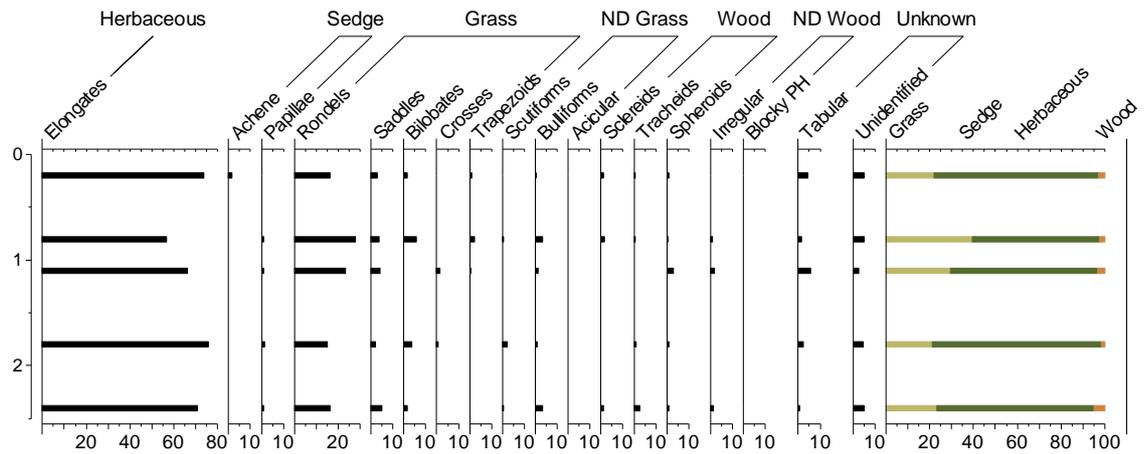
Figure 5.25: Phytolith morphotypes counted at GT9 and their respective percentages. Morphotypes are categorised into vegetation types (Herbaceous, Sedges, Grasses, nondiagnostic (ND) Grasses, Wood, ND Wood and Unknown). The percentages of these vegetation types are presented on the right of the diagram (ND morphotypes are not included here)

the top of the trench. Wood phytoliths are present throughout in low abundances of <5%; sedge phytoliths show a similar trend and are almost absent.

5.2.10. Establishing Sedimentary units

By evaluating these geological trenches, it has been possible to divide the sedimentary sequence at Nyayanga into four different units (NY-1 to 4) across the site. This will be discussed herein and will provide a framework to interpret the palaeoenvironment at Nyayanga. Figure 5.26 displays the previously described geological trenches within the context of these sedimentary units.

5.2.10.1.NY-1

NY-1 has the most extensive presence throughout the geological trenches; it is visible in all trenches. The lithology of this unit varies laterally, although it is largely composed of grey clay/silt rich deposits interbedded with orange sands, the latter of which are associated with granule-cobble grade material. The largest exposures of this unit appear in the southwest of the site at Geotrench 1 to 5, as well as at an excavation which was placed nearby (Figure 5.26); smaller exposures to the northeast further up the canyon are also visible. Due to the variable lithology of this unit, subunits have also been identified.

NY-1A, located between 5.3 m and 4.8 m in GT1 (Figure 5.3), is the lowermost subunit of NY-1 and is seen overlying sediments believed to predate this unit. It is largely structureless and characterised by clasts up to cobbles in size suspended in
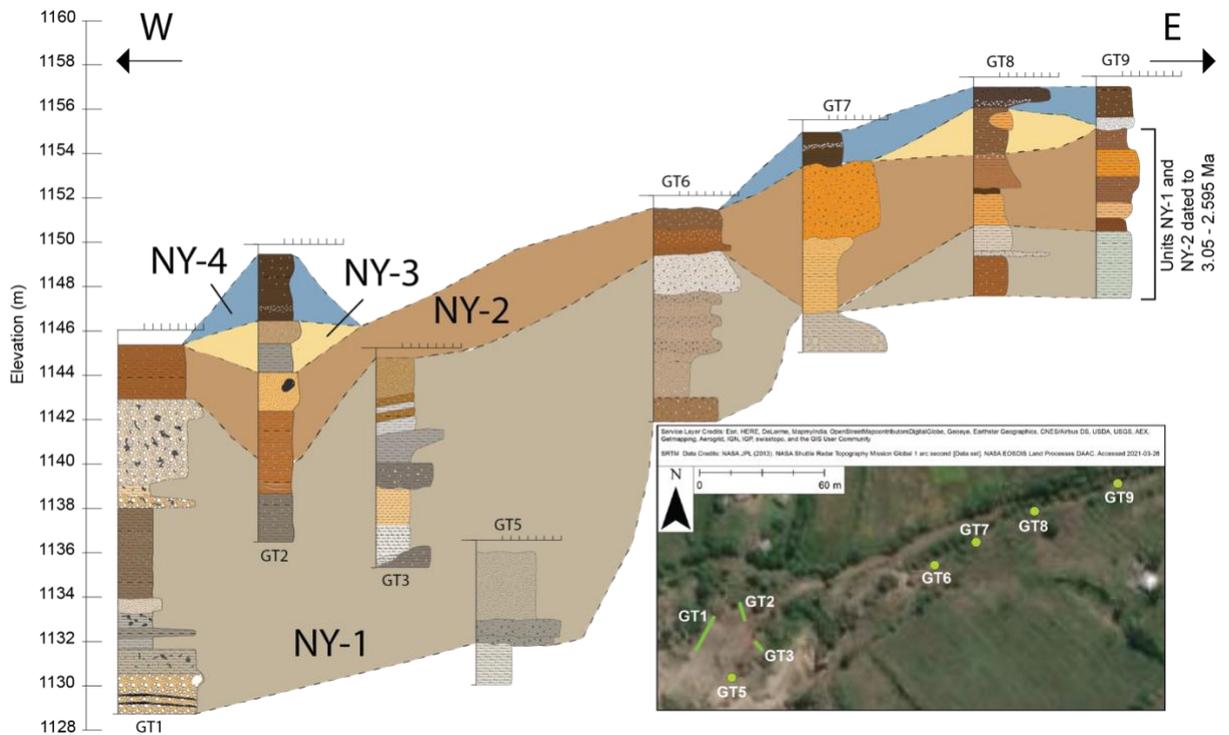
Figure 5.26: Sedimentary units identified site wide at Nyayanga across geotrenches. Vertical placement of geotrenches is representative of their elevation at the site. Horizontal placement of trenches roughly represents their position from west to east of the site. Precise locations of each Geotrench are shown in the inset figure, which is enlarged in Figure 2.3. Sediments from units NY-1 and NY-2 date to 3.05 – 2.595 Ma, based on previously acquired ages from biostratigraphy and magnetostratigraphy (Finestone, 2019)

a fine clayey silt matrix. EM1 is present here in abundances of up to 45%, yet EM2 is dominant. Phytoliths here are dominated by grass and herbaceous indicating phytoliths, although wood and sedge indicating phytoliths remain present in low percentages during this interval.

NY-1B is visible at GT1 (Figure 5.3, 4.8 m – 3.9 m), GT3 (Figure 5.9, 3.1 m – 1.3 m), GT5 (Figure 5.12, 2 m – 0.3 m) and GT6 (Figure 5.14, 3.1 m – 2.2 m). These sediments include interbedded massive muddy matrix supported pebbles and massive muds. Throughout this interval, EM1 and EM2 are most dominant, although EM3 is present, occasionally in abundance. In GT1 and GT3, EM1 and EM2 alternate in dominance. EM1 is frequently abundant when associated with the massive muddy matrix supported pebbles, whilst EM2 is frequently more abundant when associated with the massive muds with some exceptions. EM3 is present in its greatest abundance in the first instance of the massive muds, following which it is less abundant, but still present. In GT5 and GT6 EM1 is less abundant (~ 25%) and the subfacies is largely dominated by EM2 (>50%), whilst in GT6 EM3 is more abundant than elsewhere (>25%). Grass and herbaceous indicating phytoliths are

most abundant in this subfacies, although in GT1 and GT3, wood and sedge indicating phytoliths reach their highest abundance (~ 15%) site wide. However, in GT5 and GT6 they are almost absent.

NY-1C is seen overlying NY-1B in GT1 (3.9 m – 3.7 m), GT3 (1.3 m – 0.6 m), GT5 (0.3 m – 0 m) and GT6 (2.2 m – 1.2 m). In GT1, these sediments are characterised by poorly sorted massive silty sands which have an erosive contact with the underlying massive muds previously described. Increased sand content is characteristic of this subunit, up to coarse sand in size. Similarly, in GT3 an erosive contact exists with underlying sediments, whilst sand content and size also increases. Fluctuations occur in the sand content in GT3 between 1 m and 0.6 m, with sand content generally decreasing, before increasing sharply again. Similarly, in GT6 sand content and size increases sharply at 2 m, before sharply decreasing and then steadily increasing up to 1.2 m. In GT5 sand content also increases at 0.3 m, where before it was absent. Unlike the sediments at the other trenches, sands here are not as coarse. EM2 and EM3 are most abundant throughout this subunit. GT1 and GT5 are dominated by EM3, where it accounts for ~ 50% of the EM composition, whilst in GT3 and GT6, EM2 is most abundant. EM1 is poorly represented throughout this subunit, with abundances of ~ 25% or lower throughout all of the trenches. Phytoliths samples were not taken for instances of this subunit in GT1 and GT5. However, in GT3 and GT6 phytoliths in these sediments are characterised by grass and herbaceous indicating phytoliths.

NY-1D is seen overlying NY-1C in GT1 (Figure 5.3, 3.7 m – 2.3 m) and GT3 (Figure 5.9, 0.6 m – 0 m). It is also visible in GT2 (Figure 5.6, 4.2 m – 3.5 m) and GT8 (Figure 5.20, 3.1 m – 2.5 m). Sediments in this subunit are characterised by massive grey brown clayey silts with carbonate nodules and occasional granules in GT1 and GT2. At GT3, sediments in this subunit are slightly coarser and are characterised by massive orange brown sandy silts with carbonate nodules. In GT8 NY-1D is comprised of a massive red brown silt with carbonate nodules, similar to sediments in GT1 and GT2. EM2 is dominant throughout much of this subunit, apart from GT1 where it is present in low percentages. Here, EM1 is largely dominant. EM3 is also present throughout this subunit with abundances of approximately 15 – 25%. Vegetation throughout this subunit is characterised by large percentages of grass

and herbaceous indicating phytoliths. Sedge indicating phytoliths are also present in low percentages (<10%). Wood indicating phytoliths are largely absent other than in GT1 where they are present throughout this subunit in low percentages (<10%).

NY-1E is the uppermost subunit of NY-1. It is visible in GT1 (Figure 5.3, 2.4 m – 0.9 m), GT6 (Figure 5.14, 1.2 m – 0.8 m), GT7 (Figure 5.17, 3.2 m – 2.8 m), GT8 (Figure 5.20, 2.5 m – 2 m) and GT9 (Figure 5.23, 3.1 m – 2.1 m). This subunit is characterised by carbonaceous clayey silts. In GT1, it is massive, light orange in colour and contains coalescing carbonate nodules up to pebbles in size. In GT6 it is a massive grey clayey silt with carbonate nodules up to pebbles in size dispersed throughout. In GT7, carbonate nodules are absent, but sediment are light grey buff clayey silts, with occasional pebbles and cobbles at its base. At GT8, the base of this subunit is comprised of a thin grey brown clayey silt with coalescing carbonate nodules. Overlying this is a massive grey silt with cemented carbonate nodules. In GT9, massive grey green silts with occasional carbonate nodules characterise this subunit. Throughout these exposures, EM2 is particularly dominant comprising at least 50% of the EM composition. The only exception to this is GT9, where EM3 is mostly dominant (~ 50%). EM3 is also present in all other exposures, generally with abundances of 30% or less. EM1 is most poorly represented throughout this subunit. It is almost completely absent from all exposures with the exception of GT1. Here it is dominant (>50%) in two instances, but generally present in abundances of ~ 25%. Phytoliths in this subunit are characterised by abundant grass and herbaceous indicating phytoliths. Wood and sedge indicating phytoliths are infrequent and never present in abundances higher than 10%.

5.2.10.2.NY-2
NY-2 is well exposed throughout the entirety of Nyayanga (Figure 5.26), with the exceptions of Geotrench 4 and 5. Most commonly, it is a massive red brown strongly pedogenically altered clayey silt with sandy intercalations of coarse sand to granules, much of which is stained with manganese. However, some due to lateral variance in the unit, subunits have been identified.

NY-2A is the lowermost subunit of unit NY-2. It is visible in GT1 (Figure 5.3, 0.8 m – 0 m), GT2 (Figure 5.6, 3.5 m – 2.3 m), GT6 (Figure 5.14, 0.7 m – 0 m) and GT9 (Figure 5.23, 2.1 m – 1.9 m). This subunit is characterised by massive clayey silts

with pedogenic carbonates dispersed throughout much of the subunit. Sediment are frequently red brown in colour and occasionally incorporate granules in some areas (GT6). EM characteristics throughout this subunit are laterally variable. In GT1, EM1 and EM2 fluctuate in abundance significantly from as much as 75% to as little as 10% of the EM composition. EM3 is present here throughout in low percentages (<25). In GT2, EM2 is largely dominant throughout this subunit (>70%), with the exception of two instances upon which EM1 is most abundant (>75%). EM3 is less frequently absent from this subunit here, and only present in very low abundances (<10%). EM2 is also consistently dominant throughout GT6 (>50%), although not as abundant as in GT2. EM1 and EM3 are also both consistently present throughout in similar percentages to one another (<25%). In GT9, EM3 is dominant throughout this subunit (>50%), whilst EM2 comprises the rest of the EM composition. EM1 is almost entirely absent here. Phytoliths throughout this subunit are dominated by herbaceous indicating phytoliths in all trenches other than GT1, where grass indicating phytoliths are dominant. Grass indicating phytoliths are present throughout all of this subunit, whilst wood and sedge indicating phytoliths are almost entirely absent.

NY-2B is exposed in GT2 (Figure 5.6, 2.3 m – 1.7 m), GT7 (Figure 5.17, 2.7 – 1.8 m), GT8 (Figure 5.20, 2.1 m – 1.5 m) and GT9 (Figure 5.23, 1.9 m – 1.7 m). This subunit is characterised by massive orange grey clayey silts with carbonate nodules dispersed throughout, as well as light cementing. EM1 is only present in GT2, where it fluctuates in abundance between 25% and 75%. EM2 is more abundant here for most of the exposure, whilst EM3 is almost entirely absent. EM2 and EM3 account for the entire composition in all other exposures. EM2 is generally dominant although only marginally. Grass and herbaceous indicating phytoliths are most abundant in these sediments, with herbaceous phytoliths mostly dominant. Wood and sedge phytoliths are present in low abundances (<15%).

NY-2C is visible in GT7 (Figure 5.17, 1.5 m – 0.5 m), GT8 (Figure 5.20, 1.5 m – 1 m) and GT9 (Figure 5.23, 1.7 m – 0.9 m). Sediments in this subunit vary laterally. In GT7, sediments belonging to this subunit are characterised by orange sandy silts supporting pebbles and carbonate nodules. At GT8, there is a small reduction in sand content and sediments are composed of light brown silts. In GT9, sand content

reduces further and sediments are characterised by brown clayey silts which lighten in colour to orange clayey silts incorporating carbonate nodules. The absence of EM1 and abundances of EM2 and EM3 characterise this subunit. In GT7, EM3 is most dominant, and increases in abundance moving upward throughout the subunit. EM2 is present throughout and displays the opposite trend, whilst EM1 is largely absent. In GT8, EM2 and EM3 are relatively equal in abundance throughout, whilst EM1 is absent for much of this exposure. EM2 is most abundant at GT9, although EM3 is dominant in the upper part of this subunit. EM1 is more abundant here than in other exposures, but still in low percentages. Herbaceous indicating phytoliths dominate this subunit throughout. Grass indicating phytoliths are present in abundances of ~ 25%. Wood indicating phytoliths are present in low abundances (<10%), whilst sedge indicating phytoliths are absent.

5.2.10.3. NY-3

NY-3 is the most poorly exposed sedimentary unit throughout Nyayanga, only visible in GT2 (Figure 5.6, 1.7 m – 1 m) and GT8 (Figure 5.20, 1 m – 0.3 m). The lower part of this subunit is composed of grey orange granular silts with carbonate nodules. In its upper part, it is characterised by orange/brown silts with increased amounts of carbonate nodules. EM2 and EM3 are present in relatively equal abundances for the lower part of this subunit, whilst EM2 becomes largely dominant (>75%) in the upper parts. EM1 is present in very low percentages throughout the subunit (<15%). Grass and herbaceous indicating phytoliths are most abundant throughout this subunit. Grass indicating phytoliths have a slightly higher abundance in the lower parts, whilst herbaceous indicating phytoliths are more abundant in the upper parts. Wood indicating phytoliths increase in abundance throughout this subunit, yet are still very low in percentage. Sedge indicating phytoliths show the opposite trend.

5.2.10.4. NY-4

NY-4 is exposed throughout GT2 (Figure 5.6, 0.8 m – 0 m), GT7 (Figure 5.17, 0.5 m – 0 m), GT8 (0.3 m – 0 m) and GT9 (0.9 m – 0 m). Sediments throughout this subunit are characterised by massive brown silts with pedogenic carbonates throughout, at times coalescing to form cemented horizons. EM2 and EM3 compose much of this subunit. EM3 is dominant in GT7 and GT8, whilst EM2 dominates GT9

and much of GT2. EM1 is present in all exposure in low abundances, apart from in GT9 where it is particularly abundant (>40%). Herbaceous indicating phytoliths dominate this subunit, whilst grass indicating phytoliths are also moderately abundant (~ 30%). Wood and sedge indicating phytoliths are present in very low percentages (<10%).

5.2.11. Closing Statement/Table of lithology

In summary, Nyayanga displays four sedimentary units that have been identified and described through various analytical techniques (Table 5.1). These units vary laterally over a ~ 200 m transect between the southwest and northeast of the site, the former of which shows larger exposures than the latter. The site is generally characterised by carbonate rich fine grained sediment with occasional coarser material up to cobbles in size. Sediments are poorly sorted throughout and often multimodal in nature. These sediments have been 'unmixed' into three EMs, which may shed light on the sedimentary processes that occurred surrounding the time of deposition. Known phytolith assemblages are heavily dominated by grass and herbaceous indicating phytoliths, particularly elongates and rondels. Wood and sedge indicating phytoliths are much less frequent and at times absent.

Unit	Subunit	Exposure	Sedimentology/Particle size	EMMA	Phytoliths
NY-1	NY-1A	GT1	Massive poorly sorted clayey silts with clasts up to cobbles matrix supported. Carbonate nodules present	EM2 is most abundant. EM1 present in abundances of up to 45%. EM3 absent	Dominated by grasses and herbs. Wood and sedges present in low percentages
	NY-1B	GT1, GT3, GT5, GT6	Interbedded poorly sorted massive muddy matrix supported pebbles and poorly sorted massive muds.	EM1 and EM2 most abundant throughout, EM3 occasionally abundant. EM1 associated with massive muddy matrix supported pebbles. EM2 associated with massive muds. EM3 abundant with first instance of massive muds	Grasses and herbs most abundant throughout. Wood and sedges their highest abundance site wide (~ 15%) in GT1 and GT3.
	NY-1C	GT1, GT3, GT5, GT6	Poorly sorted massive silty sands and sandy silts with erosive contact to underlying sediments in places. Sand up to coarse sand in size. Fluctuating sand content throughout.	EM2 and EM3 dominant throughout. EM3 dominant in GT1 and GT5, EM2 dominant in GT3 and GT6. EM1 poorly represented throughout (<25%).	Grasses and herbs characteristic of this subunit.
	NY-1D	GT1, GT2, GT3, GT8	Poorly sorted massive silts with carbonate nodules and occasional granules. Colour varies throughout exposures. Grey brown in GT1 and GT2, orange brown in GT3 and red brown in GT8.	EM2 dominant throughout most exposures other than GT1 where EM1 is dominant. EM3 present throughout all exposures.	Grasses and herbs dominant. Sedges present in low percentages. Wood absent other than GT1
	NY-1E	GT1, GT6, GT7, GT8, GT9	Poorly sorted carbonaceous clayey silts. Light orange in colour at GT1. Light grey in colour at other exposures. Coalescing carbonate nodules in GT1. Dispersed carbonate nodules elsewhere.	EM2 dominant throughout, other than at GT9 where EM3 is dominant. EM1 poorly represented throughout subunit, other than in GT1.	Grasses and herbs dominant throughout. Wood and sedges infrequent
NY-2	NY-2A	GT1, GT2, GT6, GT9	Poorly sorted massive clayey silts with pedogenic carbonates dispersed throughout. Red brown in colour with occasional granules.	Laterally variable EM characteristics. EM1 and EM2 fluctuate in abundance and dominate GT1. EM2 dominant throughout GT2 and GT6. EM3 dominates GT9, but EM2 abundant.	Herbs dominant throughout. Grasses abundant. Absence of wood and sedges.
	NY-2B	GT2, GT7, GT8, GT9	Poorly sorted massive orange grey clayey silts with carbonate nodules dispersed throughout and occasional cementing.	EM2 and EM3 most abundant in relatively even proportions. EM1 only present in GT2, where it fluctuates in abundance and is occasionally dominant; EM3 absent here.	Grasses and herbs most abundant. Wood and sedges present but in low abundances (<15%)

	NY-2C	GT7, GT8, GT9	Laterally variable sediments. Poorly sorted orange sandy silts supporting pebbles and carbonate nodules in GT7. Light brown poorly sorted sandy silts in GT8. Poorly sorted brown clayey silts with carbonate nodules in GT9.	EM1 largely absent throughout. EM2 and EM3 dominant in relatively equal abundances.	Herbs most abundant, but grasses present in abundance of ~ 25%. Wood present in low abundances. Sedges absent.
NY-3	-	GT2, GT8	Grey orange granular silts with infrequent carbonate nodules comprise the lower parts of this subunit. Orange/brown silts with increased carbonate nodules form the upper parts.	EM2 and EM3 present in relatively equal abundances for the lower part this subunit. EM2 dominant in upper parts. EM1 present in very low percentages throughout.	Grass and herb dominated. Grasses most abundant in lower parts, whilst herbs more abundant in upper parts. Wood increases in abundance throughout subunit, but remains low in percentage.
NY-4	-	GT2, GT7, GT8, GT9	Poorly sorted massive brown silts. Pedogenic carbonates throughout, at times coalescing to form cemented horizons.	Largely dominated by EM2 and EM3. EM3 dominant in GT7 and GT8, whilst EM2 dominant in GT9 and GT2. EM1 present throughout in low percentages, other than in GT9 where it is particularly abundant.	Herbs dominate throughout, whilst grasses are also moderately abundant. Wood and sedges are present in very low percentages.

Table 5.1: A summary of the different sedimentary units identified at Nyayanga, as well as their lateral variance. Their EM characteristics and phytolith distribution are also included

5.3. Sare River
5.3.1. EMMA

At Sare River, a two EM model best represents the dataset without overfitting (Figure 5.27). A high coefficient of determination was achieved (r^2=0.989), in addition to a low linear correlation between the two EMs (r^2=0.299). A very low angular deviation was also obtained (θ=4.616). The EM model was well fitted to all samples; no samples deviated from the r^2 value significantly. The same process applied to the Nyayanga EM model was applied here.
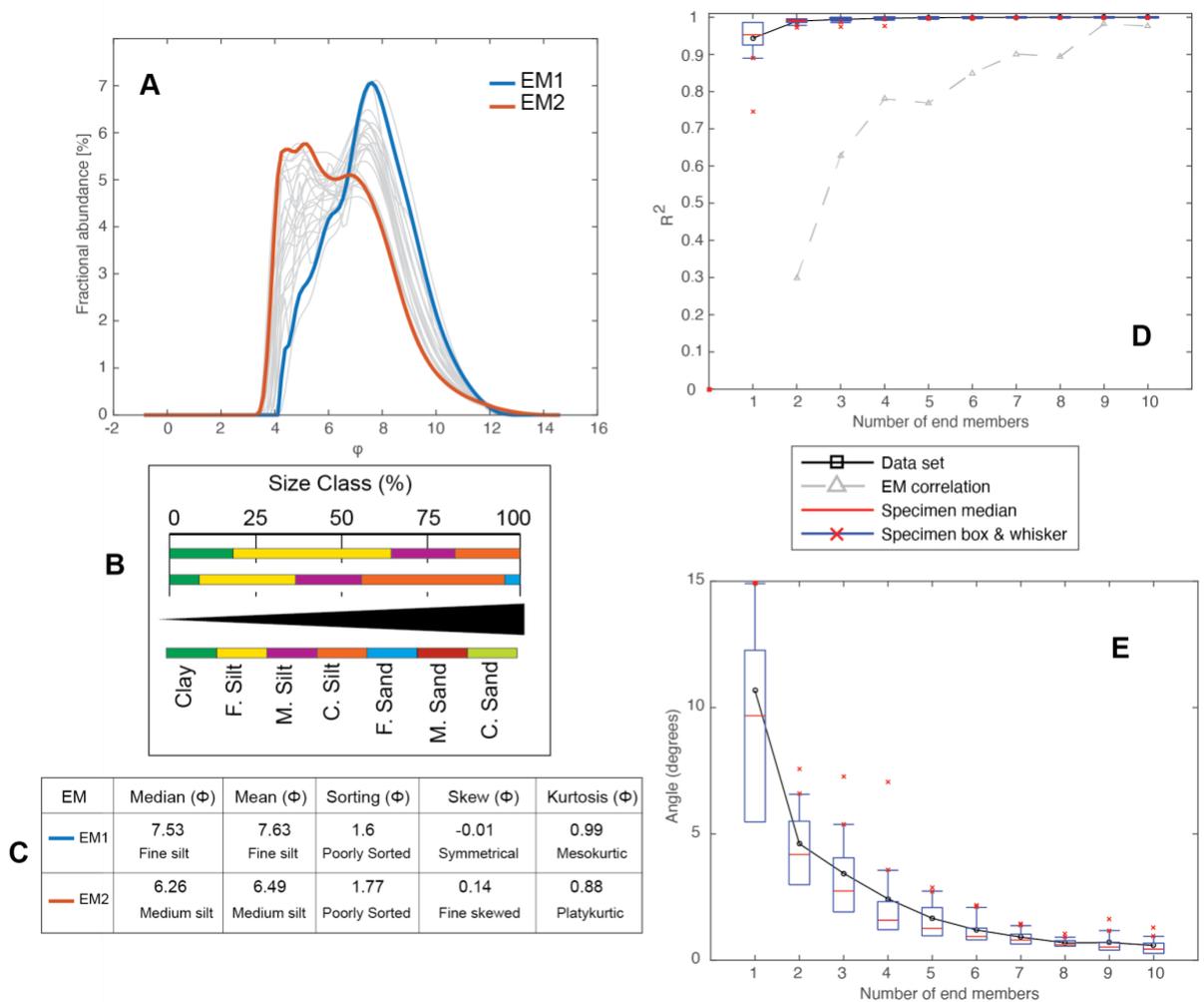
Figure 5.27: EM plots for particle size distributions at Sare River. (A) The two EM model overlaid on particle size distributions from Nyayanga, (B) Size fractions of each EM, (C) Textural parameters of each EM, (D) Linear correlations for each EM scenario (E) Angular deviations for each EM scenario

5.3.1.1. EM1

EM1 is a unimodal symmetrical poorly sorted clayey silt (Figure 5.27), with an average grain size of 7.63 Φ which resembles a fine silt. With a kurtosis value of

0.99, EM1 is classed as mesokurtic; this indicates the sorting is consistent at both the tails and central portion of the distribution.

5.3.1.2.EM2

EM2 is a multimodal fine skewed poorly sorted silt (Figure 5.27). The median is more appropriate to use as a descriptor of average grain size whilst the distribution is multimodal. This is coarser than EM1, with a value of 6.26 Φ, making it a medium silt. The kurtosis of EM2 is 0.88, making it platykurtic; this suggests that the distribution is better sorted in its tail than in its central portion.

5.3.2. Excavation 4

5.3.2.1.Sedimentology

Excavation 4 is 1.4 m in depth (Figure 5.28). At its base, it is a poorly sorted grey brown granular silt. Within this are coarser orange silts. Unlike previous excavations, it has no evidence of any carbonate. Some roots are present. This gradationally shifts into the overlying poorly sorted granular orange silts at 0.6 m. Very infrequent small traces of carbonate nodules are present in this horizon. This gradationally
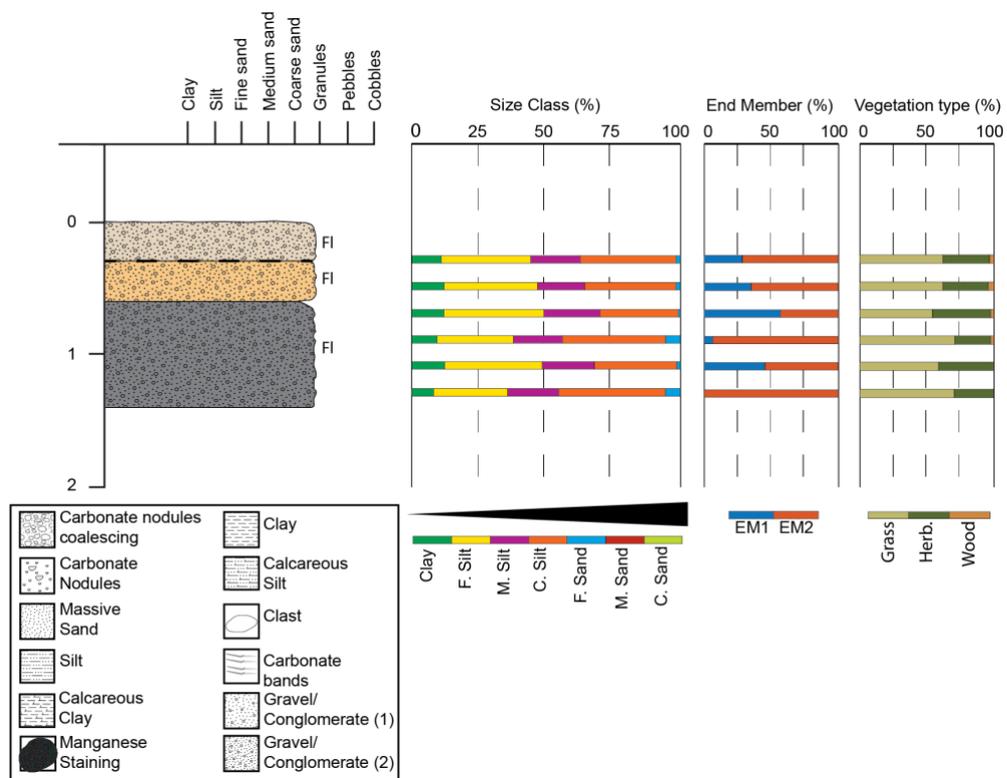
Figure 5.28: Sediment log of Excavation 4 (Figure 2.8) at Sare River. Sediment log depth is presented in metres. Facies codes outlined by Miall (2013) are included on sediment logs. Particle size distributions, EM abundances and vegetation types are also included at corresponding sample depths

shifts into an orange grey poorly sorted granular silt; only a change in colour can be observed.

5.3.2.2. EMMA

Excavation 4 is dominated by EM2, although EM1 is present throughout the excavation; at 0.8 m it is the most dominant EM, and at 1.2 m it accounts for almost 50% of the EM composition (Figure 5.28).

5.3.2.3. Phytoliths

A similar trend in phytolith distributions to Excavations 1 and 5 emerges in Excavation 4 (Figure 5.29). Grass phytoliths dominate the phytolith distribution throughout the excavation, with an abundance >55%. Within the grass phytoliths, bilobates decrease throughout the excavation from ~ 15% to <5%. Herbaceous phytoliths are generally present in abundance of 30%. Wood phytoliths show an increase in percentage from the base of the excavation to the top, yet still account for <5% of the known phytolith distribution. Like previous excavations at Sare River, there are a significant number of nondiagnostic wood phytoliths present throughout.
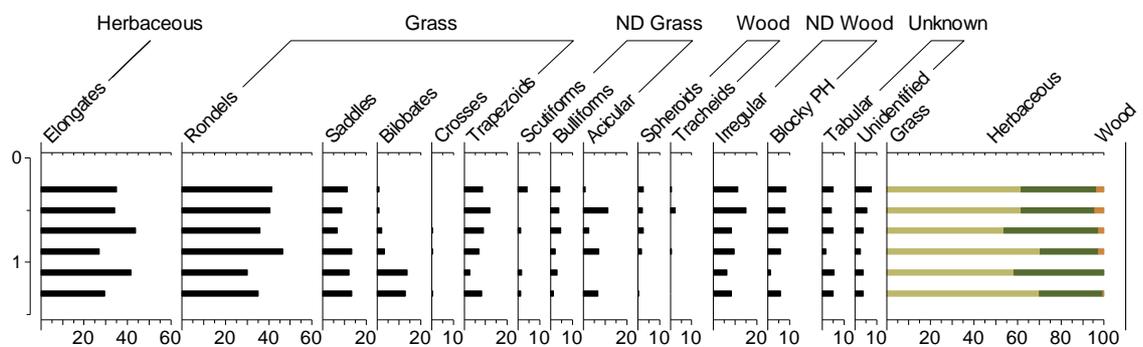
Figure 5.29: Phytolith morphotypes counted at EXC4 and their respective percentages. Morphotypes are categorised into vegetation types (Herbaceous, Grasses, nondiagnostic (ND) Grasses, Wood, ND Wood and Unknown). The percentages of these vegetation types are presented on the right of the diagram (ND morphotypes are not included here).

5.3.3. Excavation 1
5.3.3.1. Sedimentology

Excavation 1 at Sare River is 1.6 m in depth (Figure 5.30). At its base, it is composed of a massive poorly sorted orange grey tuffaceous silt, with occasional carbonate nodules. Overlying this at 1.1 m in depth is a massive poorly sorted grey brown silt with frequent carbonate nodules. Occasional roots are also present in the upper part of this horizon. This is overlain by a dark brown black silty topsoil at 0.4 m in depth.

5.3.3.2.EMMA

Excavation 1 is consistently dominated by EM1 throughout with very little fluctuation. EM2 is present throughout much of the excavation, accounting for ~ 25 – 35% of the EM composition (Figure 5.30).
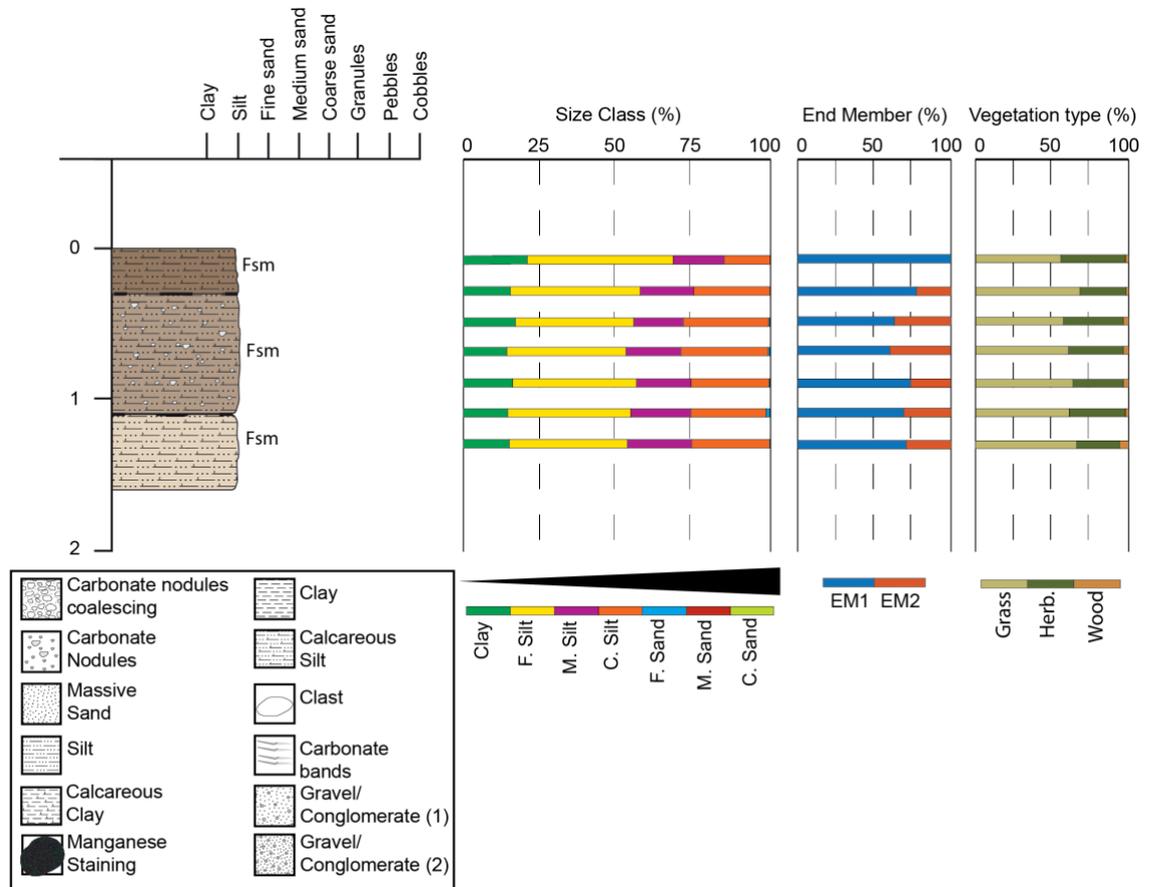
Figure 5.30: Sediment log of Excavation 1 (Figure 2.8) at Sare River. Sediment log depth is presented in metres. Facies codes outlined by Miall (2013) are included on sediment logs. Particle size distributions, EM abundances and vegetation types are also included at corresponding sample depths

5.3.3.3.Phytoliths

Excavation 1 displays a consistent phytolith distribution throughout (Figure 5.31). It is dominated by grass phytoliths, which have an abundance >60% throughout. Herbaceous phytoliths have an abundance of ~ 35% throughout, whilst wood phytoliths are present in abundances of <10%. However, a significant number of irregular and blocky polyhedral phytoliths can be observed throughout the excavation, which likely originate from wooded plants, but are not diagnostic of such.
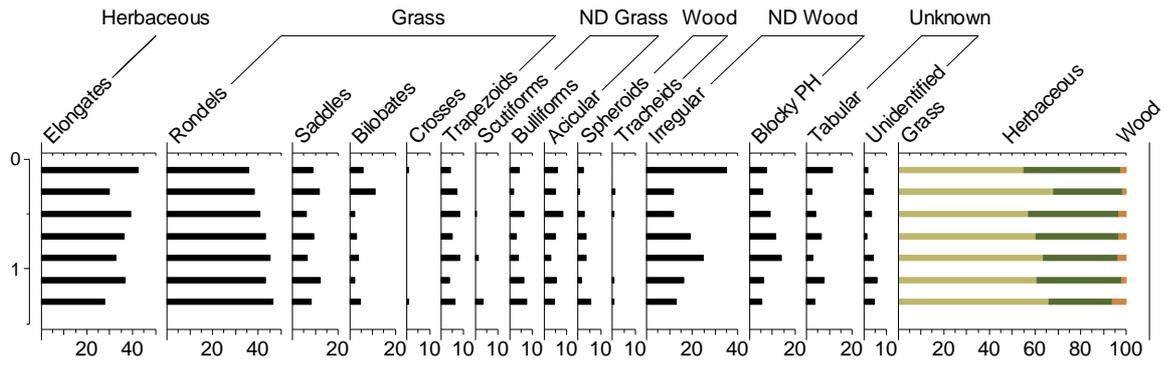
Figure 5.31: Phytolith morphotypes counted at EXC1 and their respective percentages. Morphotypes are categorised into vegetation types (Herbaceous, Grasses, nondiagnostic (ND) Grasses, Wood, ND Wood and Unknown). The percentages of these vegetation types are presented on the right of the diagram (ND morphotypes are not included here).

5.3.4. Excavation 5
5.3.4.1. Sedimentology

Excavation 5 is 1.8 m in depth (Figure 5.32). At its base is the same massive poorly sorted orange grey tuffaceous silt as Excavation 1, although occasional granule grade sediment is present. Carbonate nodules are also present throughout the
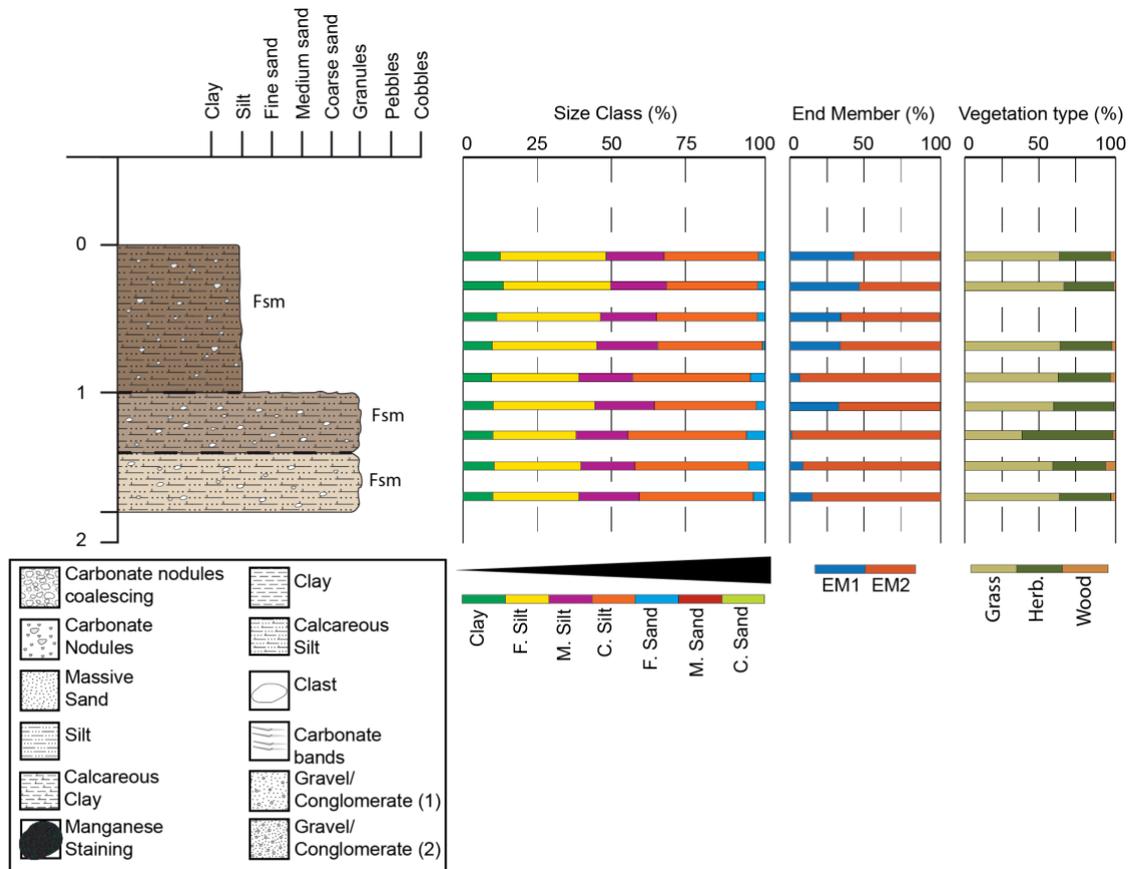
Figure 5.32: Sediment log of Excavation 5 (Figure 2.8) at Sare River. Sediment log depth is presented in metres. Facies codes outlined by Miall (2013) are included on sediment logs. Particle size distributions, EM abundances and vegetation types are also included at corresponding sample depths

horizon. This gradationally changes into a massive poorly sorted grey brown silt at 1.4 m; occasional granules remain present. At 1 m, a gradational change into finer brown silts occurs. Carbonate nodules also increase in presence and size, with some reaching up to pebble grade sizes.

5.3.4.2. EMMA

EM2 dominates Excavation 5 (Figure 5.32). At the base of the trench it accounts for ~ 80% of the EM composition, but steadily decreases up sequence and accounts for ~ 55% of the EM composition at the top of the excavation. EM1 displays the opposite trend.

5.3.4.3. Phytoliths

Excavation 5 displays a similar consistent trend to that of excavation 1 (Figure 5.33). Grass phytoliths dominate the excavation throughout, with an abundance generally >60%. At 1.3 m, a lower abundance of ~ 40% is observed. Herbaceous phytoliths have an abundance of ~ 35% throughout the trench, but at a singular instance at 1.3 m, they have an abundance of ~ 50% and are more dominant than grass phytoliths. Wood phytoliths are present throughout with a low abundance of <5%, however like Excavation 1, there are a significant number of nondiagnostic wood phytoliths.
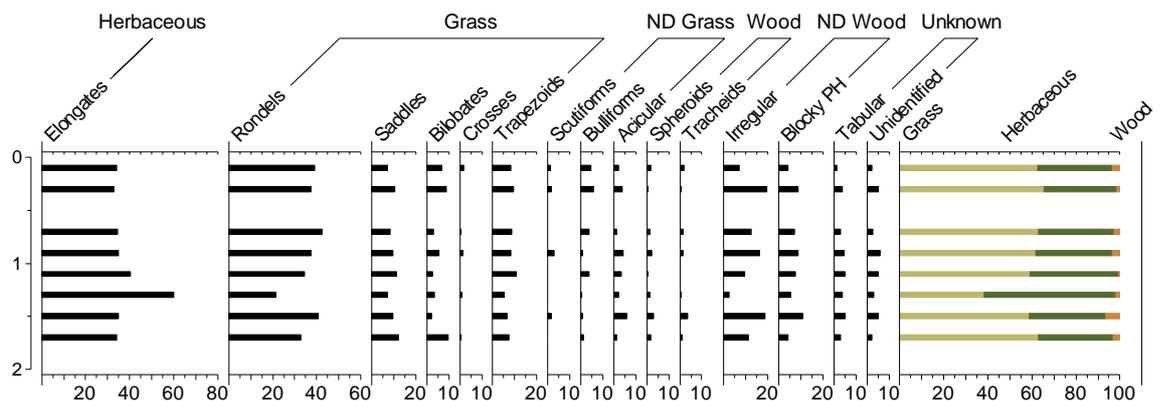
Figure 5.33: Phytolith morphotypes counted at EXC5 and their respective percentages. Morphotypes are categorised into vegetation types (Herbaceous, Grasses, nondiagnostic (ND) Grasses, Wood, ND Wood and Unknown). The percentages of these vegetation types are presented on the right of the diagram (ND morphotypes are not included here).

5.3.5. Establishing sedimentary units

From the excavations and the surrounding sediments at Sare River, two sedimentary units can be identified (SARE-1 and SARE-2); these units are described herein.

5.3.5.1.SARE-1

SARE-1 is the base of the sedimentary sequence seen at Sare River in this research. It is only seen throughout all of Excavation 4 (Figure 5.28). Poorly sorted granular silts comprise the sediments here, with little to no evidence of carbonates developing. At its base, SARE-1 is grey brown in colour with some orange silts, the latter of which gradationally become the dominant lithology of the unit. This unit can be traced across the site upstream, where an orange grey tuff can be seen to overly these sediments. EM2 is dominant throughout this unit, yet EM1 is present and occasionally abundant.

Phytolith assemblages are dominated by grass-indicating phytoliths in SARE-1, although herbaceous phytoliths comprise a significant proportion of the phytolith assemblage (>25%). Wood phytoliths increase in percentage throughout this unit, but still have a low abundance (<10%).

5.3.5.2.SARE-2

Overlying the previously noted tuff is SARE-2. This unit is characterised by poorly sorted orange grey tuffaceous silts at its base, with occasional granule grade sediment. The orange grey tuffaceous sediment is likely related to the underlying tuff. Carbonate nodules are infrequent here. These orange grey tuffaceous silts gradationally shift to grey brown poorly sorted silts. The colour shift is most likely owed to the lack of exposure of the tuff, which would reduce the availability of this sediment. Moving up the sequence, carbonate nodules become more frequent and increase in size. This unit is overlain by a brown black topsoil. EM1 dominates the sediments at Excavation 1 (Figure 5.30), whilst EM2 is present throughout (~ 30%). To contrast this, EM2 is dominant at Excavation 5 (Figure 5.32). EM1 is present here and becomes more abundant up sequence, from 20% to 45%.

Phytolith assemblages in this unit follow a consistent trend. They are grass-dominated (>55%) with a significant abundance of herbaceous phytoliths (~ 30%). The percentage of wood phytoliths fluctuates between 5% and 10%.

5.3.6. Closing Statement/Table of lithology

Sare River displays two sedimentary units that have been identified and described through various analytical techniques (Table 5.2). The site is mainly characterised

Unit	Sedimentology/Particle size	EMMA	Phytoliths
SARE-1	Poorly sorted granular silts with little to no evidence of carbonates. Grey brown in colour at base with some orange silts. Gradationally, orange silts become dominant lithology	EM2 dominates throughout. EM1 present throughout, at times abundant	Dominated by grass phytoliths throughout. Significant abundance of herbaceous phytoliths (>25%). Increase in wood phytoliths throughout, but low in abundance (<10%)
SARE-2	Poorly sorted orange grey tuffaceous silt with occasional granule grade sediment at base, with infrequent carbonate nodules. Gradational shift to overlying poorly sorted grey brown silts with increased carbonate nodule frequency and size	Dominated by EM1 at excavation 1, although EM2 present throughout (~ 30%). EM2 dominant at excavation 5. EM1 present and becomes more frequent up sequence, from 20% to 45%	Grass-dominated throughout (>55%). Herbaceous phytoliths comprise a significant proportion of assemblage (~ 30). Wood phytoliths present in low abundances (5 − 10%)

Table 5.2: A summary of the different sedimentary units identified at Sare River, as well as their lateral variance. Their EM characteristics and phytolith distribution are also included

by massive poorly sorted fine grained sediment throughout, with variations in the frequency of carbonate nodules. Sediments are multimodal in nature and have thus been 'unmixed' into two EMs, which will allow for interpretations to be made on sedimentary dynamics at the time of deposition in greater detail. Phytolith assemblages are dominated by grass and herbaceous indicating phytoliths. Wood indicating phytoliths are present in low abundances throughout the site.

5.3.7. Chronology – Cosmogenic nuclide dating

AMS measurements were obtained for both ^{26}Al and ^{10}Be for nine samples taken at Sare River (Table 5.3). The sediments sampled are thought to be laterally contemporaneous with those in SARE-1, and underlie the tuff which separates SARE-1 and SARE-2. An average basin altitude of 1259 m was calculated using SRTM data from the USGS data server. Under the assumption that all the samples taken received the same amount of post-burial cosmogenic irradiation, the isochron method (Figure 5.34) yields a burial age of 1.512 ± 0.089 Ma (slope R^2=0.97). All samples lie on this isochron, indicating that samples are all consistent with a single age of deposition at the stated time.

Sample	^{10}Be (x10^6 atoms per gram)	^{26}Al (x10^6 atoms per gram)	^{26}Al/^{10}Be (x10^6)
SR1	0.920 ± 0.026	5.120 ± 0.164	5.56 ± 0.24
SR2	0.157 ± 0.006	1.061 ± 0.053	6.74 ± 0.43
SR3	1.01 ± 0.036	5.143 ± 0.316	4.68 ± 0.32
SR4	1.808 ± 0.05	7.853 ± 0.246	4.34 ± 0.18
SR5	1.139 ± 0.032	5.969 ± 0.215	5.24 ± 0.24
SR6	0.916 ± 0.031	4.61 ± 0.242	5.03 ± 0.31
SR8	2.527 ± 0.067	8.743 ± 0.261	3.46 ± 0.14
SR9	0.445 ± 0.012	2.796 ± 0.133	6.29 ± 0.34
SR10	0.451 ± 0.014	2.63 ± 0.088	5.83 ± 0.27

Table 5.3: AMS measurements of samples taken from Sare River. ^{10}Be concentrations are based on 2:79·10^{-11} ^{10}Be/Be ratio for NIST SRM4325. ^{26}Al concentrations are based on 4:11 · 10□11 ^{26}Al/Al ratio for Purdue Z92-0222 standard
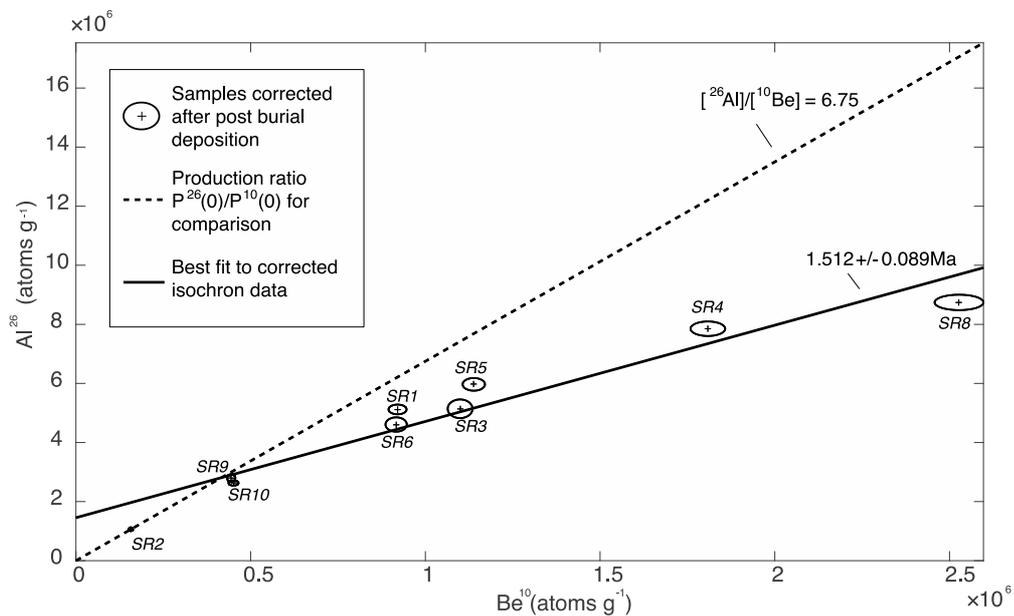
Figure 5.34: Cosmogenic ^{26}Al and ^{10}Be concentrations for samples taken at Sare River. The black ellipses represent the correction of the measured data to remove post-burial nuclide production. The dashed line displays the production ratio $P_{26}(0)/P_{10}(0)$ for comparison. The dark line resembles the best fit to the isochron data, which all samples lie on. This indicates that samples are consistent with a single age of deposition at 1.512 ± 0.089 Ma

CHAPTER 6.   DISCUSSION

6.1. Introduction

This chapter begins by interpreting EM characteristics presented in Chapter 5 from both Nyayanga and Sare River and subsequently attributes each EM to transport/depositional mechanisms or sediment sources. Leading on from this, results of the various reconstructive techniques applied are interpreted and the palaeoenvironments of the various sedimentary units identified at each site are reconstructed. Driving mechanisms of palaeoenvironmental change at both sites are then discussed. Finally, the palaeoenvironmental reconstructions of both sites are evaluated in terms of hominin activity in East Africa. Consideration is also given to which of the various hypotheses linking hominin evolution to palaeoenvironmental change this research provides support for.

6.2. EM interpretation
6.2.1. Introduction

The interpretation of EM characteristics obtained in Chapter 5 will give detailed information on the sedimentary processes that were involved in site formation at both Nyayanga and Sare River (section 4.3.2.1). In this section each EM will be attributed to a sedimentary process. Information acquired from field inspection of sediments will be used to constrain interpretations made from EMs and underpin the geometry of sedimentary processes The distribution of EMs in samples gathered across each site can then be analysed, and the major sedimentary processes involved in sediment deposition spatially and temporally can be identified.

6.2.2. Nyayanga
6.2.2.1. EM1

EM1 (Figure 5.2) is primarily composed of clay and silt, but also incorporates a small percentage of coarser particles up to coarse sand in size. Additionally, it often occurs in conjunction with the presence of clasts up to pebbles and even cobbles in size that are matrix-supported. Some of these clasts are carbonaceous, ranging from granules to pebbles in size (e.g. Figure 5.3). These carbonates are individual clasts and lack evidence of developing laminae or coalescing, which could indicate that they are not *in situ* and were instead reworked (Machette, 1985). Alternatively, these could have formed in flow hiatuses. The presence of clasts and coarser

particles found in relation to EM1 suggests that this is not a low energy environment, despite much of the EM being composed of fine sediment (Pierson, 2005). Moreover, the poor sorting of EM1 might also suggest that these sediments were deposited rapidly, under a variable flow regime, or were infrequently reworked (McLaren & Bowles, 1985; Pye & Blott, 2004). This is further supported by the absence of sedimentary structures such as channel features, where EM1 is seen in high percentages (Pierson, 2005) (e.g. Figure 5.3). Such characteristics are indicative of viscous, sediment-rich hyperconcentrated flows at Nyayanga, which likely occurred quickly and infrequently and were unconfined in nature. These types of flow are characterised by poor sorting, matrix-supported clasts, and massive structureless deposits. Erosive features are often absent in such instances, as the viscous nature and low shear stress bases of such flows often bury underlying sediment rather than erode it (Pierson, 2005; Stanistreet et al., 2018; de la Torre et al., 2018). EM1 also appears to be multimodal, which is also a common feature of hyperconcentrated flows (Pierson, 2005).

6.2.2.2. EM2

EM2 (Figure 5.2) is composed almost entirely of silts, with only a small percentage of clays present. The highest percentages of this EM are most frequently associated with sediments where coarse particles and clasts are absent, as well as sedimentary structures (e.g. Figure 5.6). In some areas of the site, high percentages of EM2 are associated with the presence of coalescing carbonate nodules and *in situ* carbonate nodules. This suggests that EM2 is related to a low energy depositional environment, which at times was stable enough for soil development to take place (Folk & Ward, 1957; Machette, 1985; Marriott & Wright, 1993; Ditchfield et al., 1999; Clarke et al., 2014; Wang et al., 2015; Liu et al., 2016). This, as well as the poor sorting of EM2, suggests that its sediments were likely to have been infrequently reworked (McLaren & Bowles, 1985; Pye & Blott, 2004). Resultantly, EM2 may represent periods of landscape stability at Nyayanga, or potentially flow hiatuses. This aligns with the interpretation of EM1, as hyperconcentrated flows are often separated by periods of landscape stability and pedogenic development (Ditchfield et al., 2018). In these periods, represented by EM2, deposition most likely occurred as fluvial runoff and aeolian deposition (Vandenberghe, 2013; de Haas et al., 2014; Vandenberghe et al., 2018; Ditchfield et al., 2018). Additionally, during such stable

periods pedogenesis was likely to have occurred (Machette, 1985; Ditchfield et al., 2018).

6.2.2.3. EM3

The higher percentages of coarse silt and sand grade sediment that characterise EM3 (Figure 5.2) suggest that it may represent mechanisms associated with higher transport/depositional energies than EM2 (Folk & Ward, 1957; Clarke et al., 2014; Wang et al., 2015; Liu et al., 2016). EM3 is often observed in higher percentages associated with matrix-supported gravel grade sediment that incorporates granules and occasionally pebbles (e.g. Figure 5.17). These clasts are frequently carbonaceous, but show little evidence of coalescing or the development of laminae, suggesting they may be reworked (Machette, 1985). Sedimentary structures including erosive contacts and faint laminations can also be observed in these instances and point towards fluvial/alluvial activity, yet no channel features are evident (Miall, 2013). Like previous EM's, EM3 is poorly sorted suggesting that it may be rapidly deposited or deposited under a variable flow regime (McLaren & Bowles, 1985; Pye & Blott, 2004). The presence of laminations may indicate that the latter is more likely, as rapid deposition would be more likely to result in massive structureless deposits (Pierson, 2005; North & Davidson, 2012; Miall, 2013). The absence of any channel features suggests that activity associated with this EM may have been unconfined in nature (Pierson, 2005; North & Davidson, 2012; Miall, 2013). The evidence presented above suggests that EM3 is representative of unconfined fluvial flows. Such flows would periodically have sufficient energy to entrain coarser sediment like the sands observed in EM3, as well as the gravel grade sediment often seen in association with this EM. Matrix-supported deposits are likely the result of flow deceleration as flows expanded and the concentration of suspended sediment increased, causing the flow to become hyperconcentrated and more debris flow like at times (North & Davidson, 2012). This would be fitting with the very fine skew of this EM (McLaren & Bowles, 1985).

6.2.3. Sare River
6.2.3.1. EM1

EM1 (Figure 5.27) at Sare River is composed almost entirely of silts, with a small percentage of clay. Coupled with the absence of clasts throughout all the excavations (Figure 5.28, Figure 5.30, Figure 5.32) this indicates that EM1 either

represents a low energy depositional environment, or a source area defined by a dominance of fine sediment availability (Paterson & Heslop, 2015a). The poor sorting of EM1 suggests that deposition of sediments may have occurred either rapidly or under a variable flow regime, or that sediments were infrequently reworked (McLaren & Bowles, 1985; Pye & Blott, 2004). The lack of sedimentary structures associated with this EM, as well as the presence of soft carbonate nodules attests that these sediments were infrequently reworked (Machette, 1985). Periods of landscape stability and flow hiatuses are most likely represented by this EM. Aeolian deposition and deposition via fluvial runoff most likely occurred during these intervals (Pope & Wilkinson, 2005; Vandenberghe, 2013; de Haas et al., 2014; Vandenberghe et al., 2018).

6.2.3.2.EM2

EM2 (Figure 5.27) is composed primarily of coarse silts, with a small percentage of fine sand. It is poorly sorted, which suggests that these sediments may have been either rapidly deposited or infrequently reworked (McLaren & Bowles, 1985; Pye & Blott, 2004). The fine skew of this EM attests to this, as sediments were likely deposited as there was a reduction in flow energy (McLaren & Bowles, 1985). The presence of gradational contacts (Figure 5.28Figure 5.30Figure 5.32) suggests that rapid deposition is less likely, as sharper contacts would be observed in such instances (Miall, 2013). The absence of any channel features observed in sediments suggests that deposition associated with this EM was unconfined in nature. These lines of evidence suggest that EM2 most likely represents low energy unconfined fluvial activity that was potentially ephemeral in nature, or had a variable flow regime. This would allow for the transport of coarser sediment, such as the sand and granule sized sediment observed. A variable flow regime would also produce poor sorting throughout the sediment, as well as a fine skew with a reduction in energy (McLaren & Bowles, 1985). The lack of erosive features and an average grain size of medium silt suggests that these flows were low in energy throughout the time these sediments were deposited (Folk & Ward, 1957; Visher, 1969). Additionally, the lack of channel features may suggest that sediments were deposited in unconfined flow events, rather than in the confines of a channel (Miall, 2013).

6.2.4. Summary

At Nyayanga, the three EMs identified are attributed to different sedimentary processes. Field observations were used underpin the geometry of sedimentary processes and to geomorphologically constrain interpretations. EM1 is interpreted as representing episodic viscous, sediment-rich hyperconcentrated flows which were unconfined in nature. EM2 is suggested to relate to a low energy depositional environment in which fluvial runoff, aeolian deposition and soil development occurred. EM3 represents relatively unconfined fluvial activity that periodically had sufficient energy to erode and entrain coarser sediment.

Two EMs were attributed to different depositional mechanisms/environments at Sare River. EM1 likely relates to periods of landscape stability in which aeolian deposition and fluvial runoff also occurred. EM2 is interpreted as representing low energy unconfined fluvial activity that was potentially ephemeral in nature, or had a variable flow regime.

6.3. Palaeoenvironmental reconstruction
6.3.1. Nyayanga
6.3.1.1. Introduction

Here, the palaeoenvironmental setting of each sedimentary unit identified at Nyayanga is interpreted based on the results obtained in Chapter 5, specifically the description of sediments in section 5.2.10. This is summarised in Table 6.1, whilst the sections below explore this in more detail. Driving mechanisms of palaeoenvironmental change here are also discussed.

Table 6.1: A summary of palaeoenvironmental characteristics interpreted for each sedimentary unit and subunit identified at Nyayanga based on sediment descriptions in section 5.2.10.

Unit	Subunit	Palaeoenvironment characteristics
NY-1	NY-1A	Deposition via episodic hyperconcentrated flows capable of entraining cobble grade sediment. Flow hiatuses characterised by stable land surface development and secondary processes (fluvial runoff, aeolian deposition). Open bushy grassland with infrequent woodland and sedges
	NY-1B	Variable environment. Deposition fluctuates between episodic hyperconcentrated flows and intermittent unconfined fluvial flows capable of eroding underlying sediment. Flow hiatuses characterised by landscape stability and secondary processes. Open bushy grasslands with infrequent woodland and sedges persisted

	NY-1C	Shift to a more frequently wet environment. Intermittent unconfined fluvial flows with a variable flow regime occurred throughout deposition of sediments. These were more water laden and capable of eroding underlying sediments. Flow hiatuses were not lengthy enough for significant pedogenesis. Similar palaeovegetation structure remained
	NY-1D	Environment became more stable and was characterised by pedogenic development and secondary processes including fluvial runoff and aeolian deposition. Intermittent unconfined flows may have occurred, but with a lower frequency. Bushy grasslands with infrequent woodland and sedges persisted
	NY-1E	Environment becomes increasingly stable. Significant stages of soil maturity developed. Infrequent unconfined fluvial flows lower in energy occurred. Flow hiatuses characterised by secondary processes. Bushy grassland/grassy bushlands characterise palaeovegetation
NY-2	NY-2A	Low energy environment with frequent periods of landscape stability. Intermittent unconfined fluvial activity occurred, potentially attributable to secondary fluvial runoff. Landscape characterised by grassy bushlands
	NY-2B	Increasingly stable environment with soil development reaching greater stages of maturity. Intermittent unconfined fluvial activity occurred throughout with higher transport energy, indicating a wetter environment. An increase in woodland and sedges attest this. Landscape remained dominated by grassy bushlands
	NY-2C	Unconfined fluvial activity became more common and increased in flow velocity, but remained intermittent. Flow hiatuses characterised by stable land development and early stages of pedogenesis. Grassy bushlands characterised the landscape
NY-3	-	Intermittent unconfined fluvial activity with stable land surface development in flow hiatuses. Early stages of pedogenesis. Palaeovegetation characterised by bushy grasslands/grassy bushlands with infrequent woodland and sedges
NY-4	-	Stable environment in which mature soils developed with late stages of pedogenesis. Unconfined fluvial activity occurred intermittently. Grassy bushlands with infrequent woodland and sedges characterised palaeovegetation

6.3.1.2. NY-1 interpretation

The lowermost sedimentary unit at Nyayanga, NY-1 (Figure 5.26) is suggested to have been deposited between 3.05 – 2.595 Ma (Finestone, 2019). It has the largest exposures site wide, particularly in the southwest of the site. High abundances of

EM1 (~ 45%) and the presence of massive poorly sorted matrix supported clasts throughout NY-1A (section 5.2.10.1) suggest sediments are characteristic of hyperconcentrated flow deposits (Pierson, 2005). The higher abundance of EM2 suggests these flows are likely to be episodic, and separated by periods of landscape stability, as is common of hyperconcentrated flows (Pierson, 2005; Ditchfield et al., 2018). During periods of landscape stability, deposition most likely took place via secondary processes including fluvial runoff and aeolian deposition (Pope & Wilkinson, 2005; Harvey et al., 2005; Vandenberghe, 2013; de Haas et al., 2014; Vandenberghe et al., 2018). The presence of pedogenic carbonates attests to this, although the lack of coalescing or development of laminae suggests that these may have been reworked or are immature in development (Machette, 1985). The relative abundance of wooded vegetation (~ 15%) during this period might indicate that soil formation did take place, and that carbonates were subsequently reworked. Grasses and herbaceous vegetation were most abundant and the landscape was most likely that of an open one characterised by bushy grasslands with infrequent woodland and sedges.

The shift to interbedded poorly sorted massive muddy matrix supported pebbles and poorly sorted massive muds belonging to NY-1B (section 5.2.10.1) suggest that the environment began to become more variable at this time. The two instances of massive muddy matrix supported pebbles (Figure 5.3, Figure 5.9, Figure 5.12) are characteristic of hyperconcentrated flows and debris rich flows, as represented by EM1 which is most abundant here. More frequent clasts are present in GT1 (Figure 5.3) than in the laterally equivalent sediments at GT3 (Figure 5.9) and GT5 (Figure 5.12) in this facies. This might suggest that GT1 was more central to the most active parts of the hyperconcentrated flows, whilst GT3 and GT5 were more marginal. The reduction in EM2 suggests that the development of stable land surfaces did not occur as frequently as in the underlying sediments in GT1 (Figure 5.3), other than in the upper instances of this facies in GT5 (Figure 5.12) and GT6 (Figure 5.14), again suggesting these locations were likely marginal. This is reflected by the reduction/absence of wooded vegetation and the increase in grasses, yet this may also be a climate signal (deMenocal, 1995; Ehleringer & Cerling, 2002; Tipple & Pagani, 2007; Hopley et al., 2007). With the absence of channel features and an increase in the abundance of EM3 here, unconfined fluvial activity more water laden

than that of the hyperconcentrated flows likely became more frequent and was potentially capable of eroding and entraining sand sized sediment (Pierson, 2005; de Haas et al., 2014; Ditchfield et al., 2018; de la Torre et al., 2018).

In contrast, the massive muds that these sediments are interbedded with do not display the same evidence for hyperconcentrated flows (section 5.2.10.1). The dominance of EM2 suggests that these massive muds are characteristic of periods of landscape stability. The increase in abundance of EM3 at these times also indicates that during these periods, fluvial runoff most likely took place, as well as aeolian deposition (Vandenberghe, 2013; de Haas et al., 2014). The reduction in EM1 and the lack of evidence for hyperconcentrated flows in the lower massive muds may reflect an increase in the frequency of precipitation, as fine sediment may have been reworked more often, rather than in less frequent/higher magnitude events (de Haas et al., 2014). In GT3 (Figure 5.9), GT5 (Figure 5.12) and GT6 (Figure 5.14) greater sediment accumulation as well as lighter coloured carbonaceous sediment indicates that these sediments were deposited on a relatively stable land surface, more so than that of the laterally contemporaneous sediments in GT1. The carbonaceous sediment suggests that soil development likely took place during this time (Machette, 1985). The presence of wooded vegetation and sedges attests to this, although the landscape was still dominated by grasses and herbaceous vegetation. The higher abundance of EM1 in the upper massive muds is most likely a result of the unconfined fluvial activity represented by EM3. These flows entrained more sediment as the flow expanded and decelerated, causing the concentration of sediment to increase and the flow to become hyperconcentrated (North & Davidson, 2012).

The overlying sediments of NY-1C (section 5.2.10.1) might indicate the shift to a more frequently wet environment. The erosive contact that these sediments have with underlying sediments suggests that more water laden flows occurred during this time (Pierson, 2005; de Haas et al., 2014; Ditchfield et al., 2018; de la Torre et al., 2018). The coarse sand present in these sediments is most likely a product of these erosional events, which may explain why they are not observed in the underlying sediments characterised by hyperconcentrated flows as these flows are more likely to bury sediments than erode them (Pierson, 2005; Ditchfield et al.,

2018). The partially and weakly cemented sandstones underlying NY-1 are most likely the source of the coarse sands observed in NY-1C. The lack of any channel features and the higher abundances of EM3 here suggest that these flows were unconfined in nature (Miall, 2013). The low abundance of EM1 could be a product of the deceleration of these unconfined flows as previously discussed (North & Davidson, 2012). EM2 is also abundant throughout these sediments, though carbonate nodules are absent suggesting short periods of landscape stability were common. Resultantly, unconfined fluvial activity might have been intermittent and possess a variable flow regime (McLaren & Bowles, 1985; Pye & Blott, 2004). The fluctuations in sand and granule content in GT3 (Figure 5.9) and GT6 (Figure 5.14) are indicative of this, as are the fine skew and poor sorting of EM3 (Visher, 1969; McLaren & Bowles, 1985; Pye & Blott, 2004). The low abundance of wooded vegetation and sedges and the dominance of grasses and herbaceous vegetation suggests the environment at this time was an open bushy grassland. This environment is commonly associated with such unconfined flows (North & Davidson, 2012).

The dominance of EM2 in the overlying sediments of NY-1D (section 5.2.10.1) suggests the environment was characterised by more frequent periods of landscape stability than the underlying sediments. Carbonate nodules throughout these sediments suggests that some of these periods were sufficiently sustained for soil development to take place (Machette, 1985). The reduction in EM3 indicates that higher energy fluvial activity was not as frequent during this time, and deposition most likely took place as low energy fluvial runoff (de Haas et al., 2014). This is supported by the lack of coarser sands as well as an overall decrease in sand content (Visher, 1969; McLaren & Bowles, 1985). Sediment exhaustion might also explain the overall decrease in sand content observed, although the development of stable land surfaces indicates it was most likely due to a reduction in flow velocity. The landscape remained relatively open during this period, characterised by bushy grasslands with infrequent wooded vegetation and sedges. The dominance of EM1 in GT1 (Figure 5.3) may suggest that sediments deposited here were at the margins of the unconfined flows, where deceleration occurred and particles as small as clay were deposited, potentially indicating a standing water environment (North &

Davidson, 2012). Aeolian deposition may also be responsible for the deposition of such sediments (Vandenberghe, 2013; de Haas et al., 2014)

The environment appears to become increasingly stable during NY-1E (section 5.2.10.1). The carbonaceous sediment here and the frequent carbonate nodules which in places form laminae or coalesce suggest that periods of landscape stability were long enough for significant pedogenic development to take place and reach more matures stages (Machette, 1985; Ditchfield et al., 1999; 2018). The dominance of EM2 throughout these sediments attests to this. The presence of EM3 and the lack of channel features suggests that unconfined fluvial activity still took place at times, potentially as fluvial runoff (de Haas et al., 2014). The decrease in percentages of EM3 and in sand sized sediment from GT9 to GT1 indicates that these flows were focussed in the southeast of the site, whilst much of the sediment toward the northwest was marginal. This is reflected by the increase in abundances of EM1 across the same transect. An open landscape characterised by grassy bushlands/bushy grasslands persisted here.

6.3.1.3. NY-2 interpretation

The sediments of NY-2 (Figure 5.26) were deposited subsequently to NY-1, but also within the age of 3.05 – 2.595 Ma (Finestone, 2019). Sediments from this unit differ to those from NY-1, with abundances of EM1 generally absent. The absence of sedimentary structures, clasts other than pedogenic carbonate nodules, as well as the reduced percentage of sand sized sediment suggests that the lowermost sediments belonging to NY-2A (section 5.2.10.2) were characteristic of a low energy environment (Visher, 1969; Miall, 2013). The abundances of EM2 throughout this subunit support this, and indicate that stable land surfaces were common. The presence of carbonate nodules further indicates soil development occurred during this time, although the lack of coalescing or development of laminae indicate these were not mature soils (Machette, 1985). The absence of channel features throughout these sediments and the frequency of EM3, indicate that low energy intermittent and unconfined fluvial activity continued to occur. Like the uppermost sediments of NY-1, a reduction in the frequency of EM3 from the southeast of the site at GT9 to northwest at GT1 occurs, suggesting the most active area of these flows remained in the southeast of the site. EM1 displays the opposite trend,

indicating flow deceleration still occurred in the northwest of the site near to GT1. The landscape remains characterised by grassy bushlands. The lack of wooded vegetation and sedges might be owed to increased aridity (Tipple & Pagani, 2007; Ségalen et al., 2007; Cerling et al., 2013; Maslin et al., 2014).

Similar environmental conditions can be observed in the sediment of NY-2B (section 5.2.10.2). The dominance of poorly sorted clayey silts containing carbonate nodules is suggestive of a low energy environment in which soil formation occurred (Folk & Ward, 1957; Visher, 1969; McLaren & Bowles, 1985; Machette, 1985; Pye & Blott, 2004). The degree of cementation associated with these sediments suggests these soils may have been more mature than those of the underlying sediments (Machette, 1985). Abundances of EM2 align with this, as periods of stable land surface development appear common. An increase in sand content and in the abundance of EM3 in these sediments points towards a wetter environment at this time, as unconfined fluvial activity appears to be more common and have a higher entrainment capacity (Visher, 1969). Increases in the abundance of wooded vegetation and sedges may reflect this, however the environment remains as an open grassy bushland. EM3 follows the same trend of decreasing from southeast to northwest in abundance. Its absence is replaced by abundances of EM1 in GT2, suggesting that this is where flow deceleration of unconfined flows may have occurred (North & Davidson, 2012).

In the overlying sediments of NY-2C (section 5.2.10.2), small changes in the environment can be observed. The increase in EM3 throughout these sediments, as well as the increase in sand content, the presence of some pebbles and the lack of any channel features, indicates that unconfined fluvial activity throughout this interval had higher flow velocities and was potentially more frequent (Visher, 1969; McLaren & Bowles, 1985; Miall, 2013). The relatively even abundance of EM2 highlights that these flows remained intermittent, and were characterised by periods of stable land development in flow hiatuses. The presence of carbonate nodules in these sediments is indicative of soil development, however the lack of laminae or coalescing suggests these were immature, or potentially reworked by the intermittent unconfined fluvial activity (Machette, 1985). The increase in herbaceous vegetation suggests that the landscape was characterised by grassy bushlands

during this time. The decreases in percentages of wooded vegetation may be related to the less frequent periods of stable land surface development.

6.3.1.4. NY-3 interpretation

The sediments of NY-3 (section 5.2.10.3, Figure 5.26) are ill-defined due to their lack of exposure throughout the site. In the southeast of the site an extremely consistent environment persisted, as is evident from the PSDs and EM composition. Relatively even abundances of EM2 and EM3 within massive sediments are indicative of an environment upon which intermittent unconfined flow events persisted, with flow hiatuses marked by periods of stable land development. Although the presence of carbonate nodules throughout these sediments is indicative of soil development, the lack of laminae and coalescing suggests that soil development here is moderately immature, or that nodules have been reworked (Machette, 1985). In the northwest of the site, stable land surfaces appear to become more frequent throughout this interval, as evidenced by the increase in EM2 and the reduction in EM3. The increase in wooded vegetation attests to this. The overall landscape during this time appears to be characterised by that of a bushy grassland/grassy bushland with occasional wooded vegetation and sedges.

6.3.1.5. NY-4 interpretation

The environment of NY-4 (section 5.2.10.4, Figure 5.26) was most likely one that experienced lengthy periods of stable land formation, allowing for soil development to take place. This is evidenced by the abundance of pedogenic carbonates throughout this unit, which display evidence for a higher degree of maturity from coalescing and forming laminae, as well as thick horizons (Machette, 1985). The presence of sand sized sediment and the lack of any channel features, as well as an abundance of EM3 suggest that unconfined fluvial activity continued to occur throughout these sediments (Visher, 1969). The higher abundances of EM3 in GT7 (Figure 5.17) and GT8 (Figure 5.20) suggest that these flows were most active in this area, whilst the higher abundance of EM2 in GT2 (Figure 5.6) and GT9 (Figure 5.23) indicates that sediments deposited here were marginal to the area of activity. A grassy bushland best characterises this landscape with infrequent wooded vegetation and sedges.

6.3.1.6. Palaeoenvironmental reconstruction

The depositional environment throughout Nyayanga is interpreted as having been characterised by a combination of hyperconcentrated flows, intermittent unconfined fluvial activity with a variable energy regime, and flow hiatuses in which aeolian deposition and stable land development occurred. This largely occurred within an open landscape on the slopes leading from Homa Mountain which were dominated by grasses and herbaceous vegetation, with infrequent woodland and sedges.

The characteristics listed above are indicative of an alluvial fan/plain environmental setting at Nyayanga (Blair & McPherson, 1994a; 1994b; Mather & Stokes, 2003; Harvey et al., 2005; Mather & Hartley, 2005; Waters et al., 2010; North & Davidson, 2012; de Haas et al., 2014; Mather et al., 2017). Hominin activity has been identified in this type of environment elsewhere during the Plio-Pleistocene of East Africa (Brown & Feibel, 1991; Hay & Kyser, 2001; Ashley et al., 2009; Feibel, 2011; Drapeau et al., 2014; Brugal et al., 2004; Uribelarrea et al., 2017; Ditchfield et al., 2018). Alluvial plains form between highlands and depositional lows, where highlands act as sediment sources and depositional lows provide ample space for sediment accumulation (Blair & McPherson, 1994a; Harvey et al., 2005; Waters et al., 2010; de Haas et al., 2014). The rapid elevation changes from Homa Mountain towards the expansive depositional low in the west (Figure 2.1, Figure 2.3) make Nyayanga a likely area for this formation (Le Bas, 1977; Blair & McPherson, 1994a; Harvey et al., 2005). The thicker exposure of sediments in the northwest of the site most likely represent a depositional sink with greater accommodation space for sediments to accumulate (Harvey et al., 2005).

Additionally, alluvial environments are frequently characterised by episodic mass flow and/or unconfined fluvial events (Blair & McPherson, 1994a; Harvey et al., 2005; de Haas et al., 2014), much like those thought to have occurred throughout the sediments at Nyayanga. Similar flows have been interpreted at other hominin sites dating to the Plio-Pleistocene and show evidence for them burying and preserving underlying sediments, rather than eroding them (Ditchfield et al., 2018; Stanistreet et al., 2018; de la Torre et al., 2018). This is essential in establishing whether traces of hominin activity are in fact *in situ* (Ditchfield et al., 2018).

Erosion/aggradation is also usually confined to smaller active sectors of an alluvial plain, and during periods of inactivity and on inactive sectors, aeolian deposition and fluvial runoff frequently occur, as well as pedogenic development (Hartley et al., 2013; de Haas et al., 2014). This can be observed throughout the sediments at Nyayanga. Moreover, lower energy unconfined fluvial activity identified at Nyayanga may in fact be attributable to fluvial runoff as a secondary process (Harvey et al., 2005; de Haas et al., 2014).

The sediments underlying lowermost NY-1 at Nyayanga resemble thick (10 m+) sequences of interbedded sandstones and weakly cemented conglomeratic layers. These most likely relate to a period in which an active alluvial belt was central to the site and deposition occurred in frequent unconfined flow events (Harvey et al., 2005; de Haas et al., 2014).

In NY-1 deposition on the alluvial plain becomes more episodic. Low frequency hyperconcentrated flow events capable of mobilising sediment up to cobbles in size at times deposited structureless beds of sediment across an open bushy grassland. These flows varied in energy, with the highest energy flows at the base of this unit. Periods of landscape stability and pedogenic development separated these flows, in which fluvial runoff and aeolian deposition most likely took place on the inactive surface (de Haas et al., 2014; Vandenberghe et al., 2018). Intermittent unconfined fluvial events also took place and likely decelerated in velocity moving west across the site. Here, flows expanded and became more sediment laden causing them to become hyperconcentrated and at times debris rich and more debris flow like (North & Davidson, 2012). At times, these unconfined fluvial events were more water laden and had higher flow velocities. This most likely resulted in erosion into harder sandstones observed throughout the site, causing the appearance of sand sized sediment in the deposits (Harvey et al., 2005; Pierson, 2005; Miall, 2013; de Haas et al., 2014; Ditchfield et al., 2018; de la Torre et al., 2018). Hyperconcentrated flows became less frequent throughout this unit, whilst lengthy periods of landscape stability with intermittent unconfined fluvial events became more common. This might reflect this section of the alluvial plain becoming less active (Figure 6.1).

During the deposition of NY-2 a similar environment to that of NY-1 persisted, although with lower energy. Periods of stable land surface development and

pedogenesis were common suggesting activity on this part of the alluvial plain was infrequent, particularly during the deposition of NY-2B. Fluvial runoff and aeolian deposition likely occurred during these periods (Vandenberghe, 2013; de Haas et al., 2014). Unconfined fluvial activity lower in energy than that observed in NY-1 persisted throughout the environment, and similarly most likely became hyperconcentrated as the flow decelerated towards the depositional low in the west of the site (North & Davidson, 2012). The increased occurrence of stable land surfaces as well as the reduction in hyperconcentrated flow events suggests that this sector of the alluvial plain became inactive, migrated laterally (Figure 6.1), or prograded during the deposition of NY-2, which is why an overall reduction in energy
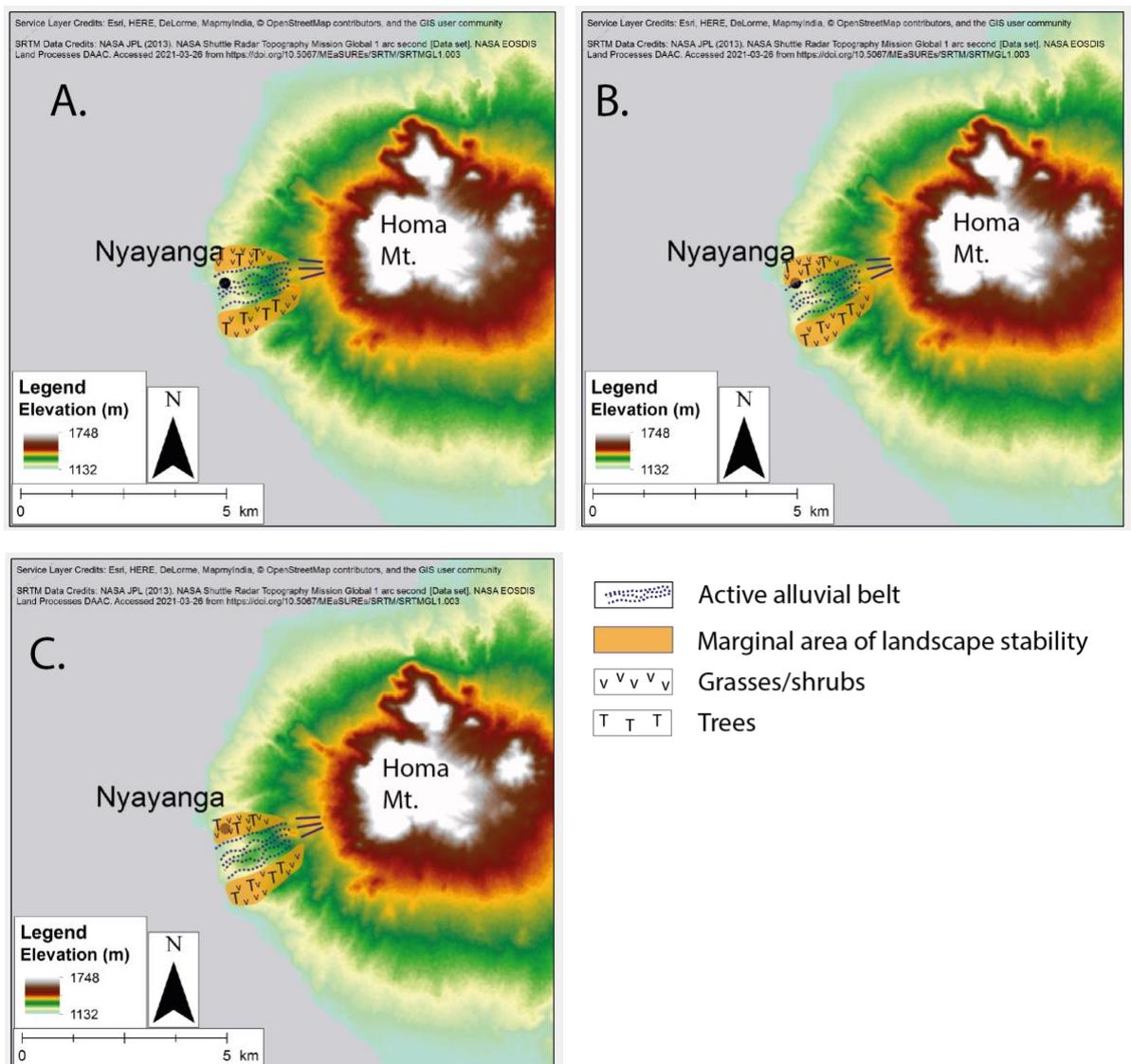
Figure 6.1: Conceptual model displaying how the active sector of the alluvial plain may have migrated laterally. A. displays Nyayanga situated on the alluvial belt at where intermittent fluvial flows and episodic hyperconcentrated flows occurred during the deposition of NY-1. B. displays how the active sector of the alluvial plain may have migrated laterally during deposition of NY-2, with Nyayanga now closer to the margins of the active sector. C. illustrates further migration of the

can be observed in the depositional environment here (Blair & McPherson, 1994a; Harvey et al., 2005; de Haas et al., 2014). The increased frequency of unconfined fluvial activity at the top of these sediments, as well as the increased energy of said activity indicates that this part of the alluvial plain began to become more active during the deposition of NY-2C. This all persisted across a landscape characterised by grassy bushlands and bushy grasslands with infrequent wooded vegetation.

Little change in the environment occurs in NY-3. The frequency of unconfined fluvial activity appears to increase here, suggesting that a continuation of the environment represented by NY-2C is likely. Regular periods of landscape stability and the increase in frequency of wooded vegetation suggest that this sector of the alluvial plain remained relatively inactive at the time these sediments were deposited, or at least experienced periods of inactivity (de Haas et al., 2014). Consequently, fluvial activity most likely occurred in the form of fluvial runoff across the inactive surface. The landscape remained characterised by open bushy grasslands and grassy bushlands.

Lengthy periods of stable land formation and soil development suggest that at the time the sediments of NY-4 were deposited this was a relatively stable environment. By this time, it is likely that the alluvial belt had migrated and that Nyayanga was located in an inactive area of the alluvial plain (Blair & McPherson, 1994a; Harvey et al., 2005; de Haas et al., 2014). Alternatively, the alluvial plain may have become inactive as a result of increased aridity at the site, reducing the frequency of flows (deMenocal, 1995; 2004). This allowed for extensive pedogenic horizons to form. Secondary processes may have characterised the inactive surface in the form of fluvial runoff and aeolian deposition. The unconfined flows represented by EM3 in this unit most likely relate to the aforementioned fluvial runoff, rather than unconfined flow events relating to an active alluvial belt (Vandenberghe, 2013; de Haas et al., 2014). The landscape remained characterised by a grassy bushland with infrequent wooded vegetation and sedges.

6.3.1.7. Drivers of palaeoenvironmental change at Nyayanga

Much like other alluvial environments, palaeoenvironmental evolution at Nyayanga was most likely driven by a complex interplay of several controlling factors (Blair & McPherson, 1994a; Harvey et al., 2005; Waters et al., 2010; de Haas et al., 2014; Stokes & Mather, 2015; Mather et al., 2017). Regional and local tectonics may have had one of the largest impacts on environmental change here. The Homa Mountain carbonatite complex creates significant changes in relief from the east to the west of the site, whilst the development of the EARS created depositional lows and basins suitable for lake formation to the west of the site, whilst also amplifying the relief of Homa Mountain through uplift (Le Bas, 1977; Sepulchre et al., 2006; Bergner et al., 2009; Trauth et al., 2010; Olaka et al., 2010; Maslin et al., 2014). The location of Nyayanga on the slopes at the foot of Homa Mountain most likely meant that sediments prograded towards the expansive depositional low to the west, as well as aggraded (Blair & McPherson, 1994a; Harvey et al., 2005; Waters et al., 2010; de Haas et al., 2014).

Additionally, the development and destruction of palaeolakes by faulting to the west of the site would have led to changes in base-level, which may have ultimately dictated periods of incision or deposition across the site (Stokes & Mather, 2000; Maher et al., 2007; Maher & Harvey, 2008). Similar environmental settings have shown evidence for palaeolake fluctuations impacting the depositional environment in this way (Baker et al., 1988; Strecker et al., 1990; Trauth et al., 2010). However, the impact of base-level change on alluvial evolution is also very much controlled by sediment supply, which can also be driven by climate (Blair & McPherson, 1994a; Harvey et al., 1999; Harvey et al., 2005; Waters et al., 2010). Local faulting throughout the Homa Peninsula may also have led to changes in sediment supply throughout time by breakdown of sediment (Harvey et al., 2005; Waters et al., 2010). Drainage was likely also effected by faulting, potentially causing variations in the active sector of the alluvial plain that Nyayanga was located upon, with river capture also a possibility (Harvey et al., 2005; Maher et al., 2007; de Haas et al., 2014).

Climate may also have been a significant driver of environmental change at Nyayanga. Changes in climate dictate the abundance of sediment supply (erosion), the release of sediment throughout the catchment, and the abundance/composition

of vegetation cover which stabilises sediment (Blair & McPherson, 1994a; Harvey et al., 2005; Pope & Wilkinson, 2005; Waters et al., 2010; Stokes & Mather, 2015). Precipitation largely drives sediment supply to alluvial plains, with periods of higher precipitation resulting in an increase in sediment supply (Blair & McPherson, 1994a; Pope & Wilkinson, 2005; Harvey et al., 2005; Waters et al., 2010). Additionally, larger amounts of precipitation can result in higher sediment entrainment capacities, particularly in higher magnitude episodic events (Mather & Hartley, 2005; Harvey et al., 2005; de Haas et al., 2014). Moister climates can often also attest to increased vegetation cover which stabilises sediments leading to a reduction in sediment supply (Harvey et al., 2005; Pope & Wilkinson, 2005; Maher et al., 2007; Waters et al., 2010).

The sediments at Nyayanga, particularly in unit NY-1 point towards a variable climate regime. Hyperconcentrated flows here were likely a product of episodic high magnitude periods of precipitation resulting in an increased sediment supply due to erosion, as well as higher sediment entrainment capacities (Blair & McPherson, 1994a; Pierson, 2005; Harvey et al., 2005; North & Davidson, 2012; de Haas et al., 2014). Evidence from phytoliths suggest that a largely open environment existed, indicating that sediments were relatively unstable at these times (Pope & Wilkinson, 2005; Harvey et al., 2005; Maher et al., 2007; Waters et al., 2010;). As flows moved west from Homa mountain, they became more viscous and sediment laden, causing them to become hyperconcentrated. Upon reaching the gentler relief of the alluvial plain at Nyayanga, these flows decelerated and resulted in aggradation throughout the site, particularly in the depositional low to the northwest (Pierson, 2005; North & Davidson, 2012; de Haas et al., 2014).

Periods of unconfined fluvial activity and fluvial runoff may have been the result of frequent precipitation resulting in more water laden flows capable of erosion/incision, rather than large episodic events (Blair & McPherson, 1994a; Harvey et al., 2005; North & Davidson, 2012; de Haas et al., 2014). Throughout the deposition of NY-1, as well as through NY-2, 3 and 4, periods of landscape stability and flow hiatuses become more common, and the environment is characterised by less frequent wooded vegetation and more vegetation indicative of open environments. This could indicate that aridification generally occurred throughout

time at Nyayanga (deMenocal, 1995; 2004; Tipple & Pagani, 2007; Ségalen et al., 2007; Edwards et al., 2010). Fluvial flows like those observed throughout these units, rather than that of hyperconcentrated flows are often more characteristic of such climates in alluvial plains (Harvey et al., 2005; Waters et al., 2010).

The variability in climate observed at Nyayanga may be owed to orbital forcing. Precession cycles largely influenced moisture availability and seasonality throughout the time that the sediments Nyayanga were deposited, which may explain the intermittent nature of flows and their periodic hiatuses (deMenocal, 1995; Teaford & Ungar, 2000; Bobe & Eck, 2001; Trauth et al., 2003; Clement et al., 2004; Denison et al., 2005; Reed & Fish, 2005; Deino et al., 2006; Hopley et al., 2007; Kingston, 2007; Lepre et al., 2007; Wilson, 2011; Joordens et al., 2011; Magill et al., 2013b; Ashley et al., 2014a; Maslin et al., 2014).

Additionally, the aridification interpreted at Nyayanga may relate to the iNHG (section 3.4.3.), which coincides with the supposed age (3.05 – 2.595 Ma) of sediments here (Maslin et al., 2014; Finestone, 2019). This would have resulted in a variable climate regime with an increase in regional aridity, which can also be observed at Nyayanga (Keigwin, 1978; 1982; Ruddiman et al., 1988; Keller et al., 1989; Mann & Corrigan, 1990; Raymo, 1991; 1994; Wright & Miller, 1996; Li et al., 1998; Haug & Tiedemann, 1998; Maslin et al., 1998; 2014; Crowley & Hyde, 2008; DeConto et al., 2008; Fedorov et al., 2013; Abe-Ouchi et al., 2013).

The openness of the environment and lack of stabilising vegetation observed throughout the sediments at Nyayanga could also relate to the expansion of C_4 grasses (Tipple & Pagani, 2007; Ségalen et al., 2007; Edwards et al., 2010; Cerling et al., 2013; Maslin et al., 2014). These became more common with increased aridity (section 3.4.3.), and explain the lack of wooded vegetation throughout the site. However, the low frequency of wood may also be related to phytolith production rates. Wooded vegetation produce lower amounts of phytoliths than that of grasses and herbaceous vegetation, causing them to become underrepresented in the phytolith distribution (Piperno, 1988; 2006; Piperno & Pearsall, 1998; Albert et al., 1999; Barboni et al., 1999; Strömberg, 2004; Mercader et al., 2009; Kinyanjui, 2012).

6.3.2. Sare River
6.3.2.1. Introduction

The palaeoenvironmental setting of the two sedimentary units identified at Sare River are interpreted based on the results obtained in Chapter 5, specifically the description of sediments in section 5.3.5. This is summarised in Table 6.2, whilst the sections below explore this in more detail. Driving mechanisms of palaeoenvironmental change here are also discussed.

Table 6.2: A summary of palaeoenvironmental characteristics interpreted for each sedimentary unit and subunit identified at Sare River based on sediment descriptions in section 5.3.5

Unit	Palaeoenvironment
SARE-1	Sediments primarily deposited via intermittent low energy unconfined fluvial activity. The frequency of these flow reduced throughout deposition of this unit. Flow hiatuses were characterised by stable land surface development and secondary processes. Open environment characterised by bushy grasslands/grassy bushlands with infrequent wooded vegetation. Wooded vegetation increases in frequency throughout this unit
SARE-2	Similar environment to SARE-1. Intermittent low energy unconfined fluvial activity deposited sediments here, with lengthier/more frequent flow hiatuses. Pedogenic development took place during these periods. Open environment characterised by bushy grasslands with infrequent wooded vegetation

6.3.2.2. SARE-1 interpretation

Deposition of SARE-1 was previously thought to have occurred at ~ 1.77 Ma, based on magnetostratigraphy and the correlation of reversed polarity sediments with the Olduvai Subchron (Finestone, 2019). However, new evidence from cosmogenic dates which provide an absolute date of sediment deposition suggest that sediments were deposited more recently than previously thought, with an age of 1.512 ± 0.089 Ma. This highlights the importance of utilising multiple methods of chronological control, particularly independent numerical dating methods (Barham et al., 2011; Gibbon et al., 2014; Granger et al., 2015). However, one must be aware that post burial production of cosmogenic nuclides can complicate dating when using this method (Granger & Muzikar, 2001).

With only EXC4 (Figure 2.8) containing exposures of SARE-1 (section 5.3.5.1), it is difficult to accurately interpret the palaeoenvironment that sediments belonging to this unit were deposited in. From what can be observed, a low energy environment

is evident, with poorly sorted silt sized sediment dominant throughout (Visher, 1969; McLaren & Bowles, 1985; Pye & Blott, 2004). The dominance of EM2 throughout this unit suggests that sediments were primarily deposited by low energy intermittent fluvial flows. The lack of evidence for a channel suggests that this was most likely unconfined fluvial activity (North & Davidson, 2012; Miall, 2013;). The increase in EM1 throughout this unit suggests that these flows became more infrequent and were separated by periods of landscape stability during flow hiatuses. The lack of any pedogenic features indicates these periods were not long enough for the development of soils (Machette, 1985). Alternatively, these flows might have migrated laterally allowing for periods of landscape stability to take place, which is common in alluvial plains (Blair & McPherson, 1994a; Harvey et al., 2005; de Haas et al., 2014;). The increase in wooded vegetation throughout this unit aligns with more frequent periods of landscape stability. Vegetation remains dominated by grasses and herbaceous vegetation and points towards a largely open landscape characterised by bushy grasslands/grassy bushlands with occasional wooded vegetation.

6.3.2.3. SARE-2 interpretation

A similar environment persists throughout SARE-2 (section 5.3.5.2). The lack of sedimentary structures and the abundance of EM2 throughout EXC5 (Figure 2.8) suggests that unconfined fluvial activity was concentrated here. The relatively lower abundances of EM1 indicates that periods of landscape stability were infrequent. Flow hiatuses and periods of landscape stability appear to become more frequent throughout this unit, as reflected by the increase in EM1 and the absence of granule grade sediment (Visher, 1969; McLaren & Bowles, 1985). The laterally equivalent sediments at EXC1 (Figure 2.8) appear to experience less frequent unconfined fluvial activity than that of EXC5, and may have been located close to the margins of the flows. An increase in silt and clay sized sediment as well as the dominance of EM1 suggests that sediments here were exposed to greater periods of landscape stability (Visher, 1969). The presence of carbonate nodules attests to this, yet their low frequency suggests that soils did not develop to significant maturity (Machette, 1985). It is likely that the unconfined fluvial activity throughout this unit was subject to lateral migration, allowing for periods of landscape stability to occur in laterally equivalent sediments (Blair & McPherson, 1994a; Harvey et al., 2005; de Haas et

al., 2014). Like SARE-1, the environment may still be characterised as a bushy grassland with infrequent wooded vegetation.

6.3.2.4. Palaeoenvironmental reconstruction

The depositional environment at Sare River is similar to that of Nyayanga. It is interpreted as a more distal alluvial plain than that of Nyayanga, having been subject to intermittent unconfined fluvial activity, as well as fluvial runoff and aeolian deposition in periods of inactivity. Stable land surfaces developed in these flow hiatuses, characterised by pedogenic development of the wider landscape. Deposition of sediments largely occurred across an open envionrment characterised by bushy grasslands and grassy bushlands, with infrequent wooded vegetation.

Alluvial plains at Sare River were likely formed as a result of the greater relief to the southeast at Nyamira (Figure 6.2) which created a reduction in relief towards the depositional low in the west, formed by the EARS. Sare River is located in the intermediate area between the highlands and depositional low, where broad plains with mild changes in relief were likely to have existed.
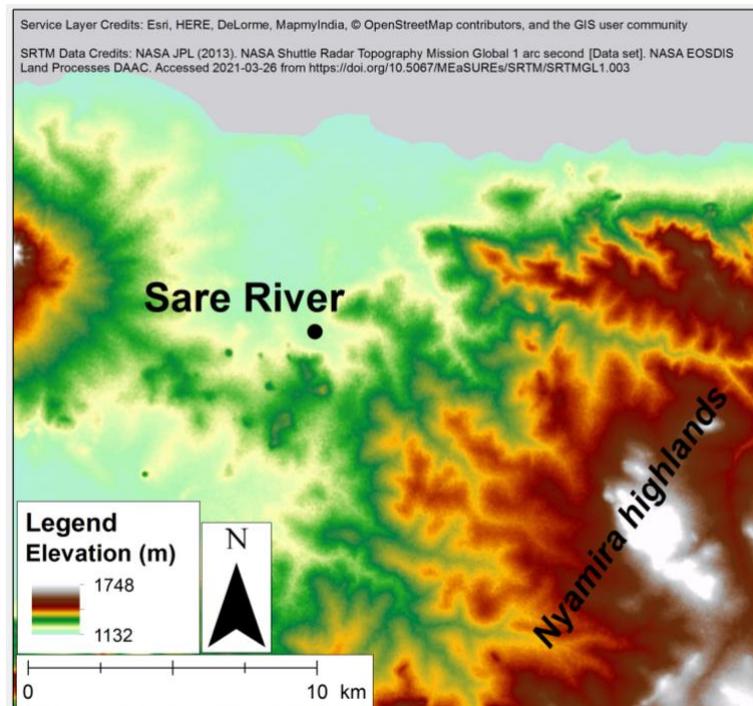
Figure 6.2: Topographic map of western Kenya displaying the elevation change between Sare River and Nyamira.

Deposition of SARE-1 at 1.512 ± 0.089 Ma may represent a period in which this sector of the alluvial plain saw more frequent activity (Figure 6.3), with few periods

of landscape stability, as evidenced by the lack of pedogenic development (Machette, 1985). These periods of landscape stability became more common throughout the deposition of this unit, suggesting that fluvial activity likely migrated laterally from this area, which is common in alluvial plain settings (Blair & McPherson, 1994a; Harvey et al., 2005; de Haas et al., 2014). Alternatively, aridification at the site may have reduced moisture availability over time, resulting in lengthier and more frequent flow hiatuses (deMenocal, 1995; 2004; Tipple & Pagani, 2007; Ségalen et al., 2007; Edwards et al., 2010). Secondary processes including fluvial runoff and aeolian deposition are thought to have occurred during periods of inactivity. Deposition occurred across an open landscape characterised by bushy grasslands/grassy bushlands (Vandenberghe, 2013; de Haas et al., 2014).

The later deposition of SARE-2 represents a continuation of the previous environmental characteristics. Stable land surfaces characterised by pedogenic development became increasingly frequent (Machette, 1985; Ditchfield et al., 1999).
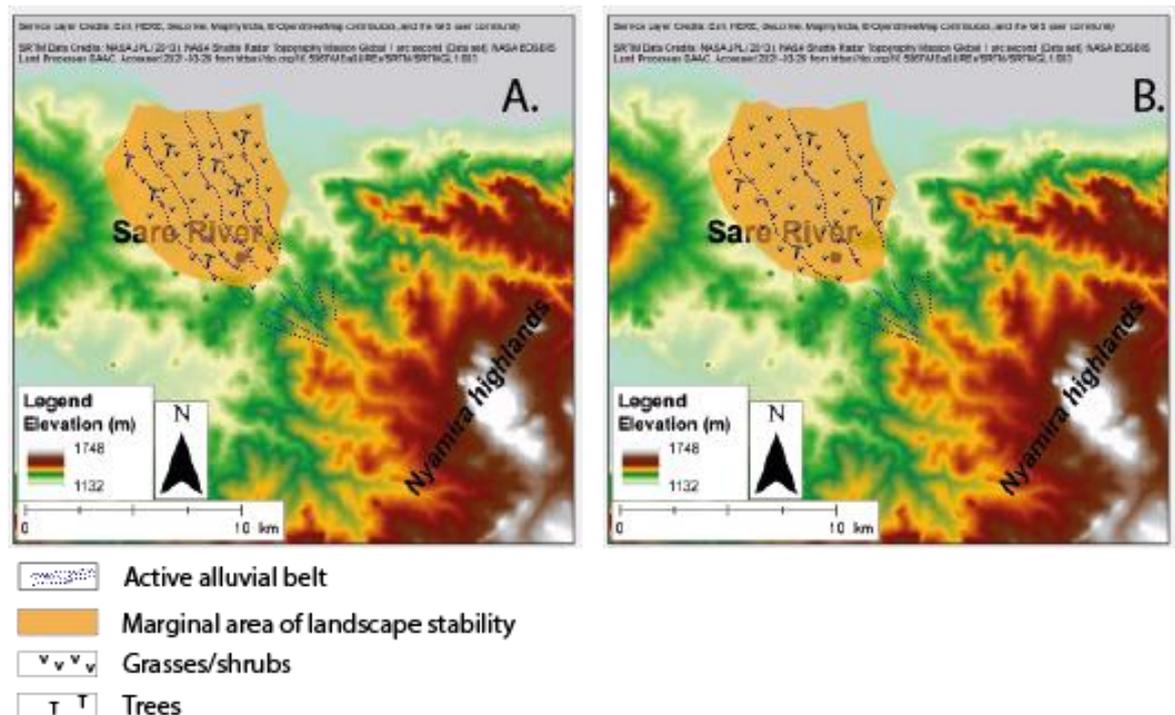
Figure 6.3: Conceptual model displaying how the alluvial plain which Sare River is located upon may have experienced less activity due to the trend towards increased aridity. A. shows the SARE-1 landscape which has increased fluvial activity owed to higher moisture availability. B. shows how this fluvial activity likely became more infrequent by SARE-2, leaving larger spaces of landscape stability subject to secondary processes of deposition

This in combination with the low energy characteristics throughout this unit suggest that migration of the active area of the alluvial plain had occurred by this time, and that deposition probably occurred through secondary processes across the

landscape in the form of fluvial runoff and aeolian deposition (Vandenberghe, 2013; de Haas et al., 2014). This continued to occur across an open landscape characterised by bushy grasslands with infrequent wooded vegetation (Figure 6.3).

6.3.2.5. Drivers of palaeoenvironmental change

Much like palaeoenvironmental evolution at Nyayanga, a combination of regional and local tectonics as well as changes in climate most likely drove environmental change at Sare River. The development of the EARS created a depositional low in the west for the accumulation of sediments most likely sourced from areas of greater relief in the east where uplift occurred (Le Bas, 1977; Sepulchre et al., 2006; Bergner et al., 2009; Trauth et al., 2010; Olaka et al., 2010; Maslin et al., 2014). Sediments likely aggraded on the broad plains in the intermediate area between these two locations at Sare River (Blair & McPherson, 1994a; Harvey et al., 2005; Waters et al., 2010; de Haas et al., 2014). Changes in base-level caused by the formation and destruction of palaeolakes throughout the EARS would have influenced periods of incision and aggradation at Sare River (Stokes & Mather, 2000; Maher et al., 2007; Maher & Harvey, 2008). Additionally, local faulting would have had an influence on sediment supply and geomorphological changes to the catchment that Sare River was located in, with river capture a possibility in the area surrounding the Nyamira highlands (Harvey et al., 2005; Waters et al., 2010). The Kaniamwia Fault is located in close proximity to Sare River and may have had an influence on the envionrment (Le Bas, 1977).

The lack of a rapid change in sedimentary characteristics or palaeovegetation indicates that tectonics were not the main driver of palaeoenvironmental change at Sare River. Climate may have had a more gradual impact on palaeoenvironmental evolution at Sare River. The increase in frequency of periods of inactivity and stable land surface development as well as the openness of the landscape indicates that the site suffered a gradual reduction in moisture availability and experienced aridification over time (deMenocal, 1995; 2004; Trauth et al., 2009; Maslin et al., 2014). This may also relate to the expansion of C_4 grasses, which are frequently linked to more arid environments (deMenocal, 1995; 2004; Tipple & Pagani, 2007; Ségalen et al., 2007; Edwards et al., 2010).

Aridification here may be related to the DWC, which resulted in increased aridity in East Africa from ~ 2 Ma throughout the Pleistocene, similar to the time these sediments were deposited (Saji et al., 1999; Ravelo et al., 2004; McClymont & Rosell-Melé, 2005; Liu et al., 2008; Brierley et al., 2009; Trauth et al., 2009; Fedorov et al., 2013; Larrasoaña et al., 2013; Maslin et al., 2014). Intermittent unconfined fluvial activity is also characteristic of arid alluvial environments (Harvey et al., 2005; Waters et al., 2010). Alternatively, periods of inactivity may instead be owed to a migration of the drainage network on the alluvial plain, allowing stable land surfaces to develop at Sare River (Blair & McPherson, 1994a; Harvey et al., 2005; de Haas et al., 2014).

6.4. Hominin activity on the Homa Peninsula and its place in the wider East African context

The Homa Peninsula provides two new records of Hominin activity throughout the Plio-Pleistocene. At Nyayanga where sediments are dated to ~ 2.6 Ma (Finestone, 2019), hominins (*Paranthropus* sp.) inhabited or frequented an alluvial environment that was characterised by intermittent flows and periods of stable land surface development. The climate here appeared to be variable, but experienced gradual aridification and was characterised by an open landscape with bushy grasslands and grassy bushlands. Such environments are typical of *Paranthropus* (Wynn, 2004; Bamford, 2005; Wood & Leakey, 2011; Bobe, 2011; Albert et al., 2015), whom had craniodental morphology adapted to processing large quantities of low-quality vegetation such as grasses and sedges typical of an open environment, rather than harder objects such as wood (Cerling et al., 2011b). It has previously been highlighted that although it is evident that the diet of *Paranthropus* was largely C_4 based, it has been difficult to identify if this is largely sedge based or grass based with isotopic evidence alone (Cerling, 2014). Phytolith evidence from this research shows that sedges are largely infrequent throughout Nyayanga, suggesting that *Paranthropus* indulged on C_4 based grasses and shrubs. *Paranthropus* is also frequently linked to increased aridification and the development of savanna ecosystems as a result (deMenocal, 1995; 2011; Wynn, 2004). Remains of *Paranthropus* are often found in association with fluvial, deltaic and alluvial environments characterised by low proportions of wooded vegetation (Wynn, 2004; Bobe, 2011; Cerling et al., 2011b; Maslin et al., 2014; Albert et al., 2015). Evidence

from Nyayanga supports current knowledge about the environmental preferences of *Paranthropus* whilst also expanding it to a new spatial context.

Of the different hypotheses linking palaeoenvironmental change to hominin evolution (section 3.2.), Nyayanga provides further detail to previous studies and increases our understanding of environmental linkages. The trend towards greater aridity at Nyayanga as well as the largely open environments provide support that aridity was a major driver in hominin evolution and environmental change (deMenocal, 1995; 2011). The interpretation that the expansion of the EARS and the formation/destruction of lakes throughout it influenced base-level and periods of incision/aggradation throughout the area may also support the notion that the formation/destruction of deep lakes throughout East Africa drove key events in hominin evolution (Trauth et al., 2007; 2010). The most likely hypothesis that palaeoenvironmental change at Nyayanga provides support for is that of the pulsed-climate hypothesis (Maslin & Trauth, 2009). In addition to the evidence for the formation/destruction of lakes, a period of variability whilst trending towards greater aridity is evident at Nyayanga in unit NY-1. This unit also bares the most abundant evidence for hominin activity during this time (Finestone, 2019).

The abundance of hominin tools uncovered at Sare River, particularly in the sediments of SARE-2 suggest that hominin activity was ongoing throughout the time of deposition here (Finestone, 2019). This activity thrived in the low-energy alluvial plains that were characterised by bushy grasslands and grassy bushlands, potentially in a more arid climate. Similar evidence for hominins inhabiting open grasslands and wooded grasslands exists from the Pleistocene period at the Olorgesaillie formation (Table 3.2). Despite this, activity largely occurred in close proximity to a shallow freshwater lake, rather than on a broad alluvial plain like that of Sare River. Similarly, evidence from Olduvai Gorge suggests that hominins inhabited a range of habitats, which included relatively open grasslands during the Pleistocene (Table 3.2). This included alluvial environments that experienced intermittent fluvial activity like that of Sare River. Hominin activity was also interpreted to have taken place on the alluvial plains characterised by wooded grasslands and open grasslands at Kanjera South, although higher energy characteristics are apparent here (Table 3.2). Grassland habitats surrounding a

fluvial system are also evident in the Koobi Fora formation in the mid-Pleistocene (Table 3.2). The dominance of grasslands was also evident at the Nachukui formation, which was characterised by fluvial and alluvial deposition (Table 3.2). The Shungura formation also developed a significant increase in the presence of grassland following 2 Ma, and was again characterised by fluvial deposition (Table 3.2).

Resultantly, the deposits at Sare River support and provide additional evidence for Hominin activity having occurred in more open environments throughout the Pleistocene, particularly in environments characterised by alluvial/fluvial deposition. Its trend towards more open environments that showed longer periods of inactivity might also point towards gradual aridification. This suggests that hominin activity at Sare River might provide additional support to the aridity hypothesis (deMenocal, 1995; 2011)

CHAPTER 7. CONCLUSIONS

7.1. Introduction

It was the aim of this thesis to provide palaeoenvironmental context for evidence of hominin activity across the Homa Peninsula at two sites, Nyayanga and Sare River, whilst also expanding knowledge on hominin environmental preferences to a new spatial context — the Homa Peninsula. To achieve this, objectives for both sites included: (1) reconstruct the depositional environment, (2) reconstruct the palaeovegetation, (3) identify drivers of palaeoenvironmental change by analysing changes in (1) and (2) throughout time and (4) determine the relationship between hominin activity and palaeoenvironmental change, as well its linkage with driving mechanisms.

Utilising a multi-proxy approach which incorporated field sedimentary analyses, particle size analysis, EMMA and analyses of phytoliths, similar environments were identified at both sites. Deposition is thought to have occurred in an alluvial plain setting at both sites, with Nyayanga being more proximal to the sediment source than that of Sare River. This occurred in a largely open landscape characterised by bushy grasslands with infrequent wooded vegetation and sedges. Palaeoenvironmental evolution at both sites is attributed to an interplay of driving mechanisms including tectonic activity and climate, similar to other palaeoenvironmental records from the Plio-Pleistocene of East Africa. The hominin active palaeoenvironments identified align with previous research findings from other hominin bearing sedimentary records from East Africa, whilst also expanding our understanding to a new spatial context — the Homa Peninsula. Fluctuations in climate and an overall trend towards more arid environments, creating largely open landscapes appears to be one of the primary influences on hominin activity.

7.2. Key Findings

7.2.1. Palaeoenvironmental reconstructions

A multi-proxy approach to reconstructing the palaeoenvironment at both sites was utilised. The identification of sedimentary dynamics was enabled using field sedimentary analysis, particle size analysis and EMMA. The latter of these methods allowed for multimodal PSDs to be 'unmixed' and interpreted in detail. Analyses of phytoliths produced reconstructions of palaeovegetation and thus palaeoclimate.

These methods used in conjunction provided detailed insights into the evolution of the palaeoenvironment of the Homa Peninsula.

At Nyayanga, an alluvial plain environment was identified for the deposition of sediments ~ 2.6 Ma. Initially, deposition occurred via episodic hyperconcentrated flows capable of mobilising cobble grade sediment, yet likely to bury underlying sediments rather than erode. Intermittent unconfined fluvial flows more water laden than the hyperconcentrated flows also occurred intermittently, and were capable of eroding underlying sediments. These flows likely decelerated with expansion and became low energy hyperconcentrated flows. Flow hiatuses were characterised by secondary processes including fluvial runoff and aeolian deposition, as well as pedogenic development. Throughout time, higher energy hyperconcentrated flows became absent, whilst unconfined fluvial activity became more infrequent. Pedogenic development and deposition by secondary processes increased in frequency. These changes were likely caused by a migration of the active sector of the alluvial plain, although aridification at may also be responsible for the reduction in the frequency of flows here. The landscape throughout this time remained open, with palaeovegetation fluctuating between bushy grasslands and grassy bushlands with infrequent woodland and sedges.

Similarly, an alluvial plain was identified as the depositional environment for sediments at Sare River at ~ 1.5 Ma, although more distal from the sediment source than that of Nyayanga. Here, intermittent unconfined fluvial activity deposited sediments across the gentle slopes. These became more infrequent throughout time. During flow hiatuses, secondary process deposited sediments on the inactive sector of the plain, whilst stable land surface development and pedogenesis also occurred. The reduced frequency of unconfined fluvial activity is attributed to a migration of the active sector of the alluvial plain. This all occurred in an open landscape characterised by bushy grasslands with infrequent woodland.

7.2.2. Drivers of environmental change on the Homa Peninsula

Palaeoenvironmental change on the Homa Peninsula appears to the result of a complex interplay of driving mechanisms including both regional and local tectonics, as well as climate. At both sites, the development of the EARS created depositional lows with extensive space for the accumulation of sediment, a key feature in alluvial

environments. During its development, the formation and destruction of palaeolakes most likely also influenced changes in base level throughout the peninsula, driving incision and aggradation within the alluvial systems. The formation of the Homa Mountain carbonatite complex created steep changes in relief across the area, as well as a more proximal sediment source for Nyayanga than that of Sare River. These factors account for the occurrence of hyperconcentrated flows at Nyayanga, as well as unconfined fluvial activity with higher energy than those at Sare River.

The most significant driver of palaeoenvironmental change at both sites appears to be that of climate. At Nyayanga, hyperconcentrated flows were most likely caused by episodic high magnitude periods of precipitation which resultantly led to an increased sediment supply and higher sediment entrainment capacities. Intermittent unconfined fluvial activity was likely controlled by lower magnitude higher frequency periods of precipitation. A trend towards a more arid climate is inferred from the increased frequency of flow hiatus and periods of stable land surface development. The timing of this aridification coincides with that of the iNHG, which is thought to have resulted in a variable climate regime with increased regional aridity throughout East Africa. The openness of the environment here can be attributed to this aridification, which resulted in the expansion of C_4 grasslands and the reduced frequency of woodland.

A similar trend is evident at Sare River, where unconfined fluvial activity became more infrequent and periods of landscape stability become more common. This trend is more consistent throughout the sequence at Sare River, unlike the variability in climate observed in the sediments at Nyayanga. Aridification at Sare River coincides with the DWC, which resulted in aridification throughout East Africa from ~ 2 Ma.

7.2.3. Implications for Hominin research

This thesis has provided environmental context for hominin activity (specifically *Paranthropus*) ~ 2.6 Ma in an alluvial environment at Nyayanga, as well as hominin activity ~ 1.5 Ma on the alluvial plains at Sare River. Environmental preferences of *Paranthropus* at Nyayanga align with pre-existing research findings, suggesting these hominins inhabited or frequented similar depositional settings in open landscapes characterised by bushy grasslands with infrequent wooded vegetation.

This is consistent with their largely C_4 based diet. Where isotopic evidence has been unable to identify whether this diet is largely sedge based or grass based, evidence from phytoliths demonstrate that the latter is more likely. Evidence from Nyayanga also corroborates previous linkages between *Paranthropus* and increased aridification and the development of savanna ecosystems. The formation/destruction of lakes as well as the climate variability identified in the hominin baring sediments of NY-1 at Nyayanga provides support for the pulsed-climate hypothesis linking environmental change to hominin evolution.

Similar to other Pleistocene palaeoenvironmental records, Sare River proves support that hominin activity during this period thrived in open environments characterised by alluvial/fluvial deposition. The trend towards greater aridity throughout the sediments at this site suggests that hominin activity at Sare River could provide support for the aridity hypothesis linking palaeoenvironmental change to hominin evolution.

7.2.4. The use of EMMA in interpreting depositional environments

The novel use of EMMA to interpret sedimentary dynamics in Plio-Pleistocene palaeoenvironmental records from East Africa has proven successful in this context. PSA alone is incapable of highlighting various depositional mechanisms that may have occurred throughout a site, particularly where sediments are multimodal, which most often they are. By utilising EMMA in conjunction with field sedimentary analyses, it has been possible to infer the sedimentary dynamics that occurred throughout the Homa Peninsula and to what extent they are represented at spatially and temporally varying locations. This is invaluable when assessing how depositional environments are likely to have evolved.

Additionally, the use of EMMA and sedimentology allowed for the identification of hyperconcentrated flows that may bury underlying sediments rather than eroding them, which is detrimental in establishing whether traces of hominin activity uncovered at Nyayanga are in fact *in situ*.

7.2.5. Phytoliths as a tool for reconstructions of palaeovegetation

Phytoliths have proven a competent tool in assessing the palaeovegetation structure of the Plio-Pleistocene environment of the Homa Peninsula. Due to their

excellent preservative characteristics, this has allowed for the reconstruction of vegetation structure where other methods may have failed. Due to the age of sediments, particularly at Nyayanga, pollen is not preserved well. Additionally, isotopic evidence fails to distinguish the types of vegetation throughout a site. Such information has proven valuable to this work, as more detailed information on the diet of *Paranthropus* has been revealed, as well as the environments in which hominin activity took place.

7.2.6. Cosmogenic dating as an independent chronological constraint

Previously, chronology at Sare River was based on magnetostratigraphy and its correlation with a tuff alone. The lack of an absolute date here made interpretations of chronology difficult, as an independent date could not be used to constrain the relative dating of magnetostratigraphy. Cosmogenic nuclide dates obtained from sediments at Sare River have provided an independent chronological constraint on sediments and better inform chronological inferences from magnetostratigraphy. The age of sediments acquired form cosmogenic dating suggests that sediments are younger than previously thought, although limitations surrounding post burial production of cosmogenic radionuclides should also be acknowledged.

7.3. Limitations of this research

It is essential that the limitations of this research are addressed to best inform interpretations and the direction of future work here. One of these limitations is sampling resolution. Samples were not taken at regular intervals, and instead targeted spot samples were taken. More detailed information on palaeoenvironmental change may have been acquired through the acquisition of samples from regular intervals. At Sare River, the spatial resolution of sampling was also limited due to the lack of exposures available to sample, as well as the time constraints faced whilst in the field. More detailed information about the palaeoenvironment and its lateral variability could be acquired by improving spatial resolution of sampling.

The analyses of phytoliths in this study is also limited to an extent. Phytoliths can provide more detailed information on plant taxa and resultantly attribute them to C_3/C_4 mechanisms, providing information on climate dynamics. However, in this

study phytoliths were only used to provide information on the types of vegetation present at the time of deposition, with delineations between grasses, herbaceous vegetation, sedges and woodland. This was largely due to the time constraints faced in sufficiently developing this technique for such inferences to be made, as this method is largely subjective and operator dependant. As previously discussed, phytolith counts for Sare River were completed prior to the awareness of several morphotypes. Due to time constraints, it was not possible to complete these counts again. For this reason, the sedge and wood components of the vegetation structure at Sare River may be under-represented.

Chronological control at Nyayanga requires improvement. Here, no independent absolute dates of sediments exist, which makes it difficult to constrain the timing of sediment deposition. Only biostratigraphy and magnetostratigraphy are used throughout this site, both of which are relative dating techniques and cannot provide accurate numerical dates on the deposition of sediment.

7.4. Direction of future work

This research has provided the basis for more in depth reconstructions of the palaeoenvironment at Nyayanga and Sare River. Sedimentary units have been identified and their lithofacies described, providing a framework for future analyses. Such analyses might include that of plant wax lipid biomarkers (e.g. Magill et al., 2013a; 2016; Uno et al., 2011; 2016b) or $\delta^{13}C$ isotopic analyses (e.g. Levin et al., 2004; Quinn et al., 2007; Plummer et al., 2009b; Cerling et al., 2011b; 2011c) to further inform the palaeovegetation structure at both sites, due to the limitations faced with analyses of phytoliths. Additionally, more detailed information could be obtained on the moisture availability at both sites through the analysis of $\delta^{18}O$ isotopes (e.g. Cerling et al., 2003; Wynn, 2004; Quinn et al., 2007; Sikes & Ashley, 2007; Levin et al., 2011). This would allow for more accurate conclusions to be drawn on the drivers of palaeoenvironmental change at both sites, particularly if it is thought that climate is one of the main drivers.

Future work would also benefit from increasing the resolution of sampling, which would allow for more discrete changes in sediments to be identified, thus allowing for more detailed insights into palaeoenvironmental trends to be obtained (Hartmann, 2007). This would also allow the facies model created herein to be

further refined, with the potential of better describing existing lithofacies and possibly identify sub-facies within these. Additionally, by increasing the spatial resolution of sampling at Sare River, more detailed interpretations of the environments lateral variability could be obtained.

It is essential that future work on the Homa Peninsula prioritises chronological control. Independent absolute dates for sediments at Nyayanga would aid in attributing driving mechanisms to palaeoenvironmental change here, whilst also informing on rates of deposition. This would allow for more detailed information to be provided on the timing of hominin activity here and the environmental factors which influenced such. Further dating at Sare River would also be beneficial in order to validate dates acquired for the site thus far.

REFERENCE LIST

Abe-Ouchi, A., Saito, F., Kawamura, K., Raymo, M.E., Okuno, J., Takahashi, K. & Blatter, H. (2013). Insolation-driven 100,000-year glacial cycles and hysteresis of ice-sheet volume. *Nature.* 500 (7461), pp. 190–193.

Albert, R.M., (2003). Quantitative Phytolith Study of Hearths from the Natufian and Middle Palaeolithic Levels of Hayonim Cave (Galilee, Israel). *Journal of Archaeological Science.* 30 (4), pp. 461–480.

Albert, R.M., (1999). Study of ash layers through phytolith analyses from the Middle palaeolithic levels of Kebara and Tabun caves (Israel). *University of Barcelona*, p. 250.

Albert, R.M. & Weiner, S. (2001). Study of phytoliths in prehistoric ash layers from Kebara and Tabun caves using a quantitative approach. In: *Phytoliths application in earth sciences and human history.* pp. 251–266.

Albert, R.M., Bamford, M.K. & Cabanes, D. (2009). Palaeoecological significance of palms at Olduvai Gorge, Tanzania, based on phytolith remains. *Quaternary International.* 193 (1-2), pp. 41–48.

Albert, R.M., Bamford, M.K. & Cabanes, D. (2006). Taphonomy of phytoliths and macroplants in different soils from Olduvai Gorge (Tanzania) and the application to Plio-Pleistocene palaeoanthropological samples. *Quaternary International.* 148 (1), pp. 78–94.

Albert, R.M., Bamford, M.K., Stanistreet, I., Stollhofen, H., Rivera-Rondón, C. & Rodr i guez-Cintas, A. (2015). Vegetation landscape at DK locality, Olduvai Gorge, Tanzania. *Palaeogeography, Palaeoclimatology, Palaeoecology.* 426, pp. 34–45.

Albert, R.M., Lavi, O., Estroff, L., Weiner, S., Tsatskin, A., Ronen, A. & Lev-Yadun, S. (1999). Mode of Occupation of Tabun Cave, Mt Carmel, Israel During the Mousterian Period: A Study of the Sediments and Phytoliths. *Journal of Archaeological Science.* 26 (10), pp. 1249–1260.

Albert, R.M., Weiner, S., Bar-Yosef, O. & Meignen, L. (2000). Phytoliths in the Middle Palaeolithic Deposits of Kebara Cave, Mt Carmel, Israel: Study of the Plant Materials used for Fuel and Other Purposes. *Journal of Archaeological Science.* 27 (10), pp. 931–947.

Alemseged, Z. (2003). An integrated approach to taphonomy and faunal change in the Shungura Formation (Ethiopia) and its implication for hominid evolution. *Journal of Human Evolution.* 44 (4), pp. 451–478.

Alexandre, A., Meunier, J.D., Lézine, A.M., Vincens, A. & Schwartz, D. (1997). Phytoliths: Indicators of grassland dynamics during the late Holocene in intertropical Africa. *Palaeogeography, Palaeoclimatology, Palaeoecology.* 136 (1-4), pp. 213–229.

Amireh, B.S. (2015). Grain size analysis of the Lower Cambrian-Lower Cretaceous clastic sequence of Jordan: Sedimentological and paleo-hydrodynamical implications. *Journal of Asian Earth Sciences*. 97, pp. 67–88.

Andrews, P. & Bamford, M. (2008). Past and present vegetation ecology of Laetoli, Tanzania. *Journal of Human Evolution*. 54 (1), pp. 78–98.

Andrews, P. & Humphrey, L. (1999). African Miocene environments and the transition to early hominines. In: *African Biogeography, Climate Change and Human Evolution*. Oxford: Oxford University Press, pp. 282–300.

Antón, S.C. (2003). Natural history of Homo erectus. *American Journal of Physical Anthropology*. 122 (S37), pp. 126–170.

Aronson, J.L., Hailemichael, M. & Savin, S.M. (2008). Hominid environments at Hadar from paleosol studies in a framework of Ethiopian climate change. *Journal of Human Evolution*. 55 (4), pp. 532–550.

Ashley, G.M. (1978). Interpretation of Polymodal Sediments. *The Journal of Geology*. 86 (4), pp. 411–421.

Ashley, G.M. (2007). Orbital rhythms, monsoons, and playa lake response, Olduvai Basin, equatorial East Africa (ca. 1.85–1.74 Ma). *Geology*. 35 (12), pp. 1091–1094.

Ashley, G.M. & Driese, S.G. (2000). Paleopedology and paleohydrology of a volcaniclastic paleosol interval: Implications for Early Pleistocene stratigraphy and paleoclimate record: Olduvai Gorge, Tanzania. *Journal of Sedimentary Research*. 70 (5), pp. 1065–1080.

Ashley, G.M., Barboni, D., Dominguez-Rodrigo, M., Bunn, H.T., Mabulla, A.Z.P., Diez-Martin, F., Barba, R. & Baquedano, E. (2010a). Paleoenvironmental and paleoecological reconstruction of a freshwater oasis in savannah grassland at FLK North, Olduvai Gorge, Tanzania. *Quaternary Research*. 74 (3), pp. 333–343.

Ashley, G.M., Beverly, E.J., Sikes, N.E. & Driese, S.G. (2014a). Paleosol diversity in the Olduvai Basin, Tanzania: Effects of geomorphology, parent material, depositional environment, and groundwater on soil development. *Quaternary International*. 322, pp. 66–77.

Ashley, G.M., Bunn, H.T., Delaney, J.S., Barboni, D., Dominguez-Rodrigo, M., Mabulla, A.Z.P., Gurtov, A.N., Baluyot, R., Beverly, E.J. & Baquedano, E. (2014b). Paleoclimatic and paleoenvironmental framework of FLK North archaeological site, Olduvai Gorge, Tanzania. *Quaternary International*. 322, pp. 54–65.

Ashley, G.M., Dominguez-Rodrigo, M., Bunn, H.T., Mabulla, A.Z.P. & Baquedano, E. (2010b). Sedimentary Geology and Human Origins: A Fresh Look at Olduvai Gorge, Tanzania. *Journal of Sedimentary Research*. 80, pp. 703–709.

Ashley, G.M., Tactikos, J.C. & Owen, R.B. (2009). Hominin use of springs and

wetlands: Paleoclimate and archaeological records from Olduvai Gorge (~ 1.79-1.74 Ma). *Palaeogeography, Palaeoclimatology, Palaeoecology*. 272 (1-2), pp. 1–16.

Baker, B.H., Mitchell, J.G. & Williams, L.A.J. (1988). Stratigraphy, geochronology and volcano-tectonic evolution of the Kedong- Naivasha-Kinangop region, Gregory Rift Valley, Kenya. *Journal of the Geogogical Society, London*. 145, pp. 107–116.

Balco, G. & Rovey, C.W. (2008). An isochron method for cosmogenic-nuclide dating of buried soils and sediments. *American Journal of Science*. 308 (10), pp. 1083–1114.

Bamford, M.K. (2005). Early Pleistocene fossil wood from Olduvai Gorge, Tanzania. *Quaternary International*. 129 (1), pp. 15–22.

Bamford, M.K. (2011a). Fossil Leaves, Fruits and Seeds. In: T. Harrison (ed.). *Paleontology and Geology of Laetoli: Human Evolution in Context*. Dordrecht: Springer Netherlands, pp. 235–252.

Bamford, M.K. (2012). Fossil sedges, macroplants, and roots from Olduvai Gorge, Tanzania. *Journal of Human Evolution*. 63 (2), pp. 351–363.

Bamford, M.K. (2011b). Fossil Woods. In: T. Harrison (ed.). *Paleontology and Geology of Laetoli: Human Evolution in Context*. Dordrecht: Springer Netherlands, pp. 217–233.

Bamford, M.K. (2017). Pleistocene fossil woods from the Okote Member, site FwJj 14 in the Ileret region, Koobi Fora Formation, northern Kenya. *Journal of Human Evolution*. 112, pp. 134–147.

Bamford, M.K., Albert, R.M. & Cabanes, D. (2006). Plio–Pleistocene macroplant fossil remains and phytoliths from Lowermost Bed II in the eastern palaeolake margin of Olduvai Gorge, Tanzania. *Quaternary International*. 148 (1), pp. 95–112.

Bamford, M.K., Stanistreet, I.G., Stollhofen, H. & Albert, R.M. (2008). Late Pliocene grassland from Olduvai Gorge, Tanzania. *Palaeogeography, Palaeoclimatology, Palaeoecology*. 257 (3), pp. 280–293.

Barber, K.E., Maddy, D., Rose, N., Stevenson, A.C., Stoneman, R. & Thompson, R. (2000). Replicated proxy-climate signals over the last 2000 yr from two distant UK peat bogs: new evidence for regional palaeoclimate teleconnections. *Quaternary Science Reviews*. 19 (6), pp. 481–487.

Barboni, D. (2014). Vegetation of Northern Tanzania during the Plio-Pleistocene: A synthesis of the paleobotanical evidences from Laetoli, Olduvai, and Peninj hominin sites. *Quaternary International*. 322, pp. 264–276.

Barboni, D. & Bremond, L. (2009). Phytoliths of East African grasses: An assessment of their environmental and taxonomic significance based on floristic data. *Review of Palaeobotany and Palynology*. 158 (1-2). pp. 29–41.

Barboni, D., Ashley, G.M., Dominguez-Rodrigo, M., Bunn, H.T., Mabulla, A.Z.P. & Baquedano, E. (2010). Phytoliths infer locally dense and heterogeneous paleovegetation at FLK North and surrounding localities during upper Bed I time, Olduvai Gorge, Tanzania. *Quaternary Research*. 74 (3), pp. 344–354.

Barboni, D., Bonnefille, R., Alexandre, A. & Meunier, J.D. (1999). Phytoliths as paleoenvironmental indicators, West Side Middle Awash Valley, Ethiopia. *Palaeogeography, Palaeoclimatology, Palaeoecology*. 152 (1-2), pp. 87–100.

Barboni, D., Bremond, L. & Bonnefille, R. (2007). Comparative study of modern phytolith assemblages from inter-tropical Africa. *Palaeogeography, Palaeoclimatology, Palaeoecology*. 246 (2-4), pp. 454–470.

Barham, L., Phillips, W.M., Maher, B.A., Karloukovski, V., Duller, G.A.T., Jain, M. & Wintle, A.G. (2011). The dating and interpretation of a Mode 1 site in the Luangwa Valley, Zambia. *Journal of Human Evolution*. 60 (5), pp. 549–570.

Barr, W.A. (2015). Paleoenvironments of the Shungura Formation (Plio-Pleistocene: Ethiopia) based on ecomorphology of the bovid astragalus. *Journal of Human Evolution*. 88, pp. 97–107.

Bedaso, Z.K. (2011). *Stable Isotope Studies of Paleoenvironment and Paleoclimate from Afar, Ethiopia*. Ph. D. University of South Florida.

Behrensmeyer, A., Potts, R., Plummer, T., Tauxe, L., Opdyke, N. & Jorstad, T. (1995). The Pleistocene locality of Kanjera, Western Kenya: stratigraphy, chronology and paleoenvironments. *Journal of Human Evolution*. 29 (3), pp. 247-274.

Behrensmeyer, A.K. (1997). Late Pliocene Faunal Turnover in the Turkana Basin, Kenya and Ethiopia. *Science*. 278 (5343), pp. 1589–1594.

Bement, L.C., Carter, B.J., Varney, R.A., Cummings, L.S. & Sudbury, J.B. (2007). Paleo-environmental reconstruction and bio-stratigraphy, Oklahoma Panhandle, USA. *Quaternary International*. 169, pp. 39–50.

Bennett, C.E., Marshall, J.D. & Stanistreet, I.G. (2012). Carbonate horizons, paleosols, and lake flooding cycles: Beds I and II of Olduvai Gorge, Tanzania. *Journal of Human Evolution*. 63 (2), pp. 328–341.

Berger, A., Loutre, M.F. & Melice, J.L. (2006). Equatorial insolation: from precession harmonics to eccentricity frequencies. Climate of the Past. *European Geosciences Union (EGU)*. 2 (2), pp. 131–136.

Berger, W.H. & Jansen, E. (1994). Mid-pleistocene climate shift-the Nansen connection. The polar oceans and their role in shaping the global environment. *American Geosciences Union (AGU)*. 85, pp. 295–311.

Bergner, A.G., Trauth, M.H. & Bookhagen, B. (2003). Paleoprecipitation estimates for the Lake Naivasha basin (Kenya) during the last 175 ky using a lake-balance model. *Global and Planetary Change*. 36 (1-2), pp. 117–136.

Bergner, A.G.N., Strecker, M.R., Trauth, M.H., Deino, A., Gasse, F., Blisniuk, P. & DUhnforth, M. (2009). Tectonic and climatic control on evolution of rift lakes in the Central Kenya Rift, East Africa. *Quaternary Science Reviews*. 28 (25-26), pp. 2804–2816.

Beuselinck, L., Govers, G., Poesen, J., Degraer, G. & Froyen, L. (1998). Grain-size analysis by laser diffractometry: Comparison with the sieve-pipette method. *Catena*. 32 (3-4), pp. 193–208.

Bickert, T., Haug, G.H. & Tiedemann, R. (2004). Late Neogene benthic stable isotope record of Ocean Drilling Program Site 999: Implications for Caribbean paleoceanography, organic carbon burial, and the Messinian Salinity Crisis. *Paleoceanography*. 19 (1), pp. 1-11

Bishop, L.C., Plummer, T.W., Ferraro, J.V., Braun, D., Ditchfield, P.W., Hertel, F., Kingston, J.D., Hicks, J. & Potts, R. (2006). Recent research into oldowan hominin activities at Kanjera South, Western Kenya. *African Archaeological Review*. 23 (1-2), pp. 31–40.

Bishop, L.C., Plummer, T.W., Hertel, F. & Kovarovic, K. (2011). Paleoenvironments of Laetoli, Tanzania as Determined by Antelope Habitat Preferences. In: *Paleontology and Geology of Laetoli: Human Evolution in Context*. Dordrecht, Springer. pp. 355–366.

Blair, T.C. & McPherson, J.G. (1994a). Alluvial Fan Processes and Forms. In: *Geomorphology of Desert Environments*. Dordrecht, Springer. pp. 354–402.

Blair, T.C. & McPherson, J.G. (1994b). Alluvial Fans and their Natural Distinction from Rivers Based on Morphology, Hydraulic Processes, Sedimentary Processes, and Facies Assemblages. *Journal of Sedimentary Research*. 64 (3a), pp. 450–489.

Blisniuk, P. & Strecker, M.R. (1990). Asymmetric rift-basin development in the central Kenya Rift. *Terra Abstr.,* 2, p. 51.

Blott, S.J. & Pye, K. (2001). Gradistat: A grain size distribution and statistics package for the analysis of unconsolidated sediments. *Earth Surface Processes and Landforms*. 26 (11), pp. 1237–1248.

Blott, S.J., Croft, D.J., Pye, K., Saye, S.E. & Wilson, H.E. (2004). Particle size analysis by laser diffraction. *Geological Society, London, Special Publications*. 232 (1), pp. 63–73.

Blumenschine, R.J., Peters, C.R., Masao, F.T., Clarke, R.J., Deino, A.L., Hay, R.L., Swisher, C.C., Stanistreet, I.G., Ashley, G.M., McHenry, L.J., Sikes, N.E., Van Der Merwe, N.J., Tactikos, J.C., Cushing, A.E., Deocampo, D.M., Njau, J.K. & Ebert, J.I. (2003). Late Pliocene Homo and hominid land use from Western Olduvai Gorge, Tanzania. *Science*. 299 (5610), pp. 1217–1221.

Blumenschine, R.J., Stanistreet, I.G. & Masao, F.T. (2012). Olduvai Gorge and the Olduvai Landscape Paleoanthropology Project. *Journal of Human Evolution*. 63 (2), pp. 247–250.

Bobe, R. (2011). Fossil Mammals and Paleoenvironments in the Omo-Turkana Basin. *Evolutionary Anthropology: Issues, News, and Reviews*. 20 (6), pp. 254–263.

Bobe, R. (2006). The evolution of arid ecosystems in eastern Africa. *Journal of Arid Environments*. 66 (3), pp. 564–584.

Bobe, R. & Behrensmeyer, A.K. (2004). The expansion of grassland ecosystems in Africa in relation to mammalian evolution and the origin of the genus Homo. *Palaeogeography, Palaeoclimatology, Palaeoecology*. 207 (3), pp. 399–420.

Bobe, R. & Eck, G.G. (2001). Responses of African Bovids to Pliocene Climatic Change. *Paleobiology*. 27 (2), pp. 1–47.

Bobe, R. & Leakey, M.G. (2009). Ecology of Plio-Pleistocene mammals in the Omo—Turkana Basin and the emergence of Homo. In: *The First Humans--Origin and Early Evolution of the Genus Homo*. Springer. pp. 173–184.

Bobe, R., Behrensmeyer, A.K. & Chapman, R.E. (2002). Faunal change, environmental variability and late Pliocene hominin evolution. *Journal of Human Evolution*. 42 (4), pp. 475–497.

Bobe, R., Behrensmeyer, A.K., Eck, G.G. & Harris, J.M. (2007). Patterns of abundance and diversity in late Cenozoic bovids from the Turkana and Hadar Basins, Kenya and Ethiopia. In: *Hominin environments in the East African Pliocene: An assessment of the faunal evidence*. Springer. pp. 129–157.

Boggs, S. (1995). *Principles of Sedimentology and Stratigraphy* (Vol. 774). New Jersey, Prentice Hall.

Bonnefille, R. (2010). Cenozoic vegetation, climate changes and hominid evolution in tropical Africa. *Global and Planetary Change*. 72 (4), pp. 390–411.

Bonnefille, R. (1983). Evidence for a cooler and drier climate in the Ethiopian uplands towards 2.5 Myr ago. *Nature*. 303 (5917), pp. 487–491.

Bonnefille, R. (1976). Implications of pollen assemblage from the Koobi Fora Formation, East Rudolf, Kenya. *Nature*. 264 (5585), pp. 403–407.

Bonnefille, R. (1984). Palynological research at Olduvai Gorge. *National Geographic Society Research Reports*. 17, pp. 227–243.

Bonnefille, R. & Dechamps, R. (1983). Data on fossil flora. *Ann. Mus. roy. Afr. Centr., Tervuren, Sci. geol.* 85, pp. 191–207.

Bonnefille, R. & Mohammed, U. (1994). Pollen-inferred climatic fluctuations in Ethiopia during the last 3000 years. *Palaeogeography, Palaeoclimatology, Palaeoecology*. 109, pp. 331–343.

Bonnefille, R. & Riollet, G. (1987). Palynological spectra from the upper Laetolil Beds. In: M.D. Leakey, J.M. Harris (eds.), *Laetoli: A Pliocene site in northern Tanzania*. Oxford, Oxford University Press. pp. 52–61.

Bonnefille, R., Potts, R., Chalie, F., Jolly, D. & Peyron, O. (2004). High-resolution vegetation and climate change associated with Pliocene Australopithecus afarensis. *Proceedings of the National Academy of Sciences.* 101 (33), pp. 12125–12129.

Bonnefille, R., Vincens, A. & Buchet, G. (1987). Palynology, stratigraphy and palaeoenvironment of a pliocene hominid site (2.9-3.3 M.Y.) at Hadar, Ethiopia. *Palaeogeography, Palaeoclimatology, Palaeoecology.* 60, pp. 249–281.

Borchardt, S. & Trauth, M.H. (2012). Remotely-sensed evapotranspiration estimates for an improved hydrological modeling of the early Holocene mega-lake Suguta, northern Kenya Rift. *Palaeogeography, Palaeoclimatology, Palaeoecology.* 361, pp. 14–20.

Borchers, A., Dietze, E., Kuhn, G., Esper, O., Voigt, I., Hartmann, K. and Diekmann, B. (2016). Holocene ice dynamics and bottom-water formation associated with Cape Darnley polynya activity recorded in Burton Basin, East Antarctica. *Marine Geophysical Research.* 37(1), pp. 49-70.

Bordy, E.M., Sztanó, O., Rampersadh, A., Almond, J. & Choiniere, J.N. (2019). Vertebrate scratch traces from the Middle Triassic Burgersdorp Formation of the main Karoo Basin, South Africa: Sedimentological and ichnological assessment. *Journal of African Earth Sciences.* 160, p. 103594.

Boswell, P.G.H. (1935). Human Remains from Kanam and Kanjera, Kenya Colony. *Nature.* p. 371.

Brachert, T.C., Brügmann, G.B., Mertz, D.F., Kullmer, O., Schrenk, F., Jacob, D.E., Ssemmanda, I. & Taubald, H. (2010). Stable isotope variation in tooth enamel from Neogene hippopotamids: monitor of meso and global climate and rift dynamics on the Albertine Rift, Uganda. *International Journal of Earth Sciences.* 99 (7), pp. 1663–1675.

Bramble, D.M. & Lieberman, D.E. (2004). Endurance running and the evolution of Homo. *Nature.* 432 (7015), pp. 345–352.

Braun, D.R., Plummer, T., Ditchfield, P., Ferraro, J.V., Maina, D., Bishop, L.C. & Potts, R. (2008). Oldowan behavior and raw material transport: perspectives from the Kanjera Formation. *Journal of Archaeological Science.* 35 (8), pp. 2329–2345.

Braun, D.R., Plummer, T., Ferraro, J.V., Ditchfield, P. & Bishop, L.C. (2009a). Raw material quality and Oldowan hominin toolstone preferences: evidence from Kanjera South, Kenya. *Journal of Archaeological Science.* 36 (7), pp. 1605–1614.

Braun, D.R., Plummer, T.W., Ditchfield, P.W., Bishop, L.C. & Ferraro, J.V. (2009b). Oldowan technology and raw material variability at Kanjera South. In: E. Hovers & D. R. Braun (eds.). *Interdisciplinary Approaches to the Oldowan.* Dordecht, Springer.

Bremond, L., Alexandre, A., Hély, C. & Guiot, J. (2005a). A phytolith index as a proxy of tree cover density in tropical areas: calibration with Leaf Area Index along a forest--savanna transect in southeastern Cameroon. *Global and Planetary Change*. 45 (4), pp. 277–293.

Bremond, L., Alexandre, A., Peyron, O. & Guiot, J. (2008). Definition of grassland biomes from phytoliths in West Africa. *Journal of Biogeography*. 35 (11), pp. 2039–2048.

Bremond, L., Alexandre, A., Peyron, O. & Guiot, J. (2005b). Grass water stress estimated from phytoliths in West Africa. *Journal of Biogeography*. 32 (2), pp. 311–327.

Bridge, J.S. (1993). Description and interpretation of fluvial deposits: a critical perspective. *Sedimentology*. 40 (4), pp. 801–810.

Brierley, C.M., Fedorov, A.V., Liu, Z., Herbert, T.D., Lawrence, K.T. & LaRiviere, J.P. (2009). Greatly expanded tropical warm pool and weakened Hadley circulation in the early Pliocene. *Science*. 323 (5922), pp. 1714–1718.

Brown, D.A. (1984). Prospects and Limits of a Phytolith Key for Grasses in the Central United States. *Journal of Archaeological Science*. 11 (4), pp. 345–368.

Brown, F.H. & Feibel, C.S. (1986). Revision of lithostratigraphic nomenclature in the Koobi Fora region, Kenya. *Journal of the Geological Society, London*. 143 (2), pp. 1–14.

Brown, F.H. & Feibel, C.S. (1991). Stratigraphy, depositional environments and palaeogeography of the Koobi Fora Formation. *Koobi Fora research project*. 3, pp. 1–30.

Brown, F.H. & McDougall, I. (2011). Geochronology of the Turkana Depression of Northern Kenya and Southern Ethiopia. *Evolutionary Anthropology: Issues, News, and Reviews*. 20 (6), pp. 217–227.

Brown, F.H., Shuey, R.T. & Croes, M.K. (1978). Magnetostratigraphy of the Shungura and Usno Formations, southwestern Ethiopia: new data and comprehensive reanalysis. *Geophysical Journal International*. 54 (3), pp. 519–538.

Brown, N.J., Newell, C.A., Stanley, S., Chen, J.E., Perrin, A.J., Kajala, K. & Hibberd, J.M. (2011). Independent and parallel recruitment of preexisting mechanisms underlying C4 photosynthesis. *Science*. 331 (6023), pp. 1436–1439.

Brugal, J.P., Roche, H., Delagnes, A., Feibel, C., Harmand, S., Kibunjia, M., Prat, S., Texier, P.J. & Teircelin, J.J. (2004). Plio-Pleistocene Hominids and Paleoenvironments from the Nachukui Formation (West Turkana, Kenya). *CR Palevol*. 2 (8), pp. 663–673.

Brunet, M., Guy, F., Pilbeam, D., Mackaye, H.T., Likius, A., Ahounta, D., Beauvilain, A., Blondel, C., Bocherens, H., Boisserie, J.R. and De Bonis, L.

(2002). A new hominid from the Upper Miocene of Chad, Central Africa. *Nature.* 418(6894), pp. 145-151.

Campisano, C.J. (2012). Geological summary of the Busidima formation (Plio-Pleistocene) at the Hadar paleoanthropological site, Afar Depression, Ethiopia. *Journal of Human Evolution.* 62 (3), pp. 338–352.

Campisano, C.J. (2007). *Tephrostratigraphy and hominin paleoenvironments of the Hadar Formation, Afar depression, Ethiopia.* Ph. D. Rutgers University.

Campisano, C.J. & Feibel, C.S. (2008). Depositional environments and stratigraphic summary of the Pliocene Hadar formation at Hadar, Afar depression, Ethiopia. *The geology of early humans in the Horn of Africa.* 446, pp. 179–201.

Cerling, T.E. (1992). Development of grasslands and savannas in East Africa during the Neogene. *Palaeogeography, Palaeoclimatology, Palaeoecology.* 97, pp. 241–247.

Cerling, T.E. (2014). Stable Isotope Evidence for Hominin Environments in Africa. *Treatise Geochem.* 14, pp. 157–167.

Cerling, T.E. & Hay, R.L. (1986). An Isotopic Study of Paleosol Carbonates from Olduvai Gorge. *Quaternary Research.* 25 (1), pp. 63–78.

Cerling, T.E., Andanje, S.A., Blumenthal, S.A., Brown, F.H., Chritz, K.L., Harris, J.M., Hart, J.A., Kirera, F.M., Kaleme, P., Leakey, L.N., Leakey, M.G., Levin, N.E., Manthi, F.K., Passey, B.H. & Uno, K.T. (2015). Dietary changes of large herbivores in the Turkana Basin, Kenya from 4 to 1 Ma. *Proceedings of the National Academy of Sciences.* 112 (37), pp. 11467–11472.

Cerling, T.E., Bowman, J.R. & ONeil, J.R. (1988). An Isotopic Study of a Fluvial-Lacustrine Sequence: The Plio-Pleistocene Koobi Fora Sequence, East Africa. *Palaeogeography, Palaeoclimatology, Palaeoecology.* 63, pp. 335–336.

Cerling, T.E., Cerling, B.W., Curtis, G.H., Drake, R.E. & Brown, F.H. (1979). Preliminary correlations between the Koobi Fora and Shungura Formations, East Africa. *Nature.* 279 (5709), pp. 118–121.

Cerling, T.E., Harris, J.M. & Leakey, M.G. (2003). Isotope paleoecology of the Nawata and Nachukui Formations at Lothagam, Turkana Basin, Kenya. In: M. Leakey and J. Harris (eds.). *Lothagam: The Dawn of Humanity in Eastern Africa.* New York, Columbia University Press. pp. 605–624.

Cerling, T.E., Levin, N.E. & Passey, B.H. (2011a). Stable Isotope Ecology in the Omo-Turkana Basin. *Evolutionary Anthropology: Issues, News, and Reviews.* 20 (6), pp. 228–237.

Cerling, T.E., Levin, N.E., Quade, J., Wynn, J.G., Fox, D.L., Kingston, J.D., Klein, R.G. & Brown, F.H. (2010). Comment on the Paleoenvironment of Ardipithecus ramidus. *Science.* 328 (5982), pp. 1105–1105.

Cerling, T.E., Manthi, F.K., Mbua, E.N., Leakey, L.N., Leakey, M.G., Leakey, R.E., Brown, F.H., Grine, F.E., Hart, J.A., Kaleme, P.others (2013). Stable isotope-based diet reconstructions of Turkana Basin hominins. *Proceedings of the National Academy of Sciences*. 110 (26), pp. 10501–10506.

Cerling, T.E., Mbua, E.N., Kirera, F.M., Manthi, F.K., Grine, F.E., Leakey, M.G., Sponheimer, M. & Uno, K. (2011b). Diet of Paranthropus boisei in the early Pleistocene of East Africa. *Proceedings of the National Academy of Sciences*. 108 (23), pp. 9337–9341.

Cerling, T.E., Wynn, J.G., Andanje, S.A., Bird, M.I., Korir, D.K., Levin, N.E., Mace, W., Macharia, A.N., Quade, J. & Remien, C.H. (2011c). Woody cover and hominin environments in the past 6 million years*. Nature*. 476 (7358), pp. 51–56.

Clarke, D.W., Boyle, J.F., Chiverrell, R.C., Lario, J. & Plater, A.J. (2014). A sediment record of barrier estuary behaviour at the mesoscale: Interpreting high-resolution particle size analysis. *Geomorphology*. 221, pp. 51–68.

Clement, A.C., Hall, A. & Broccoli, A.J. (2004). The importance of precessional signals in the tropical climate. *Climate Dynamics*. 22 (4), pp. 327–341.

Collins, J.D., O'Grady, P., Langford, R.P. and Gill, T.E. (2017). End-member mixing analysis (EMMA) applied to sediment grain size distributions to characterize formational processes of the main excavation block, Unit 2, of the Rimrock Draw Rockshelter (35HA3855), Harney Basin, Eastern Oregon (USA). *Archaeometry*. 59(2), pp. 331-345.

Crossley, R. & Knight, R.M. (1981). Volcanism in the Western Part of the Rift Valley in Southern Kenya. *Bulletin of Volcanology*. 44 (2), pp. 117–128.

Crowley, T.J. & Hyde, W.T. (2008). Transient nature of late Pleistocene climate variability. *Nature*. 456 (7219), pp. 226–230.

Curray, J.R. (1960). Tracing sediment masses by grain size modes. In: *Proceedings of the 21st International Geological Congress, Copenhagen*. pp. 119-130.

Çiner, A., Doğan, U., Yıldırım, C., Akçar, N., Ivy-Ochs, S., Alfimov, V., Kubik, P.W. & Schlüchter, C. (2015). Quaternary uplift rates of the Central Anatolian Plateau, Turkey: insights from cosmogenic isochron-burial nuclide dating of the Kızılırmak River terraces. *Quaternary Science Reviews*. 107, pp. 81–97.

de Haas, T., Ventra, D., Carbonneau, P.E. & Kleinhans, M.G. (2014). Debris-flow dominance of alluvial fans masked by runoff reworking and weathering. *Geomorphology*. 217, pp. 165–181.

DeConto, R.M., Pollard, D., Wilson, P.A., Pälike, H., Lear, C.H. & Pagani, M. (2008). Thresholds for Cenozoic bipolar glaciation. *Nature*. 455 (7213), pp. 652–656.

Deino, A. & Potts, R. (1992). Age-Probability Spectra for Examination of Single-

Crystal ^{40}Ar/^{39}Ar Dating Results: Examples from Olorgesailie, Southern Kenya Rift. *Quaternary International*. 13, pp. 47–53.

Deino, A., Kingston, J.D., Glen, J.M., Edgar, R.K. & Hill, A. (2006). Precessional forcing of lacustrine sedimentation in the late Cenozoic Chemeron Basin, Central Kenya Rift, and calibration of the Gauss/Matuyama boundary. *Earth and Planetary Science Letters*. 247 (1-2), pp. 41–60.

Deino, A.L. (2012). ^{40}Ar/^{39}Ar dating of Bed I, Olduvai Gorge, Tanzania, and the chronology of early Pleistocene climate change. *Journal of Human Evolution*. 63 (2), pp. 251–273.

Deino, A.L. (2011). ^{40}Ar/^{39}Ar Dating of Laetoli, Tanzania. In: T. Harrison (eds.). *Paleontology and Geology of Laetoli: Human Evolution in Context*. Dordrecht, Springer Netherlands, pp. 77–97.

de la Torre, I., Albert, R.M., Macphail, R., McHenry, L.J., Pante, M.C., Rodríguez-Cintas, Á., Stanistreet, I.G. & Stollhofen, H. (2018). The contexts and early Acheulean archaeology of the EF-HR paleo-landscape (Olduvai Gorge, Tanzania). *Journal of Human Evolution*. 120, pp. 274–297.

deMenocal, P.B. (2004). African climate change and faunal evolution during the Pliocene–Pleistocene. *Earth and Planetary Science Letters*. 220 (1-2), pp. 3–24.

deMenocal, P.B. (2011). Climate and human evolution. *Science*. 331 (6017), pp. 540–542.

deMenocal, P.B. (1995). Plio-Pleistocene African Climate. *Science*. 270 (5233), pp. 53–59.

Denison, S.M., Maslin, M.A., Boot, C., Pancost, R.D. & Ettwein, V.J. (2005). Precession-forced changes in South West African vegetation during Marine Isotope Stages 101–100 (~2.56–2.51 Ma). *Palaeogeography, Palaeoclimatology, Palaeoecology*. 220 (3-4), pp. 375–386.

Deocampo, D.M. & Tactikos, J.C. (2010). Geochemical gradients and artifact mass densities on the lowermost Bed II eastern lake margin (~ 1.8 Ma), Olduvai Gorge, Tanzania. *Quaternary Research*. 74 (3), pp. 411–423.

Deocampo, D.M., Behrensmeyer, A.K. & Potts, R. (2010). Ultrafine clay minerals of the pleistocene olorgesailie formation, Southern Kenya rift: Diagenesis and paleoenvironments of early hominins. *Clays and Clay Minerals*. 58 (3), pp. 294–310.

Deocampo, D.M., Cuadros, J., Wing-dudek, T., Olives, J. & Amouric, M. (2009). Saline lake diagenesis as revealed by coupled mineralogy and geochemistry of multiple ultrafine clay phases: Pliocene Olduvai Gorge, Tanzania. *American Journal of Science*. 309 (9), pp. 834–868.

Di Stefano, C., Ferro, V. & Mirabile, S. (2010). Comparison between grain-size analyses using laser diffraction and sedimentation methods. *Biosystems*

Engineering. 106 (2), pp. 205–215.

Dietze, E., Hartmann, K., Diekmann, B., IJmker, J., Lehmkuhl, F., Opitz, S., Stauch, G., W nnemann, B. & Borchers, A. (2012). An end-member algorithm for deciphering modern detrital processes from lake sediments of Lake Donggi Cona, NE Tibetan Plateau, China. *Sedimentary Geology.* 243, pp. 169-180.

Dietze, E., Wünnemann, B., Hartmann, K., Diekmann, B., Jin, H., Stauch, G., Yang, S., and Lehmkuhl, F. (2013). Early to mid-Holocene lake high-stand sediments at Lake Donggi Cona, northeastern Tibetan Plateau, China. *Quaternary Research.* 79, pp. 325–336.

Dietze, E., Maussion, F., Ahlborn, M., Diekmann, B., Hartmann, K., Henkel, K., Kasper, T., Lockot, G., Opitz, S. & Haberzettl, T. (2014). Sediment transport processes across the Tibetan Plateau inferred from robust grain-size end members in lake sediments. *Climate of the Past.* 10 (1), pp. 91-106

Dietze, E. and Dietze, M. (2019). Grain-size distribution unmixing using the R package EMMAgeo. *E&G Quaternary Science Journal.* 68(1), pp. 29-46.

Dirks, P.H. and Berger, L.R. (2013). Hominin-bearing caves and landscape dynamics in the Cradle of Humankind, South Africa. *Journal of African Earth Sciences.* 78, pp. 109-131.

Ditchfield, P. & Harrison, T. (2011). Sedimentology, Lithostratigraphy and Depositional History of the Laetoli Area. In: T. Harrison (ed.). *Paleontology and Geology of Laetoli: Human Evolution in Context.* Dordrecht, Springer Netherlands, pp. 47–76.

Ditchfield, P., Hicks, J., Plummer, T., Bishop, L.C. & Potts, R. (1999). Current research on the Late Pliocene and Pleistocene deposits north of Homa Mountain , southwestern Kenya. *Journal of Human Evolution.* 36 (2), pp. 123–150.

Ditchfield, P.W., Whitfield, E., Vincent, T., Plummer, T., Braun, D., Deino, A., Hertel, F., Oliver, J.S., Louys, J. & Bishop, L.C. (2018). Geochronology and physical context of Oldowan site formation at Kanjera South, Kenya. *Geological Magazine.* 156 (7), pp. 1190–1200.

Drapeau, M.S.M., Bobe, R., Wynn, J.G., Campisano, C.J., Dumouchel, L. & Geraads, D. (2014). The Omo Mursi Formation: A window into the East African Pliocene. *Journal of Human Evolution.* 75, pp. 64–79.

Dunai, T.J. (2010). *Cosmogenic Nuclides: Principles, concepts and applications in the Earth surface sciences.* Cambridge, Cambridge University Press.

Dunseth, Z.C., Fuks, D., Langgut, D., Weiss, E., Melamed, Y., Butler, D.H., Yan, X., Boaretto, E., Tepper, Y., Bar-Oz, G. and Shahack-Gross, R. (2019). Archaeobotanical proxies and archaeological interpretation: A comparative study of phytoliths, pollen and seeds in dung pellets and refuse deposits at Early Islamic Shivta, Negev, Israel. *Quaternary Science Reviews.* 211, pp. 166-185.

Ebinger, C.J., Yemane, T., Harding, D.J., Tesfaye, T., Kelley, S. & Rex, D.C. (2000). Rift deflection, migration, and propagation: Linkage of the Ethiopian and Eastern rifts, Africa. *Geological Society America Bulletin*. 112 (2), pp. 163–176.

Edwards, D.C. (1940). A vegetation map of Kenya with particular reference to grassland types. *Journal of Ecology*. 28 (2), pp. 377–385.

Edwards, E.J., Osborne, C.P., Strömberg, C.A., Smith, S.A., and C4 Grasses Consortium (2010). The origins of C4 grasslands: integrating evolutionary and ecosystem science. *Science*. 328 (5978), pp. 587–591.

Ehleringer, J.R. & Cerling, T.E. (2002). C3 and C4 photosynthesis. *Encyclopedia of Global Environmental Change*. 2, pp. 186–190.

Elenga, H., Schwartz, D. & Vincens, A. (1994). Pollen evidence of late Quaternary vegetation and inferred climate changes in Congo. *Palaeogeography, Palaeoclimatology, Palaeoecology*. 109 (2-4), pp. 345–356.

Eshel, G., Levy, G.J., Mingelgrin, U. & Singer, M.J. (2004). Critical Evaluation of the Use of Laser Diffraction for Particle-Size Distribution Analysis. *Soil Science Society of America Journal*. 68 (3), pp. 736–743.

Feakins, S.J., DeMenocal, P.B. & Eglinton, T.I. (2005). Biomarker records of late Neogene changes in northeast African vegetation. *Geology*. 33 (12), pp. 977–980.

Fedorov, A.V., Brierley, C.M., Lawrence, K.T., Liu, Z., Dekens, P.S. & Ravelo, A.C. (2013). Patterns and mechanisms of early Pliocene warmth. *Nature*. 496 (7443), pp. 43–49.

Feibel, C.S. (2011). A Geological History of the Turkana Basin. *Evolutionary Anthropology: Issues, News, and Reviews*. 20 (6), pp. 206–216.

Feibel, C.S. (2003). Stratigraphy and depositional setting of the Pliocene Kanapoi Formation, lower Kerio valley, Kenya. *Natural History Museum of Los Angeles County, Contributions in Science*. 498, pp. 9–20.

Feibel, C.S., Brown, F.H. & McDougall, I. (1989). Stratigraphic Context of Fossil Hominids From the Omo Group Deposits: Northern Turkana Basin, Kenya and Ethiopia. *American Journal of Physical Anthropology*. 78 (4), pp. 595–622.

Fernandez-Jalvo, Y., Denys, C., Andrews, P., Williams, T., Dauphin, Y. & Humphreys, L. (1998). Taphonomy and palaeoecology of Olduvai Bed-I (Pleistocene, Tanzania). *Journal of Human Evolution*. 34 (2), pp. 137–172.

Ferraro, J.V., Plummer, T.W., Pobiner, B.L., Oliver, J.S., Bishop, L.C., Braun, D.R., Ditchfield, P.W., Binetti, K.M., Seaman, J.W., Hertel, F. & Potts, R. (2013). Earliest Archaeological Evidence of Persistent Hominin Carnivory. *PLoS ONE*. 8 (4), p. e62174.

Ficken, K.J., Wooller, M.J., Swain, D.L., Street-Perrott, F.A. & Eglinton, G. (2002).

Reconstruction of a subalpine grass-dominated ecosystem, Lake Rutundu, Mount Kenya: A novel multi-proxy approach. *Palaeogeography, Palaeoclimatology, Palaeoecology*. 177 (1-2), pp. 137–149.

Field, D.J. (2020). Preliminary paleoecological insights from the Pliocene avifauna of Kanapoi, Kenya: Implications for the ecology of Australopithecus anamensis. *Journal of Human Evolution*. 140 (102384), pp. 1-10

Finestone, E.M. (2019). *Oldowan Tool Behaviors Through Time on the Homa Peninsula, Kenya*. Ph.D. Dissertation, CUNY Academic Works.

Flood, R.P., Orford, J.D., McKinley, J.M. & Roberson, S. (2015). Effective grain size distribution analysis for interpretation of tidal-deltaic facies: West Bengal sundarbans. *Sedimentary Geology*. 318, pp. 58–74.

Folk, R.L. & Ward, W.C. (1957). *Brazos River Bar: A Study in the Significance of Grain Size Parameters. Journal of Sedimentary Research*. 27 (1), pp. 3-26.

Foster, A., Ebinger, C., Mbede, E. & Rex, D. (1997). Tectonic development of the northern Tanzanian sector of the East African rift system. *Journal of the Geological Society, London*. 154 (4), pp. 689–700.

Fredlund, G.G. & Tieszen, L.T. (1994). Modern phytolith assemblages from the North American great plains. *Journal of Biogeography*. 21 (3), pp. 321–335.

Frenz, M., Hoppner, R., Stuut, J.-B.W., Wagner, T. & Henrich, R. (2003). Surface Sediment Bulk Geochemistry and Grain-Size Composition Related to the Oceanic Circulation along the South American Continental Margin in the Southwest Atlantic. In: G. Wefer, S. Mulitza, & V. Ratmeyer (eds.). *The South Atlantic in the Late Quaternary Reconstructions of Material Budgets and Current Systems*. Berlin, Springer. pp. 347–373.

Friedman, G.M. (1979). Differences in size distributions of population particles among sands of various origins. *Sedimentology*. 26 (6), pp. 859–862.

Garzanti, E., Vezzoli, G., Andò, S., Lavé, J., Attal, M., France-Lanord, C. and DeCelles, P. (2007). Quantifying sand provenance and erosion (Marsyandi River, Nepal Himalaya). *Earth and Planetary Science Lettera*. 258(3-4), pp. 500–515.

Gathogo, P.N. & Brown, F.H. (2006). Stratigraphy of the Koobi Fora Formation (Pliocene and Pleistocene) in the Ileret region of northern Kenya. *Journal of African Earth Sciences*. 45 (4-5), pp. 369–390.

Gathogo, P.N., Brown, F.H. & McDougall, I. (2008). Stratigraphy of the Koobi Fora Formation (Pliocene and Pleistocene) in the Loiyangalani region of northern Kenya. *Journal of African Earth Sciences*. 51 (5), pp. 277–297.

Gibbon, R.J., Pickering, T.R., Sutton, M.B., Heaton, J.L., Kuman, K., Clarke, R.J., Brain, C.K. & Granger, D.E. (2014). Cosmogenic nuclide burial dating of hominin-bearing Pleistocene cave deposits at Swartkrans, South Africa. *Quaternary Geochronology*. 24, pp. 10–15.

Gibbons, A., 2017. World's oldest Homo sapiens fossils found in Morocco. *Science*.

Granger, D.E. (2014). Cosmogenic nuclide burial dating in archaeology and paleoanthropology. *Treatise on Geochemistry*. 14, pp. 81–97.

Granger, D.E. & Muzikar, P.F. (2001). Dating sediment burial with in situ-produced cosmogenic nuclides: Theory, techniques, and limitations. *Earth and Planetary Science Letters*. 188 (1-2), pp. 269–281.

Granger, D.E., Gibbon, R.J., Kuman, K., Clarke, R.J., Bruxelles, L. & Caffee, M.W. (2015). New cosmogenic burial ages for Sterkfontein Member 2 Australopithecus and Member 5 Oldowan. *Nature*. 522 (7554), pp. 85–88.

Gray, A.B., Pasternack, G.B. & Watson, E.B. (2010). Hydrogen peroxide treatment effects on the particle size distribution of alluvial and marsh sediments. *The Holocene*. 20 (2), pp. 293–301.

Haile-Selassie, Y., Suwa, G. & White, T.D. (2004). Late Miocene teeth from Middle Awash, Ethiopia, and early hominid dental evolution. *Science*. 303 (5663), pp. 1503–1505.

Hailemichael, M. (2001). *The Pliocene environment of Hadar, Ethiopia: A comparative isotopic study of paleosol carbonates and lacustrine mollusk shells of the Hadar Formation and of modern analogs.* Ph.D. Dissertation, Case Western Reserve University

Hailemichael, M., Aronson, J.L., Savin, S., Tevesz, M.J. & Carter, J.G. (2002). $\delta^{18}O$ in mollusk shells from Pliocene Lake Hadar and modern Ethiopian lakes: Implications for history of the Ethiopian monsoon. *Palaeogeography, Palaeoclimatology, Palaeoecology*. 186 (1-2), pp. 81–99.

Hamann, Y., Ehrmann, W., Schmiedl, G., Krüger, S., Stuut, J.B. & Kuhnt, T. (2008). Sedimentation processes in the Eastern Mediterranean Sea during the Late Glacial and Holocene revealed by end-member modelling of the terrigenous fraction in marine sediments. *Marine Geology*. 248 (1-2), pp. 97–114.

Harris, J.M. & Leakey, M.G. (2003). *Geology and vertebrate paleontology of the early Pliocene site of Kanapoi, northern Kenya, vol. 498*. Los Angeles, Natural History Museum of Los Angeles County.

Harris, J.M., Cerling, T.E., Leakey, M.G. & Passey, B.H. (2008). Stable isotope ecology of fossil hippopotamids from the Lake Turkana Basin of East Africa. *Journal of Zoology*. 275 (3), pp. 323–331.

Harris, J.M., Leakey, M.G. & Brown, F.H. (1988). *Stratigraphy and paleontology of Pliocene and Pleistocene localities west of Lake Turkana, Kenya*. Los Angeles, Natural History Museum of Los Angeles County.

Harrison, T. (2017). The Paleoecology of the Upper Ndolanya Beds, Laetoli, Tanzania, and Its Implications for Hominin Evolution. In: *Human Paleontology*

and Prehistory. Springer, pp. 31–44.

Hartley, A.J., Weissmann, G.S., Bhattacharayya, P., Nichols, G.J., Scuderi, L.A., Davidson, S.K., Leleu, S., Chakraborty, T., Ghosh, P., Mather, A.E. and Driese, S., (2013). Soil development on modern distributive fluvial systems: preliminary observations with implications for interpretation of paleosols in the rock record. *New Frontiers in Paleopedology and Terrestrial Paleoclimatology: SEPM, Special Publication*. 104, pp. 149–158.

Hartmann, D. (2007). From reality to model: Operationalism and the value chain of particle-size analysis of natural sediments. *Sedimentary Geology*. 202 (3), pp. 383–401.

Harvey, A.M., Mather, A.E. & Stokes, M. (2005). Alluvial fans: geomorphology, sedimentology, dynamics. *Geological Society, London, Special Publications*. 251, pp. 1–7.

Harvey, A.M., Wigand, P.E. & Wells, S.G. (1999). Response of alluvial fan systems to the late Pleistocene to Holocene climatic transition: contrasts between the margins of pluvial Lakes Lahontan and Mojave, Nevada and California, USA. *Catena*. 36 (4), pp. 255 - 281.

Hassan, F.A. (1979). Geoarchaeology: The Geologist and Archaeology. *American Antiquity*. 44 (2), pp. 267–270.

Hassan, F.A. (1978). Sediments in Archaeology: Methods and Implications for Palaeoenvironmental and Cultural Analysis. *Journal of Field Archaeology*. 5 (2), pp. 197–213.

Haug, G.H. & Tiedemann, R. (1998). Effect of the formation of the Isthmus of Panama on Atlantic Ocean thermohaline circulation. *Nature*. 393 (6686), pp. 673–676.

Hay, R.L. (1976). *Geology of the Olduvai Gorge: a study of sedimentation in a semiarid basin*. Berkeley, University of California Press.

Hay, R.L. & Kyser, T.K. (2001). Chemical sedimentology and paleoenvironmental history of Lake Olduvai, a Pliocene lake in northern Tanzania. *Bulletin of the Geological Society of America*. 113 (12), pp. 1505–1521.

Hernández Fernández, M. & Vrba, E.S. (2006). Plio-Pleistocene climatic change in the Turkana Basin (East Africa): Evidence from large mammal faunas. *Journal of Human Evolution*. 50 (6), pp. 595–626.

Holz, C., Stuut, J.-B.W. & Henrich, R. (2004). Terrigenous sedimentation processes along the continental margin off NW Africa: implications from grain-size analysis of seabed sediments. *Sedimentology*. 51 (5), pp. 1145–1154.

Holz, C., Stuut, J.B.W., Henrich, R. & Meggers, H. (2007). Variability in terrigenous sedimentation processes off northwest Africa and its relation to climate changes: Inferences from grain-size distributions of a Holocene marine sediment record. *Sedimentary Geology*. 202 (3), pp. 499–508.

Hopf, F.A., Valone, T.J. & Brown, J.H. (1993). Competition theory and the structure of ecological communities. *Evolutionary Ecology*. 7 (2), pp. 142–154.

Hopley, P.J. & Maslin, M.A. (2010). Climate-averaging of terrestrial faunas: an example from the Plio-Pleistocene of South Africa. *Paleobiology*. 36 (1), pp. 32–50.

Hopley, P.J., Marshall, J.D., Weedon, G.P., Latham, A.G., Herries, A.I.R. & Kuykendall, K.L. (2007). Orbital forcing and the spread of C4 grasses in the late Neogene: stable isotope evidence from South African speleothems. *Journal of Human Evolution*. 53 (5), pp. 620–634.

Hover, V.C.A. & Ashley, G.M.B. (2003). Geochemical signatures of paleodepositional and diagenetic environments: A STEM/AEM study of authigenic clay minerals from an arid rift basin, Olduvai Gorge, Tanzania. *Clays and Clay Minerals*. 51 (3), pp. 231–251.

Howell, F.C., Haesaerts, P. & de Heinzelin, J. (1987). Depositional environments, archaeological occurrences and hominids from Members E and F of the Shungura Formation (Omo basin, Ethiopia). *Journal of Human Evolution*. 16 (7-8), pp. 665–700.

Hsü, K.J., Ryan, W.B. & Cita, M.B. (1973). Late Miocene desiccation of the Mediterranean. *Nature*. 242 (5395), pp. 240–244.

Huang, Y., Freeman, K.H. & Eglinton, T.I. (1999). $\delta^{13}C$ analyses of individual lignin phenols in Quaternary lake sediments: A novel proxy for deciphering past terrestrial vegetation changes. *Geology*. 27 (5), pp. 471–474.

IJmker, J., Stauch, G., Dietze, E., Hartmann, K., Diekmann, B., Lockot, G., Opitz, S., Wünnemann, B. & Lehmkuhl, F. (2012). Characterisation of transport processes and sedimentary deposits by statistical end-member mixing analysis of terrestrial sediments in the Donggi Cona lake catchment, NE Tibetan Plateau. *Sedimentary Geology*. 281, pp. 166–179.

Imbrie, J., Boyle, E., Clemens, S., Duffy, A., Howard, W., Kukla, G., Kutzbach, J., Martinson, D., McIntyre, A., Mix, A.C., Molfino, B., Morley, J.J., Peterson, L.C., Pisias, N.G. & Prell, W.L. (1992). On the Structure and Origin of Major Glaciation Cycles. 1, Linear Responses to Milankovitch Forcing. *Paleoceanography*. 7 (6), pp. 701–738.

Johanson, D. (2017). The paleoanthropology of Hadar, Ethiopia. *Comptes rendus - Palevol*. 16 (2), pp. 140–154.

Joordens, J.C.A., Vonhof, H.B., Feibel, C.S., Lourens, L.J., Dupont-Nivet, G., van der Lubbe, J.H.J.L., Sier, M.J., Davies, G.R. & Kroon, D. (2011). An astronomically-tuned climate framework for hominins in the Turkana Basin. *Earth and Planetary Science Letters*. 307 (1-2), pp. 1–8.

Katz, O., Cabanes, D., Weiner, S., Maeir, A.M., Boaretto, E. & Shahack-Gross, R. (2010). Rapid phytolith extraction for analysis of phytolith concentrations and assemblages during an excavation: an application at Tell es-Safi/Gath, Israel.

Journal of Archaeological Science. 37 (7), pp. 1557–1563.

Keigwin, L. (1982). Isotopic paleoceanography of the Caribbean and East Pacific: role of Panama uplift in late Neogene time. *Science.* 217 (4557), pp. 350–353.

Keigwin, L.D. (1978). Pliocene closing of the Isthmus of Panama, based on biostratigraphic evidence from nearby Pacific Ocean and Caribbean Sea cores. *Geology.* 6 (10), pp. 630–634.

Keller, G., Zenker, C.E. & Stone, S.M. (1989). Late Neogene history of the Pacific-Caribbean gateway. *Journal of South American Earth Sciences.* 2 (1), pp. 73–108.

Kent, P.E. (1942). The Pleistocene beds of Kanam and Kanjera, Kavirondo, Kenia. *Geological Magazine.* 79 (2), pp. 117–132.

Kibunjia, M., Roche, H., Brown, F.H. & Leakey, R.E. (1992). Pliocene and Pleistocene archeological sites west of Lake Turkana, Kenya. *Journal of Human Evolution.* 23 (5), pp. 431–438.

King, G. and Bailey, G. (2006). Tectonics and human evolution. *Antiquity.* 80(308), pp. 265-286.

Kingston, J.D. (2007). Shifting adaptive landscapes: Progress and challenges in reconstructing early hominid environments. *American Journal of Physical Anthropology.* 134 (S45), pp. 20–58.

Kingston, J.D. (2011). Stable Isotopic Analyses of Laetoli Fossil Herbivores. In: *Paleontology and Geology of Laetoli: Human Evolution in Context.* Vertebrate Paleobiology and Paleoanthropology. Dordrecht, Springer, Dordrecht, pp. 293–328.

Kinyanjui, R. (2012). *Phytolith Analysis as a Palaeoecological Tool for Reconstructing Mid-to Late- Pleistocene Environments in the Olorgesailie Basin, Kenya.* Msc. Dissertation. University of Cape town

Konert, M. & Vandenberghe, J. (1997). Comparison of laser grain size analysis with pipette and sieve analysis: a solution for the underestimation of the clay fraction. *Sedimentology.* 44 (3), pp. 523–535.

Kovarovic, K. & Andrews, P. (2011). Environmental Change within the Laetoli Fossiliferous Sequence: Vegetation Catenas and Bovid Ecomorphology. In: *Vertebrate Paleobiology and Paleoanthropology.* Dordrecht, Springer Netherlands, pp. 367–380.

Krijgsman, W., Langereis, C.G., Zachariasse, W.J., Boccaletti, M., Moratti, G., Gelati, R., Laccarino, S., Papani, G. & Villa, G. (1999). Late Neogene evolution of the Taza-Guercif Basin (Rifian Corridor, Morocco) and implications for the Messinian salinity crisis. *Marine Geology.* 153 (1) pp. 147–160.

Langford, R.P., Gill, T.E. & Jones, S.B. (2016). Transport and mixing of eolian sand from local sources resulting in variations in grain size in a gypsum dune

field, White Sands, New Mexico, USA. *Sedimentary Geology*. 333, pp. 184–197.

Larrasoaña, J.C., Roberts, A.P. & Rohling, E.J. (2013). Dynamics of Green Sahara Periods and Their Role in Hominin Evolution. *PLoS ONE*. 8 (10), pp. e76514

Larrasoaña, J.C., Roberts, A.P., Rohling, E.J., Winklhofer, M. & Wehausen, R. (2003). Three million years of monsoon variability over the northern Sahara. *Climate Dynamics*. 21 (7-8), pp. 689–698.

Le Bas, M.J. (1977). *Carbonatite Nephelnite Volcanism: An African Case History*. London, John Wiley and Sons.

Le Roux, J.P. & Rojas, E.M. (2007). Sediment transport patterns determined from grain size parameters: Overview and state of the art. *Sedimentary Geology*. 202 (3), pp. 473–488.

Leakey, L.S.B. (1935). *The stone age races of Kenya*. London, Oxford University Press

Leakey, M.G., Feibel, C.S., Bernor, R.L., Harris, J.M., Cerling, T.E., Stewart, K.M., Storrs, G.W., Walker, A., Werdelin, L. & Winkler, A.J. (1996). Lothagam: a record of faunal change in the Late Miocene of East Africa. *Journal of Vertebrate Paleontology*. 16 (3), pp. 556–570.

Leakey, M.G., Feibel, C.S., McDougall, I. & Walker, A. (1995). *New four-million-year-old hominid species from Kanapoi and Allia Bay, Kenya*. 376 (6541), p. 565.

Leakey, R.E.F. (1971). Further Evidence of Lower Pleistocene Hominids from East Rudolf, North Kenya. *Nature*. 231 (5300), pp. 241-245.

Lee, R.K.L., Owen, R.B., Renaut, R.W., Behrensmeyer, A.K., Potts, R. & Sharp, W.D. (2013). Facies, geochemistry and diatoms of late Pleistocene Olorgesailie tufas, southern Kenya Rift. *Palaeogeography, Palaeoclimatology, Palaeoecology*. 374, pp. 197–217.

Lee-Thorp, J.A., Sponheimer, M. & Luyt, J. (2007). Tracking changing environments using stable carbon isotopes in fossil tooth enamel: an example from the South African hominin sites. *Journal of Human Evolution*. 53 (5), pp. 595–601.

Lemorini, C., Plummer, T.W., Braun, D.R., Crittenden, A.N., Ditchfield, P.W., Bishop, L.C., Hertel, F., Oliver, J.S., Marlowe, F.W., Schoeninger, M.J. & Potts, R. (2014). Old stones' song: Use-wear experiments and analysis of the Oldowan quartz and quartzite assemblage from Kanjera South (Kenya). *Journal of Human Evolution*. 72, pp. 10–25.

Lepre, C.J. (2009). *Plio-pleistocene stratigraphy and paleogeography for hominin remains from areas 130 and 133, Koobi Fora, Kenya*. Ph.D Dissertation. Rutgers University Graduate School New Brunswick.

Lepre, C.J., Quinn, R.L., Joordens, J.C.A., Swisher, C.C., III & Feibel, C.S. (2007). Plio-Pleistocene facies environments from the KBS Member, Koobi Fora Formation: implications for climate controls on the development of lake-margin hominin habitats in the northeast Turkana Basin (northwest Kenya). *Journal of Human Evolution*. 53 (5), pp. 504–514.

Levin, N.E., Brown, F.H., Behrensmeyer, A.K., Bobe, R. & Cerling, T.E. (2011). Paleosol carbonates from the Omo Group: Isotopic records of local and regional environmental change in East Africa. *Palaeogeography, Palaeoclimatology, Palaeoecology*. 307 (1-4), pp. 75–89.

Levin, N.E., Quade, J., Simpson, S.W., Semaw, S. & Rogers, M. (2004). Isotopic evidence for Plio–Pleistocene environmental change at Gona, Ethiopia. *Earth and Planetary Science Letters*. 219 (1-2), pp. 93–110.

Lewin R., Foley R.A. (2004). *Principles of Human Evolution*, Malden: Blackwell.

Lezine, A.-M. (1991). West African Paleoclimates during the Last Climatic Cycle Inferred from an Atlantic Deep-Sea Pollen Record. *Quaternary Research*. 35 (3), pp. 456–463.

Li, X.S., Berger, A., Loutre, M.-F., Maslin, M.A., Haug, G.H. & Tiedemann, R. (1998). Simulating late Pliocene Northern Hemisphere climate with the LLN 2-D model. *Geophysical Research Letters*. 25 (6), pp. 915–918.

Liu, B., Qu, J., Ning, D., Gao, Y., Zu, R. & An, Z. (2014). Grain-size study of aeolian sediments found east of Kumtagh Desert. *Aeolian Research*. 13. pp. 1–6.

Liu, X., Shen, G., Tu, H., Lu, C. & Granger, D.E. (2015). Initial ^{26}Al/^{10}Be burial dating of the hominin site Bailong Cave in Hubei Province, central China. *Quaternary International*. 389, pp. 235–240.

Liu, X., Vandenberghe, J., An, Z., Li, Y., Jin, Z., Dong, J. & Sun, Y. (2016). Grain size of Lake Qinghai sediments: Implications for riverine input and Holocene monsoon variability. *Palaeogeography, Palaeoclimatology, Palaeoecology*. 449, pp. 41–51.

Liu, Z., Altabet, M.A. & Herbert, T.D. (2008). Plio-Pleistocene denitrification in the eastern tropical North Pacific: Intensification at 2.1 Ma. *Geochemistry, Geophysics, Geosystems*. 9 (11), pp. 1-14

Liutkus, C.M. & Ashley, G.M. (2003). Facies Model of a Semiarid Freshwater Wetland, Olduvai Gorge, Tanzania. *Journal of Sedimentary Research*. 73 (5), pp. 691–705.

Liutkus, C.M., Wright, J.D., Ashley, G.M. & Sikes, N.E. (2005). Paleoenvironmental interpretation of lake-margin deposits using δ^{13}C and δ^{18}O results from early Pleistocene carbonate rhizoliths, Olduvai Gorge, Tanzania. *Geology*. 33 (5), pp. 377–380.

Lu, H.Y., Wu, N.Q., Liu, K.B., Jiang, H. & Liu, T.S. (2007). Phytoliths as

quantitative indicators for the reconstruction of past environmental conditions in China II: palaeoenvironmental reconstruction in the Loess Plateau. *Quaternary Science Reviews.* 26 (5-6), pp. 759–772.

Ma, L., Wu, J., Abuduwaili, J. & Liu, W. (2015). Aeolian particle transport inferred using a ~ 150-year sediment record from Sayram Lake, arid northwest China. *Journal of Limnology.* 74 (3), pp. 1–10.

Machette, M.N. (1985). Calcific soils of the southwestern United States. *Geological Society of America Special Paper.* 203, pp. 1–21.

Macho, G.A., Leakey, M.G., Williamson, D.K. & Jiang, Y. (2003). Palaeoenvironmental reconstruction: Evidence for seasonality at Allia Bay, Kenya, at 3.9 million years. *Palaeogeography, Palaeoclimatology, Palaeoecology.* 199 (1-2), pp. 17–30.

Madella, M., Alexandre, A. & Ball, T. (2005). International code for phytolith nomenclature 1.0. *Annals of Botany.* 96 (2), pp. 253–260.

Magill, C.R., Ashley, G.M. & Freeman, K.H. (2013a). Ecosystem variability and early human habitats in eastern Africa. *Proceedings of the National Academy of Sciences.* 110 (4), pp. 1167–1174.

Magill, C.R., Ashley, G.M. & Freeman, K.H. (2013b). Water, plants, and early human habitats in eastern Africa. *Proceedings of the National Academy of Sciences.* 110 (4), pp. 1175–1180.

Magill, C.R., Ashley, G.M., Dom i nguez-rodrigo, M. & Freeman, K.H. (2016). Dietary options and behavior suggested by plant biomarker evidence in an early human habitat Archaeological trenches. *Proceedings of the National Academy of Sciences.* 113 (15), pp. 2–7.

Maher, E. & Harvey, A.M. (2008). Fluvial system response to tectonically induced base-level change during the late-Quaternary: The Rio Alias southeast Spain. *Geomorphology.* 100 (1-2), pp. 180–192.

Maher, E., Harvey, A.M. & France, D. (2007). The impact of a major Quaternary river capture on the alluvial sediments of a beheaded river system, the Rio Alias SE Spain. *Geomorphology.* 84 (3-4), pp. 344–356.

Mann, P. & Corrigan, J. (1990). Model for late Neogene deformation in Panama. *Geology.* 18 (6), pp. 558–562.

Manthi, F.K. (2006). *The Pliocene micromammalian fauna from Kanapoi, northwestern Kenya, and its contribution to understanding the environment of Australopithecus anamensis.* Ph.D. Dissertation. University of Cape Town.

Manthi, F.K., Cerling, T.E., Chritz, K.L. & Blumenthal, S.A. (2017). Diets of mammalian fossil fauna from Kanapoi, northwestern Kenya. *Journal of Human Evolution.* 140, p. 102338

Marchant, R., Mumbi, C., Behera, S. & Yamagata, T. (2007). The Indian Ocean

dipole-the unsung driver of climatic variability in East Africa. *African Journal of Ecology*. 45 (1), pp. 4–16.

Marriott, S.B. & Wright, V.P. (1993). Palaeosols as indicators of geomorphic stability in two Old Red Sandstone alluvial suites, South Wales. *Journal of the Geological Society*. 150 (6), pp. 1109–1120.

Marshall, W.A., Gehrels, W.R., Garnett, M.H., Freeman, S.P.H.T., Maden, C. & Xu, S. (2007). The use of 'bomb spike' calibration and high-precision AMS ^{14}C analyses to date salt-marsh sediments deposited during the past three centuries. *Quaternary Research*. 68 (3), pp. 325–337.

Maslin, M.A. & Christensen, B. (2007). Tectonics, orbital forcing, global climate change, and human evolution in Africa: introduction to the African paleoclimate special volume. *Journal of Human Evolution*. 53 (5), pp. 443–464.

Maslin, M.A. & Ridgwell, A.J. (2005). Mid-Pleistocene revolution and the 'eccentricity myth'. *Geological Society, London, Special Publications*. 247 (1), pp. 19–34.

Maslin, M.A. & Trauth, M.H. (2009). Plio-Pleistocene East African pulsed climate variability and its influence on early human evolution. In: *The First Humans-- Origin and Early Evolution of the Genus Homo*. Dordrecht, Springer. pp. 151– 158.

Maslin, M.A., Brierley, C.M., Milner, A.M., Shultz, S., Trauth, M.H. & Wilson, K.E. (2014). East African climate pulses and early human evolution. *Quaternary Science Reviews*. 101, pp. 1–17.

Maslin, M.A., Li, X.S., Loutre, M.F. & Berger, A. (1998). The Contribution of Orbital Forcing to the Progressive Intensification of Northern Hemisphere Glaciation. *Quaternary Science Reviews*. 17, pp. 411–426.

Mather A.E. (2011) '29. Interpreting Quaternary Environments' in: Gregory K.J.; Goudie A.S., ed. 2011. *The SAGE Handbook of Geomorphology*. SAGE Publications Limited. pp. 513-534

Mather, A.E. & Hartley, A. (2005). Flow events on a hyper-arid alluvial fan: Quebrada Tambores, Salar de Atacama, northern Chile. *Geological Society, London, Special Publications*. 251 (1), pp. 9–24.

Mather, A.E. & Stokes, M. (2003). Long-term landscape development in southern Spain. *Geomorphology (Amsterdam)*. 50 (1-3), p. 293

Mather, A.E., Stokes, M. & Whitfield, E. (2017). River terraces and alluvial fans: The case for an integrated Quaternary fluvial archive. *Quaternary Science Reviews*. 166, pp. 74–90.

Maurin, T., Bertran, P., Delagnes, A. & Boisserie, J.-R. (2017). Early hominin landscape use in the Lower Omo Valley, Ethiopia: Insights from the taphonomical analysis of Oldowan occurrences in the Shungura Formation (Member F). *Journal of Human Evolution*. 111, pp. 33–53.

McClymont, E.L. & Rosell-Melé, A. (2005). Links between the onset of modern Walker circulation and the mid-Pleistocene climate transition. *Geology*. 33 (5), pp. 389–392.

McLaren, P. & Bowles, D. (1985). The effects of sediment transport on grain size distributions. *Journal of Sedimentary Research*. 55 (4), pp. 457–470.

Mercader, J., Astudillo, F., Barkworth, M., Bennett, T., Esselmont, C., Kinyanjui, R., Grossman, D.L., Simpson, S. & Walde, D. (2010). Poaceae phytoliths from the Niassa Rift, Mozambique. *Journal of Archaeological Science*. 37 (8), pp. 1953–1967.

Mercader, J., Bennett, T., Esselmont, C., Simpson, S. & Walde, D. (2009). Phytoliths in woody plants from the Miombo woodlands of Mozambique. *Annals of Botany*. 104 (1), pp. 91–113.

Mercader, J., Runge, F., Vrydaghs, L., Doutrelepont, H., Ewango, C. & Juan-Tresseras, J. (2000). Phytoliths from Archaeological Sites in the Tropical Forest of Ituri, Democratic Republic of Congo. *Quaternary Research*. 54, pp. 102–112.

Meyer, I., Davies, G.R., Vogt, C., Kuhlmann, H. & Stuut, J.-B.W. (2013). Changing rainfall patterns in NW Africa since the Younger Dryas. *Aeolian Research*. 10, pp. 111–123.

Miall, A.D. (2013). *The geology of fluvial deposits: sedimentary facies, basin analysis, and petroleum geology*. New York, Springer.

Middleton, G.V. (1976). Hydraulic Interpretation of Sand Size Distributions. *The Journal of Geology*. 84 (4), pp. 405–426.

Moore, P.D., Webb, J.A. and Collinson, M.E (1991). *Pollen Analysis*, Blackwell, Oxford.

Moreno, A., Cacho, I., Canals, M., Prins, M.A., Sanchez-Goni, M.-F., Grimalt, J.O. & Weltje, G.J. (2002). Saharan Dust Transport and High-Latitude Glacial Climatic Variability: The Alboran Sea Record. *Quaternary Research*. 58 (3), pp. 318–328.

Mtelela, C., Roberts, E.M., Hilbert-Wolf, H.L., Downie, R., Hendrix, M.S., OConnor, P.M. & Stevens, N.J. (2017). Sedimentology and paleoenvironments of a new fossiliferous late Miocene-Pliocene sedimentary succession in the Rukwa Rift Basin, Tanzania. *Journal of African Earth Sciences*. 129, pp. 260–281.

Mudelsee, M. & Stattegger, K. (1997). Exploring the structure of the mid-Pleistocene revolution with advanced methods of time-series analysis. *International Journal of Earth Sciences: Geologische Rundschau*. 86 (2), p. 499.

Mulholland, S.C. & Rapp, G. (1992). Phytolith systematics: an introduction. In: *Phytolith systematics*. Springer, pp. 1–13.

Murphy, L.N., Kirk-Davidoff, D.B., Mahowald, N. & Otto-Bliesner, B.L. (2009). A numerical study of the climate response to lowered Mediterranean Sea level during the Messinian Salinity Crisis. *Palaeogeography, Palaeoclimatology, Palaeoecology*. 279 (1), pp. 41–59.

Mutai, C.C. & Ward, M.N. (2000). East African rainfall and the tropical circulation/convection on intraseasonal to interannual timescales. *Journal of Climate*. 13 (22), pp. 3915–3939.

Neumann, K., Fahmy, A., Lespez, L., Ballouche, A. & Huysecom, E. (2009). The Early Holocene palaeoenvironment of Ounjougou (Mali): Phytoliths in a multi-proxy context. *Palaeogeography, Palaeoclimatology, Palaeoecology*. 276 (1-4), pp. 87–106.

Nicholson, S.E. (2018). The ITCZ and the seasonal cycle over equatorial Africa. *Bulletin of the American Meteorological Society*. 99 (2), pp. 337–348.

North, C.P. & Davidson, S.K. (2012). Unconfined alluvial flow processes: recognition and interpretation of their deposits, and the significance for palaeogeographic reconstruction. *Earth-Science Reviews*. 111 (1-2), pp. 199–223.

Novello, A., Lebatard, A.-E., Moussa, A., Barboni, D., Sylvestre, F., Bourlès, D.L., Paillès, C., Buchet, G., Decarreau, A., Duringer, P., Ghienne, J.F., Maley, J., Mazur, J.-C., Roquin, C., Schuster, M. & Vignaud, P. (2015). Diatom, phytolith, and pollen records from a $^{10}Be/^{9}Be$ dated lacustrine succession in the Chad basin: Insight on the Miocene–Pliocene paleoenvironmental changes in Central Africa. *Palaeogeography, Palaeoclimatology, Palaeoecology*. 430, pp. 85–103.

Olaka, L.A., Odada, E.O., Trauth, M.H. & Olago, D.O. (2010). The sensitivity of East African rift lakes to climate fluctuations. *Journal of Paleolimnology*. 44 (2), pp. 629–644.

Ollendorf, A.L. (1992). Toward a classification scheme of sedge (Cyperaceae) phytoliths. In: *Phytolith systematics*. Springer, pp. 91–111.

Oswald, F. (1914). *The Miocene Beds of the Victoria Nyanza and the Geology of the Country between the Lake and the Kisii Highlands. Q.J. Geological Society of London*. 70, pp. 128-188.

Owen, R.B., Potts, R., Behrensmeyer, A.K. & Ditchfield, P. (2008). Diatomaceous sediments and environmental change in the Pleistocene Olorgesailie Formation, southern Kenya Rift Valley. *Palaeogeography, Palaeoclimatology, Palaeoecology*. 269 (1-1), pp. 17–37.

Owen, R.B., Renaut, R.W., Behrensmeyer, A.K. & Potts, R. (2014). Quaternary geochemical stratigraphy of the Kedong–Olorgesailie section of the southern Kenya Rift valley. *Palaeogeography, Palaeoclimatology, Palaeoecology*. 396, pp. 194–212.

Owen, R.B., Renaut, R.W., Potts, R. & Behrensmeyer, A.K. (2011). Geochemical

trends through time and lateral variability of diatom floras in the Pleistocene Olorgesailie Formation, southern Kenya Rift Valley. *Quaternary Research*. 76 (1), pp. 167–179.

Owen, R.B., Renaut, R.W., Scott, J.J., Potts, R. & Behrensmeyer, A.K. (2009). Wetland sedimentation and associated diatoms in the Pleistocene Olorgesailie Basin, southern Kenya Rift Valley. *Sedimentary Geology*. 222 (1-2), pp. 124–137.

Paterson, G.A. & Heslop, D. (2015a). *AnalySize Software for grain size unmixing and analysis v1.0.1*. 1st Ed.

Paterson, G.A. & Heslop, D. (2015b). New methods for unmixing sediment grain size data. *Geochemistry, Geophysics, Geosystems*. 16, pp. 4494–4506.

Pickford, M. (1987). Fort Ternan (Kenya) Palaeoecology. *Journal of Human Evolution*. 16, pp. 305–309.

Pickford, M. (1984). Kenya palaeontology gazetteer. *National useums of Kenya, Dept. of Sites and Monuments Documentation*. 1.

Pickford, M. (1982). The tectonics, volcanics and sediments of the Nyanza Rift Valley, Kenya. *Z. Geomorphol*. 42, pp. 1–33.

Pierson, T.C. (2005). Hyperconcentrated flow - transitional process between water flow and debris flow. In: *Debris-flow Hazards and Related Phenomena*. Berlin, Spinger. pp. 159–202.

Pik, R., Marty, B., Carignan, J., Yirgu, G. & Ayalew, T. (2008). Timing of East African Rift development in southern Ethiopia: Implication for mantle plume activity and evolution of topography. *Geology*. 36 (2), pp. 167–6.

Pilbeam, D. & Gould, S.J. (1974). Size and scaling in human evolution. *Science*. 186 (4167), pp. 892–901.

Piperno, D.R. (1997). Phytoliths and Microscopic charcoal from Leg 155: a vegetational and fire history of the Amazon basin during the last 75 K.Y. *Proceeding of the Ocean Drilling Program*. 155, pp. 411–418.

Piperno, D.R. (2006). *Phytoliths: A Comprehensive Guide for Archaeologists and Paleoecologists*. Oxford, Rowman Altamira.

Piperno, D.R. (1988). *Phytoliths: An arcaeological and geological perspective*. San Diego, Academic Press.

Piperno, D.R. & Pearsall, D.M. (1998). The silica bodies of tropical American grasses: morphology, taxonomy, and implications for grass systematics and fossil phytolith identification. *Smithsonian contributions to botany*. 85, pp. 1-40.

Plummer, T., Bishop, L.C., Ditchfield, P. & Hicks, J. (1999). Research on late Pliocene Oldowan sites at Kanjera South, Kenya. *Journal of Human Evolution*. 36 (2), pp. 151–170.

Plummer, T.W. & Bishop, L.C. (1994). Hominid paleoecology at Olduvai Gorge, Tanzania as indicated by antelope remains. *Journal of Human Evolution*. 27 (1-3). pp. 47–75.

Plummer, T.W. & Bishop, L.C. (2016). Oldowan hominin behavior and ecology at Kanjera South, Kenya. *Jounral of Anthropological Sciences*. 94. pp. 1–12.

Plummer, T.W. & Finestone, E. (2017). Archeological Sites from 2.6-2.0 Ma: Toward a Deeper Understanding of the Early Oldowan. In: *Rethinking Human Evolution*. Cambridge, MIT Press pp. 1–31.

Plummer, T.W. & Potts, R. (1989). Excavations and new findings at Kanjera, Kenya. *Journal of Human Evolution*. 18 (3), pp. 269–276.

Plummer, T.W., Bishop, L.C., Ditchfield, P.W., Ferraro, J.V., Kingston, J.D., Hertel, F. & Braun, D.R. (2009a). The environmental context of Oldowan hominin activities at Kanjera South, Kenya. In: E. Hovers & D. R. Braun (eds.). *Interdisciplinary approaches to the* Oldowan. Dordrecht, Springer. pp. 149-160

Plummer, T.W., Ditchfield, P.W., Bishop, L.C., Kingston, J.D., Ferraro, J.V., Braun, D.R., Hertel, F. & Potts, R. (2009b). Oldest evidence of tool making hominins in a grassland-dominated ecosystem. D. S. Strait (ed.). *PLoS ONE*. 4 (9), p. e7199.

Plummer, T.W., Ferraro, J.V., Louys, J., Hertel, F., Alemseged, Z., Bobe, R. & Bishop, L.C. (2015). Bovid ecomorphology and hominin paleoenvironments of the Shungura Formation, lower Omo River Valley, Ethiopia. *Journal of Human Evolution*. 88, pp. 108–126.

Pope, R.J. & Wilkinson, K.N. (2005). Reconciling the roles of climate and tectonics in Late Quaternary fan development on the Spartan piedmont, Greece. *Geological Society, London, Special Publications*. 251 (1), pp. 133–152.

Potts, R. (1998). Environmental Hypotheses of Hominin Evolution. *American Journal of Physical Anthropologists*. 107 (S27), pp. 93-136.

Potts, R. (1996). Evolution and climate variability. *Science*. 273 (5277), pp. 922-923.

Potts, R. (2013). Hominin evolution in settings of strong environmental variability. *Quaternary Science Reviews*. 73. pp. 1–13.

Potts, R. (1989). Olorgesailie: new excavations and findings in Early and Middle Pleistocene contexts, southern Kenya rift valley. *Journal of Human Evolution*. 18 (5), pp. 477–484.

Potts, R. (2016). *Relevance of East African Drill Cores to Human Evolution: the Case of the Olorgesailie Drilling Project.* American Geophysical Union, Fall Meeting 2016*, pp. PP23A-2308

Potts, R. (1994). Variables versus models of early Pleistocene hominid land use. *Journal of Human Evolution*. 27, pp. 7–24.

Potts, R., Behrensmeyer, A.K. & Ditchfield, P. (1999). Paleolandscape variation and early pleistocene hominid activities: members 1 and 7, Olorgesailie formation, Kenya. *Journal of Human Evolution*. 37 (5), pp. 747–788.

Potts, R., Ditchfield, P., Hicks, J. & Deino, A. (1997). Paleoenvironments of late Miocene and early Pliocene strata of Kanam, western Kenya. *American Journal of Physical Anthropology*. 24, pp. 188–189.

Prell, W.L. (1984). Covariance patterns of foraminiferal delta ^{18}O: an evaluation of pliocene ice volume changes near 3.2 million years ago. *Science*. 226, pp. 692–695.

Prins, M.A. (1999). Pelagic, hemipelagic and turbidite deposition in the Arabian Sea during the late quaternary: unravelling the signals of eolian and fluvial sediment supply as functions of tectonics, sea-level and climate change by means of end-member modelling siliciclastic grain-size distributions. *Geologica Ultraiectina*. 168, pp1-192

Prins, M.A., Postma, G., Cleveringa, J., Cramp, A. & Kenyon, N.H. (2000). Controls on terrigenous sediment supply to the Arabian Sea during the late quaternary: The Indus fan. *Marine Geology*. 169 (3-4), pp. 327–349.

Prins, M. A., Bouwer, L. M., Beets, C. J., Troelstra, S. R., Weltje, G. J., Kruk, R. W., Kuijpers, A., and Vroon, P. Z. (2002). Ocean circulation and iceberg discharge in the glacial North Atlantic: inferences from unmixing of sediment size distributions. *Geology*. 30 (6), pp. 555–558.

Prins, M.A., Vriend, M., Nugteren, G., Vandenberghe, J., Lu, H., Zheng, H. & Jan Weltje, G. (2007). Late Quaternary aeolian dust input variability on the Chinese Loess Plateau: inferences from unmixing of loess grain-size records. *Quaternary Science Reviews*. 26 (1-2), pp. 230–242.

Prömmel, K., Cubasch, U. & Kaspar, F. (2013). A regional climate model study of the impact of tectonic and orbital forcing on African precipitation and vegetation. *Palaeogeography, Palaeoclimatology, Palaeoecology*. 369, pp. 154–162.

Pye, K. & Blott, S.J. (2004). Particle size analysis of sediments, soils and related particulate materials for forensic purposes using laser granulometry. *Forensic Science International*. 144 (1), pp. 19–27.

Quade, J., Levin, N., Semaw, S., Stout, D., Renne, P., Rogers, M. & Simpson, S. (2004). Paleoenvironments of the earliest stone toolmakers, Gona, Ethiopia. *Geological Society of America Bulletin*. 116 (11-12), pp. 1529–1544.

Quinn, R.L., Lepre, C.J., Feibel, C.S., Wright, J.D., Mortlock, R.A., Harmand, S., Brugal, J.-P. & Roche, H. (2013). Pedogenic carbonate stable isotopic evidence for wooded habitat preference of early Pleistocene tool makers in the Turkana Basin. *Journal of Human Evolution*. 65 (1), pp. 65–78.

Quinn, R.L., Lepre, C.J., Wright, J.D. & Feibel, C.S. (2007). Paleogeographic variations of pedogenic carbonate δ^{13}C values from Koobi Fora, Kenya:

implications for floral compositions of Plio-Pleistocene hominin environments. *Journal of Human Evolution*. 53 (5), pp. 560–573.

Radosevich, S.C., Retallack, G.J. & Taieb, M. (1992). Reassessment of the Paleoenvironment and Preservation of Hominid Fossils From Hadar, Ethiopia. *American Journal of Physical Anthropology*. 87, pp. 15–27.

Ravelo, A.C., Andreasen, D.H., Lyle, M., Lyle, A.O. & Wara, M.W. (2004). Regional climate shifts caused by gradual global cooling in the Pliocene epoch. *Nature*. 429 (6989), pp. 263–267.

Raymo, M.E. (1991). Geochemical evidence supporting TC Chamberlin's theory of glaciation. *Geology*. 19 (4), pp. 344–347.

Raymo, M.E. (1994). The initiation of Northern Hemisphere glaciation. *Annual Review of Earth and Planetary Sciences*. 22 (1), pp. 353–383.

Reed, D.N. & Denys, C. (2011). The taphonomy and paleoenvironmental implications of the Laetoli micromammals. In: *Paleontology and geology of Laetoli: human evolution in context*. Dordrecht, Springer, pp. 265–278.

Reed, D.N. & Geraads, D. (2012). Evidence for a Late Pliocene faunal transition based on a new rodent assemblage from Oldowan locality Hadar A.L. 894, Afar Region, Ethiopia. *Journal of Human Evolution*. 62 (3), pp. 328–337.

Reed, K.E. (1997). Early hominid evolution and ecological change through the African Plio-Pleistocene. *Journal of Human Evolution*. 32 (2-3), pp. 289–322.

Reed, K.E. (2008). Paleoecological patterns at the Hadar hominin site, Afar Regional State, Ethiopia. *Journal of Human Evolution*. 54 (6), pp. 743–768.

Reed, K.E. & Fish, J.L. (2005). Tropical and temperate seasonal influences on human evolution. In: D. K. Brockman & C. P. van Schmik (eds.). *Seasonality in Primates Studies of Living and Extinct Human and Non-Human Primates*. Cambridge, Cambridge University Press. pp. 491–520.

Roach, N.T., Venkadesan, M., Rainbow, M.J. & Lieberman, D.E. (2013). Elastic energy storage in the shoulder and the evolution of high-speed throwing in Homo. *Nature*. 498 (7455), pp. 483–486.

Rogers, M.J., Harris, J.W.K. & Feibel, C.S. (1994). Changing patterns of land use by Plio-Pleistocene hominids in the Lake Turkana Basin. *Journal of Human Evolution*. 27 (1-3), pp. 139-158

Rossouw, L. (2009). *The application of fossil grass-phytolith analysis in the reconstruction of Cainozoic environments in the South African interior*. Ph. D Dissertation. Bloemfontein, South Africa, University of the Free State.

Rossouw, L. & Scott, L. (2011). Phytoliths and Pollen, the Microscopic Plant Remains in Pliocene Volcanic Sediments Around Laetoli, Tanzania. In: T. Harrison (ed.). *Paleontology and Geology of Laetoli: Human Evolution in Context*. Dordrecht, Springer Netherlands, pp. 201–215.

Roveri, M., Lugli, S., Manzi, V. & Schreiber, B.C. (2008). The Messinian Sicilian stratigraphy revisited: new insights for the Messinian salinity crisis. *Terra Nova*. 20 (6), pp. 483–488.

Ruddiman, W.F., Raymo, M.E., Lamb, H.H. & Andrews, J.T. (1988). Northern Hemisphere climate regimes during the past 3 Ma: possible tectonic connections. *Philosophical Transactions of the Royal Society of London. B, Biological Sciences*. 318 (1191), pp. 411–430.

Saggerson, E.P. (1952). *Geology of the Kisumu District.* Report 21. Nairobi: Geological Survey of Kenya, 86 pp.

Saji, N.H., Goswami, B.N., Vinayachandran, P.N. & Yamagata, T. (1999). A dipole mode in the tropical Indian Ocean. *Nature*. 401 (6751), pp. 360–363.

Saylor, B.Z., Gibert, L., Deino, A., Alene, M., Levin, N.E., Melillo, S.M., Peaple, M.D., Feakins, S.J., Bourel, B., Barboni, D. and Novello, A. (2019). Age and context of mid-Pliocene hominin cranium from Woranso-Mille, Ethiopia. *Nature*. 573 (7773), pp. 220–224.

Scardia, G., Parenti, F., Miggins, D.P., Gerdes, A., Araujo, A.G. & Neves, W.A. (2019). Chronologic constraints on hominin dispersal outside Africa since 2.48 Ma from the Zarqa Valley, Jordan. *Quaternary Science Reviews*. 219, pp. 1–19.

Schefuß, E., Schouten, S. & Schneider, R.R. (2005). *Central African hydrologic changes during the past 20,000 years.* American Geophysical Union, Fall meeting. pp. PP13C-07

Schillereff, D.N., Chiverrell, R.C., Macdonald, N. & Hooke, J.M. (2014). Flood stratigraphies in lake sediments: A review. *Earth-Science Reviews*. 135, pp. 17–37.

Schillereff, D.N., Chiverrell, R.C., Macdonald, N. & Hooke, J.M. (2015). Hydrological thresholds and basin control over paleoflood records in lakes. *Geology*. 44 (1), pp. 43-46

Schneck, R., Micheels, A. & Mosbrugger, V. (2010). Climate modelling sensitivity experiments for the Messinian Salinity Crisis. *Palaeogeography, Palaeoclimatology, Palaeoecology*. 286 (3), pp. 149–163.

Schoeninger, M.J., Reeser, H. & Hallin, K. (2003). Paleoenvironment of Australopithecus anamensis at Allia Bay, East Turkana, Kenya: evidence from mammalian herbivore enamel stable isotopes. *Journal of Anthropological Archaeology*. 22 (3), pp. 200–207.

Senut, B., Pickford, M., Gommery, D., Mein, P., Cheboi, K. & Coppens, Y. (2001). First hominid from the Miocene (Lukeino formation, Kenya). *Comptes Rendus de l'Académie des Sciences-Series IIA-Earth and Planetary Science*. 332 (2), pp. 137–144.

Senut, B., Pickford, M., Gommery, D. and Ségalen, L. (2018). Palaeoenvironments

and the origin of hominid bipedalism. *Historical Biology*. 30(1-2), pp. 284-296.

Sepulchre, P., Ramstein, G., Fluteau, F., Schuster, M., Tiercelin, J. & Brunet, M. (2006). Tectonic Uplift and Eastern Africa Aridification. *Science*. 313 (5792), pp. 1419–1423.

Ségalen, L., Lee-Thorp, J.A. & Cerling, T. (2007). Timing of C 4 grass expansion across sub-Saharan Africa. *Journal of Human Evolution*. 53 (5), pp. 549–559.

Shackleton, N.J., Imbrie, J., Pisias, N.G. & Rose, J. (1988). The evolution of oceanic oxygen-isotope variability in the North Atlantic over the past three million years. *Philosophical Transactions of the Royal Society of London. Series B, Biological Sciences*. 318 (1191), pp. 679–688.

Sheridan, M.F., Wohletz, K.H. & Dehn, J. (1987). Discrimination of grain-size subpopulations in pyroclastic deposits. *Geology*. 15, pp. 367–370.

Sier, M.J., Langereis, C.G., Dupont-Nivet, G., Feibel, C.S., Joordens, J.C., van der Lubbe, J.H., Beck, C.C., Olago, D. and Cohen, A. (2017). The top of the Olduvai Subchron in a high-resolution magnetostratigraphy from the West Turkana core WTK13, hominin sites and Paleolakes Drilling Project (HSPDP). *Quaternary Geochronology*. 42, pp.117-129.

Sikes, N., Potts, R. & Behrensmeyer, A.K. (1997). Isotopic study of Pleistocene paleosols from the Olorgesailie Formation, southern Kenya rift. *Journal of Human Evolution*. 32 (4), pp. A20-A21.

Sikes, N.E. & Ashley, G.M. (2007). Stable isotopes of pedogenic carbonates as indicators of paleoecology in the Plio-Pleistocene (upper Bed I), western margin of the Olduvai Basin, Tanzania. *Journal of Human Evolution*. 53 (5), pp. 574–594.

Sikes, N.E., Potts, R. & Behrensmeyer, A.K. (1999). Early pleistocene habitat in member 1 Olorgesailie based on paleosol stable isotopes. *Journal of Human Evolution*. 37, pp. 721–746.

Smith, J.N. (2001). Why should we believe 210 Pb sediment geochronologies ? *Geochimica*. 55, pp. 121–123.

Spiegel, C., Kohn, B.P., Belton, D.X. & Gleadow, A.J.W. (2007). Morphotectonic evolution of the central Kenya rift flanks: Implications for late Cenozoic environmental change in East Africa. *Geology*. 35 (5), pp. 427–430.

Stanistreet, I.G. (2012). Fine resolution of early hominin time, Beds I and II, Olduvai Gorge, Tanzania. *Journal of Human Evolution*. 63 (2), pp. 300–308.

Stanistreet, I.G., Stollhofen, H., Njau, J.K., Farrugia, P., Pante, M.C., Masao, F.T., Albert, R.M. & Bamford, M.K. (2018). Lahar inundated, modified, and preserved 1.88 Ma early hominin (OH24 and OH56) Olduvai DK site. *Journal of Human Evolution*. 116, pp. 27–42.

Stern, J.T., Jr & Susman, R.L. (1983). The locomotor anatomy of Australopithecus

afarensis. *American Journal of Physical Anthropology*. 60 (3), pp. 279–317.

Stokes, M. & Mather, A.E. (2015). Controls on modern tributary-junction alluvial fan occurrence and morphology: High Atlas Mountains, Morocco. *Geomorphology*. 248, pp. 344–362.

Stokes, M. & Mather, A.E. (2000). Response of Plio-Pleistocene alluvial systems to tectonically induced base-level changes, Vera Basin, SE Spain. *Journal of the Geological Society*. 157 (2), pp. 303–316.

Stone, J. (2004). Extraction of Al and Be from quartz for isotopic analysis. *UW Cosmogenic Nuclide Lab Methods and Procedures*.

Strauss, J., Schirrmeister, L., Wetterich, S., Borchers, A. and Davydov, S.P. (2012). Grain-size properties and organic-carbon stock of Yedoma Ice Complex permafrost from the Kolyma lowland, northeastern Siberia. *Global biogeochemical cycles*, 26(3).

Strecker, M.R., Blisniuk, P.M. & Eisbacher, G.H. (1990). Rotation of extension direction in the central Kenya Rift. *Geology*. 18, pp. 299–302.

Strömberg, C.A. (2004). Using phytolith assemblages to reconstruct the origin and spread of grass-dominated habitats in the great plains of North America during the late Eocene to early Miocene. *Palaeogeography, Palaeoclimatology, Palaeoecology*. 207 (3-4), pp. 239–275.

Stuut, J.-B.W., Prins, M.A., Schneider, R.R., Weltje, G.J., Jansen, J.H.F. & Postma, G. (2002). A 300-kyr record of aridity and wind strength in southwestern Africa: inferences from grain-size distributions of sediments on Walvis Ridge, SE Atlantic. *Marine Geology*. (180), pp. 221–233.

Su, D.F. (2011). Large Mammal Evidence for the Paleoenvironment of the Upper Laetolil and Upper Ndolanya Beds of Laetoli, Tanzania. In: T. Harrison (ed.). *Paleontology and Geology of Laetoli: Human Evolution in Context*. Dordrecht, Springer Netherlands, pp. 381–392.

Su, D.F. & Harrison, T. (2015). The paleoecology of the Upper Laetolil Beds, Laetoli Tanzania: A review and synthesis. *Journal of African Earth Sciences*. 101, pp. 405–419.

Taieb, M., Coppens, Y., Johanson, D.C. & Kalb, J. (1972). Dépôts sédimentaires et faunes du Plio-Pléistocene de la basse vallée de l'Awash (Afar central, Ethiopie). *CR Acad. Sci. D*. 275, pp. 819–882.

Teaford, M.F. & Ungar, P.S. (2000). Diet and the evolution of the earliest human ancestors. *Proceedings of the National Academy of Sciences*. 97 (25), pp. 13506–13511.

Thorn, V.C. (2004). Phytolith evidence for C4-dominated grassland since the early Holocene at Long Pocket, northeast Queensland, Australia. *Quaternary Research*. 61 (2), pp. 168–180.

Tiedemann, R., Sarnthein, M. & Shackleton, N.J. (1994). Astronomic timescale for the Pliocene Atlantic $\delta^{18}O$ and dust flux records of Ocean Drilling Program Site 659. *Paleoceanography.* 9 (4), pp. 619–638.

Tipple, B.J. & Pagani, M. (2007). The early origins of terrestrial C4 photosynthesis. *Annual Review of Earth and Planetary Sciences.* 35, pp. 435–461.

Toonen, W.H., Winkels, T.G., Cohen, K.M., Prins, M.A. and Middelkoop, H. (2015). Lower Rhine historical flood magnitudes of the last 450 years reproduced from grain-size measurements of flood deposits using End Member Modelling. *Catena.* 130, pp. 69-81.

Trauth, M.H., Deino, A.L., Bergner, A.G.N. & Strecker, M.R. (2003). East African climate change and orbital forcing during the last 175 kyr BP. *Earth and Planetary Science Letters.* 206 (3-4), pp. 297–313.

Trauth, M.H., Larrasoaña, J.C. & Mudelsee, M. (2009). Trends, rhythms and events in Plio-Pleistocene African climate. *Quaternary Science Reviews.* 28 (5), pp. 399–411.

Trauth, M.H., Maslin, M.A., Deino, A. & Strecker, M.R. (2005). Late cenozoic moisture history of East Africa. *Science.* 309 (5743), pp. 2051–2053.

Trauth, M.H., Maslin, M.A., Deino, A.L., Junginger, A., Lesoloyia, M., Odada, E.O., Olago, D.O., Olaka, L.A., Strecker, M.R. & Tiedemann, R. (2010). Human evolution in a variable environment: the amplifier lakes of Eastern Africa. *Quaternary Science Reviews.* 29 (23-24), pp. 2981–2988.

Trauth, M.H., Maslin, M.A., Deino, A.L., Strecker, M.R., Bergner, A.G.N. & Dühnforth, M. (2007). High- and low-latitude forcing of Plio-Pleistocene East African climate and human evolution. *Journal of Human Evolution.* 53 (5), pp. 475–486.

Turner, T.E., Swindles, G.T. & Roucoux, K.H. (2014). Late Holocene ecohydrological and carbon dynamics of a UK raised bog: Impact of human activity and climate change. *Quaternary Science Reviews.* 84, pp. 65–85.

Twiss, P.C., Suess, E. & Smith, R.M. (1969). Morphological Classification of Grass Phytoliths. *Soil Science of America Proceedings.* 33 (1), pp. 109–115.

Uno, K.T., Cerling, T.E., Harris, J.M., Kunimatsu, Y., Leakey, M.G., Nakatsukasa, M. & Nakaya, H. (2011). Late Miocene to Pliocene carbon isotope record of differential diet change among East African herbivores. *Proceedings of the National Academy of Sciences.* 108 (16), pp. 6509-6514.

Uno, K.T., Polissar, P.J., Jackson, K.E. & DeMenocal, P.B. (2016a). Neogene biomarker record of vegetation change in eastern Africa. *Proceedings of the National Academy of Sciences.* 113 (23), pp. 6355–6363.

Uno, K.T., Polissar, P.J., Kahle, E., Feibel, C., Harmand, S., Roche, H. & DeMenocal, P.B. (2016b). A Pleistocene palaeovegetation record from plant wax biomarkers from the Nachukui Formation, West Turkana, Kenya.

Philosophical Transactions of the Royal Society. B, Biological Sciences. 371 (1698). pp. 1–10.

Uribelarrea, D., Martín-Perea, D., Diez-Martin, F., Sánchez-Yustos, P., Dominguez-Rodrigo, M., Baquedano, E. & Mabulla, A. (2017). A reconstruction of the paleolandscape during the earliest Acheulian of FLK West: The co-existence of Oldowan and Acheulian industries during lowermost Bed II (Olduvai Gorge, Tanzania). *Palaeogeography, Palaeoclimatology, Palaeoecology*. 488, pp. 50-58

Vandenberghe, J. (2013). Grain size of fine-grained windblown sediment: A powerful proxy for process identification. *Earth-Science Reviews*. 121, pp. 18–30.

Vandenberghe, J., Sun, Y., Wang, X., Abels, H.A. & Liu, X. (2018). Grain-size characterization of reworked fine-grained aeolian deposits. *Earth-Science Reviews*. 177, pp. 43–52.

Van Hateren, J.A., Prins, M.A. and Van Balen, R.T. (2018). On the genetically meaningful decomposition of grain-size distributions: A comparison of different end-member modelling algorithms. *Sedimentary geology*. 375, pp. 49-71.

Varga, G., Újvári, G. and Kovács, J. (2019). Interpretation of sedimentary (sub) populations extracted from grain size distributions of Central European loess-paleosol series. *Quaternary International.* 502, pp. 60-70.

Verardo, D.J. & Ruddiman, W.F. (1996). Late Pleistocene charcoal in tropical Atlantic deep-sea sediments: Climatic and geochemical significance. *Geology*. 24 (9), pp. 855–857.

Verschuren, D., Damsté, J.S.S., Moernaut, J., Kristen, I., Blaauw, M., Fagot, M., Haug, G.H. (2009). Half-precessional dynamics of monsoon rainfall near the East African Equator. *Nature*. 462 (3), pp. 637–641.

Visher, G.S. (1969). Grain Size Distributions and Depositional processes. *Journal of Sedimentary Research*. 39 (3), pp. 1074–1106.

Vrba, E.S. (1985). Environment and evolution: alternative causes of the temporal distribution of evolutionary events. *South African Journal of Science*. 81 (5), pp. 229–236.

Vriend, M. and Prins, M.A. (2005). Calibration of modelled mixing patterns in loess grain-size distributions: an example from the north-eastern margin of the Tibetan Plateau, China. *Sedimentology.* 52(6), pp. 1361-1374.

Vrydaghs, L., Ball, T.B. and Devos, Y. (2016). Beyond redundancy and multiplicity. Integrating phytolith analysis and micromorphology to the study of Brussels Dark Earth. *Journal of archaeological science.* 68, pp. 79-88.

Wan, S., Li, A., Clift, P.D. & Stuut, J.B.W. (2007). Development of the East Asian monsoon: Mineralogical and sedimentologic records in the northern South China Sea since 20 Ma. *Palaeogeography, Palaeoclimatology, Palaeoecology*.

254 (3-4), pp. 561–582.

Wang, J., Li, A., Xu, K., Zheng, X. & Huang, J. (2015). Clay mineral and grain size studies of sediment provenances and paleoenvironment evolution in the middle Okinawa trough since 17ka. *Marine Geology*. 366, pp. 49–61.

Wang, R., Biskaborn, B.K., Ramisch, A., Ren, J., Zhang, Y., Gersonde, R. & Diekmann, B. (2016). Modern modes of provenance and dispersal of terrigenous sediments in the North Pacific and Bering Sea: implications and perspectives for palaeoenvironmental reconstructions. *Geo-Marine Letters*. 36 (4), pp. 259-270

Wang, W.P.P., Liu, J.L.L., Zhang, J.B.B., Li, X.P.P., Cheng, Y.N.N., Xin, W.W.W. & Yan, Y.F.F. (2013). Evaluation of Laser Diffraction Analysis of Particle Size Distribution of Typical Soils in China and Comparison With the Sieve-Pipette Method. *Soil Science*. 178 (4), pp. 194–204.

Waters, J.V., Jones, S.J. & Armstrong, H.A. (2010). Climatic controls on late Pleistocene alluvial fans, Cyprus. *Geomorphology*. 115 (3-4), pp. 228–251.

Weltje, G.J. (1997). End-member modeling of compositional data: Numerical-statistical algorithms for solving the explicit mixing problem. *Mathematical Geology*. 29 (4), pp. 503–549.

Weltje, G.J. & Prins, M.A. (2007). Genetically meaningful decomposition of grain-size distributions. *Sedimentary Geology*. 202 (3), pp. 409–424.

Weltje, G.J. & Prins, M.A. (2003). Muddled or mixed? Inferring palaeoclimate from size distributions of deep-sea clastics. *Sedimentary Geology*. 162 (1-2), pp. 39–62.

White, T.D., Ambrose, S.H., Suwa, G. & WoldeGabriel, G. (2010). Response to Comment on the Paleoenvironment of Ardipithecus ramidus. *Science*. 328, p. 1105

White, T.D., Asfaw, B., Beyene, Y., Haile-Selassie, Y., Lovejoy, C.O., Suwa, G. & WoldeGabriel, G. (2009). Ardipithecus ramidus and the paleobiology of early hominids. *Science*. 326 (5949), pp. 64–86.

Wichura, H., Bousquet, R., Oberhänsli, R., Strecker, M. & Trauth, M. (2010). *Mid-Miocene Uplift of the East African Plateau*. American Geosciences Union, Fall Meeting, pp. T31B-1801

Williams, M., Williams, F.M., Gasse, F., Curtis, G.H. & Adamson, D.A. (1979). Plio--Pleistocene environments at Gadeb prehistoric site, Ethiopia. *Nature*. 282 (5734), pp. 29-33

Wilson, K.E. (2011). *Plio-Pleistocene reconstruction of East African and Arabian Sea palaeoclimate*. Ph. D. Dissertation. University College London

Wilson, K.E., Maslin, M.A., Leng, M.J., Kingston, J.D., Deino, A.L., Edgar, R.K. & Mackay, A.W. (2014). East African lake evidence for Pliocene millennial-scale

climate variability. *Geology*. 42 (11), pp. 955–958.

WoldeGabriel, G., Olago, D., Dindi, E. & Owor, M. (2016). Genesis of the East African Rift System. In: M. Schagerl (ed.). *Soda Lakes of East Africa*. Cham, Springer, pp. 25–59.

Wood, B. & Leakey, M. (2011). The Omo-Turkana Basin Fossil Hominins and Their Contribution to Our Understanding of Human Evolution in Africa. *Evolutionary Anthropology: Issues, News, and Reviews*. 20 (6), pp. 264–292.

Wright, J.D. & Miller, K.G. (1996). Control of North Atlantic deep water circulation by the Greenland-Scotland Ridge. *Paleoceanography*. 11 (2), pp. 157–170.

Wündsch, M., Haberzettl, T., Kirsten, K.L., Kasper, T., Zabel, M., Dietze, E., Baade, J., Daut, G., Meschner, S., Meadows, M.E. and Mäusbacher, R. (2016). Sea level and climate change at the southern Cape coast, South Africa, during the past 4.2 kyr. *Palaeogeography, Palaeoclimatology, Palaeoecology*. 446, pp. 295-307.

Wynn, J.G. (2004). Influence of Plio-Pleistocene Aridification on Human Evolution: Evidence from Paleosols of the Turkana Basin, Kenya. *American Journal of Physical Anthropology: The Official Publication of the American Association of Physical Anthropologists*. 123 (2), pp. 106–118.

Wynn, J.G. (2000). Paleosols, stable carbon isotopes, and paleoenvironmental interpretation of Kanapoi, Northern Kenya. *Journal of Human Evolution*. 39, pp. 411–432.

Wynn, J.G., Roman, D.C., Alemseged, Z., Reed, D., Geraads, D. & Munro, S. (2008). Stratigraphy, depositional environments, and basin structure of the Hadar and Busidima Formations at Dikika, Ethiopia. *The Geology of Early Humans in the Horn of Africa Geological Society of America Special Paper*. 446, pp. 1–32.